entropy

Non-additive Entropy Formulas

Motivation and Derivations

Edited by
Tamás Sándor Bíró and Airton Deppman

MDPI

Non-additive Entropy Formulas: Motivation and Derivations

Non-additive Entropy Formulas: Motivation and Derivations

Editors

Tamás Sándor Bíró
Airton Deppman

Editors

Tamás Sándor Bíró   Airton Deppman
Wigner Research Centre   Universidade de São Paulo
for Physics   São Paulo, Brazil
Budapest, Hungary

This is a reprint of articles from the Special Issue published online in the open access journal *Entropy* (ISSN 1099-4300) (available at: https://www.mdpi.com/journal/entropy/special_issues/nonadditive_entropy).

For citation purposes, cite each article independently as indicated on the article page online and as indicated below:

Lastname, A.A.; Lastname, B.B. Article Title. *Journal Name* **Year**, *Volume Number*, Page Range.

Contents

About the Editors

Tamás Sándor Bíró

Tamás Sándor Biró is a theoretical physicist working at the Wigner Research Centre for Physics in Budapest, Hungary and associated with the University Babes Bolyai in Cluj, Romania as a researcher. Furthermore, he is an external member in the Complexity Science Hub, Vienna, Austria. His research interests range from high-energy physics (including quark–gluon plasma) through statistical physics (generalized entropies, inequality measures) with present experiments on nanotechnological improvements in prospective laser-initiated fusion targets.

Airton Deppman

Airton Deppman is an accomplished researcher in Nuclear and Particle Physics. With a Ph.D. in Nuclear Physics earned in 1993, his work skillfully merges theoretical models with experimental data to advance our comprehension of fundamental particles and astrophysical processes. His research has revealed the intricate nature of nuclear forces, explored the dynamics of quark–gluon plasma, and illuminated the nonextensive attributes of non-Abelian fields. Introducing an inventive approach based on fractal structures, Dr. Deppman pioneered the concept of thermofractals, offering fresh perspectives on Yang–Mills fields. His recent investigations have delved into the mathematical correlations between fractal geometry, fractal and fractional calculus, and q-deformed calculus.

Editorial

Non-Additive Entropy Formulas: Motivation and Derivations

Tamás Sándor Biró [1,2,*,†] and Airton Deppman [3]

[1]   Wigner Research Centre for Physics, 1121 Budapest, Hungary
[2]   Institute for Physics, University Babeş-Bolyai, 400294 Cluj, Romania
[3]   Instituto de Física, University of São Paolo, São Paolo 05508-090, Brazil; deppman@usp.br
[*]   Correspondence: biro.tamas@wigner.hu
[†]   External Faculty Member at Complexity Science Hub, 1080 Vienna, Austria.

Entropy is a great tool in thermodynamics and statistical physics. Originally conceptualized by Clausius as a state descriptor that was distinguished from heat, it became a basic principle for statistical and informatics calculations. Its classical form, Boltzmann entropy, is widely used. Moreover, its generalizations are numerous: altered, non-logarithmic formulas concerning the relationship between the probability of a given state and the total entropy of a system proliferate.

This Special Issue is devoted to the mathematical background and physical motivation behind using non-additive entropy formulas, which are, in most cases, still group entropies, defined as expectation values, and incorporate, in one way or another, nontrivial correlations in the investigated systems and processes. Despite the vast number of studies on applying such formulas in informatics, mathematics, and statistical physics approaches to a wide range of physical, biological, economical, and social phenomena, we felt that a collection of their derivations, beyond simple axiomatization and usage, would be useful for modern statistical communities.

The concept of entropy has been changing swiftly since C. Tsallis and, before him, a series of mathematicians and informatics experts proposed various generalizations of Boltzmann–Gibbs entropy. The most distinguishing property of these formulas is their non-additivity with respect to factorizing probabilities, with the notable exception of Rényi entropy, which is, on the other hand, not an expectation value.

The determination of a non-additive entropy formula has motivated investigations in many directions. Some works have considered the theoretical and axiomatic implications of the new form of entropy. Others have proposed physical mechanisms that could lead to non-additive entropy. Evidence for the applicability of generalized thermodynamics appears in many branches of physics and other fields, such as biological systems, socio-economic environments, information theory, and complex networks, among many others.

This Special Issue is dedicated to reviewing these developments, sharing new results and opening new perspectives as to the advancement of our knowledge of entropy. We have gathered contributions on the following topics:

(1)   The implications and applications of non-additive entropy;
(2)   Advances in the theoretical aspects of entropy;
(3)   The mathematical aspects of non-additive entropy;
(4)   The thermodynamic consequences of generalized entropy;
(5)   The origins of non-additivity in the entropy of complex systems.

The contributors to this Special Issue include colleagues who have been working on these ideas and related concepts for decades. The included papers cover issues ranging from derivation discussions of given formula groups to the applications of a given entropy formula for contemporary problems—and solving them—and the statistical data analysis of COVID-19 infections.

We have received eleven papers, including an extended review by Angle R. Plastino and Angelo Plastino titled "on the Connection Between the Microcanonical Ensemble

and the S_q-canonical Probability Distribution" (i.e., the Tsallis–Pareto cut power law distribution). This work is connected to the classical thermodynamics background in the micro-canonical approach, as is the paper by Tamás Sándor Biró entitled "Non-Additive Entropy Composition Rules Connected With Finite Heat-Bath Effects", which concerns the finite heat capacity of the reservoir determining the Tsallis-q parameter. Also of a general background nature, the contribution by Ozgur Afsar and Tirnakli investigates the self-organization process in non-extensive open systems. This paper also reveals the connections to chaotic dynamics and discusses a simple example.

A review-like contribution on the mathematical relations regarding q-entropy is presented by Angel R. Plastino, Constantino Tsallis, Rosell S. Wedemann, and Hans J. Hubold, concentrating on entropy optimization issues and the use of generalized logarithms—simultaneously implying generalizationsof the logarithmic entropy formula—and some interesting duality relations between various q parameters. In the direction of more abstract mathematical tools, two contributions in this Special Issue cover fractal derivatives. The first of which, which was written by Airton Deppman, Eugenio Megías, and Roman Pasechnik and concerns "Fractal Derivatives, Fractional Derivatives and q-Deformd Calculus", dives deeper into formalism. A similarly motivated article written by Jin-Wen Kang, Ke-Ming Shen, and Ben-Wei Zhang considers the h-Derivative in relation to non-additive entropy. Finally, we have the paper by F. Nobre and E. Curado, wherein the dynamical evolution of non-additive entropies is considered on the basis of a generalized H-theorem, resulting in non-linear equations for a class of systems.

The rest of the submissions deal with applications, but what incredible applications they are! Jin Yan and Christian Beck discuss an information shift model, which they demonstrate to be equivalent with $q = 3$ entropy in a compact phase space. It is intended to be applied to a pre-universe before ordinary spacetime was created and the natural laws as we know them were formed. The authors show that the electromagnetic fine structure constant's value, 1/137, can be interpreted as a special "equilibrium" state for Chebisev maps describing a chaotic pre-universe. This is quite an interesting perspective.

More earthbound but also more controllable applications are provided in relation to well-studied phenomena. Grzgeorz Wilk and Zbigbiew Wlodarczyk present a review of applying non-extensive entropy to multi-particle production in high-energy collisions inside accelerators. In their contribution, Elif Tuna, Alif Evren, Erhan Ustaoglu, Busra Sahin, and Zehra Zeynep Sahinbasoglu discuss an application with importance in hypothesis testing. Lastly, we have collected a genuine non-physics application to the statistics of COVID-19 infections written by Markos N. Xenakis estimating the risk of indoor infection.

In closing this Editorial, we thank the contributing authors for being responsive to our call and providing such a remarkable variety of thoughtful and interesting papers on non-additive entropy. The invaluable help provided by the MDPI Editorial Office is also gratefully acknowledged.

Article

Non-Additive Entropic Forms and Evolution Equations for Continuous and Discrete Probabilities

Evaldo M. F. Curado and Fernando D. Nobre *

Centro Brasileiro de Pesquisas Físicas and National Institute of Science and Technology for Complex Systems
Rua Xavier Sigaud 150, Urca, Rio de Janeiro 22290-180, Brazil
* Correspondence: fdnobre@cbpf.br; Tel.: +55-(21)-2141-7513

Abstract: Increasing interest has been shown in the subject of non-additive entropic forms during recent years, which has essentially been due to their potential applications in the area of complex systems. Based on the fact that a given entropic form should depend only on a set of probabilities, its time evolution is directly related to the evolution of these probabilities. In the present work, we discuss some basic aspects related to non-additive entropies considering their time evolution in the cases of continuous and discrete probabilities, for which nonlinear forms of Fokker–Planck and master equations are considered, respectively. For continuous probabilities, we discuss an H-theorem, which is proven by connecting functionals that appear in a nonlinear Fokker–Planck equation with a general entropic form. This theorem ensures that the stationary-state solution of the Fokker–Planck equation coincides with the equilibrium solution that emerges from the extremization of the entropic form. At equilibrium, we show that a Carnot cycle holds for a general entropic form under standard thermodynamic requirements. In the case of discrete probabilities, we also prove an H-theorem considering the time evolution of probabilities described by a master equation. The stationary-state solution that comes from the master equation is shown to coincide with the equilibrium solution that emerges from the extremization of the entropic form. For this case, we also discuss how the third law of thermodynamics applies to equilibrium non-additive entropic forms in general. The physical consequences related to the fact that the equilibrium-state distributions, which are obtained from the corresponding evolution equations (for both continuous and discrete probabilities), coincide with those obtained from the extremization of the entropic form, the restrictions for the validity of a Carnot cycle, and an appropriate formulation of the third law of thermodynamics for general entropic forms are discussed.

Keywords: nonlinear Fokker–Planck equations; generalized entropies; nonextensive thermostatistics

1. Introduction

The area of complex systems has attracted the attention of many researchers in recent years and has exhibited a large variety of novel phenomena, such as nonlinear dynamics, slow relaxation processes, and nonextensivity in some thermodynamic quantities [1–4]. These systems are usually characterized by a large number of components immersed in random or disordered media that interact through long-range forces and/or possess long time memories; as a consequence, they may present a collective behavior very different from those of their individual components. Many of the above-mentioned phenomena have been understood appropriately by means of proposals of generalized entropies [4–12], which have found grounds on diverse applications within the realm of complex systems (see, e.g., Ref. [9] for a comprehensive list of entropic forms available in the literature up to 2011). In its statistical formulation, a given entropic form should be a functional only of a set $\{P_i(t)\}$, i.e., $S \equiv S(\{P_i(t)\})$, where $P_i(t)$ stands for the probability of finding a

given system on a state i at time t [13,14]. Most of these generalized entropies violate the additivity property and are usually referred to as non-additive entropic forms. This property concerns two probabilistically independent systems (A and B), described by two sets of probabilities $\{P_i^{(A)}\}$ and $\{P_j^{(B)}\}$, respectively, such that the probabilities for the composed system are given by $P_{ij}^{(A+B)} = P_i^{(A)} P_j^{(B)}$ ($\forall (i,j)$). A given entropic form is considered non-additive if

$$S^{(A+B)}(\{P_{ij}\}) \neq S^{(A)}(\{P_i\}) + S^{(B)}(\{P_j\}) \,. \tag{1}$$

Among the many proposals of generalized (or non-additive) entropies, the most commonly known is Tsallis entropy S_q [12], which is characterized by an index q ($q \in \mathbb{R}$),

$$S_q(\{P_i\}) = k \frac{1 - \sum_{i=1}^{W} P_i^q}{q - 1} \,, \tag{2}$$

so as to recover the Boltzmann–Gibbs (BG) entropy,

$$S_{\mathrm{BG}}(\{P_i\}) = -k \sum_i P_i(t) \ln P_i(t) \,, \tag{3}$$

in the limit $q \to 1$, i.e., $S_1 \equiv S_{\mathrm{BG}}$.

One of the most successful theories of contemporary theoretical physics is BG statistical mechanics [13–17]; this theory is based on BG entropy, which is additive. The time evolution of $S_{\mathrm{BG}}(\{P_i(t)\})$, and consequently, its approach to the equilibrium state, is directly related to the evolution of the probabilities $\{P_i(t)\}$, which follow some fundamental equation, e.g., a master equation. For continuous probability densities $P(\vec{x}, t)$, the linear Fokker–Planck equation (FPE) appears to be an appropriate candidate for describing the evolution of probabilities and represents one of the most important equations of nonequilibrium BG statistical mechanics. The FPE delineates the time evolution of the probability density $P(\vec{x}, t)$ for finding a given particle at a position $\vec{x}$ at time t while diffusing under an external potential [14–18]. Usually one considers a confining external potential, leading to the possibility of a stationary-state solution after a sufficiently long time. Particular interest in the literature has been given to a harmonic confining potential, which leads to a Gaussian distribution as the stationary-state solution of the FPE [17,18]. In the absence of an external potential, the FPE reduces to the linear diffusion equation, which does not present a stationary-state solution and is also associated with many out-of-equilibrium applications, such as the celebrated Brownian motion and related phenomena.

A clear understanding of the range of applicability of BG statistical mechanics has been emerging in the latest years; for example, it has become evident that it should be used for systems characterized by weakly interacting particles and/or short time memories. As typical counter-examples, regarding diffusion, it is very frequent nowadays to find dynamical behavior that falls out of the ambit of the linear cases, which are commonly called anomalous diffusion and usually take place in media presenting randomness, porosity, and heterogeneity [19]. To deal with these phenomena, one habitually uses a nonlinear (power-like) diffusion equation, known in the literature as a porous media equation [20]. Similar to the linear FPE, by adding a confining potential contribution, one obtains a nonlinear Fokker–Planck equation (NLFPE) [21], as introduced in Refs. [22,23]. For a harmonic confining potential, this NLFPE presents a q-Gaussian distribution typical of nonextensive statistical mechanics [4–6] as its stationary-state solution. This distribution is expressed as

$$P_q(u) = P_0 \exp_q(-\beta u^2) \tag{4}$$

and can be defined in terms of the q-exponential function,

$$\exp_q(u) = [1 + (1-q)u]_+^{1/(1-q)} \,; \quad (\exp_1(u) = \exp(u)) \,, \tag{5}$$

where $P_0 \equiv P_q(0)$ and $[y]_+ = y$ for $y > 0$ (zero otherwise). In this way, the NLFPE introduced in Refs. [22,23] is associated with the Tsallis entropy, S_q, since its q-Gaussian solution coincides with the distribution that maximizes S_q. Additionally, proofs of an H-theorem connect the linear FPE with BG entropy [17,18], as well as NLFPEs with generalized entropies [21,24–35], and particularly, they relate the NLFPE of Refs. [22,23] to the entropy S_q.

In the present work, we analyze general entropic forms (typically non-additive) for both continuous and discrete probabilities whose time evolution follows a NLFPE, or a master equation, respectively. Some important novel results from the thermodynamical point of view, related to their corresponding equilibrium states, are studied. In the next section, we define general NLFPEs and explore their relationship to non-additive entropies by means of an H-theorem. Additionally, the corresponding stationary-state solutions are discussed; due to the H-theorem, after a sufficiently long time, the system should reach an equilibrium state for which a given stationary-state solution holds as the equilibrium solution. At equilibrium, we show that the Carnot cycle applies for these entropic forms under very common conditions. In Section 3, we consider the case of discrete probabilities, whose time evolution follows a master equation, while also proving an H-theorem; moreover, the third law of thermodynamics is discussed for both S_q and general entropic forms. Finally, in Section 4, we present our main conclusions.

2. Continuous Probabilities: Non-Additive Entropic Forms and NLFPEs

Although one may pursue an analysis in arbitrary dimensions, by considering a probability density $P(x_1, x_2, \cdots, x_N, t)$ (such as, e.g., in Ref. [34]) herein for simplicity, we will restrict ourselves to a one-dimensional space described in terms of a probability density $P(x, t)$ and following the normalization condition

$$\int_{-\infty}^{\infty} P(x,t) dx = 1 . \tag{6}$$

In this case, a general NLFPE may be defined as [30,31]

$$\frac{\partial P(x,t)}{\partial t} = -\frac{\partial}{\partial x}\{A(x)\Psi[P(x,t)]\} + D\frac{\partial}{\partial x}\left\{\Omega[P(x,t)]\frac{\partial P(x,t)}{\partial x}\right\}, \tag{7}$$

where D represents a diffusion coefficient with dimensions of energy, and the external force $A(x)$ is associated with a confining potential $\phi(x)$ $[A(x) = -d\phi(x)/dx]$. The functionals $\Psi[P(x,t)]$ and $\Omega[P(x,t)]$ should satisfy certain mathematical requirements, e.g., positiveness and monotonicity with respect to $P(x,t)$ [30,31]; moreover, to ensure the normalizability of $P(x,t)$ for all times, one must impose the conditions

$$P(x,t)|_{x\to\pm\infty} = 0 ; \quad \left.\frac{\partial P(x,t)}{\partial x}\right|_{x\to\pm\infty} = 0 ; \quad A(x)\Psi[P(x,t)]|_{x\to\pm\infty} = 0 \quad (\forall t) . \tag{8}$$

The NLFPE of Equation (7) recovers some well-known cases as particular limits: (i) the linear FPE [14–18] for $\Psi[P(x,t)] = P(x,t)$ and $\Omega[P(x,t)] = 1$ and (ii) the NLFPE introduced in Refs. [22,23], which are associated with nonextensive statistical mechanics, for $\Psi[P(x,t)] = P(x,t)$ and $\Omega[P(x,t)] = \mu[P(x,t)]^{\mu-1}$, where μ represents a real number related to the entropic index through $\mu = 2 - q$. It should be mentioned that a large variety of NLFPEs, such as the one related to nonextensive statistical mechanics, the one in the general form of Equation (7), or even those presenting nonhomogeneous diffusion coefficients in the nonlinear diffusion term, have been derived in the literature by generalizing standard procedures applied to the linear FPE [14–18], e.g., from approximations in the master equation [34,36–39] or from a Langevin approach considering a multiplicative noise [40–45].

Almost two decades ago, NLFPEs presenting more than one diffusive term appeared in the literature [36,46–52], and a special interest was given to a concrete physical application,

namely, a system of interacting vortices, which is currently used as a suitable model for type II superconductors, that exhibited such a behavior [47–52]. A general discussion of NLFPEs with two diffusive contributions was presented in Ref. [33], where one can be identified in Equation (7),

$$\Omega[P(x,t)] = \frac{D_1}{D}\,\Omega_1[P(x,t)] + \frac{D_2}{D}\,\Omega_2[P(x,t)]\,. \tag{9}$$

Next, we discuss the H-theorem associated with Equation (7), leading to a direct connection between this equation and entropic forms; we also comment on the above case of two diffusive contributions.

2.1. Generalized Forms of the H-Theorem from NLFPEs

The H-theorem represents one of the most important results of nonequilibrium statistical mechanics since it ensures that after a sufficiently long time, the associated system will reach an equilibrium state. In standard nonequilibrium statistical mechanics, it is usually proven by considering the BG entropy S_{BG} and making use of an equation that describes the time evolution of the associated probability density, such as the Boltzmann probability density, linear FPE (in the case of continuous probabilities), or the master equation (in the case of discrete probabilities) [13–17]. To our knowledge, the first proof of an H-theorem making use of a NLFPE appeared in the literature more than 30 years ago [53]. After that, proofs were extended by many authors in such a way as to cover generalized entropic forms and their relationships to NLFPEs (see, e.g., Refs. [21,24–35]); below, we closely follow those carried in Refs. [30–33].

In the case of a system under a confining external potential $\phi(x)$ (from which one obtains the external force appearing in Equation (7), $A(x) = -d\phi(x)/dx$), the H-theorem corresponds to a well-defined sign for the time derivative of the free-energy functional,

$$F[P] = U[P] - \theta S[P]\,; \qquad U[P] = \int_{-\infty}^{\infty} dx\,\phi(x)P(x,t)\,, \tag{10}$$

with θ denoting a positive parameter with dimensions of temperature. Moreover, the entropy may be considered in the general form [30–33],

$$S[P] = k \int_{-\infty}^{\infty} dx\,g[P(x,t)]\,; \quad g(0) = g(1) = 0\,; \quad \frac{d^2g}{dP^2} \leq 0\,, \tag{11}$$

where k represents a positive constant with entropy dimensions, whereas the functional $g[P(x,t)]$ should be at least twice differentiable. Furthermore, the conditions that ensure the normalizability of $P(x,t)$ for all times (cf. Equation (8)) are also used in the proof of the H-theorem. Considering $D = k\theta$, the H-theorem may be achieved by imposing the condition [30–33],

$$-\frac{d^2g[P]}{dP^2} = \frac{\Omega[P]}{\Psi[P]}\,, \tag{12}$$

which relates the entropic form to a certain time evolution described by the two functionals of Equation (7). Particular entropic forms and their associated NLFPEs were explored in Ref. [30], whereas families of NLFPEs (those characterized by the same ratio $\Omega[P]/\Psi[P]$) were studied in Ref. [32].

One should mention that the relationship of Equation (12) is applicable for a single diffusive contribution, a linear internal-energy definition (as in Equation (10)), and for a constant diffusion coefficient, as in Equation (7). Extensions of the H-theorem have been achieved, disregarding these restrictions separately, by considering: (i) two diffusive contributions, as in Equation (9) [33] (to be discussed next); (ii) a nonlinear internal-energy definition (see Refs. [31,34]). In this case, the H-theorem is fulfilled through a slight mod-

ification in the NLFPE of Equation (7), so that besides Equation (12), an extra equation appears concerning the nonlinear functional appearing in the internal energy definition; (iii) a diffusion coefficient dependent on the position, so that one needs to modify the free energy of Equation (10) [54]. Recent studies have discussed physical systems within the context of nonextensive statistical mechanics, characterized by a varying entropic index q, such as a modified cosmological scenario [55], and the phenomenon of quantum mixing, i.e., the superposition of particle states with different masses [56]. This is certainly an interesting novelty, not contemplated by Equation (7), which recovers the NLFPE introduced in Refs. [22,23] and is associated with nonextensive statistical mechanics for $\Psi[P(x,t)] = P(x,t)$ and $\Omega[P(x,t)] = (2-q)[P(x,t)]^{1-q}$, where q represents a real number. The solution of this NLFPE is the so-called q-Gaussian distribution (cf. Equation (4)), which was shown to cover a large number of experimental verifications within the context of anomalous diffusion phenomena, for which the value of q may vary for different systems [4–8]. An NLFPE with a variable index q, its solution, as well as a possible H-theorem, require a particular nontrivial analysis, which, to our knowledge, has not been addressed at present.

A detailed proof of the H-theorem in the case of two diffusive contributions, such as in Equation (9), was presented in Ref. [33]; briefly, one replaces the free energy functional of Equation (10) with

$$F[P] = U[P] - \theta_1 S_1[P] - \theta_2 S_2[P] \; ; \qquad U[P] = \int\limits_{-\infty}^{\infty} dx \, \phi(x) P(x,t) \, , \qquad (13)$$

where θ_1 and θ_2 denote positive parameters with dimensions of temperature. Similarly to Equation (11), one defines

$$S_i[P] = k \int\limits_{-\infty}^{\infty} dx \, g_i[P(x,t)] \; ; \quad g_i(0) = g_i(1) = 0 \; ; \quad \frac{d^2 g_i}{dP^2} \leq 0 \; ; \quad (i = 1,2). \qquad (14)$$

In such a case, it is sufficient to impose the conditions

$$D_1 = k\theta_1 \; ; \qquad D_2 = k\theta_2 \, , \qquad (15)$$

as well as

$$-\frac{d^2 g_1[P]}{dP^2} = \frac{\Omega_1[P]}{\Psi[P]} \; ; \qquad -\frac{d^2 g_2[P]}{dP^2} = \frac{\Omega_2[P]}{\Psi[P]} \, , \qquad (16)$$

extending the condition of Equation (12) for two diffusion contributions.

From now on, we restrict our analysis to a single diffusion contribution, as in Equation (7), and their associated free energy functional (cf. Equation (10)), entropy functional (cf. Equation (11)), as well as the relationship in Equation (12). In the discussion above, this situation occurs whenever a diffusion coefficient is much larger than the other one (e.g., $D_2 \gg D_1$) so that one may neglect the effects of the smaller contribution. As a typical example, one should mention a system of interacting vortices currently used as a suitable model for type II superconductors, for which, in typical cases, one of the diffusion coefficients has been shown to be at least 10^4 times larger than the other one [49].

2.2. Equilibrium Distribution

Now, we briefly work out the stationary-state (i.e., time-independent) solution of Equation (7), as well as the equilibrium distribution that results from an extremization procedure of the entropic functional in Equation (11) (a detailed analysis of these procedures may be found in Ref. [30])). As usual, the Lagrange parameters of this later approach will be defined appropriately so that these two results coincide; based on this, in the calculations that follow, we refer to an equilibrium state, described by a distribution $P_{eq}(x)$.

First, let us obtain the time-independent distribution of Equation (7); for this purpose, we rewrite it in the form of a continuity equation,

$$\frac{\partial P(x,t)}{\partial t} = -\frac{\partial J(x,t)}{\partial x} \, , \tag{17}$$

where the probability current density is given by

$$J(x,t) = A(x)\Psi[P(x,t)] - D\Omega[P(x,t)]\frac{\partial P(x,t)}{\partial x} \, . \tag{18}$$

The solution $P_{\text{eq}}(x)$ is obtained by setting $J_{\text{eq}}(x) = 0$ (as required by conservation of probability [30]), so that

$$J_{\text{eq}}(x) = A(x)\Psi[P_{\text{eq}}(x)] - D\Omega[P_{\text{eq}}(x)]\frac{dP_{\text{eq}}}{dx} = 0 \, , \tag{19}$$

which may still be written in the form

$$A(x) = D\frac{\Omega[P_{\text{eq}}(x)]}{\Psi[P_{\text{eq}}(x)]}\frac{dP_{\text{eq}}}{dx} \, . \tag{20}$$

Integrating the equation above over x and remembering that the external force was defined as $A(x) = -d\phi(x)/dx$, one obtains

$$\phi_0 - \phi(x) = D\int_{x_0}^{x} dx \, \frac{\Omega[P_{\text{eq}}(x)]}{\Psi[P_{\text{eq}}(x)]}\frac{dP_{\text{eq}}}{dx} = D\int_{P_{\text{eq}}(x_0)}^{P_{\text{eq}}(x)} \frac{\Omega[P_{\text{eq}}(x')]}{\Psi[P_{\text{eq}}(x')]}dP_{\text{eq}}(x') \, , \tag{21}$$

where $\phi_0 \equiv \phi(x_0)$. Now, one uses the relationship in Equation (12), and, performing the integration, can further obtain

$$D\frac{dg[P]}{dP}\bigg|_{P=P_{\text{eq}}(x)} = \phi(x) + C_1 \, , \tag{22}$$

with C_1 being a constant.

Next, we extremize the entropic functional of Equation (11) with respect to the probability under the constraints of probability normalization and an internal energy definition following Equation (10). For this, we introduce the functional

$$\mathcal{I} = \frac{S[P]}{k} + \alpha\left(1 - \int_{-\infty}^{\infty} dx \, P(x,t)\right) + \beta\left(U - \int_{-\infty}^{\infty} dx \, \phi(x)P(x,t)\right) \, , \tag{23}$$

where α and β are Lagrange multipliers. Hence, the extremization $(\delta\mathcal{I})/(\delta P)|_{P=P_{\text{eq}}(x)} = 0$ leads to

$$\frac{dg[P]}{dP}\bigg|_{P=P_{\text{eq}}(x)} - \alpha - \beta\,\phi(x) = 0 \, . \tag{24}$$

One notices that Equations (22) and (24), which result from the stationary-state solution of Equation (7) and the extremization of the entropic functional of Equation (11), respectively, coincide if one chooses the Lagrange multipliers $\alpha = C_1$ and $\beta = 1/D$.

2.3. Carnot Cycle for a General Entropic Form $S(P)$

Considering non-additive entropies, the Carnot cycle was shown to hold for the equilibrium entropy S_{2-q} (in the case that $q = 0$) and its corresponding thermodynamically conjugated parameter θ [49], which is used to define an infinitesimal heat-like quantity $\delta Q = \theta dS_2$ [50–52]; the physical system under investigation was a model for type II superconductors characterized by interacting vortices. Later on, the Carnot cycle was shown to be valid for any system of particles interacting repulsively through short-range potentials,

whose equilibrium distributions are compact q-Gaussian distributions (characterized by a cutoff) and can be described by the entropy S_{2-q} (for $q < 1$), extending the above-mentioned proof for $q = 0$ [57]. One should notice that, in the illustrations concerning the Tsallis entropy considered herein, the equilibrium distribution and the entropic form are related by means of the simple change $q \leftrightarrow (2 - q)$ [58]. This appears to be a direct consequence of a linear internal energy definition, such as the one in Equation (10), which was considered in Refs. [50–52,57]; this subtle property will be discussed in detail for the case of discrete probabilities (see the next section). Herein, we show that the Carnot cycle holds for general entropic forms, as defined in Equation (11). For this, we assume that the usual (i.e., very common) conditions apply for the system under investigation, as described below.

(i) The equilibrium distribution $P_{\text{eq}}(x)$, which maximizes the entropic functional of Equation (11) (as shown in Section 2.2), exists and leads to the entropy $S[P_{\text{eq}}]$ and internal energy $U[P_{\text{eq}}]$ at equilibrium. Both $S[P_{\text{eq}}]$ and $U[P_{\text{eq}}]$ are state functions in the sense that

$$\int_a^b dS[P_{\text{eq}}] = S[P_{\text{eq}}^{(b)}] - S[P_{\text{eq}}^{(a)}] = S_b - S_a \; ; \tag{25}$$

$$\int_a^b dU[P_{\text{eq}}] = U[P_{\text{eq}}^{(b)}] - U[P_{\text{eq}}^{(a)}] = U_b - U_a \; , \tag{26}$$

where a and b denote arbitrary equilibrium thermodynamic states. We introduce the short notations $S_a \equiv S[P_{\text{eq}}^{(a)}]$ and $U_a \equiv U[P_{\text{eq}}^{(a)}]$ (similar notations holding for state b). Hence, one may define an infinitesimal type of heat, $\delta Q = \theta dS$, where θ represents the positive parameter with the temperature dimensions introduced in Equation (10).

(ii) The system under investigation can, in principle, perform work in several ways, leading to an infinitesimal contribution, $\delta W = \sum_i \sigma_i d\alpha_i$, where for each contribution i, σ_i and α_i are pairs of thermodynamically conjugate variables. However, for simplicity, we restrict the following analysis to a single "external field", σ, and its conjugate, α. The parameter α is also considered a state function following conditions similar to those in Equations (25) and (26).

(iii) Using the quantities defined in (i) and (ii), we formulate the equivalent to the first law,

$$dU = \delta Q + \delta W = \theta dS + \sigma d\alpha \; , \tag{27}$$

where δW corresponds to the work carried out by the external field σ *on* the system.

(iv) Equation (27) implies that $U = U(S, \alpha)$; we assume that $U(S, \alpha)$ is invertible, yielding $S = S(U, \alpha)$ (with the same condition holding for $S(U, \alpha)$), leading to

$$dS = \frac{1}{\theta} dU - \frac{\sigma}{\theta} d\alpha \; . \tag{28}$$

From Equation (27) (or equivalently, from Equation (28)) one obtains the fundamental relationship

$$\theta = \left(\frac{\partial U}{\partial S} \right)_\alpha \; , \tag{29}$$

as well as the equation of state

$$\sigma = \left(\frac{\partial U}{\partial \alpha} \right)_S \; . \tag{30}$$

Let us now consider four equilibrium states, yielding a Carnot cycle $a \to b \to c \to d \to a$, defined by two isothermal (constant θ) transformations: $a \to b$ at a temperature θ_1 and $c \to d$ at a temperature θ_2, with $\theta_1 > \theta_2$. These transformations are intercalated by two adiabatic transformations (where S is constant) ($b \to c$ and $d \to a$),

so that $\Delta S_{bc} = \Delta S_{da} = 0$. Considering that both S and U are state functions (according to Equations (25) and (26)), and using Equation (27), one has for the whole cycle

$$\Delta S = \Delta S_{ab} + \Delta S_{cd} = 0 \quad \Rightarrow \quad \Delta S_{ab} = -\Delta S_{cd} ; \tag{31}$$

$$\Delta U = (W_{ab} + Q_{ab}) + W_{bc} + (W_{cd} + Q_{cd}) + W_{da} = 0 . \tag{32}$$

From this later equation, one can obtain that the total work W carried out *on* the system is given by

$$W = W_{ab} + W_{bc} + W_{cd} + W_{da} = -(Q_{ab} + Q_{cd}) = -\mathcal{W} , \tag{33}$$

where we have defined $\mathcal{W}$ ($\mathcal{W} > 0$) as the total work completed *by* the system. For the two isothermal transformations, one has

$$Q_{ab} = \theta_1 \int_a^b dS = \theta_1(S_b - S_a) = \theta_1 \Delta S_{ab} ; \tag{34}$$

$$Q_{cd} = \theta_2 \int_c^d dS = \theta_2(S_d - S_c) = \theta_2 \Delta S_{cd} , \tag{35}$$

and using Equation (31), one obtains that

$$\frac{Q_{ab}}{Q_{cd}} = -\frac{\theta_1}{\theta_2} , \tag{36}$$

showing that Q_{ab} and Q_{cd} present different signs. Therefore, as usually considered for a Carnot Cycle, we assume that $Q_{ab} > 0$ and $Q_{cd} < 0$, i.e., heat gets into (out of) the system along the isothermal transformation at temperature θ_1 (θ_2). Let us now redefine $Q_1 = Q_{ab}$ and $Q_2 = |Q_{cd}|$, leading to the fundamental relationship for the Carnot Cycle,

$$\frac{Q_1}{Q_2} = \frac{\theta_1}{\theta_2} , \tag{37}$$

as well as to the conservation of energy along the whole cycle, which can be expressed as

$$Q_1 = \mathcal{W} + Q_2 , \tag{38}$$

Tn these two equations above, all quantities are positive. Consequently, one has the celebrated efficiency for the Carnot cycle,

$$\eta = \frac{\mathcal{W}}{Q_1} = \frac{Q_1 - Q_2}{Q_1} = 1 - \frac{\theta_2}{\theta_1} \qquad (0 \le \eta \le 1). \tag{39}$$

Therefore, we have shown that the Carnot cycle, which represents a fundamental thermodynamical process, holds for general entropic forms as defined in Equation (11) and for the internal energy of Equation (10) under the usual requirements for its equilibrium state. Within the framework of non-additive entropies, the most serious restrictions are: (a) at equilibrium, $S \equiv S[P_{eq}]$ and $U \equiv U[P_{eq}]$, so that one must express $S = S(U, \{\alpha_i\})$, where $\{\alpha_i\}$ represents state functions, whose small changes define infinitesimal work contributions; (b) the entropy $S = S(U, \{\alpha_i\})$ should be invertible, leading to the possibility of expressing $U = U(S, \{\alpha_i\})$. Only if these conditions are satisfied may one be able to calculate an effective temperature in two different (but equivalent) ways,

$$\theta = \left(\frac{\partial U}{\partial S}\right)_{\{\alpha_i\}} \quad \text{and} \quad \frac{1}{\theta} = \left(\frac{\partial S}{\partial U}\right)_{\{\alpha_i\}} , \tag{40}$$

using Equations (27) and (28), respectively.

To our knowledge, at present, the only successful proofs of a Carnot cycle for non-additive entropies have been carried for the equilibrium entropy S_{2-q} (in the case that $q = 0$) and its corresponding thermodynamically conjugate parameter θ in an application of a system of type II superconducting vortices [49–52], as well as an extension for the equilibrium entropy S_{2-q} (for $q < 1$) associated with a system of particles interacting repulsively through short-range potentials, whose equilibrium distributions are compact q-Gaussian distributions (characterized by a cutoff) [57]. The proof above opens the way for the validation of the Carnot cycle considering other non-additive entropic forms available in the literature.

3. Discrete Set of Probabilities: H-Theorem and Equilibrium Solutions for Generalized Entropies

We now consider a system characterized by discrete states, with associated probabilities $\{P_i(t)\}$ ($i = 1, 2, \cdots, W$), where $P_i(t)$ represents the probability of finding the system on a state i at time t, following the normalization condition

$$\sum_{i=1}^{W} P_i(t) = 1 \qquad (\forall t). \tag{41}$$

For discrete probabilities, an H-theorem was proven for $S_{\mathrm{BG}}(\{P_i\})$ (cf. Equation (3)) in both cases of an isolated system (expressed by $dS_{\mathrm{BG}}/dt \geq 0$) and a system in contact with a heat bath at a temperature T, where one can consider the time-derivative of the free-energy functional to be

$$F = U - TS_{\mathrm{BG}} \; ; \qquad U = \sum_i \varepsilon_i P_i \, , \tag{42}$$

leading to $dF/dt \leq 0$ (see, e.g., Ref. [13]).

Recently, there has been a growing interest in generalized entropic forms for an appropriate description of complex systems [4–11]. In most cases, these entropic forms may be written as

$$S[\{P_i\}] = k \sum_{i=1}^{W} g[P_i] \; ; \quad g(0) = g(1) = 0 \, , \tag{43}$$

where the functional $g[P_i]$ should be concave and at least twice-differentiable, i.e., $(d^2 g/dP_i^2) \leq 0$ ($\forall i$). Moreover, the free-energy functional is considered similar to the one in Equation (42),

$$F = U - \theta S \; ; \qquad U = \sum_i \varepsilon_i P_i \, , \tag{44}$$

where θ represents a positive quantity with dimensions of temperature, which in some cases may coincide with the usual absolute temperature T, although it may present a different concept in some complex systems (see, e.g., Refs. [49–52]).

The extremization of the entropic form of Equation (43), considering the constraints for the probability normalization of Equation (41) (with the Lagrange multiplier α) and the internal energy definition of Equation (44) (with its corresponding Lagrange multiplier β), leads to the following equation for the equilibrium distribution P_i^{eq}:

$$g'[P_i^{\mathrm{eq}}] - \alpha - \beta \varepsilon_i = 0 \, , \tag{45}$$

where we have defined

$$g'(X) \equiv \left. \frac{dg[P]}{dP} \right|_{P=X} . \tag{46}$$

One should notice that the functional $g'[P_i^{\mathrm{eq}}]$ is invertible, since $g[P_i]$ is concave; however, in some cases, one may deal with a transcendental equation for P_i^{eq}. The procedure above applied to BG entropy (cf. Equation (3)) yields the well-known Boltzmann weight [13,14];

let us now illustrate this method by considering the Tsallis entropy (cf. Equation (2)), for which

$$g'[P_i^{\text{eq}}] = -\frac{q}{q-1}\left(P_i^{\text{eq}}\right)^{q-1} . \tag{47}$$

Substituting the result above into Equation (45) and using Equation (41), one obtains the distribution

$$P_i^{\text{Equation (1)}} = \frac{1}{Z_q^{(1)}}[1 - (q-1)\beta^{(1)}\varepsilon_i]_+^{1/(q-1)} , \tag{48}$$

where $[y]_+ = y$ for $y > 0$ and is zero otherwise; the superscript refers to the extremization of the entropy S_q under the internal energy definition with a linear dependence on the set of probabilities, as in Equation (44), which is also known as first formulation [4]. It is important to notice that the equilibrium distribution coming out of the extremization procedure of any entropic form is directly related to the imposed constraints (see, e.g., Refs. [58–62] for detailed discussions on the role of constraints in nonextensive statistical mechanics); herein, we adopt the linear internal energy definition due to its simplicity for proving the H-theorem. However, the most common form for the equilibrium distribution, usually known as the Tsallis distribribution, is obtained from an internal energy definition with a nonlinear dependence on the set of probabilities $\{P_i\}$, i.e., a power-like P_i^q, leading to [4]

$$P_i^{\text{eq}} = \frac{1}{Z_q}[1 - (1-q)\beta\varepsilon_i]_+^{1/(1-q)} , \tag{49}$$

which will be considered the equilibrium distribution from now on. Notice that Equations (48) and (49) may be converted into one another by means of the simple change $q \leftrightarrow (2-q)$ [58]. In fact, the distribution of Equation (49) may also be derived from the extremization of S_{2-q} in Equation (45). Since in the thermodynamic application that follows, namely, the third law of thermodynamics for the Tsallis entropy, we consider an equilibrium state described by Equation (49), the corresponding entropic form can be written as S_{2-q} instead of S_q.

Below, we outline the proof of an H-theorem for general entropic forms, written as in Equation (43), which may be achieved by making use of a master equation [63],

$$\frac{\partial P_i(t)}{\partial t} = \sum_j [P_j(t)w_{ji}(t) - P_i(t)w_{ij}(t)] . \tag{50}$$

As usual, $w_{ij}(t)$ represents the probability transition rate associated with a transition from state i to state j (i.e., $w_{ij}\Delta t$ is the probability that a transition from states i to j occurs during the time interval $t \rightarrow t + \Delta t$). Herein, we will consider the most general out-of-equilibrium situation characterized by time-dependent probability transition rates, i.e., $P_i(t)w_{ij}(t) \neq P_j(t)w_{ji}(t)$. These quantities will become time-independent only at equilibrium, where the detailed balance condition holds,

$$P_i^{\text{eq}}W_{ij} = P_j^{\text{eq}}W_{ji} \qquad [W_{ij} = \lim_{t\to\infty} w_{ij}(t)] . \tag{51}$$

The procedure below essentially extends the proof of the H-theorem for BG entropy in Equation (3) for an isolated system, as well as for a system in contact with a heat bath at a temperature T, where one considers the time derivative of the free-energy functional in Equation (42) (see, e.g., Ref. [13]). Following this, we start by taking the time derivative of the entropic form in Equation (43),

$$\frac{dS}{dt} = k\frac{d}{dt}\sum_i g[P_i(t)] = k\sum_i \frac{dg}{dP_i}\frac{\partial P_i}{\partial t} , \tag{52}$$

and using Equation (50), one obtains

$$\frac{dS}{dt} = k \sum_{i,j} \frac{dg}{dP_i} [P_j(t)w_{ji}(t) - P_i(t)w_{ij}(t)] . \tag{53}$$

Interchanging $i \leftrightarrow j$ and adding the resulting equation with Equation (53), one obtains

$$\frac{dS}{dt} = \frac{k}{2} \sum_{i,j} [g'(P_i) - g'(P_j)][P_j(t)w_{ji}(t) - P_i(t)w_{ij}(t)] , \tag{54}$$

where we have used the definition of Equation (46). In a similar way, one can express the time derivative of the internal energy of Equation (44) as

$$\frac{dU}{dt} = \frac{1}{2} \sum_{i,j} [\varepsilon_i - \varepsilon_j][P_j(t)w_{ji}(t) - P_i(t)w_{ij}(t)] . \tag{55}$$

Now, using Equations (44), (54) and (55), one obtains the time derivative of the free-energy functional,

$$\frac{dF}{dt} = \frac{1}{2} \sum_{i,j} \{\varepsilon_i - \varepsilon_j - k\theta[g'(P_i) - g'(P_j)]\}[P_j(t)w_{ji}(t) - P_i(t)w_{ij}(t)] . \tag{56}$$

General proofs of the H-theorem have been carried out in Ref. [63] through algebraic manipulations of the equations above (e.g., making use of the property that $g[X]$ is concave, leading to a monotonically decreasing first derivative $g'[X]$) for two typical situations, namely, an isolated system (for which the H-theorem is expressed by $(dS/dt) \geq 0$) and a system in contact with a thermal bath)for which the H-theorem is expressed by $(dF/dt) \leq 0$. Moreover, these proofs apply to very general out-of-equilibrium situations (along which $P_i(t)w_{ij}(t) \neq P_j(t)w_{ji}(t)$) and are characterized by non-symmetric probability transition rates ($w_{ij}(t) \neq w_{ji}(t)$). Additional interesting results were achieved in Ref. [64], where the quantities above were associated with the phenomenon of entropy production for irreversible processes. Mathematically, this result may be expressed by writing the entropy time rate in the form [16,65,66]

$$\frac{d}{dt}S[P] = \Pi - \Phi, \tag{57}$$

where one can identify the contributions of the entropy production Π and entropy flux Φ. These two concepts were extended to general entropic forms, making use of general NLF-PEs [67] when dealing with continuous probabilities, as well as of a master equation [64] for discrete probabilities. Comparing the quantities above with

$$\frac{dF}{dt} = \frac{dU}{dt} - \theta \frac{dS}{dt} , \tag{58}$$

one identifies

$$\Pi = -\frac{1}{\theta}\frac{dF}{dt} ; \qquad \Phi = -\frac{1}{\theta}\frac{dU}{dt} , \tag{59}$$

so that, for a non-negative entropy production contribution, the H-theorem implies $\Pi \geq 0$, as expected [16,65,66]. All these results were illustrated for the particular cases of BG (cf. Equation (3)) and Tsallis (cf. Equation (2)) entropies [63,64].

Third Law of Thermodynamics for Generalized Entropies

Herein, we assume that the following typical conditions apply.

(i) There is a positive temperature-like parameter θ, associated with the Lagrange multiplier β, such that $\beta = 1/(k\theta)$. It is important to mention that the following analysis also applies for the absolute temperature T of standard thermodynamics.

(ii) There is a discrete non-negative energy spectrum $\{\varepsilon_i\}$, i.e., $\varepsilon_i \geq 0$ $(i = 1, 2, \cdots, W)$.

(iii) There is a non-degenerate ground state characterized by the energy $\varepsilon_1 \geq 0$.

(iv) There is a gap between the energies of the ground and first-excited states, $\Delta = \varepsilon_2 - \varepsilon_1 > 0$.

(v) As the temperature parameter θ decreases (or equivalently, as β increases), the probabilities $\{P_i\}$ associated with the lowest-energy states become larger.

Next, we illustrate the third law of thermodynamics for the entropy S_q of Equation (2) and its corresponding equilibrium distribution in Equation (49). In this case, for convenience, we set $\varepsilon_1 = 0$. Notice that the requirement for real probabilities in Equation (49) implies the condition

$$(1 - q)\beta\varepsilon_i \leq 1 \qquad (\forall i). \tag{60}$$

Whenever the inequality above is violated, one has $P_i = 0$, i.e., the corresponding energy level may not be occupied. For the third law of thermodynamics applied under the above requirements, two distinct cases should be considered, namely, $q \geq 1$ and $q < 1$, as discussed below.

Case 1: $q \geq 1$.

The condition in Equation (60) is always fulfilled, so that for $\beta \to \infty$, the system should reach a pure state, characterized by $P_1 = 1$ and leading to $S_q(1) = S_{2-q}(1) = 0$.

Case 2: $q < 1$.

The condition in Equation (60) is not always fulfilled, and it may be violated for certain ranges of β, values of q, and energies ε_i, for which $P_i = 0$. Now, we concentrate on the two lowest energy values, separated by the gap $\Delta = \varepsilon_2 - \varepsilon_1$, and define a temperature θ^* through $k\theta^* = (1 - q)\Delta$. At precisely the effective temperature θ^*, only these two energy levels are occupied with the respective probabilities P_2 and P_1 such that $P_1 + P_2 = 1$. Then, for a slightly lower temperature, one has $P_2 = 0$ and $P_1 = 1$, leading to $S_q(1) = S_{2-q}(1) = 0$. Notice that $k\theta^* \leq \Delta$ (for $0 \leq q < 1$), whereas $k\theta^* = (1 + |q|)\Delta$, yielding $k\theta^* > \Delta$ (for $q < 0$).
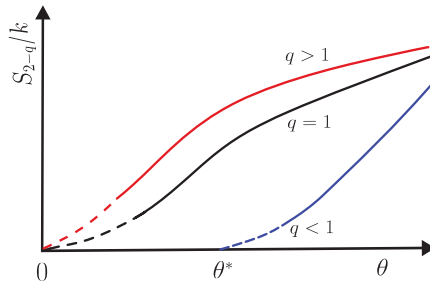
Therefore, the entropy S_{2-q} becomes zero for a positive value of temperature, $\theta^* = (1 - q)\Delta/k > 0$, so that the third law is satisfied at (and below) this temperature value. In this way, the effective temperature θ^* for $q < 1$ plays a role similar to $\theta = 0$ for $q \geq 1$; thus, in the former case, all thermodynamic quantities should be analyzed in the limit $\theta \to \theta^*$ (from above). The vanishing of S_{2-q} at an effective temperature $\theta^* > 0$ for $q < 1$ is directly related to violations in the condition of Equation (60), i.e., to the existence of a cutoff in the set of probabilities $\{P_i\}$. Qualitative plots of the entropy S_{2-q} versus the effective temperature θ are presented in Figure 1; in each case, the approach to the limits $\theta \to 0$ $(q \geq 1)$ or $\theta \to \theta^*$ $(q < 1)$ are shown in dashed lines since the corresponding slopes may depend on the system under investigation. One should mention that previous studies of the third law for the Tsallis entropy [68,69] did not take into account the effective temperature θ^* for $q < 1$, leading to misinterpretations of the third law of thermodynamics.

Below, we formulate the third law for the entropy S_q, as well as for nonadditive entropies in general.

Third law of thermodynamics for the entropy S_q:

Consider a system described by: (a) a positive effective temperature θ (for certain values of q, this temperature may coincide with the absolute temperature T of standard thermodynamics) thermodynamically conjugated to the entropy S_{q^*} (typically $q^* = 2 - q$); (b) a discrete non-negative energy spectrum $\{\varepsilon_i\}$; (c) a non-degenerate ground state with energy $\varepsilon_1 = 0$; and (d) a gap between the energies of the ground and the first-excited states, $\Delta = \varepsilon_2$. Under these conditions, the entropy S_{q^*} becomes zero for $\theta \to 0$ $(q \geq 1)$ or for $\theta \to \theta^*$ $(q < 1)$, where $\theta^* = (1 - q)\Delta/k > 0$."

For a general nonadditive entropic form, as defined in Equation (43) and possibly characterized by a set of indices $\{\alpha, \gamma, \cdots\}$ typical of nonadditive entropic forms [9–11], one should add an extra condition in the above statement concerning possible combinations of θ, energy values $\{\varepsilon_i\}$, and the indices $\{\alpha, \gamma, \cdots\}$, for which there may be restrictions on the probabilities $\{P_i\}$, such as a cutoff, yielding levels with $P_i = 0$. In this way, we formulate the third law for a general nonadditive entropy below.

Figure 1. The entropy S_{2-q} is exhibited versus an effective temperature θ (positive quantity with dimensions of temperature) in three distinct cases, namely, $q > 1$ (red curve), $q = 1$ (black curve), and $q < 1$ (blue curve). The entropy S_{2-q} becomes zero for $\theta \to 0$ ($q \geq 1$), whereas $S_{2-q} \to 0$ for $\theta \to \theta^* > 0$ ($q < 1$) (see text). In the latter case, the vanishing of S_{2-q} at an effective temperature $\theta^* > 0$ is directly related to violations in the condition of Equation (60), i.e., to the existence of a cutoff in the set of probabilities $\{P_i\}$. In these curves, the approaches $S_{2-q} \to 0$ are shown in dashed lines since the corresponding slopes may depend on the system under study.

Third law of thermodynamics for a general nonadditive entropy $S_{\alpha, \gamma, \cdots}$:

Consider a system described by: (a) a positive effective temperature, θ, thermodynamically conjugated to the entropy $S_{\alpha, \gamma, \cdots}$ (for certain values of the indices $\{\alpha, \gamma, \cdots\}$, this temperature may coincide with the absolute temperature T of standard thermodynamics); (b) a discrete non-negative energy spectrum $\{\varepsilon_i\}$; (c) a non-degenerate ground state with energy $\varepsilon_1 \geq 0$; (d) a gap between the energies of the ground and the first-excited states, $\Delta = \varepsilon_2 - \varepsilon_1 > 0$; and (e) combinations of θ, the energy values $\{\varepsilon_i\}$, and the indices $\{\alpha, \gamma, \cdots\}$, for which there are restrictions on the probabilities $\{P_i\}$, such as a cutoff, yielding levels with $P_i = 0$. Under these conditions, the entropy $S_{\alpha, \gamma, \cdots}$ becomes zero for $\theta \to \theta^*$ (with $\theta^* > 0$), where this threshold should depend on Δ and the parameters $\{\alpha, \gamma, \cdots\}$ that define the entropy; whenever the restrictions described in (e) do not apply, $S_{\alpha, \gamma, \cdots}$ becomes zero for $\theta \to 0$".

4. Discussion and Conclusions

We have discussed some basic aspects related to non-additive entropies, considering their time evolution in the cases of continuous and discrete probabilities, described by nonlinear Fokker–Planck and master equations, respectively. In both cases, forms of the H-theorem were proven, connecting functionals of the probabilities appearing in these equations with those of the entropic forms. A particular emphasis was given to their equilibrium-state distributions, showing that those obtained from the corresponding evolution equations coincide with those derived form the extremization of the associated entropic forms.

Considering the equilibrium state, we have shown that a Carnot cycle holds for a general entropic form under standard thermodynamic conditions. Within the framework of non-additive entropies, the most serious restrictions for the validity of the Carnot cycle are as follows: (a) the equilibrium functionals $S \equiv S[P_{eq}]$ and $U \equiv U[P_{eq}]$ should allow one to express $S = S(U, \{\alpha_i\})$, where $\{\alpha_i\}$ represents state functions, whose small changes define infinitesimal work contributions; (b) the entropy $S = S(U, \{\alpha_i\})$ should be invertible,

leading to the possibility of expressing $U = U(S, \{\alpha_i\})$. Only if these conditions are satisfied may one be able to calculate an effective temperature parameter, which is fundamental for the Carnot cycle. It is possible that these procedures may not be feasible for some of the entropic forms introduced in the literature (see, e.g., a comprehensive list in Ref. [9]). To our knowledge, at present, the only successful proofs of a Carnot cycle for non-additive entropies have been carried out for the equilibrium entropy S_{2-q} (in the case for which $q = 0$) and its corresponding thermodynamically conjugate parameter θ in an application of a system of type II superconducting vortices [49–52], as well as an extension for the equilibrium entropy S_{2-q} (for $q < 1$), associated with a system of particles interacting repulsively through short-range potentials, whose equilibrium distributions are compact q-Gaussian distributions (characterized by a cutoff) [57].

In the case of discrete probabilities, we have discussed how the third law of thermodynamics should apply to equilibrium non-additive entropic forms in general. Considering an equilibrium entropic form S and its thermodynamically conjugate parameter θ, one has two situations to be analyzed, which are as follows: (i) combinations of θ, energy values $\{\varepsilon_i\}$, and possible entropic indices characteristic of the generalization, for which there are restrictions on the probabilities $\{P_i\}$, such as a cutoff, which implies levels with $P_i = 0$; (ii) cases where the combinations mentioned in (i) do not lead to restrictions on the probabilities $\{P_i\}$. If there are no restrictions, one must have $S \to 0$ when $\theta \to 0$; whenever there are restrictions on the set of probabilities (such as a possible cutoff), one should have $S \to 0$ for $\theta \to \theta^*$, where $\theta^* > 0$.

The physical consequences, and particularly, the fact that the equilibrium-state distributions obtained from the corresponding evolution equations (for both continuous and discrete probabilities) coincide with those obtained from the extremization of the entropic form, become very relevant for the study of complex systems. Moreover, the validity of a Carnot cycle and a formulation of the third law of thermodynamics for general entropic forms, under standard thermodynamic requirements, opens the path for consistent thermodynamic frameworks in the context of generalized (or non-additive) entropic forms.

References

1. Nicolis, G.; Nicolis, C. *Foundations of Complex Systems: Nonlinear Dynamics, Statistical Physics, Information and Prediction*; World Scientific Publishing Co. Pte. Ltd.: Singapore, 2007.
2. Yoshida, Z. *Nonlinear Science: The Challenge of Complex Systems*; Springer: New York, NY, USA, 2010.
3. Ngai, K.L. *Relaxation and Diffusion in Complex Systems*; Springer: New York, NY, USA, 2011.
4. Tsallis, C. *Introduction to Nonextensive Statistical Mechanics: Approaching a Complex World*, 2nd ed.; Springer: New York, NY, USA, 2023.
5. Tsallis, C. An introduction to nonadditive entropies and a thermostatistical approach to inanimate and living matter. *Contemp. Phys.* **2014**, *55*, 179. [CrossRef]
6. Tsallis, C. Beyond Boltzmann-Gibbs-Shannon in physics and elsewhere. *Entropy* **2019**, *21*, 696. [CrossRef]
7. Rapisarda, A.; Thurner, S.; Tsallis, C. Nonadditive entropies and complex systems. *Entropy* **2019**, *21*, 538. [CrossRef] [PubMed]
8. Tsallis, C. Senses along Which the Entropy S_q Is Unique. *Entropy* **2023**, *25*, 743. [CrossRef] [PubMed]
9. Hanel, R.; Thurner, S. A comprehensive classification of complex statistical systems and an axiomatic derivation of their entropy and distribution functions. *Europhys. Lett.* **2011**, *93*, 20006. [CrossRef]

10. Hanel, R.; Thurner, S. When do generalized entropies apply? How phase space volume determines entropy. *Europhys. Lett.* **2011**, *96*, 50003. [CrossRef]
11. Hanel, R.; Thurner, S. Generalized (c,d)-entropy and aging random walks. *Entropy* **2013**, *15*, 5324. [CrossRef]
12. Tsallis, C. Possible generalization of Boltzmann-Gibbs statistics. *J. Stat. Phys.* **1988**, *52*, 479–487 . [CrossRef]
13. Diu, B.; Guthmann, C.; Lederer, D.; Roulet, B. *Éléments de Physique Statistique*; Hermann: Paris, France, 1989.
14. Balian, R. *From Microphysics to Macrophysics*; Springer: Berlin, Germany, 1991; Volumes I and II.
15. Reichl, L.E. *A Modern Course in Statistical Physics*, 2nd ed.; John Wiley and Sons: New York, NY, USA, 1998.
16. De Groot, S.R.; Mazur, P. *Non-Equilibrium Thermodynamics*; Dover Publications: New York, NY, USA, 1984.
17. Balakrishnan, V. *Elements of Nonequilibrium Statistical Mechanics*; CRC Press, Taylor and Francis Group: New York, NY, USA, 2008.
18. Risken, H. *The Fokker-Planck Equation*, 2nd ed.; Springer: Berlin, Germany, 1989.
19. Bouchaud, J.P.; Georges, A. Anomalous diffusion in disordered media: Statistical mechanisms, models and physical applications. *Phys. Rep.* **1990**, *195*, 127. [CrossRef]
20. Vázquez, J.L. *The Porous Medium Equation*; Oxford University Press: Oxford, UK, 2007.
21. Frank, T.D. *Nonlinear Fokker-Planck Equations: Fundamentals and Applications*; Springer: Berlin, Germany, 2005.
22. Plastino, A.R.; Plastino, A. Non-extensive statistical mechanics and generalized Fokker-Planck equation. *Physica A* **1995**, *222*, 347–354. [CrossRef]
23. Tsallis, C.; Bukman, D.J. Anomalous diffusion in the presence of external forces: Exact time-dependent solutions and their thermostatistical basis. *Phys. Rev. E* **1996**, *54*, R2197. [CrossRef]
24. Kaniadakis, G. H-theorem and generalized entropies within the framework of nonlinear kinetics. *Phys. Lett. A* **2001**, *288*, 283–291. [CrossRef]
25. Shiino, M. Free energies based on generalized entropies and H-theorems for nonlinear Fokker-Planck equations. *J. Math. Phys.* **2001**, *42*, 2540. [CrossRef]
26. Frank, T.D.; Daffertshofer, A. H-theorem for nonlinear Fokker-Planck equations related to generalized thermostatistics. *Physica A* **2001**, *295*, 455–474. [CrossRef]
27. Frank, T.D. Generalized Fokker-Planck equations derived from generalized linear nonequilibrium thermodynamics. *Physica A* **2002**, *310*, 397–412. [CrossRef]
28. Chavanis, P.-H. Generalized thermodynamics and Fokker-Planck equations: Applications to stellar dynamics and two-dimensional turbulence. *Phys. Rev. E* **2003**, *68*, 036108. [CrossRef]
29. Chavanis, P.-H. Generalized Fokker-Planck equations and effective thermodynamics. *Physica A* **2004**, *340*, 57–65. [CrossRef]
30. Schwämmle, V.; Nobre, F.D.; Curado, E.M.F. Consequences of the H theorem from nonlinear Fokker-Planck equations. *Phys. Rev. E* **2007**, *76*, 041123. [CrossRef] [PubMed]
31. Schwämmle, V.; Curado, E.M.F.; Nobre, F.D. A general nonlinear Fokker-Planck equation and its associated entropy. *Eur. Phys. J. B* **2007**, *58*, 159–165. [CrossRef]
32. Schwämmle, V.; Curado, E.M.F.; Nobre, F.D. Dynamics of normal and anomalous diffusion in nonlinear Fokker-Planck equations. *Eur. Phys. J. B* **2009**, *70*, 107–116. [CrossRef]
33. Curado, E.M.F.; Nobre, F.D. Equilibrium States in Two-Temperature Systems. *Entropy* **2018**, *20*, 183. [CrossRef] [PubMed]
34. Ribeiro, M.S.; Nobre, F.D.; Curado, E.M.F. Classes of N-Dimensional Nonlinear Fokker-Planck Equations Associated to Tsallis Entropy. *Entropy* **2011**, *13*, 1928. [CrossRef]
35. Chavanis, P.-H. Nonlinear mean field Fokker-Planck equations. Application to the chemotaxis of biological population. *Eur. Phys. J. B* **2008**, *62*, 179–208. [CrossRef]
36. Curado, E.M.F.; Nobre, F.D. Derivation of nonlinear Fokker-Planck equations by means of approximations to the master equation. *Phys. Rev. E* **2003**, *67*, 021107.
37. Boon, J.P.; Lutsko, J.F. Nonlinear diffusion from Einstein's master equation. *Europhys. Lett.* **2007**, *80*, 60006. [CrossRef]
38. Lutsko, J.F.; Boon, J.P. Generalized diffusion: A microscopic approach. *Phys. Rev. E* **2008**, *77*, 051103. [CrossRef] [PubMed]
39. Zand, J.; Tirnakli, U.; Jensen, H.J. On the relevance of q-distribution functions: The return time distribution of restricted random walker. *J. Phys. A* **2015**, *48*, 1751. [CrossRef]
40. Borland, L. Ito-Langevin equations within generalized thermostatistics. *Phys. Lett. A* **1998**, *245*, 67–72. [CrossRef]
41. Borland, L. Microscopic dynamics of the nonlinear Fokker-Planck equation: A phenomenological model. *Phys. Rev. E* **1998**, *57*, 6634. [CrossRef]
42. Beck, C. Dynamical Foundations of Nonextensive Statistical Mechanics. *Phys. Rev. Lett.* **2001**, *87*, 180601. [CrossRef]
43. Anteneodo, C.; Tsallis, C. Multiplicative noise: A mechanism leading to nonextensive statistical mechanics. *J. Math. Phys.* **2003**, *44*, 5194. [CrossRef]
44. Dos Santos, B.C.; Tsallis, C. Time evolution towards q-Gaussian stationary states through unified Itô-Stratonovich stochastic equation. *Phys. Rev. E* **2010**, *82*, 061119. [CrossRef] [PubMed]
45. Arenas, Z.G.; Barci, D.G.; Tsallis, C. Nonlinear inhomogeneous Fokker-Planck equation within a generalized Stratonovich prescription. *Phys. Rev. E* **2014**, *90*, 032118. [CrossRef]
46. Lenzi, E.K.; Mendes, R.S.; Tsallis, C. Crossover in diffusion equation: Anomalous and normal behaviors. *Phys. Rev. E* **2003**, *67*, 031104. [CrossRef] [PubMed]

47. Zapperi, S.; Moreira, A.A.; Andrade, J.S., Jr. Flux front penetration in disordered superconductors. *Phys. Rev. Lett.* **2001**, *86*, 3622. [CrossRef] [PubMed]
48. Andrade, J.S., Jr.; da Silva, G.F.T.; Moreira, A.A.; Nobre, F.D.; Curado, E.M.F. Thermostatistics of overdamped motion of interacting particles. *Phys. Rev. Lett.* **2010**, *105*, 260601. [CrossRef]
49. Nobre, F.D.; Souza, A.M.C.; Curado, E.M.F. Effective-temperature concept: A physical application for nonextensive statistical mechanics. *Phys. Rev. E* **2012**, *86*, 061113. [CrossRef] [PubMed]
50. Curado, E.M.F.; Souza, A.M.C.; Nobre, F.D.; Andrade, R.F.S. Carnot cycle for interacting particles in the absence of thermal noise. *Phys. Rev. E* **2014**, *89*, 022117. [CrossRef]
51. Ribeiro, M.S.; Casas, G.A.; Nobre, F.D. Second law and entropy production in a nonextensive system. *Phys. Rev. E* **2015**, *91*, 012140. [CrossRef]
52. Nobre, F.D.; Curado, E.M.F.; Souza, A.M.C.; Andrade, R.F.S. Consistent thermodynamic framework for interacting particles by neglecting thermal noise. *Phys. Rev. E* **2015**, *91*, 022135. [CrossRef]
53. Shiino, M. Dynamical behavior of stochastic systems of infinitely many coupled nonlinear oscillators exhibiting phase transitions of mean-field type: H theorem on asymptotic approach to equilibrium and critical slowing down of order-parameter fluctuations. *Physica Rev. A* **1987**, *36*, 2393. [CrossRef] [PubMed]
54. Sicuro, G.; Rapcan, P.; Tsallis, C. Nonlinear inhomogeneous Fokker-Planck equations: Entropy and free-energy time evolution. *Phys. Rev. E* **2016**, *94*, 062117. [CrossRef] [PubMed]
55. Nojiri, S.; Odintsov, S.D.; Saridakis, E.N. Modified cosmology from extended entropy with varying exponent. *Eur. Phys. J. C* **2019**, *79*, 242. [CrossRef]
56. Luciano, G.G.; Blasone, M. q-generalized Tsallis thermostatistics in Unruh effect for mixed fields. *Phys. Rev. D* **2021**, *104*, 045004. [CrossRef]
57. Souza, A.M.C.; Andrade, R.F.S.; Nobre, F.D.; Curado, E.M.F. Thermodynamic framework for compact q-Gaussian distributions. *Physica A* **2018**, *491*, 153–166. [CrossRef]
58. Plastino, A.R.; Tsallis, C.; Wedemann, R.S.; Haubold, H.J. Entropy Optimization, Generalized Logarithms, and Duality Relations. *Entropy* **2022**, *24*, 1723. [CrossRef]
59. Tsallis, C.; Mendes, R.S.; Plastino, A.R. The role of constraints within generalized nonextensive statistics. *Physica A* **1998**, *261*, 543–554. [CrossRef]
60. Martinez, S.; Nicolas, F.; Pennini, F.; Plastino, A. Tsallis' entropy maximization procedure revisited. *Physica A* **2000**, *286*, 489. [CrossRef]
61. Ferri, G.L.; Martinez, S.; Plastino, A. Equivalence of the four versions of Tsallis' statistics. *J. Stat. Mech. Theory Exp.* **2005**, *2005*, P04009. [CrossRef]
62. Ferri, G.L.; Martinez, S.; Plastino, A. The role of constraints in Tsallis' nonextensive treatment revisited. *Physica A* **2005**, *345*, 493. [CrossRef]
63. Casas, G.A.; Nobre, F.D.; Curado, E.M.F. H theorem for generalized entropic forms within a master-equation framework. *Phys. Rev. E* **2016**, *93*, 032145. [CrossRef] [PubMed]
64. Casas, G.A.; Nobre, F.D.; Curado, E.M.F. Generalized entropy production phenomena: A master-equation approach. *Phys. Rev. E* **2014**, *89*, 012114. [CrossRef]
65. Prigogine, I. *Introduction for the Thermodynamics of Irreversible Processes*; John Wiley and Sons: New York, NY, USA, 1967.
66. Glansdorff, P.; Prigogine, I. *Thermodynamic Theory of Structure, Stability and Fluctuations*; John Wiley and Sons: New York, NY, USA, 1971.
67. Casas, G.A.; Nobre, F.D.; Curado, E.M.F. Entropy production and nonlinear Fokker-Planck equations. *Phys. Rev. E* **2012**, *86*, 061136. [CrossRef]
68. Bento, E.P.; Viswanathan, G.M.; da Luz, M.G.E.; Silva, R. Third law of thermodynamics as a key test of generalized entropies. *Phys. Rev. E* **2015**, *91*, 022105. [CrossRef]
69. Bagci, G.B.; Oikonomou, T. Validity of the third law of thermodynamics for the Tsallis entropy. *Phys. Rev. E* **2016**, *93*, 022112. [CrossRef] [PubMed]

Fractal Derivatives, Fractional Derivatives and q-Deformed Calculus

Airton Deppman [1,*], Eugenio Megías [2] and Roman Pasechnik [3]

[1]   Instituto de Física, Universidade de São Paulo, São Paulo 05508-090, Brazil
[2]   Departamento de Física Atómica, Molecular y Nuclear and Instituto Carlos I de Física
     Teórica y Computacional, Universidad de Granada, Avenida de Fuente Nueva s/n, 18071 Granada, Spain;
     emegias@ugr.es
[3]   Department of Physics, Lund University, Sölvegatan 14A, SE-22362 Lund, Sweden;
     roman.pasechnik@hep.lu.se
*   Correspondence: deppman@usp.br

Abstract: This work presents an analysis of fractional derivatives and fractal derivatives, discussing their differences and similarities. The fractal derivative is closely connected to Haussdorff's concepts of fractional dimension geometry. The paper distinguishes between the derivative of a function on a fractal domain and the derivative of a fractal function, where the image is a fractal space. Different continuous approximations for the fractal derivative are discussed, and it is shown that the q-calculus derivative is a continuous approximation of the fractal derivative of a fractal function. A similar version can be obtained for the derivative of a function on a fractal space. Caputo's derivative is also proportional to a continuous approximation of the fractal derivative, and the corresponding approximation of the derivative of a fractional function leads to a Caputo-like derivative. This work has implications for studies of fractional differential equations, anomalous diffusion, information and epidemic spread in fractal systems, and fractal geometry.

Keywords: fractal derivatives; fractional derivatives; fractional differential equations; q-calculus; nonextensive statistics

1. Introduction

Fractional differential equations have been used to describe the behavior of complex systems. The growing interest in this mathematical tool imposes the necessity of urgent analysis of its fundamentals. The widespread use of fractional differential equations in fluid dynamics, finance, and other complex systems has led to the intense investigation of the properties of fractional derivatives and their geometrical and physical meaning. Fractional derivatives are often associated with fractal geometry, but the connections between fractional derivatives and fractal derivatives have not been clarified so far. Fractional derivatives have been used in many applications [1,2], and advancing our understanding of their geometrical meaning and their relations with fractals is necessary. The q-calculus has been frequently applied to describe the statistical properties of fractal systems [3,4]. However, the relationship between q-calculus and fractal derivatives has not been fully understood yet.

This work reviews the fundamentals of fractal derivatives and establishes their connections with fractional derivatives and q-calculus. The generalization of standard calculus to include fractional-order derivatives and integrals is an exciting field of research, and many works have been conducted in this area. Different proposals for fractional generalization are available, and applications of fractional derivatives have been used in various fields. Fractional differential equations are frequently used to describe the behavior of complex systems. In Refs. [5,6], the authors analyzed different forms of fractional derivatives and

discussed their properties. Caputo's derivative is among the most commonly used and is defined by

$$D_C^\nu h(x) = \frac{1}{\Gamma(1-\nu)} \int_{x-\delta}^{x} (x-t)^{-\nu} \frac{dh}{dt} dt ,$$

(1)

which is a particular case of the Riemann–Liouville fractional derivative [7].

Haussdorff established the fundamental aspects of spaces with fractional dimension, and an introduction to the subject can be found in [8]. One of the important quantities associated with fractal spaces is the Haussdorff measure, denoted by $\mathcal{H}^s(\mathbb{F})$. Its definition is based on the measure $\mathcal{H}^s_\delta(\mathbb{F})$, and is given by

$$\mathcal{H}^s(\mathbb{F}) = \lim_{\delta \to 0} \mathcal{H}^s_\delta(\mathbb{F}) ,$$

(2)

where the measure depends on a δ-cover of the Borel subset $\mathbb{F} \subseteq \mathbb{R}^n$. The space $\mathbb{F}$ will be referred to as a fractal space, and its Hausdorff dimension is denoted by α and defined as

$$\alpha = \inf\{s \geq 0 : \mathcal{H}^s(\mathbb{F}) = 0\} = \sup\{s : \mathcal{H}^s(\mathbb{F}) = \infty\} .$$

(3)

If $0 < \alpha < \infty$, the Haussdorff measure of the δ^α-cover is called the mass distribution, denoted by $\gamma^\alpha(\mathbb{F}, a, b)$ [9–11], which will be discussed below. Fractal derivatives and fractional derivatives are not the same concept [12], and the non-locality is a prominent aspect of the fractal derivative. For a comprehensive review of the subject and its applications, see Ref. [13]. The Parvate–Gangal derivative is defined for functions on a fractal domain. This work shows that extending the same concepts to functions with a fractal image can provide new insights into the role of fractal derivatives in the study of complex systems.

Tsallis statistics was proposed to describe the statistical properties of fractal systems. It introduces a non-additive entropy that can be used to obtain, through the ordinary thermodynamics formalism, the non-extensive thermodynamics [14,15]. To deal with non-additivity, the q-calculus was proposed [16]. One important result of q-calculus is the q-derivative, which is written as:

$$\frac{\bar{d}f}{dx} = f^{q-1} \frac{df}{dx}.$$

(4)

Notice that, if the function f is a q-exponential, the *special derivative* above results to be identical to the standard derivative of a q-exponential function. This derivative can be straightforwardly related to the conformal derivative [17].

The three different theoretical areas mentioned above have been investigated independently, evolving in parallel. Despite their many common aspects, the connections between them have not been demonstrated so far [18]. This work aims to establish connections between Caputo's derivative and the q-calculus with the continuous approximation of the fractal derivative proposed by Parvate and Gangal. In this work, we assume that the fractal derivative is correctly calculated by the definitions advanced by Parvate, Gangal, and coworkers [9–11], and discuss how some relevant forms of fractional derivatives, as well as the q-deformed derivative, can be obtained as a continuous approximation of the fractal derivative.

2. Fractal Derivatives

Lemma 1. *If $x = (x_1, \cdots, x_n) \in \mathbb{R}^n$ and $f = (f_1(x), \cdots, f_m(x)) \in \mathbb{R}^m$ is an m-dimensional vector field $f : \mathbb{R}^n \to \mathbb{R}^m$. Then, $m \leq n$.*

Proof. Suppose $m > n$, then $(f_1(x), \cdots, f_n(x))$ forms a new set of n independent variables, which are functions of the n independent variables of x. Then, $f_{n+1}(x)$ is not independent of the functions in the set. $\square$

Definition 1. *A vector field with dimension $m = 1$ is a function.*

Lemma 2. *If there is an inverse function $f^{-1}(f(x)) = x$, then $m = n$.*

Proof. It follows immediately by applying Lemma 1. □

Lemma 3. *If f is a fractal vector field $f : \mathbb{R}^n \to \mathbb{R}^\alpha$, with $\alpha \in \mathbb{R}$, then $\alpha \leq n$.*

Proof. It follows immediately by applying Lemma 1. □

Definition 2. *A fractal vector field with dimension $\alpha \leq 1$ is a fractal function.*

Definition 3. *An α-dimensional function is a fractal vector field if $\alpha > 1$ or a fractal function if $\alpha \leq 1$.*

Definition 4. *If $\gamma(\mathbb{F}, a, b)$ is the Haussdorff mass distribution for a cover F, with $a, b \in F$, then the staircase function, S^α_{F,a_o}, is defined as*

$$S^\alpha_{F,a_o} = \begin{cases} \gamma(\mathbb{F},a_o,x) \ \text{ for } x > a_o \\ \gamma(\mathbb{F},x,a_o) \ \text{ for } x < a_o \end{cases}. \tag{5}$$

Lemma 4. *The staircase function is a scalar.*

Proof. The staircase function is proportional to the Haussdorff mass function, which is the volume resulting from the union of the $\delta^\alpha(x) \in \mathbb{F}$, so it is a scalar. □

Definition 5. *If $\mathbb{F}$ is a δ^α-cover and $f : \mathbb{F} \to \mathbb{R}$, then the fractal derivative of $f(x)$ is*

$$D^\alpha_{\mathbb{F},a_o} f(x_o) = \begin{cases} F \lim_{x \to x_o} \frac{f(x)-f(x_o)}{S^\alpha_{F,a_o}(x)-S^\alpha_{F,a_o}(x_o)} & x, x_o \in \mathbb{F} \\ 0 & \text{otherwise} \end{cases}. \tag{6}$$

Theorem 1. *There is a fractal derivative of the inverse function, and it is the inverse of the fractal derivative.*

Proof. Consider that $x, x_o \in \mathbb{F}$. Suppose there exists a function $g : \mathbb{R} \to \mathbb{F}$ such that $g(f(x)) = x$. Then,

$$D^\alpha_{\mathbb{F},a_o} g(f_{x_o}) = F \lim_{x \to x_o} \frac{g(f_x) - g(f_{x_o})}{f(x) - f(x_o)} \frac{f(x) - f(x_o)}{S^\alpha_{F',a_o}(x) - S^\alpha_{F',a_o}(x_o)} = 1, \tag{7}$$

where the simplified notation $f_x = f(x)$ was adopted. It follows that

$$F \lim_{x \to x_o} \frac{g(f_x) - g(f_{x_o})}{f(x) - f(x_o)} = F \lim_{x \to x_o} \frac{S^\alpha_{F',a_o}(x) - S^\alpha_{F',a_o}(x_o)}{f(x) - f(x_o)}. \tag{8}$$

□

The fractal derivative of the inverse function can be applied to any fractal function $h : \mathbb{R} \to \mathbb{F}$. The staircase function, in this case, is applied to the fractal image space of the function h. The function f can be defined arbitrarily, with the constraint that there is an inverse function f^{-1}. One case of particular interest is the identity function $f(x) = x$, then we have

$$[D^\alpha_{\mathbb{F},\varphi}]^{-1} h(x_o) = F \lim_{x \to x_o} \frac{S^\alpha_{F,\varphi}[h(x)] - S^\alpha_{F,\varphi}[h(x_o)]}{x - x_o}, \tag{9}$$

with $\varphi = h(a_o)$.

Observe that in this case, the image space and the domain space of the function h are the same, i.e., $h \colon \mathbb{F} \to \mathbb{F}$.

Definition 6. *The result obtained above can be generalized by defining the fractal derivative of the inverse function or, equivalently, the inverse of the fractal derivative, as*

$$[D_{\mathbb{F},\varphi}^\alpha]^{-1} h(f_{x_o}) = \begin{cases} F \lim_{x \to x_o} \frac{S_{F,\varphi}^\alpha[h(x)] - S_{F,\varphi}^\alpha[h(x_o)]}{x - x_o} & x, x_o \in \mathbb{F} \\ 0 & otherwise \end{cases}. \tag{10}$$

Corollary 1. *The derivative of a fractal function is well-defined only if the function is almost always non-divergent in the interval $[a, b]$ (Following the standard terminology in the field, we say that a function is almost always non-divergent if the set of points where it is divergent has null Lebesgue measure).*

Proof. According to Definition 4, the staircase function is well-defined only if the mass distribution function can be defined. The mass distribution is equal to the Haussdorff measure when the Haussdorff dimension is $0 < \alpha < \infty$. This condition is satisfied only if the function is almost always non-divergent. $\square$

Theorem 2. *If the function $h(x)$ is almost always continuous and non-divergent in $\mathbb{F}$, and $h'(x) = [D_{\mathbb{F},\varphi}^\alpha]^{-1} h(x)$, then the Haussdorff dimension of $h(x)$ and $h'(x)$ are the same.*

Proof. Let $\mathbb{F}$ be the δ^α-cover of the fractal function $h(x)$, and $\mathbb{F}'$ the δ^β-cover of the inverse of fractal derivative. For any $\delta^\alpha[h(x)] \in \mathbb{F}$ there is a $\delta^\beta[h'(x)] \in \mathbb{F}'$, so $\beta \geq \alpha$. For $\delta^\beta[h'(x)] \in \mathbb{F}'$, there is a $\delta^\alpha[h(x)] \in \mathbb{F}$; therefore, $\alpha \leq \beta$. Hence, $\alpha = \beta$. $\square$

Definition 7. *We will denote the inverse of an α-dimensional fractal function by $D_{\mathbb{F},\varphi}^\alpha h(x)$, and we will refer to it as a fractal derivative of an α-dimensional fractal function, or simply fractal function, while the fractal derivative will be called fractal derivative over a fractal space.*

Definition 8. *The partial derivative of a fractal function is*

$$D_{\mathbb{F},\varphi}^\alpha |_i h(f_x) = \begin{cases} F \lim_{x_i \to x_{o,i}} \frac{S_{F,\varphi}^\alpha[h(x)] - S_{F,\varphi}^\alpha[h(x_o)]}{x_i - x_{o,i}} & x, x_o \in \mathbb{F} \\ 0 & otherwise \end{cases}, \tag{11}$$

where the index i indicates the component x_i of the vector x.

Corollary 2. *The dimension of $D_{\mathbb{F},\varphi}^\alpha |_i h(f_x)$ is $\alpha \leq 1$.*

Proof. It follows immediately from Lemma 1 and Theorem 2. $\square$

Definition 9. *The staircase function differential is defined by*

$$dS_{F,a_o}^\alpha(x) = \begin{cases} F \lim_{dx \to 0} \left[S_{F,a_o}^\alpha(x + dx) - S_{F,a_o}^\alpha(x) \right] & if \; x, x + dx \in \mathbb{F} \\ 0 & otherwise \end{cases} \tag{12}$$

Theorem 3. *The staircase function differential can be approximated by*

$$dS_{F,a_o}^\alpha(x) = \frac{A(\alpha)}{\alpha} dx^\alpha, \tag{13}$$

where

$$A(\alpha) := 2\pi^{\alpha/2} / \Gamma(\alpha/2). \tag{14}$$

Proof. For any volume $(\delta x)^n \in \mathbb{R}^n$, its intersection with $\mathbb{F}$ has a volume $(\delta x)^\alpha$. Consider the volume of an n-dimensional sphere of radius x given by

$$V(x) = \frac{A(n)}{n} x^n, \tag{15}$$

where $A(n) = 2\pi^{n/2}/\Gamma(n/2)$ is the surface area term, with $\Gamma(z)$ being the Euler's Gamma Function, and $x = \sqrt{x_1^2 + \cdots + x_n^2}$. Then, the volume of a spherical shell of finite width δx is given by

$$\delta V(x) = \frac{A(n)}{n} ((x + \delta x)^n - x^n). \tag{16}$$

$\square$

In the limit $\delta x \to dx$, where now dx is infinitesimal, it results

$$dV(x) = A(n) x^{n-1} dx = \frac{A(n)}{n} dx^n, \tag{17}$$

where $dx^n := d(x^n)$.

The intersection of $\delta V(x)$ with $\mathbb{F}$, which is denoted by $\delta V_\alpha(x)$, is

$$\delta V_\alpha(x) = \frac{A(\alpha)}{\alpha} ((x + \delta x)^\alpha - x^\alpha). \tag{18}$$

In the limit $\delta x \to dx$, this leads to

$$\delta V_\alpha(x) \to dV_\alpha(x) = A(\alpha) x^{\alpha-1} dx = \frac{A(\alpha)}{\alpha} dx^\alpha. \tag{19}$$

On the other hand, $dS_{F,a_o}^\alpha(x)$ is the volume of the intersection between an infinitesimal volume $dV \in \mathbb{R}^n$ with $\mathbb{F}$. (The multiplicative coefficient $A(\alpha)$ used here is valid for integer dimensions. The case of fractional dimensions is more challenging, so this coefficient needs to be considered with care. In this work, we focus on the shape of the continuous approximation.)

$$dS_{F,a_o}^\alpha(x) = \frac{A(\alpha)}{\alpha} dx^\alpha = A(\alpha) x^{\alpha-1} dx. \tag{20}$$

Definition 10. *The continuous approximation of a fractal function is defined as a set of infinitesimal elements dx such that Equation (20) is satisfied.*

Theorem 4. *The continuous approximation of the fractal derivative of a function is*

$$D_{\mathbb{F},\varphi}^\alpha h(x) = \frac{A(\alpha)}{\alpha} \frac{dh^\alpha}{dx} = A(\alpha) h^{\alpha-1}(x) \frac{dh}{dx}(x). \tag{21}$$

Theorem 5. *The continuous approximation of the fractal derivative of a fractal function is*

$$D_{\mathbb{F},\varphi}^\alpha h(x) = \frac{A(\alpha)}{\alpha} \frac{dh^\alpha}{dx} = A(\alpha) h^{\alpha-1}(x) \frac{dh}{dx}(x). \tag{22}$$

Proof. It follows directly from the definition of the fractal derivative of a function and of the continuous approximation. $\square$

Theorem 6. *Consider a fractal function $f : \mathbb{R}^n \to \mathbb{F}$, where $\mathbb{F}$ is a δ^α-cover, with $n - 1 < \alpha < n$, for $n > 1$. It defines a set of fractal functions $\{f_i(x_i)\}$ with dimensions $\{\alpha_i\}$ such that $\alpha = \alpha_1 + \cdots + \alpha_n$.*

Proof. Consider the fractal function $f_k(x_k) = f(a, \cdots, x_k, \cdots, z)$, where $a, \cdots, z$ are constants. For any interval $I = [x_k, x_k + \delta x_k]$, the intersection of I and $\mathbb{F}$ is $(\delta x_k)^{\alpha_k}$, with $\alpha_k < 1$.

For an α_{k-1}-dimensional function $h_{k-1}(x_1, \cdots, x_{k-1}, k, l, \cdots, z)$ such that for any volume $(\delta x)^{k-1}$, the intersection with $\mathbb{F}$ is $(\delta x)^{\alpha_{k-1}}$, the function $h_k(x_1, \cdots, x_{k-1}, x_k, l, \cdots, z)$ has dimension $(\delta x)^{\alpha_{k-1}} \delta x = (\delta x)^{\alpha_k}$, where $\alpha_k = \alpha_{k-1} + \alpha_k$. The theorem is proved by induction. $\square$

Definition 11. *Consider a fractal function h with dimension $\alpha < 1$. The gradient of a fractal function is defined as*

$$\mathbf{D}_{\mathbb{F},\varphi}^{\alpha} h(x_o) = \left(D_{\mathbb{F},\varphi}^{\alpha_1}|_1 h(x_o), \cdots, D_{\mathbb{F},\varphi}^{\alpha_n}|_n h(x_o) \right), \tag{23}$$

where $\alpha = \alpha_1 + \cdots + \alpha_n$.

Definition 12. *For $\alpha > 1$, the partial fractal derivative of the function is*

$$\mathbf{D}_{\mathbb{F},\varphi}^{\alpha}|_i h(x_o) = \left(D_{\mathbb{F},\varphi}^{\alpha_1}|_i h(x_o), \cdots, D_{\mathbb{F},\varphi}^{\alpha_n}|_i h(x_o) \right), \tag{24}$$

where $\alpha = \alpha_1 + \cdots + \alpha_n$.

Theorem 7. *For a finite δ, the derivative of a fractal function in the interval $[x - \delta, x]$ is*

$$D_{[\delta],\varphi}^{\alpha} h(x) = \frac{A(\alpha)}{\alpha} \int_{x-\delta}^{x} h^{\alpha-1}(t) \frac{dh}{dt} dt. \tag{25}$$

Proof. The derivative in the interval $[x - \delta, x]$ is

$$D_{[\delta],\varphi}^{\alpha} h(x) = \int_{x-\delta}^{x} D_{\mathbb{F},\varphi}^{\alpha} h(t) dt. \tag{26}$$

$\square$

Using Definition 10, the theorem is proved.

Theorem 8. *For a finite δ, the derivative of function in the interval $[x - \delta, x]$ in a fractal space is*

$$D_{[\delta],a}^{\alpha} h(x) = \frac{A(\alpha)}{\alpha} \int_{x-\delta}^{x} [h(x) - h(t)]^{\alpha-1} \frac{dh}{dt} dt. \tag{27}$$

Proof. The proof is performed by applying the continuous approximation in Equation (20) to the derivative on fractal space in Definition 5. $\square$

Observe that the α-dimensional sphere needs not to be centered at φ for the fractal derivative of a fractal function, or at a for the derivative on a fractal space. The point x, where the derivative is calculated, can be set as the center of the sphere.

Definition 13. *The continuous approximation of the derivative of a function on a fractal space, based on α-dimensional sphere centered at x is indicated by $D_{\mathbb{F},x}^{\alpha} h(x)$.*

Theorem 9. *The continuous approximation of the derivative of a function on a fractal space, $D_{\mathbb{F},x}^{\alpha} h(x)$ in the interval $[x - \delta, x]$, for finite δ, is given by*

$$D_{\mathbb{F},x}^{\alpha} h(x) = \frac{A(\alpha)}{\alpha} \int_{x-\delta}^{x} (x-t)^{1-\alpha} \frac{dh}{dt} dt, \tag{28}$$

which is proportional to Caputo's derivative.

Proof. The local continuous approximation, considering that the radius of the spherical shell is $x - t$, is determined from Theorem 5 as

$$D_{\mathbb{F},x}^{\alpha}h(t) = A(\alpha)(x - t)^{1-\alpha}\frac{dh}{dx}(t)\,. \tag{29}$$

☐

Using Definition 13, one has

$$D_{\mathbb{F}}^{\alpha}h(x) = \int_{x-\delta}^{x} D_{\mathbb{F},x}^{\alpha}h(t)dt\,, \tag{30}$$

leading to the proof of the Theorem.

Definition 14. *The continuous approximation of the derivative of a fractal function based on α-dimensional sphere centered at x is indicated by $D_{\mathbb{F}}^{\alpha}h(x)$.*

Theorem 10. *The continuous approximation of the derivative of a fractal function, $D_{\mathbb{F},\varphi_x}^{\alpha}h(x)$ in the interval $[x - \delta, x]$, for finite δ, is given by*

$$D_{\mathbb{F},\varphi_x}^{\alpha}h(x) = \frac{A(\alpha)}{\alpha}\int_{x-\delta}^{x}(\varphi_x - h(t))^{\alpha-1}\frac{dh}{dt}dt\,, \tag{31}$$

for t such that $h(t) < \varphi_x = h(x)$.

Proof. The proof follows the same lines of the proof for Theorem 9. ☐

Corollary 3. *The continuous approximation in Definition 10 is proportional to the limit of the continuous approximation in the range $[x - \delta, x]$ for $\delta \to 0$ of Caputo's derivative.*

3. Discussion and Conclusions

The fractal derivative proposed by Parvate and Gangal, presented in Definition 5, is the closest concept to the Hausdorff concept of fractional dimension spaces. Therefore, it is considered as the starting point for the analysis of fractal derivatives and fractional derivatives here.

The existence of the inverse of the Parvate–Gangal derivative is a natural consequence, i.e., a derivative of a function with a fractal image space that is defined on a domain space, which may or may not be fractal. This is proven in Theorem 1.

This work demonstrates that fractal functions with arbitrary dimension α, such as a fractal vector field with fractal dimension $\alpha > 1$, can be defined. However, the cases of most interest are those with $\alpha \leq 1$, as they are physically relevant for the present work.

The derivative of a fractal function on a fractal space allows for a continuous approximation, as demonstrated in Theorem 4. Additionally, a similar continuous approximation can be obtained for the derivative of a function in a fractal space, as shown in Theorem 5. This approximation is identical to the *special derivative* used in Ref. [19] to derive the Plastino–Plastino Equation, which is a generalization of the Fokker–Planck Equation for systems with non-local correlations.

To illustrate the behavior of the continuous approximation, we utilize the well-known Cantor Set, which has a dimension $\alpha = 0.631$. We aim to demonstrate how the continuous approximation aligns with the mass distribution, $S_{\mathbb{F},0}^{\alpha}(x)$. To achieve this, we numerically calculate the mass distribution for this fractal set up to level 4. In other words, the smallest component of the fractal has a linear length of $l = 3^{-4}$. We employ a δ-cover with $\delta = 0.01$ to calculate the mass distribution.

Next, we fit a power-law function, $y(x) = ax^b$. According to the theoretical findings presented in this work, the exponent b should closely approximate the fractal dimension α of the Cantor Set. The obtained results are displayed in Figure 1, revealing that the best fit

corresponds to $b = 0.636$, which is in close proximity to the expected value. This outcome effectively illustrates the application of the continuous approximation and provides insight into substituting the mass distribution by the continuous approximation. It should be noted that there are numerous other methods available for creating a continuous approximation of the fractal measure, and each of these approaches will result in different fractional derivatives. Investigating the coherence and convenience of different forms of approximation to the staircase function is an interesting line of research that is beyond the scope of this present study.
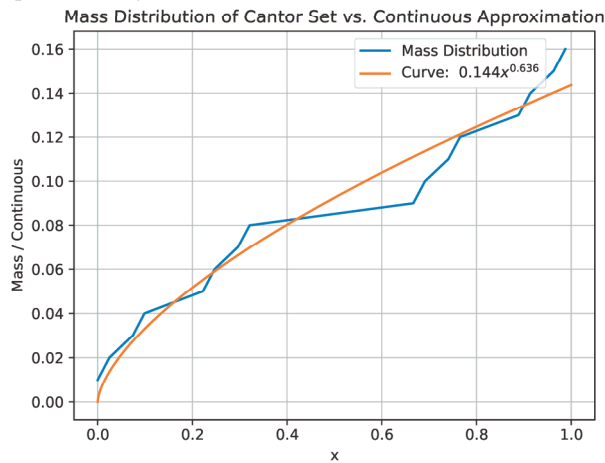
Figure 1. Plots of the mass distribution (blue line) for the Cantor Set at the 4th iteration, calculated with a δ-cover with $\delta = 0.01$, compared with the continuous approximation (orange line) represented by a function $y(x) = ax^b$ fitted to the mass distribution. The best-fit results in $b = 0.636$, in agreement with the Cantor Set dimension $\alpha = 0.631$.

The continuous approximation derivative is expressed in terms of the standard derivative operator and can be associated with the q-deformed calculus [16]. Unlike the fractal derivative, the continuous approximation is a local derivative, and the non-linear behavior of the continuous approximation is a remnant of the non-local properties of the fractal derivative.

Non-locality can be explicitly introduced into the continuous approximation by considering finite δ-covers. In the non-local continuous approximation, the derivative is obtained by integrating the local continuous derivative over a finite range δ. This non-local continuous approximation is presented in Theorem 9, and it is precisely the Caputo fractional derivative.

The derivative of a function in a fractal space and the derivative of a fractal function lead to different continuous approximations. The former can be associated with the Caputo fractional derivative, as shown in Theorem 9, while the latter leads to a Caputo-like derivative, as demonstrated in Theorem 10. Similar derivatives to Caputo's derivative can also be found in [20].

The results of the present work evidence the relations between the fractal derivative and some of the most used fractional derivatives. Comparing the result of Theorem 5 with Equation (4), it is clear that the local continuous approximation of the derivative of a fractal function is equal to the q-derivative. Thus, for the first time, the q-calculus derivative is shown to be a continuous approximation to the fractal derivative.

A consequence of the relationship between the q-derivative and the local continuous approximation of the derivative of a fractal function (Theorem 5), and of the connection between the derivative of a fractal function and the Caputo-like fractional derivative (Theorem 10) is that the q-derivative and the Caputo-like derivative are connected through

a dislocation of the center of the α-dimensional sphere around which the non-local continuous approximation is calculated. Hereby, one can conclude that different forms of fractional derivatives can be obtained from the Parvate–Gangal fractal derivative by considering the different possibilities of continuous approximation and non-locality of the fractional derivative.

Other fractal derivatives can be explored along the same lines as performed here. The Riemann–Liouville derivative bears a close relationship with Caputo's derivative [21] and it is interesting to observe the similarities between the fractal derivative proposed in Refs. [22,23] and the continuous approximations studied in the present work. The fractional derivative used in Ref. [24] is equal to the local continuous approximation of the fractal derivative of a function in a fractal space obtained in the present work. Ref. [25] studied this fractional derivative and its relationship with the q-derivative. Establishing a clear connection between the Parvate–Gangal fractal derivative and Caputo's fractional derivative, this work opens the possibility for a deeper understanding of the use of fractional differential equations, which is so common in many different areas. In this respect, let us remark that fractal and fractional differential equations have been used in applications as dynamic of the system in porous or heterogeneous media [26–28], diffusive flow [29–33], solitons [34], control of complex systems [35], epidemic process [36], polymer plasma [37] and many others. The consequences of the present study for these physical systems deserve further investigation in the future. The consequences of the present study for these physical systems deserve further investigation in the future. Its implication on the study and applications of fractal functions [38] deserves further investigation.

References

1. Tenreiro Machado, J.A.; Silva, M.F.; Barbosa, R.S.; Jesus, I.S.; Reis, C.M.; Marcos, M.G.; Galhano, A.F. Some applications of fractional calculus in engineering. *Math. Probl. Eng.* **2010**, *2010*, 639801. [CrossRef]
2. Debnath, L. Recent applications of fractional calculus to science and engineering. *Int. J. Math. Math. Sci.* **2003**, *2003*, 3413–3442. [CrossRef]
3. Deppman, A.; Andrade-II, E.O. Emergency of Tsallis statistics in fractal networks. *PLoS ONE* **2021**, *16*, e0257855. [CrossRef]
4. Deppman, A. Thermofractals, non-additive entropy, and q-calculus. *Physics* **2021**, *3*, 290–301. [CrossRef]
5. Valério, D.; Trujillo, J.J.; Rivero, M.; Machado, J.A.T.; Baleanu, D. Fractional calculus: A survey of useful formulas. *Eur. Phys. J. Spec. Top.* **2013**, *222*, 1827–1846. [CrossRef]
6. Valério, D.; Ortigueira, M.D.; Lopes, A.M. How many fractional derivatives are there? *Mathematics* **2022**, *10*, 737. [CrossRef]
7. Abdeljawad, T. On Riemann and Caputo fractional differences. *Comput. Math. Appl.* **2011**, *62*, 1602–1611. [CrossRef]
8. Falconer, K. *Fractal Geometry*, 3rd ed.; John Wiley & Sons: Nashville, TN, USA, 2014.

9. Parvate, A.; Gangal, A.D. Calculus on fractal subsets of real line—I: Formulation. *Fractals* **2009**, *17*, 53–81. [CrossRef]

10. Parvate, A.; Gangal, A.D. Calculus on fractal subsets of real line—II: Conjugacy with ordinary calculus. *Fractals* **2011**, *19*, 271–290. [CrossRef]

11. Parvate, A.; Satin, S.; Gangal, A.D. Calculus on Fractal Curves in Rn. *Fractals* **2011**, *19*, 15–27. [CrossRef]

12. Golmankhaneh, A.K.; Baleanu, D. Non-local integrals and derivatives on fractal sets with applications. *Open Phys.* **2016**, *14*, 542–548. [CrossRef]

13. Golmankhaneh, A.K. *Fractal Calculus and Its Applications: F-Alpha-Calculus*; World Scientific: Singapore, 2023.

14. Tsallis, C. Possible Generalization of the Boltzmann-Gibbs Statistics. *J. Stat. Phys.* **1988**, *52*, 479–487. [CrossRef]

15. Tsallis, C. *Introduction to the Nonextensive Statistical Mechanics*; Springer: New York, NY, USA, 2009.

16. Borges, E.P. A possible deformed algebra and calculus inspired in nonextensive thermostatistics. *Phys. A Stat. Mech. Its Appl.* **2004**, *340*, 95–101. [CrossRef]

17. Khalil, R.; Al Horani, M.; Yousef, A.; Sababheh, M. A new definition of fractional derivative. *J. Comput. Appl. Math.* **2014**, *264*, 65–70. [CrossRef]

18. Cattani, C. Fractal and Fractional. *Fractal Fract.* **2017**, *1*, 1. [CrossRef]

19. Deppman, A.; Khalili Golmankhaneh, A.; Megías, E.; Pasechnik, R. From the Boltzmann equation with non-local correlations to a standard non-linear Fokker-Planck equation. *Phys. Lett. B* **2023**, *839*, 137752. [CrossRef]

20. Almeida, R. A Caputo fractional derivative of a function with respect to another function. *Commun. Nonlinear Sci. Numer. Simul.* **2017**, *44*, 460–481. [CrossRef]

21. Srivastava, H.M. Fractional-Order Derivatives and Integrals: Introductory Overview and Recent Developments. *Kyungpook Math. J.* **2020**, *60*, 73–116. [CrossRef]

22. He, J.H. Fractal calculus and its geometrical explanation. *Results Phys.* **2018**, *10*, 272–276. [CrossRef]

23. He, J.H. A tutorial review on fractal spacetime and fractional calculus. *Int. J. Theor. Phys.* **2014**, *53*, 3698–3718. [CrossRef]

24. Chen, W. Time–space fabric underlying anomalous diffusion. *Chaos Solitons Fractals* **2006**, *28*, 923–929. [CrossRef]

25. Weberszpil, J.; Lazo, M.J.; Helayël-Neto, J.A. On a connection between a class of q-deformed algebras and the Hausdorff derivative in a medium with fractal metric. *Phys. A* **2015**, *436*, 399–404. [CrossRef]

26. Yin, Q.; Zhao, Y.; Gong, W.; Dai, G.; Zhu, M.; Zhu, W.; Xu, F. A fractal order creep-damage constitutive model of silty clay. *Acta Geotech.* **2023**. [CrossRef]

27. Bouras, Y.; Vrcelj, Z. Fractional and fractal derivative-based creep models for concrete under constant and time-varying loading. *Constr. Build. Mater.* **2023**, *367*, 130324. [CrossRef]

28. Liang, Y.; Guan, P. Improved Maxwell model with structural dashpot for characterization of ultraslow creep in concrete. *Constr. Build. Mater.* **2022**, *329*, 127181. [CrossRef]

29. Liu, F.; Yang, L.; Nadeem, M. A new fractal transform for the approximate solution of Drinfeld–Sokolov–Wilson model with fractal derivatives. *Fractals* **2023**, *31*, 2350007. [CrossRef]

30. Wang, K.L. Novel analytical approach to modified fractal gas dynamics model with the variable coefficients. *Z. Angew. Math. Mech.* **2022**, *103*, e202100391. [CrossRef]

31. Sun, H.; Nie, S.; Packman, A.I.; Zhang, Y.; Chen, D.; Lu, C.; Zheng, C. Application of Hausdorff fractal derivative to the determination of the vertical sediment concentration distribution. *Int. J. Sediment Res.* **2023**, *38*, 12–23. [CrossRef]

32. Wang, K.L. A novel variational approach to fractal Swift–Hohenberg model arising in fluid dynamics. *Fractals* **2022**, *30*, 2250156. [CrossRef]

33. El-Nabulsi, R.A.; Anukool, W. Fractal dimensions in fluid dynamics and their effects on the Rayleigh problem, the Burger's Vortex and the Kelvin–Helmholtz instability. *Acta Mech.* **2022**, *233*, 363–381. [CrossRef]

34. Manikandan, K.; Aravinthan, D.; Sudharsan, J.B.; Vadivel, R. Optical solitons in the generalized space–time fractional cubic-quintic nonlinear Schrödinger equation with a PT-symmetric potential. *Optik* **2022**, *271*, 170105. [CrossRef]

35. Sadek, L. Controllability and observability for fractal linear dynamical systems. *J. Vib. Control* **2022**. [CrossRef]

36. Policarpo, J.M.P.; Ramos, A.A.G.F.; Dye, C.; Faria, N.R.; Leal, F.E.; Moraes, O.J.S.; Parag, K.V.; Peixoto, P.S.; Buss, L.; Sabino, E.C.; et al. Scale-free dynamics of Covid-19 in a Brazilian city. *Appl. Math. Model.* **2023**, *121*, 166–184. [CrossRef]

37. Paun, M.A.; Paun, V.A.; Paun, V.P. Fractal modeling of polymer plasma laser ablation, plasma plume Tsallis entropy and its q-statistics interpretation, part I: Theory. *Entropy* **2022**, *24*, 342. [CrossRef]

38. Gowrisankar, A.; Khalili Golmankhaneh, A.; Serpa, C. Fractal calculus on fractal interpolation functions. *Fractal Fract.* **2021**, *5*, 157. [CrossRef]

Article

A Note on the Connection between Non-Additive Entropy and *h*-Derivative

Jin-Wen Kang [1], Ke-Ming Shen[1,2,*] and Ben-Wei Zhang [1,*]

[1] Key Laboratory of Quark & Lepton Physics (MOE), Institute of Particle Physics, Central China Normal University, Wuhan 430079, China; kangjinwen@mails.ccnu.edu.cn

[2] School of Science, East China University of Technology, Nanchang 330013, China

* Correspondence: shen_keming.ecut@hotmail.com (K.-M.S.); bwzhang@mail.ccnu.edu.cn (B.-W.Z.)

Abstract: In order to study as a whole a wide part of entropy measures, we introduce a two-parameter non-extensive entropic form with respect to the *h*-derivative, which generalizes the conventional Newton–Leibniz calculus. This new entropy, $S_{h,h'}$, is proved to describe the non-extensive systems and recover several types of well-known non-extensive entropic expressions, such as the Tsallis entropy, the Abe entropy, the Shafee entropy, the Kaniadakis entropy and even the classical Boltzmann–Gibbs one. As a generalized entropy, its corresponding properties are also analyzed.

Keywords: non-additive entropy; *h*-derivative; $S_{h,h'}$-entropy

1. Introduction

Since it was proposed over one hundred years ago, the conventional Boltzmann–Gibbs (BG) statistics has been developed very delicately and successfully with wide applications in many disciplines. During the last few decades, however, people noticed that more and more systems are difficult to be described by this simple BG distribution, such as the long-range interactions [1], the gravitational systems [2], the Lévy flights and fractals [3], and so on [4]. In order to cope with this challenge, some attempts have been made to generalize the BG statistics. Among them, the most investigated formalism is the non-extensive entropy. It was inspired by the geometrical theory of multi-fractals and its systematic use of powers of probabilities by C. Tsallis [5]:

$$S_q = k_B \frac{1 - \sum_{i=1}^{W} p_i^q}{q - 1},\tag{1}$$

where k_B is the Boltzmann constant (hereafter we assume $k_B = 1$ for simplicity) and q stands for the Tsallis non-extensive parameter. It describes the departure of non-extensive statistics from the BG one. This entropy goes back to the usual BG form when $q \to 1$. For more than two decades of researches and developments, the Tsallis entropy has been successfully applied to various domains: physics, chemistry, economics, computer science, biosciences, linguistics, and so on [5–10]. For the average charged-hadron yields in inelastic non-single-diffractive events, V. Khachatryan et al. observe it as the Tsallis distribution [11,12]

$$E\frac{\mathrm{d}^3 N_{ch}}{\mathrm{d}p^3} = \frac{1}{2\pi p_T}\frac{\mathrm{d}^2 N_{ch}}{\mathrm{d}\eta\,\mathrm{d}p_T} = C\frac{\mathrm{d}N_{ch}}{\mathrm{d}y}\left(1 + \frac{E_T}{nT}\right)^{-n},\tag{2}$$

where $E\frac{\mathrm{d}^3 N_{ch}}{\mathrm{d}p^3}$ is for the function of spectra with E for the total energy of the particle and p for its momentum, η denotes the pseudorapidity with y for the rapidity, p_T stands for the transverse momentum, C is for its normalization constant, T, a variational parameter representing the temperature when the system reaches equilibrium, n is the fitting parameter which connects with Tsallis' q by $n = 1/(1 - q)$, $y = 0.5\ln[(E + p_z)/(E - p_z)]$, $E_T =$

$\sqrt{m^2 + p_T^2} - m$, and m is the charged pion mass. The data fitting results show that the Tsallis distribution can well-describe both the low-p_T exponential and the high-p_T power-law behaviors [11,12]. One application in astrophysics is the study of the distribution of asteroid rotation periods from different regions of the solar system and diameter distributions of near-Earth asteroids (NEAs) [13]. A. S. Betzler and E. P. Borges analyze two samples from different years. They discover that the distribution of diameters of NEAs obeys a Tsallis-like distribution, and the rotation periods of asteroids can be well-approximated by a Tsallis–Gaussian function. According to the first conclusion, there should be 994 ± 30 NEAs with diameters greater than 1 km [13]. In another example, Y. Wang and J. Du study the viscosity of light charged particles in weakly ionized plasma with the power-law Tsallis-distributions using the generalized Boltzmann equation of transport and the motion equation of hydrodynamics [14].

The Tsallis entropy is indeed not unique. By now, a lot of different expressions of the non-additive entropies have been proposed, for instance, the Kaniadakis entropy [15], the Shafee entropy [16], the $q - q^{-1}$ symmetric modification of Tsallis entropy [17], and the two-parameter (q, q')-entropy [18]. These expressions were obtained in quite different ways and investigated by distinct motivations. Therefore, it will be of great interest to find the relationship among these formulas or to find a simple formula to study them as a whole.

In this paper, we first introduce a two-parameter non-additive entropy, $S_{h,h'}$, based on the h-derivative. The h-derivative is known as a mathematical generalization of the normal Newton–Leibniz calculus. We address that $S_{h,h'}$ unifies different types of expressions of non-extensive entropies; namely, it can connect a family of non-extensive entropies. On the other hand, we also discuss its properties in order to better understand this newly established non-additive entropic function.

2. h-Derivative

In the conventional mathematical theory, the Newton–Leibniz derivative is defined as:

$$Df(x) \equiv \frac{\mathrm{d}f(x)}{\mathrm{d}x} = \lim_{\delta \to 0} \frac{f(x + \delta) - f(x)}{\delta}. \tag{3}$$

Classically, most of the physical quantities are continuous, and it is natural to apply the Newton–Leibniz derivative. In quantum physics, on the other hand, all the physical quantities will be quantized; people then try to develop quantum calculus, which utilizes the discrete forms of derivatives instead and presents a generalization of this Newton-Leibniz derivative.

One formalism of quantum calculus is the h-derivative [19]. For an arbitrary function $f(x)$, its h-differential is defined as follows:

$$\mathrm{d}_h f(x) = f(x + h) - f(x). \tag{4}$$

It is easily verified that

$$\mathrm{d}_h x = h, \tag{5}$$

and

$$\mathrm{d}_h(f(x)g(x)) = f(x + h)\mathrm{d}_h g(x) + g(x)\mathrm{d}_h f(x). \tag{6}$$

Thus, can we obtain the h-derivative of $f(x)$:

$$D_h f(x) \equiv \frac{\mathrm{d}_h f(x)}{\mathrm{d}_h x} = \frac{f(x + h) - f(x)}{h}. \tag{7}$$

When $f(x)$ is differentiable, the following property is obviously obtained:

$$\lim_{h \to 0} D_h f(x) = \frac{\mathrm{d}f(x)}{\mathrm{d}x}, \tag{8}$$

which is nothing but the definition of the conventional Newton–Leibniz derivative. Note that we need the function $f(x)$ to be continuous for the Newton–Leibniz derivative, but this requirement becomes unnecessary for the h-derivative.

Next, some basic rules of this h-derivative are listed:

1. Sum and difference
   Considering the sum and difference rules of the h-derivative, we have

$$D_h[f(x) \pm g(x)] = D_h f(x) \pm D_h g(x). \tag{9}$$

2. Product and quotient rules
   As for the product and quotient rules,

$$D_h[f(x)g(x)] = f(x)D_h g(x) + g(x+h)D_h f(x), \tag{10}$$

$$D_h\left[\frac{f(x)}{g(x)}\right] = \frac{g(x)D_h f(x) - f(x)D_h g(x)}{g(x)g(x+h)}. \tag{11}$$

3. h-derivative of elementary functions
   Some other basic calculations of it are expressed:

$$D_h C = 0 \quad \text{(here C is constant)}, \tag{12}$$

$$D_h x = \frac{(x+h) - x}{h} = 1, \tag{13}$$

$$D_h x^n = \sum_{k=0}^{n-1} \frac{n!}{k!(n-k)!} x^k h^{n-k-1} \quad (n \in \mathbb{N}), \tag{14}$$

$$D_h \frac{1}{x} = -\frac{1}{x^2 + hx}, \tag{15}$$

$$D_h \frac{1}{x^n} = \frac{1}{h(x+h)^n} - \frac{1}{hx^n}, \tag{16}$$

$$D_h e^{bx} = \frac{e^{bh} - 1}{h} e^{bx} \quad \text{(here $b \in \mathbb{R}$)}, \tag{17}$$

$$D_h a^{bx} = \frac{a^{bh} - 1}{h} a^{bx} \quad \text{(here $b \in \mathbb{R}$)}. \tag{18}$$

In Figure 1, we illustrate the behavior of $D_h e^x$ at different values of h as an example. We could see that it behaves as an exponential when $h = 0$. For any fixed values of h, $D_h e^x$ is a monotonically increasing function with respect to the variable x. The values of this derivative also increase when the parameter h becomes larger.

With the definition of h-derivative, V. Kac and P. Cheung [19] developed a type of quantum calculus, known as h-calculus. As a matter of fact, an operator such as h-derivative is called the forward difference quotient operator. Analogously, it also has the backward difference quotient operator ∇_h and the central difference quotient operator δ_h, defined as [20]

$$\nabla_h f(x) = \frac{f(x) - f(x-h)}{h}, \tag{19}$$

$$\delta_h f(x) = \frac{f(x + \frac{1}{2}h) - f(x - \frac{1}{2}h)}{h}. \tag{20}$$

Note that the regular vector differential operator ∇ has been generalized based on h-derivative. We then explore the connection between the h-derivative entropy and its modified forms.
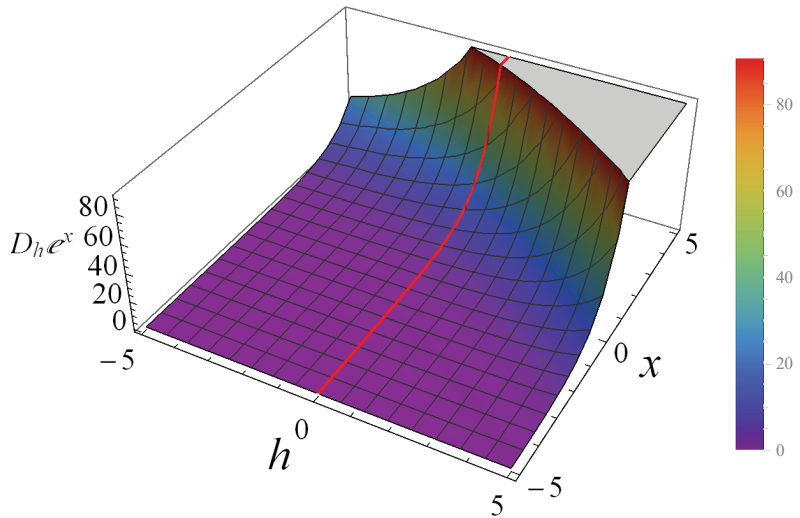
Figure 1. The behavior of $D_h e^x$ when h varying from -5 to 5. The red line denotes $(e^x)'$.

3. *h*-Derivative and Non-Additive Entropy

In order to generalize the non-additive entropic forms, one could utilize Equation (7) and give out the following equation:

$$S_h = -D_h \sum_{i=1}^{W} p_i^x \Bigg|_{x=1} = -\frac{\sum_{i=1}^{W} p_i^{1+h} - 1}{h}, \tag{21}$$

with the normalization condition $\sum_{i=1}^{W} p_i = 1$. When $h \to 0$, it will go back to the usual BG entropy. Note that it also recovers the Tsallis non-extensive entropy, S_q, cf. Equation (1) under the transformation of $h = q - 1$.

Following the ways of the central difference quotient operator of Equation (20), we define a new form of two-parameter (h, h')-derivative,

$$D_{h,h'} f(x) = \frac{f(x+h) - f(x-h')}{h+h'} \quad (h, h' \in \mathbb{R}). \tag{22}$$

The corresponding (h, h')-entropy is

$$S_{h,h'} = -D_{h,h'} \sum_{i=1}^{W} p_i^x \Bigg|_{x=1} = -\sum_{i=1}^{W} \frac{p_i^{1+h} - p_i^{1-h'}}{h+h'}. \tag{23}$$

Similarly, when $h = h' \to 0$, the entropy $S_{h,h'}$ returns to the BG one. It is shown that,

$$
\begin{aligned}
\lim_{h=h'\to 0} S_{h,h'} &= -\lim_{h=h'\to 0} \sum_{i=1}^{W} \frac{p_i^{1+h} - p_i^{1-h'}}{h + h'} \\
&= -\lim_{h=h'\to 0} \sum_{i=1}^{W} p_i \frac{e^{h \ln p_i} - e^{-h' \ln p_i}}{h + h'} \\
&= -\lim_{h=h'\to 0} \sum_{i=1}^{W} p_i \frac{e^{h \ln p_i} \ln p_i + e^{-h' \ln p_i} \ln p_i}{2} \\
&= -\sum_{i=1}^{W} p_i \ln p_i = S_{BG}.
\end{aligned}
\tag{24}
$$

Note that L'Hospital's rule has been applied within the formula $de^{\alpha x}/dx = \alpha e^{\alpha x}$ for the last step in the above.

It is constructive to explore the connections with the already known statistical distributions. For example, the Tsallis entropy is obtained by $h = q - 1, h' = 0$. While taking $h = q - 1, h' = 1 - q^{-1}$, we can obtain the Abe entropy Equation (A5) (see the discussion in the Appendix A) [17]. The non-extensive entropy given in Equation (A7) proposed by Borges and Roditi [18] (also see the Appendix A) can then be recovered with the relationship of $h = q - 1, h' = 1 - q'$. Although the non-extensive entropy of Borges and Roditi and our two-parameter (h, h')-entropy have similar forms, we gained them using different mathematical methods. Specifically, we used (h, h')-derivative developed by ourselves, which differs from the q-calculus used by Borges and Roditi. In addition to the difference in the form of expression between the two-type derivative, a conspicuous point is that our two-parameter (h, h')-derivative does not require the function $f(x)$ to be continuous and differentiable at $x = 0$.

By assuming $h' = h$, we could also obtain another new form of entropy $S_{h,h}$, which is obviously invariant under the interchange $h \leftrightarrow -h$. As a matter of fact, it is nothing new but the well-known Kaniadakis non-extensive κ-entropy [15]. Last but not least, it is set that $h' \to -h$ and $h' = -h + \delta$. Considering the limit of $\delta \to 0$ and $h' \to -h$, we could also cover the exact Shafee entropy [16,21] by taking the transformation of $q = h + 1$.

In Table 1, we summarize different entropy functions, which can be represented by this two-parameter $S_{h,h'}$ entropy through taking different values of h and h'. In addition, by choosing $h' = -1/h$ the function $S_{h,h'}$ becomes

$$
S_{h,-1/h} = -\sum_{i=1}^{W} \frac{p_i^{1+h} - p_i^{1-1/h}}{h + 1/h},
\tag{25}
$$

Note that this entropic form looks much similar to Abe entropy [17], but it is totally different in fact that Abe entropy cannot be recovered only by exchanging q and h when comparing them. Hereby, we name it the modified-Abe entropy function. Except for the entropy forms listed in Table 1, there is a well-known entropy—Renyi entropy, which can be related to $S_{h,h'}$ through the relationship between Renyi entropy and Tsallis entropy (only for $q \le 1$) [22],

$$
S_q^{\text{Renyi}} \equiv \frac{\ln \sum_{i=1}^{W} p_i^q}{1 - q} = \frac{\ln\left[1 + (1 - q) S_q^{\text{Tsallis}}\right]}{1 - q}.
\tag{26}
$$

Table 1. The two-parameter entropy $S_{h,h'}$ recovers other entropy functions by the variation of h, h'.

Entropy Type	$S_{h,h'}$
Boltzmann–Gibbs	$h = h' \to 0$
Tsallis [5]	$h = q - 1, h' = 0$ or $h = 0, h' = 1 - q$
κ [15]	$h' = h = \kappa$
(κ, r) [23]	$h = r + \kappa, h' = \kappa - r$
γ [23]	$h = 2\gamma, h' = \gamma$
Abe [17]	$h = q - 1, h' = 1 - q^{-1}$ or $h = q^{-1} - 1, h' = 1 - q$
Shafee [16,21,24]	$h' \to -h$
modified Abe	$h' = -1/h$

4. Properties

Now we shall address some properties of this (h, h')-entropy, $S_{h,h'}$. As we all know, the Boltzmann–Gibbs and the Tsallis entropy can be expressed as [6,25]

$$S_{BG} = -\langle \ln p_i \rangle = \langle \ln(1/p_i) \rangle, \quad S_q = \langle \ln_q(1/p_i) \rangle, \tag{27}$$

where $\langle \ldots \rangle \equiv \sum_{i=1}^{W} p_i (\ldots)$ is the standard mean value, and $\ln_q$ is q-logarithm. Along this line, we straightforwardly obtain

$$S_{h,h'} = \langle \ln_{h,h'}(1/p_i) \rangle, \tag{28}$$

where $\ln_{h,h'}$ is the (h, h')-logarithm, and it can be expressed as

$$\ln_{h,h'}(x) = \frac{x^{h'} - x^{-h}}{h + h'}. \tag{29}$$

4.1. Non-Negativity

First of all, we consider a thermal system within any possible state. The probability distribution of each microstate i is defined as p_i. If we assume $p_i^{1+h} \geqslant p_i^{1-h'}$, namely, $1 + h \leqslant 1 - h'$, for $0 \leqslant p_i \leqslant 1$, thus can we obtain $h + h' \leqslant 0$ and this two-parameter entropy $S_{h,h'} \geqslant 0$.

4.2. Extremal at Equal Probabilities

Utilizing the Tsallis entropy, $S_q^T = \frac{\sum_{i=1}^{W} p_i^q - 1}{1-q}$, this two-parameter entropy $S_{h,h'}$ can be expressed with it as,

$$S_{h,h'} = \frac{1}{h + h'} \left(h S_{1+h}^T + h' S_{1-h'}^T \right). \tag{30}$$

For the Tsallis entropies inside this formula, namely S_{1+h}^T and $S_{1-h'}^T$, it is easy to know that both of them reach their extreme values when all the probabilities are equal [6]. Therefore, at the state of equal probability, our entropy $S_{h,h'}$ will also approach to its extreme value since

$$\frac{\mathrm{d}}{\mathrm{d}p_i} S_{h,h'} = \frac{1}{h + h'} \left[h \frac{\mathrm{d}}{\mathrm{d}p_i} S_{1+h}^T + h' \frac{\mathrm{d}}{\mathrm{d}p_i} S_{1-h'}^T \right] = 0. \tag{31}$$

4.3. Expansibility

It is straightforwardly verified that $S_{h,h'}$ is expansible for any values of h and h', since

$$S_{h,h'}(p_1, p_2, \cdots, p_W, 0) = S_{h,h'}(p_1, p_2, \cdots, p_W). \tag{32}$$

This property trivially follows from the definition itself. It means when we add some events with zero probabilities, $S_{h,h'}$ keeps invariant.

4.4. Non-Additivity

When we consider a system that can be decomposed into two independent subsystems, A and B, ($p_{ij}^{A+B} = p_i^A p_j^B$),

$$
\begin{aligned}
S_{h,h'}(A+B) &= -\sum_{i=1}^{W_A}\sum_{j=1}^{W_B} \frac{\left(p_{ij}^{A+B}\right)^{1+h} - \left(p_{ij}^{A+B}\right)^{1-h'}}{h+h'} \\
&= S_{h,h'}(A) \cdot \sum_{j=1}^{W_B}\left(p_j^B\right)^{1+h} + S_{h,h'}(B) \cdot \sum_{i=1}^{W_A}\left(p_i^A\right)^{1-h'}.
\end{aligned}
\tag{33}
$$

The values of h and h' cannot be zero together in case (or $h = -1$ and $h' = 1$ appear at the same time). In other words, $S_{h,h'}$ is said to be non-additive similar to the Tsallis non-extensive entropy.

5. Summary and Outlook

To summarize, with the generalized h-derivative we firstly propose a two-parameter non-additive entropy, $S_{h,h'}$, in order to connect several non-extensive entropy functions. The h-derivative motivated non-additive entropy, $S_{h,h'}$, is demonstrated to recover different kinds of non-extensive entropy formalisms, such as the Tsallis entropy ($h = q - 1, h' = 0$), the Abe entropy ($h = q - 1, h' = 1 - q^{-1}$), the Borges–Roditi entropy ($h = q - 1, h' = 1 - q'$), the Kaniadakis κ-entropy ($h' = h = \kappa$) and the Shafee ($h' \to -h$ or $h' = -h + \delta$, here $\delta \to 0$) non-extensive entropy by varying values of h, h'. On the other hand, the present two-parameter entropy exhibits all the relative properties as a generalized non-extensive entropy. Furthermore, the remarkable relationship between $S_{h,h'}$ and other non-extensive entropies may cast a light on the connection of non-extensive entropy and some mathematical structures such as quantum calculus. It may lead to a deeper understanding of the mathematical and physical foundations of non-extensive statistics. We also noticed some other two-parameter distribution functions, such as the (r, q)-distribution and (α, κ)-distribution [26,27], which have been well-applied to astrophysics or space plasma physics. These two-parameter distributions provide another view to investigate the non-Maxwellian systems. It will be of great interest to associate this (h, h')-entropy with them and find out the deeper connections. There are also various elegant forms of entropy, such as fractional entropy [28] and Deng entropy [29]. Our (h, h')-entropy, $S_{h,h'}$, is indeed unable to establish a connection with theirs. Further exploration of the inherent connections between different forms of entropy is necessary.

Appendix A

S. Abe has proven an interesting property [17] that the BG entropy can be rewritten as a derivative of

$$S_{BG} = -\frac{\mathrm{d}}{\mathrm{d}x} \sum_{i=1}^{W} p_i^x \bigg|_{x=1}, \tag{A1}$$

and the Tsallis one has a similar property

$$S_q = -D_q \sum_{i=1}^{W} p_i^x \bigg|_{x=1}, \tag{A2}$$

where D_q is Jackson q-derivative [30–33],

$$D_q f(x) \equiv \frac{f(qx) - f(x)}{qx - x}. \tag{A3}$$

Abe applied the symmetric $q \leftrightarrow q^{-1}$ to give a new modified q-derivative as follows:

$$D_{q,q^{-1}} f(x) \equiv \frac{f(qx) - f(q^{-1}x)}{qx - q^{-1}x}, \tag{A4}$$

thus a symmetric modification of Tsallis entropy goes as

$$S_q^S = -\sum_{i=1}^{W} \frac{(p_i)^q - (p_i)^{q^{-1}}}{q - q^{-1}}. \tag{A5}$$

Inspired by S. Abe, Borges and Roditi define a two-parameter q-derivative [18]:

$$D_{q,q'} f(x) \equiv \frac{f(qx) - f(q'x)}{qx - q'x}, \quad q, q' \in \mathbb{R}, \tag{A6}$$

and its corresponding entropic form is

$$S_{q,q'} = -\sum_{i=1}^{W} \frac{p_i^q - p_i^{q'}}{q - q'}. \tag{A7}$$

References

1. Dauxois, T.; Ruffo, S.; Arimondo, E.; Wilkens, M. Dynamics and Thermodynamics of Systems with Long-Range Interactions: An Introduction. In *Dynamics and Thermodynamics of Systems with Long-Range Interactions*; Dauxois, T., Ruffo, S., Arimondo, E., Wilkens, M., Eds.; Springer: Berlin/Heidelberg, Germany, 2002; pp. 1–19. [CrossRef]
2. Salzberg, A.M. Exact statistical thermodynamics of gravitational interactions in one and two dimensions. *J. Math. Phys.* **1965**, *6*, 158–160. [CrossRef]
3. Montroll, E.W.; Shlesinger, M.F. Maximum entropy formalism, fractals, scaling phenomena, and 1/f noise: A tale of tails. *J. Stat. Phys.* **1983**, *32*, 209–230. [CrossRef]
4. Tsallis, C. Some comments on Boltzmann-Gibbs statistical mechanics. *Chaos Solitons Fractals* **1995**, *6*, 539–559.
5. Tsallis, C. Possible Generalization of Boltzmann-Gibbs Statistics. *J. Stat. Phys.* **1988**, *52*, 479–487.
6. Tsallis, C. *Introduction to Nonextensive Statistical Mechanics: Approaching a Complex World*; Springer: New York, NY, USA, 2009. [CrossRef]
7. Plastino, A.; Plastino, A. Non-extensive statistical mechanics and generalized Fokker-Planck equation. *Physica A* **1995**, *222*, 347–354. [CrossRef]
8. Biró, T.S.; Shen, K.M.; Zhang, B.W. Non-extensive quantum statistics with particle-hole symmetry. *Physica A* **2015**, *428*, 410–415.
9. Shen, K.M.; Zhang, B.W.; Wang, E.K. Generalized Ensemble Theory with Non-extensive Statistics. *Physica A* **2017**, *487*, 215–224.
10. Shen, K.M.; Zhang, H.; Hou, D.F.; Zhang, B.W.; Wang, E.K. Chiral Phase Transition in Linear Sigma Model with Nonextensive Statistical Mechanics. *Adv. High Energy Phys.* **2017**, *2017*, 4135329.

11. Khachatryan, V.; Sirunyan, A.M.; Tumasyan, A.; Adam, W.; Bergauer, T.; Dragicevic, M.; Erö, J.; Fabjan, C.; Friedl, M.; Frühwirth, R.; et al. Transverse-momentum and pseudorapidity distributions of charged hadrons in pp collisions at $\sqrt{s} = 7$ TeV. *Phys. Rev. Lett.* **2010**, *105*, 022002.

12. Khachatryan, V.; Sirunyan, A.M.; Tumasyan, A.; Adam, W.; Bergauer, T.; Dragicevic, M.; Erö, J.; Friedl, M.; Frühwirth, R.; Ghete, V.M.; et al. Transverse Momentum and Pseudorapidity Distributions of Charged Hadrons in pp Collisions at $\sqrt{s} = 0.9$ and 2.36 TeV. *J. High Energy Phys.* **2010**, *2010*, 41.

13. Betzler, A.S.; Borges, E.P. Nonextensive distributions of asteroid rotation periods and diameters. *Astron. Astrophys.* **2012**, *539*, A158. [CrossRef]

14. Wang, Y.; Du, J. The viscosity of charged particles in the weakly ionized plasma with power-law distributions. *Phys. Plasmas* **2018**, *25*, 062309. [CrossRef]

15. Kaniadakis, G. Non-linear kinetics underlying generalized statistics. *Physica A* **2001**, *296*, 405–425. [CrossRef]

16. Shafee, F. Generalized Entropies and Statistical Mechanics. *arXiv* **2004**, arXiv:cond-mat/0409037.

17. Abe, S. A note on the q-deformation-theoretic aspect of the generalized entropies in nonextensive physics. *Phys. Lett. A* **1997**, *224*, 326–330. [CrossRef]

18. Borges, E.P.; Roditi, I. A family of nonextensive entropies. *Phys. Lett. A* **1998**, *246*, 399–402. [CrossRef]

19. Kac, V.G.; Cheung, P. *Quantum Calculus*; Springer: Berlin/Heidelberg, Germany, 2002; Volume 113.

20. Jagerman, D.L. *Difference Equations with Applications to Queues*; CRC Press: Boca Raton, FL, USA, 2000.

21. Shafee, F. Lambert function and a new non-extensive form of entropy. *IMA J. Appl. Math.* **2007**, *72*, 785–800. [CrossRef]

22. Tsallis, C. I. Nonextensive Statistical Mechanics and Thermodynamics: Historical Background and Present Status. In *Nonextensive Statistical Mechanics and Its Applications*; Abe, S., Okamoto, Y., Eds.; Springer: Berlin/Heidelberg, Germany, 2001; pp. 3–98. [CrossRef]

23. Kaniadakis, G.; Lissia, M.; Scarfone, A.M. Two-parameter deformations of logarithm, exponential, and entropy: A consistent framework for generalized statistical mechanics. *Phys. Rev. E* **2005**, *71*, 046128.

24. Wang, Q. Extensive Generalization of Statistical Mechanics Based on Incomplete Information Theory. *Entropy* **2003**, *5*, 220–232. [CrossRef]

25. Tsallis, C. What are the numbers that experiments provide. *Quim. Nova* **1994**, *17*, 468–471.

26. Qureshi, M.N.S.; Nasir, W.; Masood, W.; Yoon, P.H.; Shah, H.A.; Schwartz, S.J. Terrestrial lion roars and non-Maxwellian distribution. *J. Geophys. Res. Space Phys.* **2014**, *119*, 10059–10067. [CrossRef]

27. Abid, A.A.; Ali, S.; Du, J.; Mamun, A.A. Vasyliunas-Cairns distribution function for space plasma species. *Phys. Plasmas* **2015**, *22*, 084507. [CrossRef]

28. Ubriaco, M.R. Entropies based on fractional calculus. *Phys. Lett. A* **2009**, *373*, 2516–2519. [CrossRef]

29. Deng, Y. Uncertainty measure in evidence theory. *Sci. China Inf. Sci.* **2020**, *63*, 210201. [CrossRef]

30. Jackson, F.H. Generalization of the differential operative symbol with an extended form of Boole's equation. *Mess. Math.* **1909**, *38*, 57.

31. Jackson, F.H. On q-definite integrals. *Quart. J. Pure Appl. Math.* **1910**, *41*, 193.

32. Ernst, T. *The History of Q-Calculus and a New Method*; UUDM Report; Department of Mathematics, Uppsala University: Uppsala, Sweden, 2000.

33. Aral, A.; Gupta, V.; Agarwal, R. *Applications of q-Calculus in Operator Theory*; SpringerLink: Bücher; Springer: New York, NY, USA, 2013.

Article

Generalizing the Wells–Riley Infection Probability: A Superstatistical Scheme for Indoor Infection Risk Estimation

Markos N. Xenakis

VTT Technical Research Centre of Finland Ltd., FI-02044 Espoo, Finland; mrksxenakis@gmail.com or markos.xenakis@vtt.fi

Abstract: Recent evidence supports that air is the main transmission pathway of the recently identified SARS-CoV-2 coronavirus that causes COVID-19 disease. Estimating the infection risk associated with an indoor space remains an open problem due to insufficient data concerning COVID-19 outbreaks, as well as, methodological challenges arising from cases where environmental (i.e., out-of-host) and immunological (i.e., within-host) heterogeneities cannot be neglected. This work addresses these issues by introducing a generalization of the elementary Wells-Riley infection probability model. To this end, we adopted a superstatistical approach where the exposure rate parameter is gamma-distributed across subvolumes of the indoor space. This enabled us to construct a susceptible (S)–exposed (E)–infected (I) dynamics model where the Tsallis entropic index q quantifies the degree of departure from a well-mixed (i.e., homogeneous) indoor-air-environment state. A cumulative-dose mechanism is employed to describe infection activation in relation to a host's immunological profile. We corroborate that the six-foot rule cannot guarantee the biosafety of susceptible occupants, even for exposure times as short as 15 min. Overall, our work seeks to provide a minimal (in terms of the size of the parameter space) framework for more realistic indoor SEI dynamics explorations while highlighting their Tsallisian entropic origin and the crucial yet elusive role that the innate immune system can play in shaping them. This may be useful for scientists and decision makers interested in probing different indoor biosafety protocols more thoroughly and comprehensively, thus motivating the use of nonadditive entropies in the emerging field of indoor space epidemiology.

Keywords: indoor biosafety; infection risk estimation; COVID-19; SEI dynamics; Tsallis entropy; superstatistics; indoor-space epidemiology

1. Introduction

As a consequence of the COVID-19 pandemic, humanity has faced an unprecedented crisis affecting every sphere of society, and causing a considerable health and economic burden. Unsurprisingly, several mitigation strategies have been proposed and implemented with the ultimate goal of controlling and, if possible, preventing the transmission of SARS-CoV-2 strains. Growing evidence suggests that air is the main pathway through which SARS-CoV-2 is transmitted [1–8]. Infection by SARS-CoV-2 is, thus, much more likely to occur indoors than outdoors. In particular, an infectious occupant can spread virus-containing aerosol particles (VCAPs) into the air via exhalation, resulting in the infection of susceptible occupants according to three main scenarios [9]: (a) the short-range airborne transmission scenario [10], where the spreader and the susceptible individual are in geometrical proximity; (b) the shared-room airborne scenario, where the spreader and susceptible individual are sharing the same indoor space, thus breathing from and exhaling into the same air container; (c) the longer-distance airborne transmission [11] scenario, where the spreader and the susceptible are not in geometrical proximity (i.e., they either do not share the same room or are far apart in an ample indoor space). Realization of any of these scenarios can trigger COVID-19 outbreaks of varying epidemiological magnitude depending on complexly interwoven biological (e.g., viral infectivity and the host's immunological preparedness) and nonbiological (e.g., indoor space geometry and ventilation

flow) factors. For example, there is a growing consensus that micrometer-sized VCAPs might underpin the transmission dynamics of so-called "superspreading events" [3,12,13], thus catalyzing the spread of SARS-CoV-2 in communities [8,14,15]. Although more than three years have passed since the beginning of the COVID-19 pandemic, the emergence of highly mutated and transmissible Omicron subvariants, such as XBB.1.5, poses significant threats to public health [16].

Mathematical modelling and simulation approaches to investigating airborne transmission indoors ultimately aim at developing comprehensive, quantitative methods for indoor infection-risk estimation (IIRE). The emergency of the COVID-19 pandemic accelerated multidisciplinary scientific efforts and provided a wealth of mathematical modelling approaches operating at various levels of abstraction, thus also claiming different degrees of biological plausibility. At a coarse-grained scale, SIR-like models can be insightful for understanding indoor infection dynamics at the occupant-group level (e.g., see [17–20]). On the other hand, refining the spatiotemporal scale leads to particle-based models attempting to shed light onto the transport mechanisms underlying airborne transmission and viral accumulation in the human body (e.g., see [21,22]). Typically, what all of these models have in common is an—at least—implicit connection between the indoor concentration (densities) of VCAPs and an infection rate parameter established via fluid mechanics. To this end, computational fluid dynamics (CFD) have been extensively applied to the study of airborne SARS-CoV-2 transmission pathways in different indoor environments (e.g., see [23–26]).

Due to the multiscale nature of the IIRE procedure, a crucial element of any modelling approach is the statistical frame upon which it relies to construct probability measures. Commonly, IIREs are obtained by either employing case-specific modifications of the classical Wells–Riley infection probability (WRIP) [27] or even developing entirely novel probabilistic approaches (e.g., see [28]). The WRIP's primary assumption, inherited from Poissonian statistics, is that of a homogeneous (i.e., well-mixed) indoor air environment, implying that the transmission range is predominantly short, and exposure events are probabilistically independent of each other. Stated differently, the WRIP is based on the idea that, under steady-state conditions, indoor-air-environment-property gradients (in short, steady-state-invariant gradients), which are the underlying cause of observed statistical distances between a well-mixed and a not well-mixed, i.e., heterogeneous, VCAP spatial configuration, can be neglected. The realization, however, that omitting effects of steady-state-invariant gradients may return underrated IIREs in the vicinity of an infectious source [29] has led many researchers to reconsidering the applicability of the WRIP scheme by carefully localising it (e.g., see [25,26,28,30,31]). In practice, this approach can yield satisfactory IIREs at locations of high epidemiological interest, e.g., the breathing zone of susceptible individuals without, however, providing any systematic way to integrate local WRIPs into a nonlocal (i.e., macroscopic) measure for evaluating the biosafety of the indoor air environment as a whole. An additional layer of complexity that, to the best of our knowledge, remains unexplored, mainly due to insufficient knowledge of the innate immune system dynamics [32], can be added here by considering the possibility of heterogeneous within-host responses to inhaled VCAPs.

In this work, we present a superstatistical [33] solution to the problem of integrating local WRIPs into epidemiologically relevant macroscopic measures in terms of a gamma mixture model encoding spatial fluctuations of the exposure rate parameter in an arbitrary indoor space volume. The decisive step is to conceptualize a spatial-epidemiology model where susceptible occupants may receive VCAPs via distinct (i.e., noninteracting) pathways under the influence of indoor-air-environment stochasticities. Accordingly, we consider local exposure rates to reflect the joint yet probabilistically independent action of intrinsically stochastic airborne transmissions occurring simultaneously, but via different spatial routes. The core assumption accompanying this kind of spatial thinking is that fast- and slow-dynamics timescales co-exist and are well-separated: in a steady-state indoor air environment, fast dynamics is given by the emission and inhalation of VCAPs, while slow dynamics describes how an indoor-air-environment-property-gradient field

may change. This implies that macroscopic changes in the VCAP (spatial) distribution occurring during a predetermined exposure period are forbidden as long as the steady-state assumption is satisfied. Our modelling procedures suggest a frameshift from Poissonian to Paretian statistics, thus leading directly to a q-exponential WRIP, with q denoting the Tsallis entropic index [34] and admitting the interpretation of the degree of heterogeneity associated with a given steady-state indoor air environment. From a spatial-epidemiology viewpoint, $q > 1$ signals a nonvanishing transmission range, thus enabling construction of a distance-sensitive susceptible (S)–exposed (E)–infected (I) dynamical model where the magnitude of the rate at which occupants are transferred from the E subgroup to the I subgroup depends on immunological traits. Specifically, the Richards growth model [35] is employed to describe the dynamical relationship among viral accumulation, infection activation, and a hypothetical innate-immune-system defence mechanism orchestrated by neutralising antibodies (NAbs), and potentially enhanced by the interferon (IFN) system (for reviews covering the crucial roles that NAbs and the IFN system play in disrupting SARS-CoV-2 pathogenesis, see [36,37], respectively). This allows for investigating the interplay between out-of-host and within-host heterogeneities in a single model that, as we show, provides a simple tool for evaluating distance-based mitigation strategies such as the six-foot rule.

2. Model Construction

2.1. Preliminaries

We consider an enclosed space of rectangular volume V (m^3) occupied by N randomly mixed individuals split into a group of susceptible individuals of size S and infectious individuals of size F. The indoor air environment was assumed to relax into a steady state. Infectious occupants act as virus spreaders by emitting VCAPs into V. Susceptible occupants can be exposed to the virus via airborne transmission, i.e., by inhaling air samples from $v_{br} < V$ containing VCAPs, with v_{br} denoting the breathing zone volume, i.e., the air volume surrounding a susceptible occupant and determining their epidemiological status. The dynamics of VCAP emission and inhalation are paced by τ_{rel}, denoting the fast-dynamics timescale. The breathing-cycle period gives the magnitude of τ_{rel}, which is ≈ 3 (s). τ_{rel} also determines the time it takes for the local equilibrium density of the indoor air particles (thus also of VCAPs) to be restored. Accordingly, perturbations in the local density of VCAPs are expected to be damped out very quickly. The time over which macroscopic environmental changes can occur, i.e., the slow-dynamics timescale, is denoted with $\mathcal{T}$. The magnitude of $\mathcal{T}$ determines the period over which an indoor-air-environment-property-gradient field might change. It is required that $\mathcal{T}/\tau_{rel} \gg 1$. The epidemiological status of susceptible occupants may be probed at any time $t' \in [t_0, t'']$, where $\tau := t'' - t_0$ (h) is the occupancy time, i.e., the total time that N occupants spend in V. It is required that $\tau < \mathcal{T}$ so that the steady-state assumption is satisfied at any t'. The average maximum time that the breathing zone of a susceptible occupant is contaminated with at least one VCAP gives the exposure time; let this be denoted with $\tau' \leq \tau$. The average maximum distance over which a VCAP can be transported during τ_{rel} delimits the transmission range; let this be denoted with ξ (m). ξ plays a similar role throughout this work to the one that the correlation length plays in superstatistical applications (e.g., see [38]). For simplicity, it is assumed that each VCAP contains an equal number of virions. An explicit connection with epidemiology is obtained via the notion of infectious quantum (IQ) (plural form abbreviation: IQa) [27] defined here as the critical number of VCAPs, Φ_{crit} (VCAPs) $\equiv 1$ (IQ), that, once deposited in the body, is expected to activate an infection.

Table 1 aims to ease the reader by presenting key parameters and highlighting their interdependencies.

Table 1. We consider two parameter sets, namely, the out-of-host set $\{N, F, V, v_{br}, \tau, r, w, W, \xi, \tau'\}$ and the within-host set $\{\Phi_{crit}, \zeta, \beta^*\}$. Out-of-host parameters r, w, and W denote the volumetric inhalation rate, the VCAP exhalation rate, and the ventilation rate, respectively, and are introduced in Section 2.2.1. Within-host parameters ζ and β^* codetermine a susceptible occupant's immunological profile and are formally introduced in Section 2.3. λ, ρ, κ, and μ may be considered summary parameters, as they are expressed as combinations of out-of- and within-host parameters. λ and ρ represent the exposure rate parameter and VCAP density, respectively, and are introduced and reinterpreted in Section 2.2.1 and Section 2.2.2, respectively. κ denotes the number of local air environments (modelled as surrounding subvolumes of volumetric size $\propto \xi^3$) determining a susceptible occupant's epidemiological status and is introduced in Section 2.2.2. μ gives the average time separating any pair of subsequent airborne transmission events and is introduced in Section 2.2.2.

Summary Param.	Out-of-Host Param.	Within-Host Param.
$\lambda = \frac{rwF}{W\Phi_{crit}}$ (1/h)	N (nr. of occupants)	Φ_{crit} (VCAPs)
$\rho = \frac{Fw}{W}$ (VCAPs/m^3)	F (nr. of infectors)	ζ (dimensionless)
$\kappa \propto \frac{v_{br}}{\xi^3}$ (dimensionless)	V (m^3)	β^* (1/h)
$\mu \propto \frac{\Phi_{crit}}{\rho}\frac{\tau'}{\xi^3}$ (h)	v_{br} (m^3)	
	τ (h)	
	r (m^3/h)	
	w (VCAPs/h)	
	W (m^3/h)	
	ξ (m)	
	τ' (h)	

2.2. Airborne Exposure Risk Statistics

2.2.1. Homogeneous Indoor Air Environment

If the indoor air environment is homogeneous (for a geometric description of a homogeneous indoor air environment, see Appendix A.1, a series of exposure events realised anywhere in V can be thought of as a Poisson process, where the probability that any pair of subsequent exposure events are timely separated by $t = t' - t_0$ is given by the exponential probability density function (PDF):

$$p(t|\lambda) = \lambda \exp(-\lambda t), \tag{1}$$

where λ (1/h) is a macroscopic rate designating the speed at which individuals are exposed to the virus via airborne transmission. It is common practice to consider substitution $\lambda = r\frac{Fw}{W\Phi_{crit}}$, where $w > 0$ (VCAPs/h) is the rate at which VCAPs are emitted into V by an infectious occupant (i.e., VCAP exhalation rate), $r > 0$ (m^3/h) is the rate at which a susceptible occupant breathes air from V (i.e., volumetric inhalation rate), and $W > 0$ (m^3/h) is the rate at which clean air is supplied to V by a ventilation system [27]. The total number of VCAPs exhaled and inhaled during t by infectious and susceptible occupants is then given by Fwt and λt, respectively, and the steady-state VCAP density reads [27]

$$\rho = \frac{K}{V} = \frac{Fw}{W} \tag{2}$$

from which it follows that

$$\lambda = r\frac{\rho}{\Phi_{crit}}. \tag{3}$$

The cumulative distribution function (CDF) associated with Equation (1) gives the classical WRIP [27]:

$$P(t|\lambda) = 1 - \exp(-\lambda t), \tag{4}$$

which is assumed to serve as a good approximation for the ratio $\frac{E}{S}$ [27], i.e., $P(t|\lambda) \approx \frac{E}{S}$, where E represents the number of susceptible occupants exposed to the virus after spending t time in V (in short, exposed occupants). For $t = 1$ and $\lambda = 1$, (4) returns an exposure risk of $\approx 63.2\%$, namely, $\approx 63.2\%$ of susceptible occupants have been exposed to the virus.

2.2.2. Heterogeneous Indoor Air Environment

If the indoor air environment is heterogeneous (for a geometric description of a heterogeneous indoor air environment, see Appendix A.1, getting a similar closed-form expression for the WRIP to (4) requires updating our knowledge concerning the location of VCAPs in V. The first step in this direction is to refine the spatial resolution of the IIRE procedure on the basis of our knowledge concerning the value of ξ (to gain some insight on what the order of magnitude of ξ might be, see Appendix A.1, relationship (A2)). For this, let us assume that V can be partitioned into $\Omega \in \mathbb{Z}_+$ nonoverlapping cubic subvolumes of size

$$v = \frac{V}{\Omega} \quad (\text{m}^3), \tag{5}$$

where Ω is chosen, so that $\sqrt[3]{v} \propto \xi$ (for an illustration, see Figure 1). With Equation (5) at hand, we can express K as $K = \sum_i^{\Omega} k_i$, where k_i gives the number of VCAPs suspended in the i-th subvolume. By doing so, we have silently introduced a random variable, namely, the random variable k accounting for fluctuations of the local VCAP number, i.e., of the number of VCAPs suspended in a v-sized subvolume. Accordingly, k_i denotes the i-th realisation of k. No assumption concerning the PDF of k is made except by requiring that the mean value of k be given by

$$\langle k \rangle = \frac{1}{\Omega} \sum_i k_i = \frac{K}{\Omega}, \tag{6}$$

where angular brackets $\langle \cdot \rangle$ indicate that the mean value calculation was performed over Ω subvolumes. k can only weakly fluctuate over τ_{rel}; specifically, large-amplitude fluctuations of k are only allowed over the slow-dynamics timescale $\mathcal{T}$, since steady-state indoor-air-environment conditions are assumed.

Given k, let us now also introduce a local version of Equation (3):

$$\lambda_i = r \frac{\rho_i}{\Phi_{crit}}, \quad \rho_i = \frac{k_i}{v}, \tag{7}$$

where, like k_i, λ_i represents a realisation of a random variable, namely, of the exposure rate random variable, λ, which accounts for local fluctuations of the exposure rate parameter. Stated differently, λ is no longer a mere phenomenological construct (as it was considered in Section 2.2.1), but it has acquired a new, microscopic interpretation: it is distributed across v-sized subvolumes with some probability $f(\lambda)$ that is shaped by steady-state-invariant gradients. Hence, like k, λ can only weakly fluctuate over τ_{rel}, since large-amplitude fluctuations of λ are forbidden during $\mathcal{T}$.

In light of (7), obtaining a macroscopic estimation for exposure risk statistics requires the calculation of marginal probability:

$$p(t) = \int_0^\infty d\lambda f(\lambda) p(t|\lambda), \tag{8}$$

which returns the mean value of $p(t|\lambda)$ over $f(\lambda)$ for a given t, with $f(\lambda)p(t|\lambda)$ denoting the joint probability (i.e., the probability for a pair of subsequent exposure events to be timely separated by t given a certain value of λ). The CDF corresponding to (8) is given by

$$P(t) = \int_0^\infty d\lambda \, f(\lambda) P(t|\lambda). \tag{9}$$

This serves as a generalisation of (4), in the sense that it quantifies the probability for a susceptible occupant to become exposed to the virus after spending t hours in a heterogeneous indoor air environment.

A question that naturally arises is what an epidemiologically motivated choice for $f(\lambda)$ could be. In what follows, we attempt to answer this question under the macroscopic constraint that the mean value of λ, $\langle\lambda\rangle$, equals $r\rho/\Phi_{crit}$, i.e., $\langle\lambda\rangle = r\rho/\Phi_{crit}$.

Plausibly, an exposure event can be thought of as the outcome of κ airborne transmissions, which do not necessarily result in the inhalation of the same amount of VCAPs. Accordingly, κ is defined as a dimensionless quantity describing the number of air samples of size v inhaled during τ', i.e.,

$$\kappa := r/\psi, \quad \psi = v/\tau', \quad \tau' > 0, \tag{10}$$

where ψ (m^3/h) re-scales r with respect to the epidemiologically relevant parameters v and τ'. Within a spatial-epidemiology context, κ is interpreted as the number of v-sized subvolumes surrounding a susceptible occupant, thus determining their epidemiological status (see Figure 1). Consequently, κv gives the volumetric size of an occupant's breathing zone, i.e., $v_{br} = \kappa v = r\tau'$. Continuing this line of thought, the κ-th surrounding subvolume is supposed to act as an airborne transmission pathway by facilitating routes through which suspended VCAPs can reach the nearest susceptible occupant. The rate at which VCAPs are transmitted via the κ-th subvolume to the nearest susceptible occupant is determined by a random variable; let it be denoted with x (1/h). We refer to x as the transmission rate, and we note that x essentially corresponds to the κ-th spatial component of λ, i.e., $\lambda \sim \sum_{i=1}^\kappa x_i, \kappa \in \mathbb{Z}_+$. Introduction of x highlights the fact that the transmission of VCAPs is an intrinsically stochastic process that can occur over a wide range of timescales averaging $1/\langle x\rangle$, where $\langle x\rangle > 0$ denotes the mean value of x. Assuming that the κ-th transmission event is probabilistically independent of all the others (which, in turn, implies that the κ-th pathway is not interacting with any of the other $\kappa - 1$ pathways), and that the transmission of a small number of VCAPs is more likely than the transmission of a large number of VCAPs, the simplest function that can be chosen for describing the PDF of x across v is the following exponential:

$$h(x|\mu) = \mu \exp(-\mu x), \tag{11}$$

where parameter $\mu = \frac{1}{\langle x\rangle}$ (h) denotes the average time separating any two transmission events and is defined as follows:

$$\mu := \tau' \frac{\Phi_{crit}}{\langle k\rangle}, \tag{12}$$

where the ratio $\frac{\langle k\rangle}{\Phi_{crit}}$ gives the local IQ number (i.e., the average size for an IQa dose). Like λ, x can only weakly fluctuate over τ_{rel}, so that changes in the functional shape of $h(x|\mu)$ during $\mathcal{T}$ are insignificant. From (12), it follows that $\langle x\rangle$ can be expressed as follows:

$$\langle x\rangle = \frac{\langle k\rangle}{\Phi_{crit}} \frac{1}{\tau'} \stackrel{(7)}{=} \frac{K}{\Omega\Phi_{crit}} \frac{1}{\tau'} \stackrel{(5)}{=} \frac{K}{V\Phi_{crit}} \frac{v}{\tau'} \stackrel{(3)}{=} \frac{\rho}{\Phi_{crit}} \psi \tag{13}$$

Given (10) and (13), the simplest possible functional form that one can assign to f so that $\lambda \sim \sum_{i=1}^{\kappa} x_i$ is guaranteed is that of a gamma distribution [39] of the form:

$$f(\lambda) = \frac{\mu^{\kappa} \lambda^{\kappa-1} \exp(-\mu\lambda)}{\Gamma(\kappa)} \tag{14}$$

with $\Gamma(\cdot)$ being the gamma function,

$$\langle \lambda \rangle = \frac{\kappa}{\mu} = r\frac{\rho}{\Phi_{crit}} \tag{15}$$

denoting the mean value of λ (note that $\langle \lambda \rangle$ satisfies the initially imposed macroscopic constraint), and $\text{Var}(\lambda) = \frac{\kappa}{\mu^2}$ denoting the variance in λ. For $\kappa = 1$ (14) becomes identical with (11) implying that $v_{br} = v$ (see Figure 1). When (14) is substituted into (8), we get:

$$p(t) = \frac{\kappa\mu^{\kappa}}{(t+\mu)^{\kappa+1}} \tag{16}$$

corresponding to a Pareto Type II distribution [40] with CDF:

$$P(t) = 1 - (1 + \frac{t}{\mu})^{-\kappa}. \tag{17}$$

For $t = 1$, $\mu = 1$, and $\kappa = 1$, (17) returns an exposure risk of 50% (i.e., 50% of susceptible occupants were exposed to the virus). To show that (17) serves as a generalisation of (4) one simply has to calculate $P(t)$ while having ψ be vanishingly small, i.e.,

$$\begin{aligned}
\lim_{\psi \to 0} P(t) &= 1 - \lim_{\psi \to 0}(1 + \frac{t}{\mu})^{-\kappa} \\
&\overset{(10)(13)}{=} 1 - \lim_{\psi \to 0}(1 + \frac{\rho\psi}{\Phi_{crit}}t)^{-r/\psi} \\
&= 1 - \exp(-\frac{r\rho}{\Phi_{crit}}t) \\
&= 1 - \exp(-\langle\lambda\rangle t) \equiv (4),
\end{aligned} \tag{18}$$

which is achieved by taking either $v \to 0$ or $\tau' \to \infty$.

Taking (7) and (14) together implies that k is realised by a rescaled (by a factor of $c = \Phi_{crit}v/r$) gamma distribution, i.e.,

$$g(k) = \frac{o^{\kappa}k^{\kappa-1}\exp(-ok)}{\Gamma(\kappa)}, \quad o = \frac{\mu}{c} = \frac{r\mu}{\Phi_{crit}v} \overset{(12)}{=} \frac{\kappa}{\langle k \rangle}, \tag{19}$$

with the required mean value $\langle k \rangle = \frac{\kappa}{o} = \frac{K}{\Omega}$, and variance $\text{Var}(k) = \frac{\kappa}{o^2} = \frac{\langle k \rangle^2}{\kappa}$.
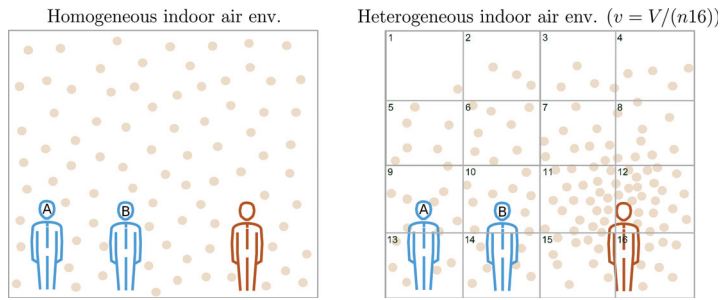
Figure 1. Schematic illustration of the proposed spatial-epidemiology model. We consider an indoor space of volume V occupied by one infector (i.e., $F = 1$) and two susceptible (i.e., $S_0 = 2$) individuals, shown in red and blue, respectively. Round dots represent steady-state VCAP densities in V. The classical WRIP scheme assumes that the indoor air environment is homogeneous, i.e., that VCAPs are roughly uniformly spaced in V (see subfigure on the **left**). On the other hand, the generalized WRIP scheme does not rely on the homogeneity assumption (e.g., as we can see in the subfigure on the **right**, VCAP density can be higher near an infectious source). To systematically capture deviations from homogeneity, we partition V into $i = 1, 2, \ldots, \Omega = n16$ subvolumes of size $v = V/\Omega$, where n denotes the number of subvolume layers used to fill V. For clarity, we illustrate only the front layer containing the first 16 subvolumes (subvolume boundaries are highlighted in black). Supposing that the epidemiological status of susceptible occupants is determined by a single surrounding subvolume (i.e., if $\kappa = 1$), then the subvolumes indexed with $i = 9$ and $i = 10$ correspond to the breathing zones of susceptible occupants A and B with $\lambda_9 = x_9$ and $\lambda_{10} = x_{10}$, respectively, representing the values of the corresponding realizations of λ with $\lambda \sim \text{Gamma}(1, \mu) = \text{Exp}(\mu)$ (see Equations (11) and (14)).

2.3. Infection-Activation Considerations

Once inside the body, SARS-CoV-2 can enter cells located on the surface of the upper respiratory tract via binding to the angiotensin-converting enzyme 2 (ACE2) receptor [41]. High replication levels during the first hours following exposure are correlated with the risk of developing symptomatic disease [42]. Although biological details concerning infection activation remain largely unknown, knowledge gained from long-lasting superspreading events, such as the Skagit Valley Chorale choir practice [13], suggests that a prolonged exposure time increases the risk of symptomatic disease. The critical size of the cumulative viral dose that could activate an infection leading with high certainty to symptomatic disease is impossible to measure. Nevertheless, it was recently suggested that the interplay between the size of the cumulative viral dose and the efficiency of the innate immune system plays a crucial role in determining the course of infection and disease severity [43]. Anti-SARS-CoV-2 NAbs are at the frontlines of the innate immune system, since they can inhibit the binding of the virus to the ACE2 receptor, thus offering protective immunity against SARS-CoV-2 infection [36,44,45]. In this work, we assume that infection activation is a necessary but not sufficient condition for the development of symptomatic disease.

The average number of IQa inhaled after spending t hours in V, i.e., the average size for the cumulative IQa dose up to time t, can be estimated with

$$\Phi = \int_{t_0}^{t'} dz \langle \lambda \rangle \overset{*}{=} \langle \lambda \rangle t \tag{20}$$

($*$ is a reminder that this equality holds only under steady-state indoor-air-environment conditions). Without loss of generality, a relationship between Φ and a hypothetical NAb-orchestrated antiviral defence mechanism can be obtained via the following generalised logistic differential equation:

$$\frac{dR}{d\Phi} = aR\left(1 - R^\zeta\right), \tag{21}$$

which is known as the Richards growth model [35], where $R \in [R_0, R_{\Phi \to \infty} = 1)$ is a hypothetical infection-activation biomarker, $R_{\Phi \to \infty}$ denotes the upper asymptotic bound of R, $R_0 > 0$ is the initial condition for R, $a > 0$ is the rate of change of R with respect to Φ, and $\zeta > 0$ is a dimensionless exponent accounting for host susceptibility. Concretely, ζ is considered inversely correlated with the neutralising capacity of NAbs. Hence, the larger ζ is, the smaller the neutralising capacity of NAbs is expected to be, which, in turn, implies a lower degree of protective immunity against SARS-CoV-2 infection. The solution of (21) reads

$$R = [1 + A \exp(-a\zeta(\Phi - \Phi_0))]^{-1/\zeta}, \quad A = R_0^{-\zeta} - 1, \quad \Phi_0 = \langle \lambda \rangle t_0. \tag{22}$$

A connection with the notion of IQ is established by requiring that the inflection point of (22)

$$\Phi_{infl} = \frac{\ln\left(\frac{A}{\zeta}\right)}{a\zeta} + \Phi_0, \tag{23}$$

is equal to $1/\zeta$, i.e.,

$$\Phi_{infl} = 1/\zeta \implies a = \frac{\ln\left(\frac{A}{\zeta}\right)}{1 - \zeta\Phi_0}. \tag{24}$$

Φ_{infl} designates the Φ value for which R attains its maximum value. Qualitatively, Φ_{infl} can be understood as the beginning (with respect to Φ) of R's asymptotic convergence towards $R_{\Phi \to \infty}$. From a disease biology viewpoint, Φ_{infl} represents a threshold value of "no return" that, once surpassed, signals a high likelihood for infection activation. For $\zeta = 1$, we have that $\Phi_{infl} = 1 = \Phi_{crit}$, implying that one IQ suffices for infection activation. Accordingly, if $\zeta > 1$ ($\zeta < 1$), then the host is considered to exhibit low (high) NAb-attributed preparedness since $\Phi_{infl} < \Phi_{crit}$ ($\Phi_{infl} > \Phi_{crit}$). Φ_{infl} can, thus, be understood as a personalised estimation for the number of IQa required to activate an infection. This can be tuned to match an occupant's immunological profile.

2.4. Indoor Infection Dynamics

Following [27], let us now claim that $(17) = \frac{E}{S}$. Then, for the initial condition $S_0 = N - F > 0$, the decrease in the number of susceptible occupants (or the increase in the number of exposed occupants) under steady-state indoor-air-environment conditions is given by

$$\frac{E}{S_0} = \frac{S_0 - S}{S_0} = 1 - (1 + \frac{t}{\mu})^{-\kappa} \implies S = S_0(1 + \frac{t}{\mu})^{-\kappa}, \tag{25}$$

which for a sufficiently small time step dt becomes the solution of the following differential equation [46,47]:

$$\frac{dS}{dt} = -\alpha S^q = -\frac{dE}{dt}, \quad \alpha := \frac{\langle \lambda \rangle}{S_0^{q-1}}, \quad q := 1 + 1/\kappa, \tag{26}$$

where α is the "effective" [46,47] exposure rate, and q is the Tsallis entropic index [34]. Equation (25) can be derived by maximising the Tsallis entropy functional [46,47]:

$$\mathcal{S}[S] = -\frac{\int_{t_0}^{t''} S(1 - S^{q-1}) dt}{1 - q} \tag{27}$$

subject to constraints $\mathcal{L}_1 = \int_{t_0}^{t''} S \, dt$ and $\mathcal{L}_2 = \int_{t_0}^{t''} tS^q \, dt$, where $\mathcal{L}_1$ and $\mathcal{L}_2$ are Lagrange multipliers with their values being manually adjusted so that the desired values for S_0 and $\langle \lambda \rangle$, respectively, may be obtained [46].

By using (22), we may now extend (26) to account for an I subgroup representing exposed occupants who are expected to develop symptomatic disease. We consider R to

determine the value of a hypothetical infection rate β (1/h), delimiting the speed at which occupants are transferred from the E subgroup to the I subgroup, i.e.,

$$\beta := \beta^* R, \tag{28}$$

where $\beta^* > 0$ (1/h) rescales R and imposes an upper asymptotic bound on β. Generally, β^* can be thought of as being inversely correlated with the rate at which successful IFN-system-driven immune responses take place (for the crucial role that the IFN system can play during the first hours following infection activation, see [42]). Hence, its value determines whether an initially activated infection is sustained or not. Altogether, our modelling considerations lead us to the following set of ordinary differential equations (ODEs) describing the indoor infection dynamics of S_0 in V:

$$\begin{aligned}
\frac{dS}{dt} &= -\alpha S^q \\
\frac{dE}{dt} &= \alpha S^q - \beta E \\
\frac{dI}{dt} &= \beta E,
\end{aligned} \tag{29}$$

for $S_0 = N - F, E_0 = 0, I_0 = 0, N = \text{const}, F = \text{const}.$

Stability analysis of the system of ODEs described in (29) is trivial; for $t \to \infty$, all occupants were expected to have been transferred to the I subgroup, i.e., $(S_{t\to\infty} \to 0, E_{t\to\infty} \to 0, I_{t\to\infty} \to N - F)$ is the unique equilibrium point globally attracting from within the positively invariant region $\{(S, E, I) \mid S + E + I \leq N - F\}$.

The presented SEI model belongs, from a mathematical point of view, to the class of q-$SEIR$ models recently introduced in [19].

The numerical integration of (29) was performed in Python [48] by employing a Runge–Kutta method of order 5(4) [49].

3. Insights Gained from Computational Analysis

3.1. Scrutinising the Generalised WRIP

To better understand the implications for indoor biosafety stemming from (17), we may focus on (18). We set $r = 1$, and considered the case where K VCAPs were suspended in V with $\langle \lambda \rangle = 1$ so that $\frac{Fw}{W\Phi_{crit}} = \frac{\rho}{\Phi_{crit}} = 1$. With this choice of parameters, we gain some insight into how (17) approaches (4), and how $f(\lambda)$ and $g(k)$ behave for decreasing the transmission range ξ while keeping the exposure time τ' (and, thus, also v_{br}) fixed.

As we can see in Figure 2a, for a vanishingly small ξ (i.e., $v \to 0$), (4) approaches its upper asymptotic bound, which is given by (17). Simply put, the classical WRIP is an overestimation of the exposure risk justified on the basis that, in the absence of any substantial knowledge concerning fluctuations of λ, the worst-case scenario may be assumed, namely, that any realisation of λ would be approximately equal to $\langle \lambda \rangle$. The necessary condition supporting this simplification is that the VCAP density is very large, i.e., K and V should be very large and small, respectively (see also Appendix A.1). On the other hand, the generalised WRIP returns a lower but more realistic estimation for the exposure risk on the basis of the expectation that $f(\lambda)$ may be well-approximated in terms of a gamma distribution. In fact, (17) serves as a more "fair" IIRE, in the sense that the chance for an occupant to become exposed to the virus after spending one hour in V is the same as tossing an unbiased coin, namely, 50% (see Figure 2a). In particular, the difference between the classical and the generalised WRIP at $t = 1$ decreases from ≈ 0.13 to ≈ 0.01 if one considers a tenfold increase in the number of subvolumes Ω (see Figure 2b and the corresponding legend text).
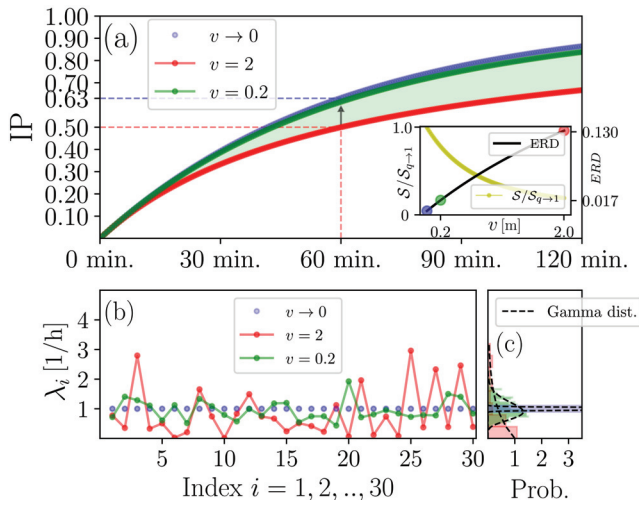
Figure 2. Classical WRIP as an upper asymptotic bound of its generalisation. (**a**), we plot (17) for $\mu = 1/\psi$ and $\kappa = 1/\psi$ with $\tau' = \tau = 2$ and $v \in (0, 2]$ (i.e., $\psi \in (0, 1]$). The black arrow indicates that the generalised WRIP measure approaches the classical one as v decreases. The shaded area between the two curves visualises the image of the generalised WRIP function for $\psi \in (0, 1]$. An estimation of the exposure risk difference (ERD), i.e., the difference between the generalised and the classical WRIP measures, calculated by $(1 + \frac{t}{\mu})^{-\kappa} - \exp(-t)$ for $v \in (0, 2]$ and $t = 1$ (=60 min) is shown in the inset graph. Colorful markers in the inset graph indicate the v key values considered in (**a**). In the same inset graph, the ratio $\mathcal{S}/\mathcal{S}_{q \to 1}$ is plotted, where $\mathcal{S}$ is calculated by using the discretised version of (27) and with $\mathcal{S}_{q \to 1}$ denoting the Boltzmann–Gibbs entropy (see Appendix A.3, Equations (A3) and (A4), respectively). (**b**), for a hypothetical volume of size $V = 60$, we plot $i = 1, 2, \ldots, 30$ randomly-chosen realisations of λ for $v \to 0$, $v = 0.2$, and $v = 2$ implying that $\Omega \to \infty$, $\Omega = 300$, and $\Omega = 30$, respectively, since $v = \frac{V}{\Omega}$ (see (5)). (**c**), The corresponding gamma distributions are shown. Different colors are used to visualise the distributions obtained for the key values appearing in (**a**,**b**).

The information content of an S trace is measured in terms of q entropy $\mathcal{S}$ (see Equation (27)) that, as we can see in the inset of Figure 2a, is inversely correlated with ξ. The loss of S-trace-related information with increasing ξ accounts for the degree of viral dispersity in V quantified in terms of the reciprocal of κ, $1/\kappa \propto \frac{\xi^3}{v_{br}}$. Intuitively, we may understand $1/\kappa$ as a rough indicator for the likelihood that a suspended VCAP misses its target due to either the smallness of v_{br} or the largeness of ξ (or both). Of particular interest is the case where ξ is large since, as we show in Figure A1 found in Appendix A.2, it may support a contaminated-air-sharing scenario where a pair of susceptible occupants are competing for the same IQa dose, i.e., a suspended VCAP could potentially reach any two susceptible occupants during τ_{rel}. Thus, one might anticipate that S-trace-related information losses associated with a composite epidemiological system $A \oplus B$ (where A and B may represent any two susceptible occupant subgroups (or "subsystems")) should be proportional to $1/\kappa$. Indeed, because $\mathcal{S}$ is nonadditive, we have that

$$\mathcal{S}[A \oplus B] = \mathcal{S}[A] + \mathcal{S}[B] - (1 - q)\mathcal{S}[A]\mathcal{S}[B]$$
$$= \mathcal{S}[A] + \mathcal{S}[B] - \frac{\mathcal{S}[A]\mathcal{S}[B]}{\kappa} \implies \tag{30}$$
$$\mathcal{S}[A \oplus B] - (\mathcal{S}[A] + \mathcal{S}[B]) \propto \frac{\xi^3}{v_{br}}\mathcal{S}[A]\mathcal{S}[B],$$

where $A := \{p_i^{(A)}\}, i = 1, 2, \ldots, W_A$, $B := \{p_j^{(B)}\}, j = 1, 2, \ldots, W_B$, and $A \oplus B := \{p_{i,j}^{(A \oplus B)} = p_i^{(A)} p_j^{(B)}\}$ are time-step-specific probabilities of escaping exposure introduced while dis-

cretising $\mathcal{S}$ (see Appendix A.3, Equation (A3)), and the term $\frac{\mathcal{S}[A]\mathcal{S}[B]}{\kappa}$ quantifies the losses in $\mathcal{S}$-trace-related information due to potential realisation of a contaminated-air-sharing scenario involving A and B as a pair. This is summarised in terms of the Tsallis entropic index q: for $v \to 0$ (i.e., $1/\kappa \to 0$), we have that $q \to 1$, indicating that indoor-air-environment homogeneity is restored. In turn, this implies that the information content of S is maximised, i.e., the Boltzmann–Gibbs entropic functional is recovered (see Appendix A.3, Equation (A4), and Figure 2b), and the likelihood of pairwisely sharing contaminated air is negligible.

To gain more insight into how steady-state-invariant gradients shape the statistics of λ and k, the asymptotes of $f(\lambda)$ and $g(k)$, respectively, are deduced. First, for $v \ll 1$, we have that

$$
\begin{aligned}
\sqrt{\mathrm{Var}(\lambda)} \ll \langle \lambda \rangle \quad \text{(a)} \\
\sqrt{\mathrm{Var}(k)} \ll \langle k \rangle \quad \text{(b)}
\end{aligned}
\tag{31}
$$

since $\langle \lambda \rangle \not\propto v$ (because $\langle \lambda \rangle$ is macroscopically constrained by construction) and $\sqrt{\mathrm{Var}(\lambda)} \propto v$, and $\langle k \rangle \propto v$ and $\sqrt{\mathrm{Var}(k)} \propto v^3$ apply, respectively. Inequality (a) in (31) implies that $f(\lambda)$ resembles a Gaussian distribution of the form [50]:

$$
\frac{\mu^\kappa}{\Gamma(\kappa)}\exp(-\frac{\mu^2}{2\kappa}(\lambda - \langle \lambda \rangle)^2) \propto \frac{v^{-1/v}}{\Gamma(1/v)}\exp(-\frac{1}{2v^2}(\lambda - \langle \lambda \rangle)^2)
\tag{32}
$$

(see Figure 2c, green distribution), and, eventually, approaches the Dirac delta distribution located at $\langle \lambda \rangle$, i.e.,

$$
f_{v \to 0}(\lambda) = \delta(\lambda - \langle \lambda \rangle)
\tag{33}
$$

is the asymptote of $f(\lambda)$ (see Figure 2c, blue distribution). Equation (33) sets the basis for constructing classical WRIPs (see Figure 2c). In fact, plugging $f_{v \to 0}(\lambda)$ into (9) gives (4).

Let us now turn our attention to Inequality (b) in (31). Its main implication is the same as previously: $g(k)$ can be approximated with the Gaussian distribution of the form [50]:

$$
\frac{o^\kappa}{\Gamma(\kappa)}\exp(-\frac{o^2}{2\kappa}(k - \langle k \rangle)^2) \propto \frac{v^{-2/v}}{\Gamma(1/v)}\exp(-\frac{1}{2v^3}(k - \rho v)^2)
\tag{34}
$$

(see Figure 3, green distribution), and, eventually, approaches the Dirac delta distribution located at zero, i.e.,

$$
g_{v \to 0}(k) = \delta(k)
\tag{35}
$$

is the asymptote of $g(k)$ (see Figure 3, blue distribution). Equation (35) tells us that V is partitioned into an infinite number of subvolumes, each containing an infinitesimally small number of VCAPs. This is because the mean value and variance of $g(k)$ are proportional to v and v^3, respectively, so that $g(k)$ is translocated towards the origin while at the same time becoming increasingly narrow as v decreases for some finite value of K (see Figure 3). For $v \to 0$, it is, thus, almost certain to find an infinitesimally small amount of VCAPs anywhere in V as if VCAPs were molecules of a well-mixed gas [27].
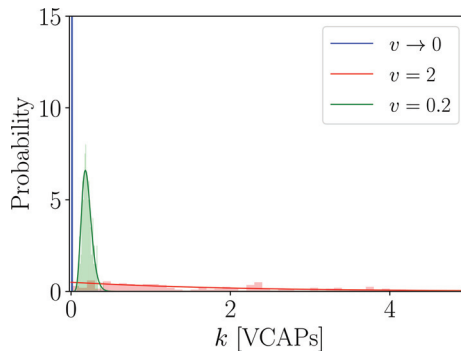
Figure 3. Instances of a VCAP distribution. We plot $g(k)$ for $\mu = 1/\psi$ and $\kappa = 1/\psi$ with $\tau' = \tau = 2$ and $v \in (0,2]$ (i.e., $\psi \in (0,1]$).

3.2. Refining the IIRE

Of particular epidemiological interest is understanding how IIREs depend not only on indoor-air-environment properties, but also on personalised immunological traits. Towards this end, we may utilise the *SEI* model described by (29) as a simple tool to probe different scenarios. In Figure 4, we demonstrate how our model refines the IIRE procedure in the sense that the classical WRIP is now represented in terms of two additive components incorporating out-of-host and within-host information, namely, *E* and *I*, respectively, so that $E + I \to S_0(1 - \exp(-\langle\lambda\rangle t))$ for $v \to 0$. Normalising *SEI* traces over S_0 turns them into personalised biosafety scores returning the *t*-dependent probabilities $\{s := S/S_0, e := E/S_0, i := I/S_0\}$ of escaping exposure, being exposed, and getting infected (i.e., developing symptomatic disease sometime in the near future), respectively. Decreasing the value of the host susceptibility parameter ζ translocates the *I* trace towards the origin, thus decelerating the transfer of occupants from the *E*-subgroup to the *I*-subgroup (see Figure 4 and the corresponding legend text) since infection activation is efficiently suppressed due to a high degree of protective immunity. This reflects the action of NAbs and is manifested as a decelerated increase in a hypothetical infection-activation biomarker, *R* (see (22)), induced by translocating inflection point Φ_{infl} away from the origin as ζ decreases (see the inset graph in Figure 4a). As one might expect, the rate of IFN-system-driven successful responses, β^*, sets the speed at which occupants are transferred from the *E* subgroup to the *I* subgroup (compare Figure 4a and Figure 4b). In principle, however, the value of β^* is unknown in the IIRE procedure; it may exhibit nontrivial time dependencies over viral replication dynamics and the host's immunological profile.

3.3. Evaluation of the Six-Foot Rule

We now demonstrate how our modelling procedures can aid in designing and testing distance-based mitigation strategies specifically targeting indoor spaces. We focused on how changes in the $\{\kappa, \zeta, \beta^*\}$ triplet affect *SEI* dynamics under different steady-state VCAP density conditions. As a concrete example, we scrutinise the effectiveness of the six-foot rule, which dictates that the maximum number of occupants should be $N_{max} = \sqrt{length \cdot width}/d_{safe}$, $V = length \cdot width \cdot height$, where $d_{safe} = 1.8 \ (\approx 6 \text{ ft})$ is the minimal distance to be kept at all times between any two occupants to guarantee biosafety. To cover the worst-case scenario, we require that (a) the average maximum distance over which virions can be transmitted is determined by the minimal distance separating any pair of occupants, i.e., $\xi = d_{safe}$, and (b) the breathing zones of susceptible occupants are uninterruptedly contaminated, i.e., we set $\tau' = \tau$, so that ψ was minimised. On this basis, we proceeded with collecting $i_\tau := i(t = t'')$ values for $\tau = 0.25, 0.5, 0.75, 1$, and $r = 0.54, 1.38, 3.30$ (breathing rates values correspond to the mean values reported for the activities of standing, light exercise, and heavy exercise, respectively [51]), and analyse their functional dependence over ρ for different values of $\{\zeta, \beta^*\}$.
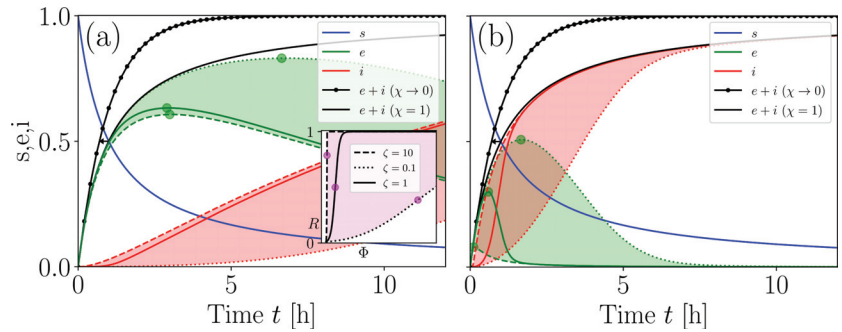
Figure 4. Refined biosafety scoring. (**a**), *s*, *e*, *i* traces are plotted for $\mu = 1/\psi$ and $\kappa = 1/\psi$ with $v = \tau' = \tau = 12$ (i.e., $\psi = 1$), $\beta^* = 0.1$, $R_0 = 0.01$, and $\zeta \in [0.1, 10]$. The shaded areas highlight the images of the E and I for $\zeta \in [0.1, 10]$. Green circular markers highlight the maxima of E (their values and locations both decreased with increasing β, indicating that the transfer of occupants from the E subgroup to the I subgroup was accelerated). The black arrow indicates that the sum $E + I$ approached the classical WRIP for $v \to 0$. Φ-dependent dynamics of R are illustrated in the inset graph. Magenta points in the inset graph highlight R values corresponding to the tunable inflection point $\Phi_{infl} = 1/\zeta$. The shaded area in the inset graph visualises the image of R for $\zeta \in [0.1, 10]$. The main and inset graphs use the same line styles to account for $\zeta = 0.1, 1, 10$. (**b**), same as (**a**), but for $\beta^* = 10$.

First, we focus on how i_τ traces behave as functions of ρ for $\zeta \in [\zeta_{min}, \zeta_{max}]$ and $\beta^* = 1$. We rely on the existence of an inflection point ρ_{infl} marking the location where the change from convex to concave in an i_τ trace takes place for increasing ρ. For small values of ζ (strong protective immunity), ρ_{infl} is translocated away from the origin, thus decelerating the increase in i_τ (see Figure 5a,c,e). On the other hand, for large values of ζ (weak protective immunity), i_τ exhibits a steep increase for $\rho < \rho_{infl}$ with ρ_{infl} being located very close to the origin (see Figure 5a,c,e). For $\rho > \rho_{infl}$, a saturation i_τ plateau is gradually formed due to epidemiological spatiotemporal constraints imposed by the magnitude of ψ (see Figure 5a,c,e and the corresponding inset graphs). Specifically, there is a large value of ρ, let this be $\rho^* > \rho_{infl}$, for which i_τ traces converge (i.e., the range within which $i_{\tau;\rho \geq \rho^*}$ values lie tends to be vanishingly small) irrespective of what the value of ζ is (see Figure 5a,c,e, and the corresponding inset graphs). This regime emerges when local VCAP densities are so high that protective immunity is inadequate in counteracting the viral threat, i.e., $k_i \gg \Phi_{infl}$; consequently, the influence of ζ on the *SEI* dynamics is rendered marginal. In computational practice, ρ^* is obtained by finding the value of ρ for which the first-order differences of i_τ drop below a threshold (for details, see the legend of Figure 5).
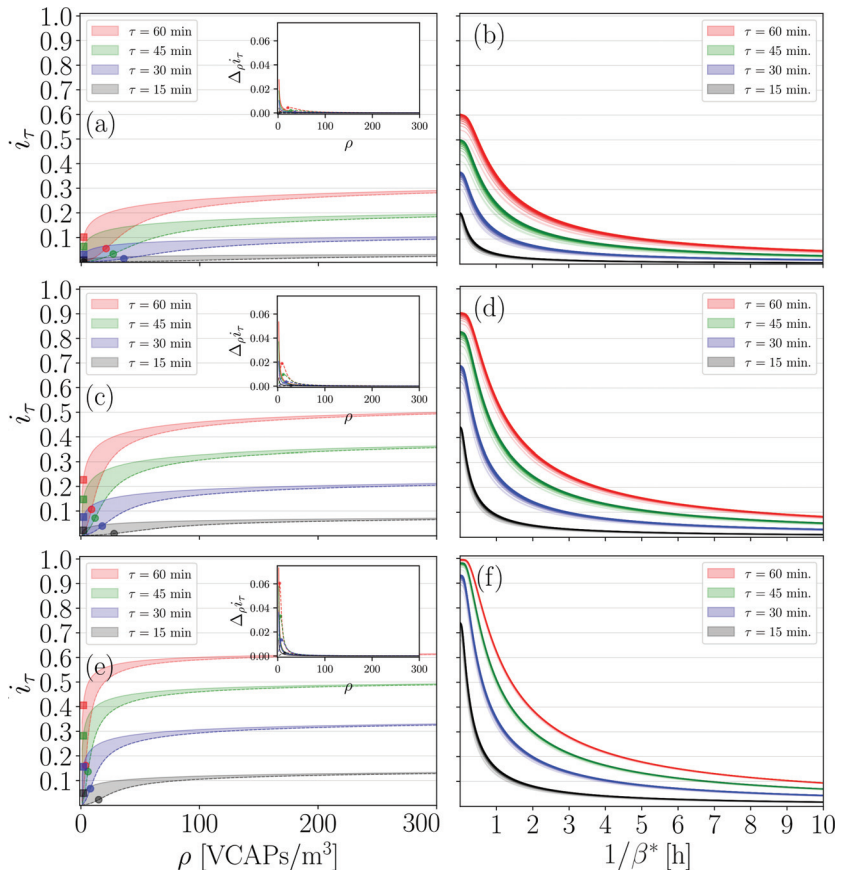
Figure 5. Evaluation of the six-foot rule. (**a**), we plot i_τ as a function of ρ for $r = 0.54$, $\zeta \in [\zeta_{min} = 0.1, \zeta_{max} = 10]$, $\beta^* = 1$, $\xi = d_{safe}$, $R_0 = 0.01$, and $\tau = 0.25, 0.5, 0.75, 1$. Continuous and dashed lines highlight the upper and lower boundaries of i_τ values range obtained for $\zeta_{min} = 0.1$ and $\zeta_{max} = 10$, respectively. (**c**), same as (**a**), but for $r = 1.38$. (**e**), same as (**a**), but for $r = 3.3$. Inset graphs in (**a**,**c**,**e**) illustrate how the first-order differences trace $\Delta_\rho i_\tau = i_{\tau;\rho+\Delta\rho} - i_{\tau;\rho}$ "flattens" for increasing ρ. The following computational criterion was used to decide whether a $\Delta_\rho i_\tau$-trace has "flattened": find ρ^* so that $\Delta_\rho i_\tau < \epsilon$, $\epsilon = 1 \times 10^{-4}$, is satisfied for any $\rho \geq \rho^*$. Once all ρ^* values had been gathered for a specific r-value, we found their maximum, $\rho^*_{max} = \max\limits_{\zeta,\tau,\beta^*=1} \{\rho^*\}$. ρ^*_{max} is provided here for convenience: it serves as a baseline value for probing the behaviour of i_τ-values with respect to $1/\beta^*$. Round and square markers in (**a**,**c**,**e**) highlight the values of i_τ at the inflection point ρ_{infl} for $\zeta = \zeta_{min}$ and $\zeta = \zeta_{max}$, respectively. For clarity, only round markers are used in the inset graphs, highlighting the maxima of $\Delta_\rho i_\tau$ for $\zeta = \zeta_{min}$. (**b**) We plot the value of i_τ obtained for $\rho = n\rho^*_{max}$, $n = 1, 2, 3, \ldots, 10$, $\rho^*_{max} = 384$ versus $1/\beta^*$ for $r = 0.54$, $\zeta \in [\zeta_{min}, \zeta_{max}]$, and $\tau = 0.25, 0.5, 0.75, 1$. (**d**), same as (**b**), but for $r = 1.38$ with $\rho^*_{max} = 354$. (**f**), same as (**b**), but for $r = 3.3$ with $\rho^*_{max} = 245$. Different colour intensities in (**b**,**d**,**f**) were used to visualize i_τ-values in ascending n-order. Black traces appearing in (**b**) are particularly interesting here, as they indicate that for exposure times as short as 15 min, i_τ can take values as high as ≈ 0.2 if the host's innate immune system falls short in counteracting the viral threat, i.e., if $1/\beta^*$ is very small.

Lastly, we evaluate the performance of the six-foot rule by ensuring again that our calculations covered the worst-case scenario. Namely, we required that $\rho \geq \rho^*$ and $\beta^* \to \infty$, implying that both NAb-orchestrated and IFN-system-driven lines of defence cannot provide sufficient protection against a viral threat. Figure 5b shows that, if N_{max} occupants

spend 15, 30, 45, and 60 min in V standing, then i_τ could attain values as high as ≈ 0.2, ≈ 0.35, ≈ 0.5, and ≈ 0.6, respectively. Crucially, this finding shows that the efficiency of the six-foot rule drops significantly after 15 min, since susceptible occupants with a weak immune system might face as high a symptomatic-disease risk as $\approx 20\%$ (notice the behaviour of the black traces shown in Figure 5b for very small $1/\beta^*$). If N_{max} occupants spend time in V while engaging in light exercise activities, then i_τ could potentially exceed 0.4, 0.6, 0.8, and 0.9, respectively (see Figure 5d). Moreover, if N_{max} occupants engage in heavy exercise activities, then i_τ can attain values larger than 0.7 and 0.9 for $\tau = 0.25$ and $\tau = 0.5, 0.75, 1$, respectively, as we can see in Figure 5f. The last two cases suggest that the six-foot rule cannot guarantee the biosafety of immunologically weak susceptible occupants in indoor spaces where exercise activities are undertaken, even if the exposure time is shorter than 30 min. Obviously, for $\beta^* \to 0$, we have that $i_\tau \to 0$, since the transfer from the E to the I subgroup is suppressed as if the IFN-system-driven response would successfully disrupt viral replication and eliminate the virus (see Figure 5b,d,f).

4. Discussion

Given the current rate of biosphere degradation, respiratory viruses of zoonotic origin capable of spreading via air, such as SARS-CoV-2, are expected not only to emerge more often, but also to carry an unprecedentedly high epidemic potential. Self-evidently, the probability of infection increases significantly indoors due to the very nature of the built environment, that is, enclosure. Thus, the biosafety of societies whose members spend most of their time indoors is likely compromised.

In this work, we presented a minimal (in terms of parameter space size) ODE-based model for describing indoor exposure to and potentially also infection by an airborne-transmitted virus. The initial motivation for this work was to construct a modelling framework that could stretch beyond the idea of environmental and biological homogeneity within the context of indoor air biosafety. We achieved this by generalising the WRIP on the basis of a κ-pathway spatial model that treats the breathing zone as a stochastic VCAP transmitter. Following this line of thought, we deduced that the most general PDF that could be used to statistically describe the spatial fluctuations of the exposure rate parameter and VCAP number is that of a gamma distribution. This pointed towards a Tsallisian entropic origin of transmission dynamics, with q measuring the departure from the homogeneous case. The connection between Tsallis entropy and superstatistics is usually established via χ^2 distribution (e.g., see [33]) which is nothing but a special case of the gamma distribution. Lastly, by extending exposure dynamics to account for the possibility of infection activation in relation to innate-immune-system defence mechanisms, we propose that i (defined in Section 3.2) can be used as a probability measure for estimating the risk for developing symptomatic COVID-19 disease. Although Tsallis entropy-based modelling approaches have proven useful in understanding the spread of SARS-CoV-2 among the general population (e.g., see [19,52]), the model curated in this work serves as a first attempt to zoom in on a single indoor space. We emphasise that even for a 15 min exposure under the six-foot-rule guideline, a symptomatic-disease risk as high as 20% might apply.

Let us now discuss some of the limitations of this work. First, theoretical predictions concerning the VCAP distribution remain to be verified (or dismissed) by CFD simulations. In practice, the values of parameters $\{\kappa, \mu\}$ can be estimated by analysing steady-state VCAP distributions obtained from CFD experiments by employing standard distribution parameter estimation procedures. If $\{r, w, W\}$ are known, then one can investigate which combinations of v and τ' offer the best description for the experimental PDF of k. Inevitably, rigorous definitions for τ' and ξ then have to be provided in accordance with the simulation details. Second, very little is known about how the innate immune system reacts to SARS-CoV-2. Therefore, the presented extension of exposure dynamics based on parameter pair $\{\zeta, \beta^*\}$ serves as a rather general starting point for investigating the role of immunologically heterogeneous responses to SARS-CoV-2 and might be updated

in the future as our knowledge increases. In particular, future studies could explore the possibility of $\beta^* := \beta^*(t)$ in order to probe the relationship among IFN-system-driven immune responses and SARS-CoV-2 replication dynamics.

Overall, our work demonstrates how superstatistics and related q-entropies can open up possibilities for systematically obtaining exposure and symptomatic-disease risk estimations in heterogeneous indoor air environments. In turn, this allows for minimising the number of parameters used when constructing personalised biosafety scores such as i. Therefore, our work provides a recipe for incorporating VCAP-related spatial information into simple ODE-based models for indoor epidemiological scenario explorations.

5. Conclusions

At the macroscopic level, the classical Wells–Riley infection probability results in an overrated exposure risk estimation. Locally, however, the situation is different: a classical Wells–Riley infection probability can either over- or under-estimate the associated risks depending on whether the corresponding realisation of exposure rate parameter λ_i is larger or smaller, respectively, than its mean value $\langle \lambda \rangle$.

The Tsallis entropic functional can serve as an information-theoretical starting point for exploring SEI dynamics in heterogeneous indoor air environments.

Institutional Review Board Statement: Not applicable.

Data Availability Statement: Not applicable.

Conflicts of Interest: The author declares that there is no conflict of interest.

Appendix A

Appendix A.1. Probing the Spatial Configuration of VCAPs

To probe the geometry underlying a steady-state VCAP distribution, one may adopt a moments-expansion scheme borrowed from molecular field theory [53]. In fact, moments-expansion schemes serve as simple, yet, informative tools for studying the spatial organisation of heterogeneous molecular systems [54,55]. Imposing periodic boundary conditions over V, we utilise the following geometrical nonuniformity index:

$$\gamma := \left\langle \frac{1}{K} \sum_i^K \|\mathbf{h}_i(t)\| \right\rangle_{t'} \quad (\text{m}),$$

$$\mathbf{h}_i(t) = \frac{1}{K'} \sum_j^{K'} \big(\overbrace{\mathbf{p}_j(t) - \mathbf{p}_i(t)}^{=\mathbf{d}_{ij}(t) \ (\text{m})} \big) \quad (\text{m}),$$

$$(\text{A1})$$

where $\mathbf{p}_i$ is a t-dependent vector from the coordinate system origin to the location of the i-th VCAP, $\mathbf{d}_{i,j}$ is a t-dependent vector difference between the i-th and j-th VCAP locations, $\mathbf{h}_i$ is the first-order geometric moment expanded about the i-th VCAP location calculated and normalised over $0 < K' \leq K - 1$ nearest-neighboring VCAP locations, $\|\cdot\|$ is the Euclidean norm, and $\langle \cdot \rangle_{t'}$ returns the mean value over all t' instances (i.e., ensemble average). $\mathbf{h}_i$ serves here as a t-dependent measure of the displacement tendency (or "imbalance" [53]) of the i-th VCAP about its current location, capturing the magnitude and direction of local VCAP density fluctuations. If VCAPs tend to be uniformly spaced in V (which is a plausible scenario if K and V are very large and small, respectively), then we expect that $\|\mathbf{h}_i\| \approx 0$ for K' would exceed a lower-value threshold value. In turn, this implies that $\gamma \to 0$, thus making the case for a homogeneous indoor air environment. On the other hand, for heterogeneous indoor air environments, γ is larger than zero, letting its maximum

value delimited by the diagonal of V be D, i.e., $\gamma \in [0, D)$. Given γ, nothing can really be said about ξ except that

$$\xi \propto \gamma. \tag{A2}$$

Proportional relationship (A2) implies that a nonvanishing value for γ sets the ground for long-range airborne transmission since the displacement of VCAPs is possible. On the other hand, for $\gamma \to 0$, the range of airborne transmission is expected to be predominantly short; large-magnitude displacements of VCAPs in homogeneous indoor air environments are unlikely to take place.

Appendix A.2. Schematic Illustration of the Contaminated-Air-Sharing Scenario
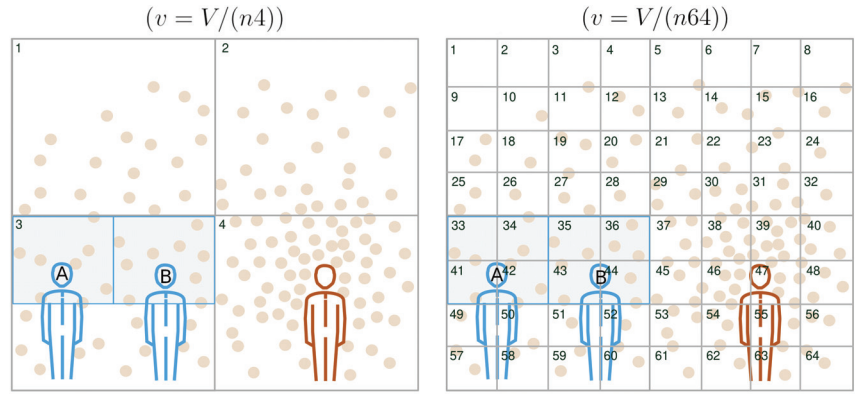
Figure A1. Investigating contaminated-air-sharing scenarios. We consider the same setup as that in Figure 1, but for V partitioned in two different ways. For simplicity, we assume that $v = \xi^3$. The susceptible occupants' breathing zones are highlighted and outlined in light grey and blue, respectively. On the **left** subfigure, we partitioned V into $i = 1, 2, \ldots, \Omega = n4$ subvolumes of size $v = V/\Omega$, so that $v_{br} = v/4$, implying that $\xi > \sqrt[3]{v_{br}}$. The susceptible occupants' breathing zones were embedded within the subvolume indexed with $i = 3$. Because $\xi > \sqrt[3]{v_{br}}$, the epidemiological status of A and B may be influenced by any of the surrounding subvolumes $i = 1, 2, 3, 4$. In fact, during τ_{rel}, a VCAP suspended within any of $i = 1, 2, 3, 4$ could reach A or B. Hence, it is likely that A and B are sharing contaminated air; imagine a VCAP originating from any of $i = 1, 2, 3, 4$ being displaced towards and inhaled by either A or B during τ_{rel}. On the **right** subfigure, we partitioned V into $i = 1, 2, \ldots, \Omega = n64$ subvolumes of size $v = V/\Omega$, so that $v_{br} = 4v$, implying that $\xi < \sqrt[3]{v_{br}}$. Those indexed with $i = 33, 34, 41, 42$ and $i = 35, 36, 43, 44$ were embedded within the breathing zone of A and B, respectively. Because $\xi < \sqrt[3]{v_{br}}$, the epidemiological status of A and B is unlikely to be influenced by any other surrounding subvolumes except from $i = 33, 34, 41, 42$ and $i = 35, 36, 43, 44$, respectively. Hence, A and B are also unlikely to share contaminated air, since VCAPs suspended in any of $i = 33, 34, 41, 42$ and $i = 35, 36, 43, 44$ are unlikely to reach B and A, respectively, during τ_{rel}.

Appendix A.3. Discretisation of the Tsallis Entropic Functional

The following discretised version of (27) was used:

$$\mathcal{S}[\{p_i\}] = -\frac{1 - \sum_i p_i^q}{1 - q}, \quad p_i = \frac{s_i}{\sum_i s_i} \tag{A3}$$

with $s_i := S(t_i)$, $t_{i=1,2,\ldots,W} = t_0 + \frac{i-1}{W-1}(t'' - t_0)$, where $p_i \propto (1 + \frac{t}{\mu})^{-\kappa} \overset{(17)}{=} 1 - P(t)$ is a time-step-specific probability of escaping exposure (i.e., not inhaling any VCAPs) after spending t hours in V. $\sum_{i=1}^{W} p_i = 1$ with W being identified as the number of accessible microstates. Accordingly, a subgroup of susceptible occupants of size smaller than S_0 may

be thought of as a subsystem visiting the *i*-th microstate with some probability p_i. The probabilistic independence of any pair of subsystems is guaranteed by model construction, since probabilistically independent airborne transmissions are assumed throughout. For $q \to 1$, (A3) gives us the Boltzmann–Gibbs entropy, i.e.,

$$\mathcal{S}_{q \to 1}[\{p_i\}] = -\sum_{i=1}^{W} p_i \ln(p_i). \tag{A4}$$

References

1. National Academies of Sciences, Engineering, and Medicine. *Airborne Transmission of SARS-CoV-2: Proceedings of a Workshop-in Brief*; The National Academies Press: Washington, DC, USA, 2020. [CrossRef]
2. Prather, K.A.; Marr, L.C.; Schooley, R.T.; McDiarmid, M.A.; Wilson, M.E.; Milton, D.K. Airborne Transmission of SARS-CoV-2. *Science* **2020**, *370*, 303–304. [PubMed]
3. Miller, S.L.; Nazaroff, W.W.; Jimenez, J.L.; Boerstra, A.; Buonanno, G.; Dancer, S.J.; Kurnitski, J.; Marr, L.C.; Morawska, L.; Noakes, C. Transmission of SARS-CoV-2 by Inhalation of Respiratory Aerosol in the Skagit Valley Chorale Superspreading Event. *Indoor Air* **2021**, *31*, 314–323. [CrossRef] [PubMed]
4. Greenhalgh, T.; Jimenez, J.L.; Prather, K.A.; Tufekci, Z.; Fisman, D.; Schooley, R. Ten Scientific Reasons in Support of Airborne Transmission of SARS-CoV-2. *Lancet* **2021**, *397*, 1603–1605. [CrossRef] [PubMed]
5. Tang, J.W.; Marr, L.C.; Li, Y.; Dancer, S.J. COVID-19 Has Redefined Airborne Transmission. *BMJ* **2021**, *373*, n913. [CrossRef] [PubMed]
6. Zhang, R.; Li, Y.; Zhang, A.L.; Wang, Y.; Molina, M.J. Identifying airborne transmission as the dominant route for the spread of COVID-19. *Proc. Natl. Acad. Sci. USA* **2020**, *117*, 14857–14863. [CrossRef]
7. Setti, L.; Passarini, F.; De Gennaro, G.; Barbieri, P.; Perrone, M.G.; Borelli, M.; Palmisani, J.; Di Gilio, A.; Piscitelli, P.; Miani, A. Airborne transmission route of COVID-19: Why 2 m/6 feet of inter-personal distance could not be enough. *Int. J. Environ. Res. Public Health* **2020**, *17*, 2932. [CrossRef]
8. Morawska, L.; Milton, D.K. It is time to address airborne transmission of coronavirus disease 2019 (COVID-19). *Clin. Infect. Dis.* **2020**, *71*, 2311–2313. [CrossRef]
9. Peng, Z.; Rojas, A.P.; Kropff, E.; Bahnfleth, W.; Buonanno, G.; Dancer, S.J.; Kurnitski, J.; Li, Y.; Loomans, M.G.; Marr, L.C.; et al. Practical Indicators for Risk of Airborne Transmission in SharedIndoor Environments and Their Application to COVID-19 Outbreaks. *Environ. Sci. Technol.* **2022**, *56*, 1125–1137. [CrossRef]
10. Dick, E.C.; Jennings, L.C.; Mink, K.A.; Wartgow, C.D.; Inborn, S.L. Aerosol Transmission of Rhinovirus Colds. *J. Infect. Dis.* **1987**, *156*, 442–448. [CrossRef]
11. Yu, I.T.; Li, Y.; Wong, T.W.; Tam, W.; Chan, A.T.; Lee, J.H.; Leung, D.Y.; Ho, T. Evidence of Airborne Transmission of the Severe Acute Respiratory Syndrome Virus. *N. Engl. J. Med.* **2004**, *350*, 1731–1739. [CrossRef]
12. Moriarty, L.F.; Plucinski, M.M.; Marston, B.J.; Kurbatova, E.V.; Knust, B.; Murray, E.L.; Pesik, N.; Rose, D.; Fitter, D.; Kobayashi, M.; et al. Public Health Responses to COVID-19 Outbreaks on Cruise Ships—Worldwide, February–March 2020. *MMWR Morb. Mortal. Wkly. Rep.* **2020**, *69*, 347–352. [CrossRef]
13. Hamner, L.; Dubbel, P.; Capron, I.; Ross, A.; Jordan, A.; Lee, J.; Lynn, J.; Ball1, A.; Narwal, S.; Russell, S.; et al. High SARS-CoV-2 attack rate following exposure at a choir practice, Skagit County, Washington, March 2020. *MMWR Morb. Mortal. Wkly. Rep.* **2020**, *69*, 606–610. [CrossRef]
14. Jayaweera, M.; Perera, H.; Gunawardana, B.; Manatunge, J. Transmission of COVID-19 virus by droplets and aerosols. *Environ. Res.* **2020**, *188*, 109819. [CrossRef]
15. Morawksa, L. Droplet fate in indoor environments, or can we prevent the spread of infection? *Indoor Air* **2006**, *16*, 335–347.
16. Tian, D.; Sun, Y.; Xu, H.; Ye, Q. The emergence and epidemic characteristics of the highly mutated SARS-CoV-2 Omicron variant. *J. Med. Virol.* **2022**, *94*, 2376–2383. [CrossRef]
17. Gaddis, M.D.; Manoranjan, V.S. Modeling the Spread of COVID-19 in Enclosed Spaces. *Math. Comput. Appl.* **2021**, *26*, 79. [CrossRef]
18. Noakes, C.J.; Beggs, C.B.; Sleigh, P.A.; Kerr, K.G. Modelling the transmission of airborne infections in enclosed spaces. *Epidemiol. Infect.* **2006**, *134*, 1082–1091. [CrossRef]
19. Tirnakli, U.; Tsallis, C. Epidemiological Model with Anomalous Kinetics: Early Stages of the COVID-19 Pandemic. *Front. Phys.* **2020**, *8*, 613168. [CrossRef]
20. Vasconcelos, G.L.; Pessoa, N.L.; Silva, N.B.; Macêdo, A.M.; Brum, A.A.; Ospina, R.; Tirnakli, U. Multiple waves of COVID-19: A pathway model approach. *Nonlinear Dyn.* **2023**, *111*, 6855–6872. [CrossRef]
21. Dhawan, S.; Biswas, P. Aerosol Dynamics Model for Estimating the Risk from Short-Range Airborne Transmission and Inhalation of Expiratory Droplets of SARS-CoV-2. *Environ. Sci. Technol.* **2021**, *55*, 8987–8999. [CrossRef]
22. Bazant, M.Z.; Bush, J.W.M. A guideline to limit indoor airborne transmission of COVID-19. *Proc. Natl. Acad. Sci. USA* **2021**, *118*, 17. [CrossRef] [PubMed]

23. He, Q.; Niu, J.; Gao, N.; Zhu, T.; Wu, J. CFD study of exhaled droplet transmission between occupants under different ventilation strategies in a typical office room. *Build. Environ.* **2011**, *46*, 397–408. [CrossRef] [PubMed]
24. Foster, A.; Kinzel, M.; Estimating, M. COVID-19 exposure in a classroom setting: A comparison between mathematical and numerical models. *Phys. Fluids* **2021**, *33*, 021904. [CrossRef] [PubMed]
25. Wang, Z.; Galea, E.R.; Grandison, A.; Ewer, J.; Jia, F. A coupled Computational Fluid Dynamics and Wells-Riley model to predict COVID-19 infection probability for passengers on long-distance trains. *Saf. Sci.* **2022**, *147*, 105572. [CrossRef]
26. Su, W.; Yang, B.; Melikov, A.; Liang, C.; Lu, Y.; Wang, F.; Li, A.; Lin, Z.; Li, X.; Cao, G.; et al. Infection probability under different air distribution patterns. *Build. Environ.* **2022**, *207*, 108555. [CrossRef]
27. Riley, E.C.; Murphy, G.; Riley, R.L. Airborne spread of measles in a suburban elementary school. *Am. J. Epidemiol.* **1978**, *107*, 421–432. [CrossRef]
28. Mittal, R.; Meneveau, C.; Wu, W. A mathematical framework for estimating risk of airborne transmission of COVID-19 with application to face mask use and social distancing. *Phys. Fluids* **2020**, *32*, 101903. [CrossRef]
29. Noakes, C.J.; Sleigh, P.A. Applying the Wells-Riley equation to the risk of airborne infection in hospital environments: The importance of stochastic and proximity effects. In Proceedings of the Indoor Air 2008, the 11th International Conference on Indoor Air Quality and Climate, Copenhagen, Denmark, 17–22 August 2008.
30. Zhang, S.; Lin, Z. Dilution-based evaluation of airborne infection risk-Thorough expansion of Wells-Riley model. *Build. Environ.* **2021**, *194*, 107674. [CrossRef]
31. Shao, X.; Li, X. COVID-19 transmission in the first presidential debate in 2020. *Phys. Fluids* **2020**, *32*, 115125. [CrossRef]
32. Li, Q.; Wang, Y.; Sun, Q.; Knopf, J.; Herrmann, M.; Lin, L.; Jiang, J.; Shao, C.; Li, P.; He, X.; et al. Immune response in COVID-19: What is next? *Cell Death Differ.* **2022**, *29*, 1107–1122. [CrossRef]
33. Beck, C.; Cohen, E.G.D. Superstatistics. *Phys. A* **2003**, *322*, 267–275. [CrossRef]
34. Tsallis, C. Possible generalization of Boltzmann-Gibbs statistics. *J. Stat. Phys.* **1988**, *52*, 479. [CrossRef]
35. Richards, F.J. A flexible growth function for empirical use. *J. Exp. Bot.* **1959**, *10*, 290. [CrossRef]
36. Gupta, S.L.; Jaiswal, R.K. Neutralizing antibody: A savior in the COVID-19 disease. *Mol. Biol. Rep.* **2022**, *49*, 2465–2474. [CrossRef]
37. Lamers, M.M.; Haagmans, B.L. SARS-CoV-2 pathogenesis. *Nat. Rev. Microbiol.* **2022**, *20*, 270–284. [CrossRef]
38. Beck, C.; Cohen, E.G.D.; Swinney, H.L. From time series to superstatistics. *Phys. Rev. E Stat. Nonlinear Soft Matter Phys.* **2005**, *72*, 056133. [CrossRef]
39. Feller, W. *An Introduction to Probability Theory and Its Applications*; John Wiley: London, UK, 1966; Volume II.
40. Arnold, B.C. *Pareto Distributions*; International Cooperative Publishing House: Fairland, MD, USA, 1983.
41. Zhou, P.; Yang, X.L.; Wang, X.G.; Hu, B.; Zhang, L.; Zhang, W.; Si, H.R.; Zhu, Y.; Li, B.; Huang, C.L.; et al. A pneumonia outbreak associated with a new coronavirus of probable bat origin. *Nature* **2020**, *579*, 270–273. [CrossRef]
42. Cheemarla, N.R.; Watkins, T.A.; Mihaylova, V.T.; Wang, B.; Zhao, D.; Wang, G.; Landry, M.L.; Foxman, E.F. Dynamic innate immune response determines susceptibility to SARS-CoV-2 infection and early replication kinetics. *J. Exp. Med.* **2021**, *218*, 8. [CrossRef]
43. Matricardi, P.M.; Dal Negro, R.W.; Nisini, R. The first, holistic immunological model of COVID-19: Implications for prevention, diagnosis, and public health measures. *Pediatr. Allergy Immunol.* **2020**, *5*, 454–470. [CrossRef]
44. Morales-Núñez, J.J.; Muñoz-Valle, J.F.; Torres-Hernández, P.C.; Hernández-Bello, J. Overview of Neutralizing Antibodies and Their Potential in COVID-19. *Vaccines* **2021**, *9*, 1376. [CrossRef]
45. Favresse, J.; Gillot, C.; Di Chiaro, L.; Eucher, C.; Elsen, M.; Van Eeckhoudt, S.; David, C.; Morimont, L.; Dogné, J.M.; Douxfils, J. Neutralizing Antibodies in COVID-19 Patients and Vaccine Recipients after Two Doses of BNT162b2. *Viruses* **2021**, *13*, 1364. [CrossRef] [PubMed]
46. Mendes, R.S.; Pedron, I.T. Nonlinear differential equations based on nonextensive Tsallis entropy and physical applications. *arXiv* **1999**, arXiv:Cond.mat/9904023v1.
47. Brouers, F.; Sotolongo-Costa, O. Generalized fractal kinetics in complex systems (application to biophysics and biotechnology). *Phys. A* **2006**, *368*, 165–175. [CrossRef]
48. Van Rossum, G.; Drake, F.L., Jr. *Python Reference Manual*; Centrum voor Wiskunde en Informatica: Amsterdam, The Netherlands, 1995.
49. Dorm, J.R.; Prince, P.J. A family of embedded Runge-Kutta formulae. *J. Comput. Appl. Math.* **1980**, *6*, 19–26.
50. Kim, E.-J.; Tenkès, L.-M.; Hollerbach, R.; Radulescu, O. Far-From-Equilibrium Time Evolution between Two Gamma Distributions. *Entropy* **2017**, *19*, 511. [CrossRef]
51. Adams, W.C. *Measurement of Breathing Rate and Volume in Routinely Performed Daily Activities: Final Report, Contract No. A033-205*; California Air Resources Board: Sacramento, CA, USA, 1993.
52. Tsallis, C.; Tirnakli, U. Predicting COVID-19 Peaks Around the World. *Front. Phys.* **2020**, *8*, 217. [CrossRef]
53. Silverman, B.D. Hydrophobic moments of protein structures: Spatially profiling the distribution. *Proc. Natl. Acad. Sci. USA* **2001**, *98*, 4996–5001. [CrossRef]

54. Xenakis, M.N.; Kapetis, D.; Yang, Y.; Heijman, J.; Waxman, S.G.; Lauria, G.; Faber, C.G.; Smeets, H.J.; Westra, R.L.; Lindsey, P.J. Cumulative hydropathic topology of a voltage-gated sodium channel at atomic resolution. *Proteins* **2020**, *88*, 1319–1328. [CrossRef]
55. Xenakis, M.N.; Kapetis, D.; Yang, Y.; Heijman, J.; Waxman, S.G.; Lauria, G.; Faber, C.G.; Smeets, H.J.; Lindsey, P.J.; Westra, R.L. Non-extensitivity and criticality of atomic hydropathicity around a voltage-gated sodium channel's pore: A modeling study. *J. Biol. Phys.* **2021**, *47*, 61–77. [CrossRef]

Article

Necessary Condition of Self-Organisation in Nonextensive Open Systems

Ozgur Afsar [1,*,†] and Ugur Tirnakli [2,†]

[1] Department of Physics, Faculty of Science, Ege University, Izmir 35100, Turkey
[2] Department of Physics, Faculty of Arts and Sciences, Izmir University of Economics, Izmir 35330, Turkey
[*] Correspondence: ozgur.afsar@ege.edu.tr
[†] These authors contributed equally to this work.

Abstract: In this paper, we focus on evolution from an equilibrium state in a power law form by means of q-exponentials to an arbitrary one. Introducing new q-Gibbsian equalities as the necessary condition of self-organization in nonextensive open systems, we theoretically show how to derive the connections between q-renormalized entropies ($\Delta \tilde{S}_q$) and q-relative entropies (KL_q) in both Bregman and Csiszar forms after we clearly explain the connection between renormalized entropy by Klimontovich and relative entropy by Kullback-Leibler without using any predefined effective Hamiltonian. This function, in our treatment, spontaneously comes directly from the calculations. We also explain the difference between using ordinary and normalized q-expectations in mean energy calculations of the states. To verify the results numerically, we use a toy model of complexity, namely the logistic map defined as $X_{t+1} = 1 - aX_t^2$, where $a \in [0, 2]$ is the map parameter. We measure the level of self-organization using two distinct forms of the q-renormalized entropy through period doublings and chaotic band mergings of the map as the number of periods/chaotic-bands increase/decrease. We associate the behaviour of the q-renormalized entropies with the emergence/disappearance of complex structures in the phase space as the control parameter of the map changes. Similar to Shiner-Davison-Landsberg (SDL) complexity, we categorize the tendencies of the q-renormalized entropies for the evaluation of the map for the whole control parameter space. Moreover, we show that any evolution between two states possesses a unique $q = q^*$ value (not a range for q values) for which the q-Gibbsian equalities hold and the values are the same for the Bregmann and Csiszar forms. Interestingly, if the evolution is from $a = 0$ to $a = a_c \simeq 1.4011$, this unique q^* value is found to be $q^* \simeq 0.2445$, which is the same value of $q_{sensitivity}$ given in the literature.

Keywords: S-theorem; q-renormalized entropy; complexity measures; logistic map

1. Introduction

The main problem for researchers who are interested in entropy-based measures is discerning which measure would be the most suitable one for the complex system under consideration. The definition of 'suitable' implies the measure which represents a behaviour that is compatible with the dynamics of the system among definitions of the measures in the literature. For example, it has been expected that the measure is able to make a distinction among possible phases of the system as the parameter set of the system slightly changes. Despite the numerous definitions [1–8], the measures can be categorized into three types (Figure 1), namely type-I, type-II and type-III that are similar to SDL complexity, formally [5]. The first type considers measure as a monotonically increasing function of disorder. In the second type, measure is a convex function of disorder. Hence, it is a minimum for both completely order and completely disorder, and a maximum at a point between them. In the last type, measure is a monotonically decreasing function of disorder. The crucial point in this classification is that classic notion of entropy by Shannon [9] is associated with the degree of disorder. It should be noted that the control parameter of the system can also

be used as the degree of disorder if the Shannon entropy *S* is a monotonically increasing function of some system parameter, say *a*, as the system evolves in its parameter space from *a* to $a + \Delta a$ [10].
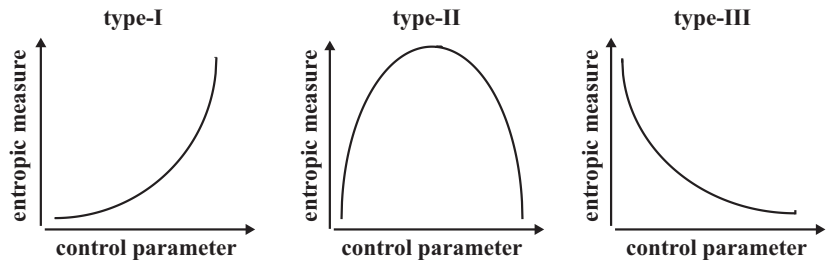
Figure 1. An example of types of entropy based measures as a function of control parameter (adapted from [5]).

Even if it seems that changing the parameter in space is not directly related to time, it always takes time from one state to another for a real system since an evolution depends on the change of conditions, i.e., of parameters, with time [11]. For the evolution of dissipative dynamical systems which pave their way to successive stable branches, and then to successive chaotic band mergings as the parameter set of the system slightly changes, the classic notion of the entropy by Shannon, the relative entropy by Kullback-Leibler and the renormalized entropy by Klimontovich are good examples for entropy-based measures of type-I, type-II and type-III, respectively [10]. The Shannon entropy monotonically increases from the first branch to the most chaotic state (type-I). The relative entropy increases monotonically from the first branch up to the edge of chaos, and then decreases monotonically up to the first chaotic band merge (type-II). The renormalized entropy decreases monotonically from the first branch up to the edge of chaos (type-III), and then increases monotonically up to the first chaotic band merge (type-I). In other words, when the sequence of branches emerges, the relative order increases, i.e., the measure of complexity, the renormalized entropy decreases [12].

The behaviour of the renormalized entropy indicates the relative degree of order in the system as first suggested by Haken [13] in the context of self-organization. The S-theorem that is a basis for the method of renormalized entropy was proved for the transition from laminar to turbulent flow [14]. Such a kind transformation confirmed that turbulent structures are more ordered, that implies highly organized, than laminar [15]. Moreover, Rayleigh–Bénard convection [16,17], Taylor instability experiment [18], bacterial [19] and Dictyostelium discoideum [20] colonies are some typical examples in which the most ordered spatial patterns emerge in the phase spaces via changing conditions of the systems, that indicates a high level of self-organization.

The Shannon entropy expression, setting $k_B = 1$, reads

$$S = - \sum_i p_i \ln p_i \tag{1}$$

where p_i are the probability of an event *i* of a sample set. Maximizing the Shannon entropy of the system subject to suitable constraints (namely, mean energy and probability normalization constraints), using Lagrange multipliers method, one can obtain the equilibrium distribution as

$$p_i^{eq} = \frac{e^{-\beta \epsilon_i}}{Z} \tag{2}$$

where β is the inverse temperature and $Z = \sum_i e^{-\beta \epsilon_i}$ is the partition function. For the evolution to the equilibrium state from an arbitrary one ($p \rightarrow p^{eq}$), the Shannon entropy can be used to find the difference between the entropies $\Delta S^{(p \rightarrow p^{eq})} = S(p^{eq}) - S(p) \geq 0$ that is known as the second law of thermodynamics. However, from both Boltzmann's

H-theorem and Gibbs theorem, it is well known that this inequality is only valid for an isolated evolution between the states. Hence, it is violated for the evolution of open systems that exchange of energy/matter with its surroundings is allowed. In other words, these theorems state that $\Delta S^{(p \to p^{eq})}$ equals relative entropy with a limitation that the mean energy $\langle E \rangle$ remains constant (i.e, $\langle E \rangle^{p^{eq}} = \langle E \rangle^p$) [21]. Therefore, in a process of such an evolution (from p to p^{eq}) as long as mean energy is the same, from these theorems, it follows that

$$\Delta S = S_{eq} - S = \sum_i p_i \ln \frac{p_i}{p_i^{eq}} = K(p||p^{eq}) \geq 0 \tag{3}$$

where p^{eq} and p are probability distributions corresponding to the equilibrium state and arbitrary one, respectively. Equation (3) implies that the equilibrium state has the greatest disorder (or chaoticity) as compared to the arbitrary state. The usual expression of the relative entropy $K(p||r) = \sum_i p_i \ln \frac{p_i}{r_i}$ gives the entropy produced by the change from the state p to the state r. Whenever $r = p^{eq}$, it can be written in terms of free energy differences of the states

$$K(p||p^{eq}) \propto (F - F^{eq}) \tag{4}$$

where $F = \langle E \rangle^p - \frac{1}{\beta}S$ and $F^{eq} = \langle E \rangle^{p^{eq}} - \frac{1}{\beta}S_{eq}$.

Due to the strong limitations on the second law, Klimontovich introduced his S-theorem, where 'S' stands for 'self-organization', that makes it possible to analyze open systems in terms of the Gibbs theorem [21]. According to the S-theorem, it is possible to compare distinct states, which are the equilibrium and a non-equilibrium stationary state, under dissipation of the energy that implies the evolution of an open system. To compensate the dissipation, a new mean energy equality $\langle E \rangle^{\tilde{p}^{eq}} = \langle E \rangle^p$ similar to the Gibbs' equality via a renormalization procedure $p^{eq} \to \tilde{p}^{eq}$ is defined. After such a renormalization, the renormalized entropy $\Delta \tilde{S}$ is defined as (noticing that evolution is from $\tilde{p}^{eq}$ to p)

$$\Delta \tilde{S} = S - \tilde{S}_{eq} = -\sum_i p_i \ln \frac{p_i}{\tilde{p}_i^{eq}} = -K(p||\tilde{p}^{eq}) \leq 0 \tag{5}$$

where $\tilde{p}^{eq}$ and p are the renormalized equilibrium and non-equilibrium stationary states, respectively (all proofs regarding Equations (3)–(5) will be given in the next part of the paper).

In Section 2, we show that the definition of mean energy equality (and also Equation (5)) in the concept of the renormalized entropy by Klimontovich is valid for an evolution to/from the canonical equilibrium distribution of exponential form in Equation (2). We also discuss the connections among the Shannon, the Kullback-Leibler relative and the renormalized entropies within a thermodynamic perspective.

In Section 3, we theoretically show how to apply this procedure on a nonextensive open system, whose generalized canonical probability distribution is of q-exponential form

$$e_q^x = [1 + (1-q)x]^{1/(1-q)} . \tag{6}$$

This distribution is the one that comes from the maximization of the Tsallis entropy given by [22]

$$S_q = \frac{1 - \sum_i p_i^q}{1 - q} , \tag{7}$$

and it recovers the Shannon entropy $S = -\sum_i p_i \ln p_i$ in the limit $q \to 1$ as a special case. It is well known that the maximization of the Tsallis entropy subject to the ordinary constraints ($\sum_i p_i \epsilon_i = \langle E \rangle$ and $\sum_i p_i = 1$) yields a canonical distribution in a q-exponential form,

$$p_i^{ord} = \frac{e_{2-q}^{-\beta^* \epsilon_i}}{Z(\beta^*)} , \tag{8}$$

where $1/Z(\beta^*)$ is a normalization constant [23]. On the other hand, normalized q-expectation is employed instead of the ordinary constraints, $(\sum_i [p_i^q \epsilon_i / \sum_i p_i^q] = \langle E \rangle_q$ and $\sum_i [p_i^q / \sum_i p_i^q] = 1)$, the canonical probability distributions reads

$$p_i^{(nor)} = \frac{e_q^{-\hat{\beta}(\epsilon_i - \langle E \rangle_q)}}{Z(\hat{\beta})} \tag{9}$$

where $\hat{\beta} = \beta / C_q$ and $C_q = \sum_i (p_i^{nor})^q$ [22]. Respectively, when the generalized version of canonical distributions in Equations (8) and (9) put into two kinds of q-generalized relative entropies, which are well known Bregman $K_q^B(p||p^{ord})$ and Csiszar types $K_q^C(p||p^{nor})$, it can be shown that the generalized relative entropies are associated with the q-generalized version of free energy differences of the states [24]:

$$K_q^B(p||p^{ord}) \propto (F_q - F_q^{ord}) \tag{10a}$$

$$K_q^C(p||p^{nor}) \propto (F_q - F_q^{nor}) \tag{10b}$$

that are similar to the Equation (4). It can be also noted that there is one more version of the formalism using unnormalized q-expectations in the constraints. However, it is shown in [25] that all these versions are equivalent to each other.

In the following subsections, we explain the necessary condition (on the q-mean energy equality) for self organization of open systems using the Bregman and Csiszar forms of generalized relative entropies, respectively. Klimontovich himself as well as some recent efforts on the generalization of the renormalized entropy [26,27] have invoked a predefined 'effective Hamiltonian' function to obtain the mean energy equality. We will theoretically show here what kind of equalities would be necessary conditions for self organization of nonextensive systems without using any predefined effective Hamiltonian function. The results will come up as a direct consequence of our approach. Moreover, we derive relations between q-renormalized entropy and the generalized relative entropies from the viewpoint of information theoretic approaches in Section 2.

In Section 4, we use a paradigmatic toy model, the logistic map, in order to numerically show the level of self-organization (or the degree of complexity from self-organisation) for a system that paves its way to successive stable branches, and then to successive chaotic band mergings as the parameter of the system slightly changes. We show the behaviour of the q-relative entropies in both Bregmann and Csiszar forms as the suitable measure for self-organisation, and define their types of complexity (type-I, -II or -III). Finally, we show a unique q^* values obtained through evolution of the states with the system parameter and relate its value at the edge of chaos with the $q_{sensitivity}$ value obtained for the logistic map [28,29].

2. Thermodynamic Perspective of the Renormalized Entropy and Connections

Let us consider an evolution from an equilibrium state p_0 to an arbitrary one p as the control parameter of the complex system slightly changes from a_0 to $a_0 + \Delta a$. Entropy produced by the change of state (i.e., corresponding information gain) in such an evolution can be given by the Kullback-Leibler relative entropy [30]

$$K(p||p_0) = \sum_i p_i \ln \frac{p_i}{p_{0i}} \geq 0 . \tag{11}$$

Adding and subtracting $\sum_i p_{0i} \ln p_{0i}$ to and from right-hand side of Equation (11), this can be rewritten as

$$K(p||p_0) = -\Delta S^{(p_0 \to p)} - \sum_i (p_i - p_{0i}) \ln p_{0i} \tag{12}$$

where $\Delta S^{(p_0 \to p)} = \sum_i p_{0i} \ln p_{0i} - \sum_i p_i \ln p_i$.

Substituting $p_{0i} = p_i^{eq}$, the canonical equilibrium distribution of exponential form in Equation (2), into the logarithmic function $\ln p_{0i}$ in Equation (12), it can be immediately shown that

$$K(p||p^{eq}) = -\Delta S^{(p^{eq} \to p)} + \beta \Delta \langle E \rangle^{(p^{eq} \to p)} \tag{13}$$

where $\Delta \langle E \rangle^{(p^{eq} \to p)} = \langle E \rangle^p - \langle E \rangle^{p^{eq}}$ is the difference between the mean energies through the evolution from the state p^{eq} to the state p. Comparing Equations (12) and (13), it follows that

$$\Delta \langle E \rangle^{(p^{eq} \to p)} = -\frac{1}{\beta} \sum_i (p_i - p_i^{eq}) \ln p_i^{eq} . \tag{14}$$

One can notice that Equations (12)–(14) lead three important connections regarding the proofs of Equations (3)–(5):

(i) Equation (3), the second law of thermodynamics $\Delta S^{(p \to p^{eq})} \geq 0$, can be derived from Equation (13) noticing that $\Delta S^{(p \to p^{eq})} = -\Delta S^{(p^{eq} \to p)}$ and $K(p||p^{eq}) \geq 0$. This derivation requires the limitation that the Gibbs equality holds, i.e., $\sum_i (p_i - p_i^{eq}) \ln p_i^{eq} \propto \Delta \langle E \rangle = 0$, which implies the evolution is isolated, i.e., the mean energy is the same through the evolution.

(ii) Equation (4) can easily obtain from Equation (13) using the definition of the free energy given as $F = \langle E \rangle^r - \frac{1}{\beta} S$ for any state (r). It means that Kullback-Leibler relative entropy is associated with the free energy difference of the states in such an evolution.

(iii) Equation (5), the result of the S-theorem by Klimontovich, can be shown from Equation (13) by a transformation $p^{eq} \to \tilde{p}^{eq}$ ensuring the renormalization of the state so that it compensates the mean energy difference between the states corresponding to the renormalized equilibrium and non-equilibrium stationary states, i.e $\Delta \langle E \rangle^{(\tilde{p}^{eq} \to p)} = 0$. The compensation requires the Gibbs equality defined as

$$\sum_i p_i \ln p_i^{eq} = \sum_i \tilde{p}_i^{eq} \ln p_i^{eq}. \tag{15}$$

Such a renormalization enables us to use the Gibbs theorem for an open system with energy flux. To compare the states in terms of the renormalized $\Delta \tilde{S}$ and Kullback-Leibler relative entropies K, the connection can be written as

$$\Delta \tilde{S} = -K(p||\tilde{p}^{eq}) \leq 0 \tag{16}$$

by means of Equations (12) and (15).

It should be noted that our assumption reveals with Equations (12)–(14) why a quantity called the effective Hamiltonian, $H_{eff} = -\ln p_{0i}$, for the reference equilibrium state was preferred by Klimontovich. In our assumption, choosing the reference state as $p_0 = p^{eq}$ yields $\Delta \langle E \rangle^{(p^{eq} \to p)}$ in Equation (13), spontaneously. The details and applications on both synthetical and real data of the renormalized entropy by Klimontovich can be found in references [10,12,21,31] and [32–35], respectively.

3. Derivation of the *q*-Renormalized Entropy and Connections

Similar to the connection in Equation (4) between Kullback-Leibler relative entropy and free energy differences, there are two types of *q*-generalized relative entropies whose connections to *q*-free energy differences exists [36]. Respectively, they are called Bregmann form given by

$$K_q^B(p||p_0) = \frac{1}{q-1} \sum_i p_i \left(p_i^{q-1} - p_{0i}^{q-1} \right) - \sum_i (p_i - p_{0i}) p_{0i}^{q-1} \tag{17}$$

and Csiszar form defined as

$$K_q^C(p||p_0) = \frac{1}{q-1} \sum_i p_i \left[\left(\frac{p_i}{p_{0i}} \right)^{q-1} - 1 \right].$$ (18)

Noticing the dependence of the generalized relative entropies on the constraints from Equation (10), we derive the q-renormalized entropies for the evolution from a stationary state in the functional forms of the inverse power law (i.e., q-exponentials in Equations (8) and (9)) within a thermodynamic perspective similar to the Section 2. The crucial point of such an approach is that a predefined effective hamiltonian function is not necessary. Moreover, we show the necessary conditions of self organization in nonextensive open system using a q-Gibbsian equality in the following subsections.

3.1. Derivation and Connection I: q-Renormalized Entropy and Bregman Form of Relative Entropy

Firstly, we reorganize the Bregman form of the generalized relative entropy in Equation (17) as

$$K_q^B(p||p_0) = \sum_i p_{0i} \ln_{2-q} p_{0i} + \sum_i p_i \ln_{2-q} p_i - q \sum_i (p_i - p_{0i}) \ln_{2-q} p_{0i}$$ (19)

where the identical relation of $(2-q)$-deformed logarithm, $\ln_{2-q} x = (x^{q-1} - 1)/(q-1)$, has been used. It should be noted that the same relation leads to the q-logarithmic form of the Tsallis entropy in Equation (7), that is given by

$$S_q = - \sum_i p_i \ln_{2-q} p_i.$$ (20)

Putting this form in Equation (19), we have a similar expression to Equation (12), which reads

$$K_q^B(p||p_0) = -\Delta S_q^{(p_0 \to p)} - q \sum_i (p_i - p_{0i}) \ln_{2-q} p_{0i}$$ (21)

where $\Delta S_q^{(p_0 \to p)} = S_q(p) - S_q(p_0)$ is the change in the Tsallis entropies through an evolution from the state p_0 to p.

Substituting $p_{0i} = p_i^{ord}$, the stationary distribution of the $(2-q)$-exponential form in Equation (8), into the $(2-q)$-logarithmic function $\ln_{2-q} p_{0i}$ in Equation (21), we can immediately write

$$K_q^B(p||p^{ord}) = -\Delta S_q^{(p^{ord} \to p)} + \beta' \sum_i (p_i - p_i^{ord}) \epsilon_i$$ (22)

where $\beta' = \frac{q\beta^*}{Z^{q-1}}$. From the transformation $p_i^{ord} \to \tilde{p}_i^{ord}$ on the reference state, one can easily obtain

$$K_q^B(p||\tilde{p}^{ord}) = -\Delta S_q^{(\tilde{p}^{ord} \to p)} + \beta' \Delta \langle E \rangle^{(p^{ord} \to p)}$$ (23)

where $\Delta \langle E \rangle^{(p^{ord} \to p)} = \langle E \rangle^p - \langle E \rangle_q^{p^{ord}}$ is the mean energy difference and $\tilde{p}_i^{ord} = (p_i^{ord})^q / \sum_i (p_i^{ord})^q$ is the distribution chosen so that it enables us to vanish the second terms in the right hand side of Equations (22) and (23) at a unique value of $q = q^*$, namely,

$$K_{q^*}^B(p||\tilde{p}^{ord}) = -\Delta S_{q^*}^{(\tilde{p}^{ord} \to p)}$$ (24)

It should be noted here that the transformation enables us to equate the mean energies, i.e., $\langle E \rangle_{q^*}^{p^{ord}} = \langle E \rangle^p$, at a unique value of q taking the normalized q-average instead of

the ordinary average in the calculation of the mean energy of the reference state. In other words, it re-normalizes the mean energy of the reference state.

Comparing Equations (21)–(24), it can be easily shown that the compensation requires a q-Gibbsian equality given by

$$\sum_i p_i \ln_{2-q^*} p_i^{ord} = \sum_i \tilde{p}_i^{ord} \ln_{2-q^*} p_i^{ord} \tag{25}$$

where the unique q^* can be found numerically.

One can easily show that Bregman form of the generalized relative entropy in Equation (22) is associated with the q-generalized version of free energy differences as can be given in Equation (10a) where $F_q = <E>^p - S_q/\beta'$ and $F_q^{ord} = <E>^{p^{ord}} - S_q/\beta'$. Moreover, as can be seen in Equation (24), there is a one-to-one correspondence between the generalized relative entropy and the q-renormalized entropy due to the compensation of the mean energy differences.

It is also worth noting that q-renormalized entropy is not a generalization of the usual renormalized entropy by Klimontovich. Although the generalized relative entropy in Equation (17) recovers the relative entropy by Kullback-Leibler in the limit $q \to 1$, the Gibbsian equality in Equation (25) is ensured at $q^* = 1$ only if the transition from p^{ord} to p belongs a cyclic process or the states possess the same degree of complexity. At $q = q^* \neq 1$, the value of q holds the Gibbsian equality as the necessary condition of self organization for the transition between distinct states and leads the connection in Equation (24). Therefore, the parameter q^*, which is the unique value of q, measures the relative degree of order/disorder between the states. We confirm it using the toy model in Section 4.

3.2. Derivation and Connection II: q-Renormalized Entropy and Csiszar Type of Relative Entropy

Substituting $p_{0i} = p_i^{nor}$, the stationary distribution of the q-exponential form in Equation (9), into Equation (18) and using the identical relation $Z^{1-q} = C_q$ where $C_q = \sum_i (p_i^{nor})^q$, the Csiszar form of the generalized relative entropy can be written as

$$K_q^C(p||p^{nor}) = -\Delta S_q^{(p^{nor} \to p)} \\ + \hat{\beta} D_q \sum_i \frac{p^q}{D_q}\left(\epsilon_i - \langle E \rangle_q^{p^{nor}}\right) \tag{26}$$

where $D_q = \sum_i p_i^q$. Using the q-deformed logarithm form, $\ln_q x$, instead of the second term in the right hand side of Equation (26), it follows that

$$K_q^C(p||p^{nor}) = -\Delta S_q^{(p^{nor} \to p)} \\ - C_q D_q \sum_i \left(\frac{p^q}{D_q} - \frac{(p_i^{nor})^q}{C_q}\right) \ln_q (p_i^{nor}) \tag{27}$$

By the transformation $p_i \to \tilde{p}_i$ on the other state, Equation (26) yields

$$K_{q^*}^C(\tilde{p}||p^{nor}) = -\Delta S_{q^*}^{(p^{nor} \to \tilde{p})} \tag{28}$$

where $\tilde{p}_i = p_i^{1/q} / \sum_i p_i^{1/q}$ is the distribution chosen so that it enables us to vanish the second terms in the right hand side of Equations (26) and (27) at a unique value of $q = q^*$, satisfying $\langle E \rangle_{q^*}^{p^{nor}} = \langle E \rangle^p$.

Comparing Equations (26) and (27), it can be easily shown that the compensation of mean energy difference requires a Gibbsian equality given by

$$\sum_i p_i \ln_{q^*} p_i^{nor} = \sum_i \frac{(p_i^{nor})^{q^*}}{C_q} \ln_{q^*} p_i^{nor} \tag{29}$$

where the unique q^* can be found numerically.

At this point, it should be emphasized that the Gibbsian equalities in Equations (25) and (29) both lead the same mean energy equality, that is $\langle E \rangle_{q^*}{}^{p_0} = \langle E \rangle^p$, if one applies a transformation on the reference state for the Bregman form of the generalized relative entropy taking $p_0 = p^{ord}$ and on the other state for the Csiszar form of the generalized relative entropy taking $p_0 = p^{nor}$.

4. Application: Logistic Map

To identify behaviour of the q-renormalized entropies for an evolution in the control parameter space and to illustrate the consistency of Bregman and Csiszar forms of the relative entropies within the context of the self-organization, we apply these procedures on the logistic map. In addition to its 'very simple expression' as a toy model, the logistic map has 'highly complicated' dynamics in the phase space [37]. Moreover, it is very convenient to search whether there exist a connection between self-organization and bifurcation processes as the system parameter slightly changes.

The expression of the logistic map reads

$$f(X_t) = X_{t+1} = 1 - aX_t^2 \tag{30}$$

where $X_t \in [-1, 1]$ is a sufficiently long phase space trajectory, t is iteration step ($t = 1, 2, \dots, N$) and $a \in [0, 2]$ is the control parameter of the map.

For the evolution of the map from a_0 to $a_0 + \Delta a$, one can easily generate the trajectories $\{X_t(a_0)\}$ and $\{X_t(a_0 + \Delta a)\}$. Respectively, the corresponding probability distributions estimated from the trajectories are $p_0 = p_0(X, a_0)$ for the reference state and $p_1 = p_1(X, a_0 + \Delta a)$ for the other state where $\sum p_0 = \sum p_1 = 1$.

For the estimation of the distributions, we use the dependence of spectral intensities on the frequency w. In other words, we use the Fourier transformation $p(w, a) = F(w, a) \cdot F^*(w, a)$ of the trajectory $\{X_t(a)\}$ instead of residence time distribution. Technically, we generate trajectories of the map in Equation (30) with the length of 65,536 points after 4096 points are discarded as transients. The spectrum is then averaged over 16 periodograms with a length of 4096 points. The details of the estimation procedure can be found in a recent paper [10].

It is well known that the bifurcation diagram of the logistic map represents a very rich dynamics where transitions with period-doubling route to chaos arise as the control parameter changes in the range of $a \in [0, 2]$ as can be seen in Figure 2. The map has a critical point at $a = a_c = 1.401155\ldots$ which can be approached from the most ordered state where the value of the control parameter is $a = 0$. From $a = 0$ (where period-1 occurs) to $a = a_c$ (where 2^∞ periods accumulate), the map shows a period-doubling procedure of 2^n periods. One can also approach the critical point from the most chaotic state (where the value of the control parameter is $a = 2$), via a band splitting procedure where 2^∞ bands split at the critical point. In other words, the map is in a periodic region from $a = 0$ up to $a = a_c$ with a period doubling procedure as it is in a chaotic region from $a = 2$ up to $a = a_c$ with a band splitting procedure. It is also possible to see narrow periodic windows in the chaotic region that possess similar structures to those of the map in the whole range of the control parameter, i.e., $a \in [0, 2]$. Moreover, the Lyapunov exponent of the map can be calculated using

$$\lambda = \lim_{N \to \infty} \frac{1}{N} \sum_{t=0}^{N-1} \log|f'(X_t)|, \tag{31}$$

by substituting the first derivative of the map function in the Equation (31) and is used to make a distinction between periodic regions ($\lambda < 0$) and chaotic ones ($\lambda > 0$) [38].

To compare the reference state of the map with all other states within q-renormalized entropies, we choose the reference state p_0 at $a = a_0 = 0$ and all other states in the region of $a \in [0, 2]$, i.e., $p_0 = p(w, a_0 = 0)$ and $p_1 = p(w, a_0 + \Delta a)$ with a parameter increase step $\Delta a = 0.01$. To calculate the entropies, we firstly numerically define the unique q^* values that

hold the Gibsian equalities in Equations (25) and (29). We then obtain the q-renormalized entropies $\Delta S_{q^*}^{(\tilde{p}_0 \to p)}$ and $\Delta S_{q^*}^{(p_0 \to \tilde{p})}$ that are associated with q-relative entropies $K_{q^*}^B(p||\tilde{p}_0)$ and $K_{q^*}^C(\tilde{p}||p_0)$, respectively.

In Figure 3, from top to bottom, we plot the bifurcation diagram, the Lyapunov exponent, the q-renormalized entropy in Bregman and Csiszar forms and evolution of the q^* values in the control parameter space. We denote some points just above the bifurcation diagram as can be seen as $a_0, a_1, a_2, \dots, \tilde{a}_2, \tilde{a}_1, \tilde{a}_0$ to divide the map in distinct regions as analogous to the periodic and chaotic band regions in Figure 2. There are 2^{n-1} number of periods and chaotic bands between the regions $a \in [a_{n-1}, a_n]$ and $a \in [\tilde{a}_{n-1}, \tilde{a}_n]$ where $n = 1, 2, 3, \dots, \infty$, respectively. As the control parameter evolves from $a_0 = 0$ to $\tilde{a}_0 = 2$, the periodic trajectories bifurcate at the critical point a_n, where the first bifurcation point is a_1, up to the chaos threshold a_c, where infinite number of periods exists. As a reverse process, an infinite number of chaotic bands which exist at the chaos threshold a_c start to merge through the critical points $\tilde{a}_n$ up to the $\tilde{a}_1$ where the last chaotic band merging exists. The Lyapunov exponent vanishes at all critical points from a_1 to $\tilde{a}_1$ as it has a negative value in the range of $a \in [a_0, a_c)$ and has a positive value in the range of $a \in (a_c, \tilde{a}_0]$. It can also be seen that the q-renormalized entropy in both Bregman and Csiszar forms point out the same relative degree of order/disorder in the range of period–1 which implies a low level of self-organization/complexity. When the sequence of branches emerges at a_1, the relative order, i.e., the level of self-organization/complexity, increases and the q-renormalized entropies decrease through successive bifurcations up to the chaos threshold point a_c. Such behaviour of q-renormalized entropy in the control parameter space of $a \in [a_1, a_c]$ is compatible with that of the entropy-based measures of type-III in Figure 1. In the range of chaotic band merging area of $a \in (a_c, \tilde{a}_1]$ as a reverse process, increase in q-renormalized entropies corresponds to the entropy-based measures of type-I in Figure 1. It means that the relative order, i.e., the level of self-organization/complexity, decreases through the band merging area. It should be noted that the q-renormalized relative entropy in Csiszar form evaluates that the level of order in the range of period–1 of $a \in [a_0, a_1]$ has the same degree of complexity with the level of disorder in the range of chaotic band–1 of $a \in (\tilde{a}_1, \tilde{a}_0]$. However, the degree of order/disorder in the range of chaotic band–1 of $a \in (\tilde{a}_1, \tilde{a}_0]$ decreases/increases except for a very thin periodic window, which is similar to the behaviour of the Lyapunov exponent in the same range of the control parameter. Moreover, q-renormalized entropy in Bregman form is more accurate for localization of the chaos threshold such that it corresponds to a local minimum between $a \in (a_1, \tilde{a}_1)$ where $a_c = 1.4011 \dots$.

The equalities between the q-generalized relative entropies and the q-renormalized entropies in Equations (24) and (28) guarantee that the evolution of the q-generalized relative entropies as complexity measures in the range of period doublings and chaotic band mergings of $a \in [a_1, \tilde{a}_1]$ at a unique $q = q^*$ value conforms with the behaviour of the entropy-based measure of type-II in Figure 1. Such behaviour of the complexity function is similar to the behaviour of complexity in coffee automaton (or to experiment of coffee with milk). It was discussed by defining a "complextropy" measure that first increases and then decreases in closed thermodynamic systems, in contrast to usual Shannon entropy (which increases monotonically) [39]. Similar to the model, in the range of $a_1 < a_c < \tilde{a}_1$, the q^*-generalized relative entropy represents the most organized spatial pattern at the chaos threshold where $a = a_c$ due to the relations roughly $K_{q^*} = -\Delta \tilde{S}_{q^*}$ where $\Delta \tilde{S}_{q^*}$ is the general definition of the q-renormalized entropy. q-relative entropy is an evaluation of the change in entropy relative to a reference state chosen. For the transition between the reference equilibrium state and the other arbitrary state, one can numerically localize the unique q^* value as the one for which the Gibbsian equalities hold. We show in the bottom of Figure 3 that the q^* values are the same for both Bregman and Csiszar forms of the q-renormalized entropies for an evolution in the control parameter space of the logistic map, satisfying the Gibbsian equalities as the necessary condition of self organization. In other words, renormalization enables us to equate mean energies of the states at a unique q^*

value in a manner that the evolution of the reference state is isolated after renormalization. For the evolution of the q^* values in the range of the control parameter $a \in [0, 2]$, the q^* values decrease from $q^* = 1$ to $q^* = 0$ where the maximum value indicates the most ordered state (period-1) and the minimum value points out the most disordered (strongly chaotic) state. The process offers a method by means of q-renormalized entropies on how to measure the level of self organization in spatially-extended fractals. On the other hand, the Shannon entropy leads to an increase since it is proportional to the logarithm of the accessible volume in phase space, however a decrease in entropy is necessary to link a connection to the self-organization.

In Figure 4, we zoom to the chaos threshold in order to localize unique q^* value at the critical point. It is intriguing that this unique q^* value happens to coincide with the $q_{sensitivity}$ value [28,29] (i.e., $q^* \simeq 0.2445$). At this point, it is worth noting that this kind of varying q parameter tendency with the control parameter of the map is very reminiscent to the behaviour of the running q parameter with the energy scale detected in recent cosmological studies [40,41].
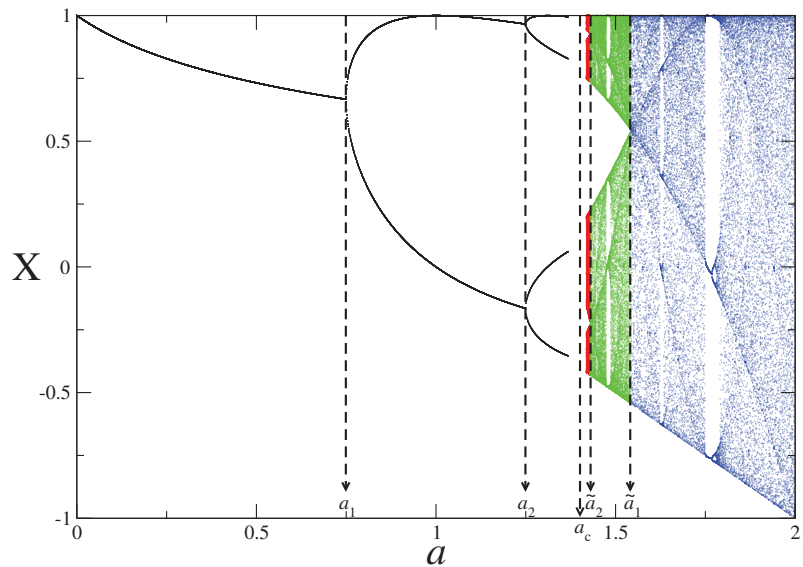
Figure 2. A representation of the pitchfork bifurcations in periodic regime (black) and the band merging structures in chaotic regime (blue, green and red) of the logistic map. The black dashed lines represent the bifurcation points (a_n) and the band merging points ($\tilde{a}_n$).
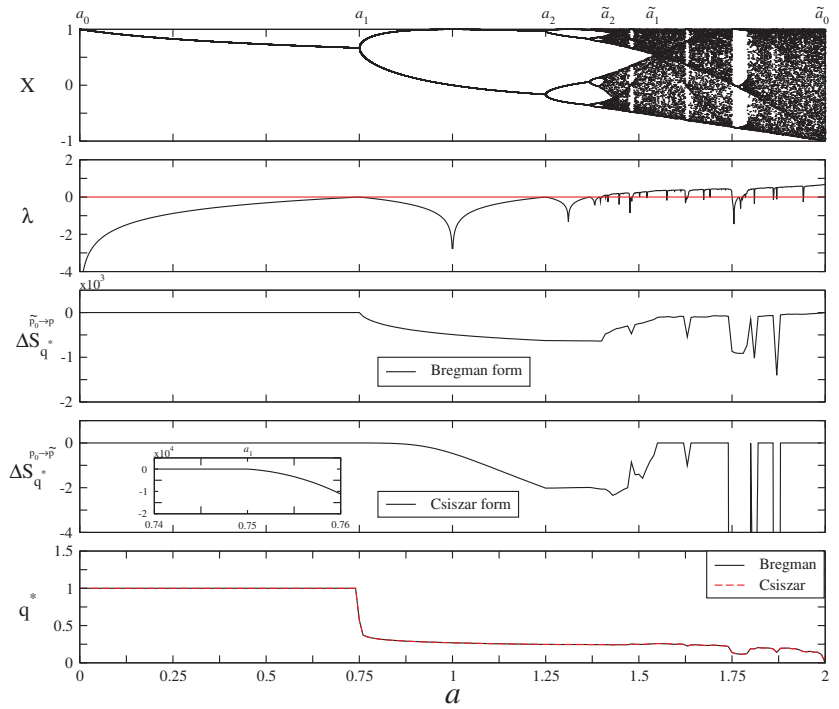
Figure 3. For the evolution of the logistic map in the control parameter space, from top to bottom: Bifurcation diagram, Lyapunov exponent, Bregman form of q-renormalized entropy, Csiszar form of q-renormalized entropy and q^* values that hold the Gibbsian equalities in Equations (25) and (29), respectively.
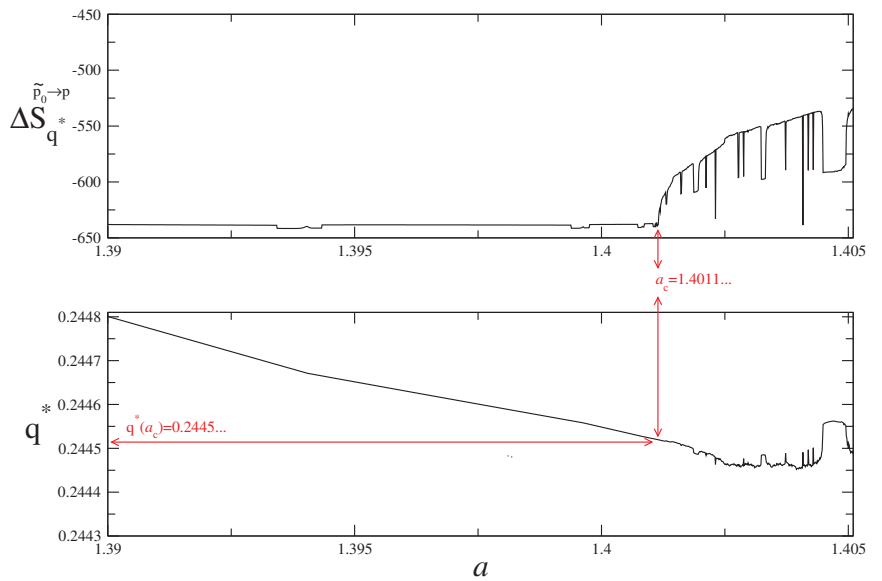
Figure 4. q-Renormalized entropy (top) and q^* values for the control parameter evolution of the logistic map near chaos threshold ($a \in [1.390, 1.4051]$).

5. Conclusions

It is well known that the second law of thermodynamic ($\Delta S \geq 0$) is only valid for an isolated evolution of an arbitrary state to an equilibrium state. This inequality can be derived by substituting Gibbs equality in the definition of Kullback-Leibler relative entropy, which implies that the equilibrium state shows the greatest disorder (or chaoticity) as compared to any arbitrary state as long as the mean energy is the same. The mean energy equality through the evolution is a consequence of Gibbs equality, that points out a strong limitation of the law. Hence, it is violated for the evolution of open systems in which the exchange of energy/matter with its surroundings is allowed. The problem was solved by Klimantovich via the S-theorem where 'S' stands for criterion of self-organization. The theorem is based on renormalization of the equilibrium distribution in a manner that Gibbs equality holds. Mean energy in terms of a predefined effective Hamiltonian function for an open system is constant through the evolution after renormalization. The renormalization on the distribution leads a renormalized entropy as a new complexity measure to compare distinct states, i.e., a renormalized equilibrium state and an arbitrary one. For an isolated evolution from the renormalized equilibrium state to an arbitrary one, a decrease in the renormalized entropy indicates an increase in the relative degree of order in the system that indicates the creation of complicated structures in the phase space as first suggested by Haken in the context of self-organization [13]. Although the renormalized entropy is a suitable measure to explain highly organised structures that emerge in phase space, we have shown that its expression ($\Delta \tilde{S} = -KL \leq 0$) is valid for the systems which evaluate from canonical equilibrium state. Moreover, choosing a reference state in exponential form spontaneously reveals the predefined effective Hamiltonian function ($H_{eff} = \ln p_0$) by Klimontovich directly from the calculations. We have also shown that such kind of relation between q-renormalized entropy and q-generalized relative entropies (in the form of both Bregmann and Csiszar) can be written by introducing new q-Gibbsian equalities as the necessary conditions of self-organisation. The crucial point for the new equalities is that they are only valid for a unique $q = q^*$ value for the transition between two states and lead to the same mean energy equality that is $\langle E \rangle_{q^*}{}^{p_0} = \langle E \rangle^p$. To achieve this result, it is necessary to apply a transformation on the reference state for the Bregman form of the generalized relative entropy taking $p_0 = p^{ord}$ and on the other state for the Csiszar form of the generalized relative entropy taking $p_0 = p^{nor}$ as the stationary distributions of the $(2-q)$-exponential and q-exponential forms, respectively. To verify the results numerically, we have used the control parameter evolution of the logistic map. As the control parameter changes in $a \in [0, 2]$, we have shown a fall in the q-renormalized entropies through period doublings in the range of $a \in [0, a_c]$ and an increase in the q-renormalized entropies through chaotic band mergings in the range of $a \in [a_c, 2]$. Such kind of behaviour of the q-renormalized entropy is compatible with the SDL complexity of type-III and type-I as the signs of emerging and destroying highly organized structures in the phase space, respectively [5]. We have also looked closely at the chaos threshold of the map, and interestingly we discovered that the unique q^* value is $q^* \simeq 0.2445$, which coincides with the value of $q_{sensitivity}$ given in the literature [28,29].

Finally, it would be good to note that these considerations could be applied to some specific class of nonextensive systems, such as black holes and other gravitational systems. An interesting future work addressing a possible discussion of our scheme for such systems would be highly welcomed.

Author Contributions: Conceptualization, O.A. and U.T.; Methodology, O.A. and U.T.; Writing—review & editing, O.A. and U.T. All authors have read and agreed to the published version of the manuscript.

Conflicts of Interest: The authors declare no conflict of interest.

References

1. Kolmogorov, A.N. Three approaches to the quantitative definition of information. *Probl. Inf. Transm.* **1965**, *1*, 1–7. [CrossRef]
2. Chaitin, G.J. On the length of programs for computing finite binary sequences. *J. ACM* **1966**, *13*, 547–569. [CrossRef]
3. Bennett, C.H. On the nature and origin of complexity in discrete, homogeneous, locally-interacting systems. *Found. Phys.* **1986**, *16*, 585–592. [CrossRef]
4. Lloyd, S.; Pagels, H. Complexity as thermodynamic depth. *Ann. Phys.* **1988**, *188*, 186–213. [CrossRef]
5. Shiner, J.S.; Davison, M.; Landsperg, P.T. Simple measure for complexity. *Phys. Rev. E* **1999**, *59*, 1459–1464. [CrossRef]
6. López-Ruiz, R.; Mancini, H.; Calbet, X. A statistical measure of complexity. *Phys. Lett. A* **1995**, *209*, 321–326. [CrossRef]
7. Feldman, D.P.; Crutchfield, J.P. Measures of statistical complexity: Why? *Phys. Lett. A* **1998**, *238*, 244–252. [CrossRef]
8. Newman, M.E.J. Resource letter cs–1: Complex systems. *Am. J. Phys.* **2011**, *79*, 800–810. [CrossRef]
9. Shannon, C.E. A mathematical theory of communication. *Bell Syst. Tech. J.* **1948**, *27*, 379–423. [CrossRef]
10. Afsar, O. A comparison of Shannon, Kullback–Leibler and renormalized entropies within successive bifurcations. *Physica D* **2019**, *390*, 62–68. [CrossRef]
11. Blum, H.F. Perspectives in: Evolution. *Am. Sci.* **1955**, *43*, 595–610.
12. Saparin, P.; Witt, A.; Kurths, J.; Anishchenko, V. The renormalized entropy—An appropriate complexity measure? *Chaos Solit. Fractals* **1994**, *4*, 1907–1916. [CrossRef]
13. Haken, H. *Information and Self-Organization: A Macroscopic Approach to Complex Systems (Springer Series in Synergetics)*; Springer: Secaucus, NJ, USA, 2006.
14. Klimontovich, Y.L. Entropy and entropy production in the laminar and turbulent flows. *Pis'ma ZhTF* **1984**, *10*, 80.
15. Klimontovich, Y.L. *Statistical Physics*; Harwood Academic Publishers: Cambridgeshire, UK, 1986.
16. Rayleigh, L. LIX. On convection currents in a horizontal layer of fluid, when the higher temperature is on the under side. *Lond. Edinb. Dubl. Philos. Mag.* **1916**, *32*, 529–546. [CrossRef]
17. Bénard, H. Les tourbillons cellulaires dans une nappe liquide. Méthodes optiques d'observation et d'enregistrement. *J. Phys. Theor. Appl.* **1901**, *10*, 254–266. [CrossRef]
18. Taylor, G.I. Viii. stability of a viscous liquid contained between two rotating cylinders. *Philos. R. Soc. Lond. Ser. A Math. Phys. Eng. Sci.* **1923**, *223*, 289–343.
19. Ben-Jacob, E.; Schochet, O.; Tenenbaum, A.; Cohen, I.; Czirók, A.; Vicsek, T. Generic modelling of cooperative growth patterns in bacterial colonies. *Nature* **1994**, *368*, 46. [CrossRef] [PubMed]
20. Pálsson, E.; Cox, E.C. Origin and evolution of circular waves and spirals in dictyostelium discoideum territories. *Proc. Natl. Acad. Sci. USA* **1996**, *93*, 1151–1155. [CrossRef]
21. Klimontovich, Y.L. Criteria of Self-organization. *Chaos Solit. Fractals* **1995**, *5*, 1985–2002. [CrossRef]
22. Tsallis, C.; Mendes, R.S.; Plastino, A.R. The role of constraints within generalized nonextensive statistics. *Physica A* **1998**, *261*, 534–554. [CrossRef]
23. Oikonomou, T.; Bagci, G.B. The maximization of Tsallis entropy with complete deformed functions and the problem of constraints. *Phys. Lett. A* **2010**, *374*, 2225–2229. [CrossRef]
24. Abe, S.; Bagci, G.B. Necessity of *q*-expectation value in nonextensive statistical mechanics. *Phys. Rev. E* **2005**, *71*, 016139. [CrossRef]
25. Ferri, G.L.; Martinez, S.; Plastino, A. Equivalence of the four versions of Tsallis's statistics. *J. Stat. Mech.* **2005**, P04009. [CrossRef]
26. Bagci, G.B. Nonadditive open systems and the problem of constraints. *Int. J. Mod. Phys. B* **2008**, *22*, 3381–3396. [CrossRef]
27. Bagci, G.B.; Tirnakli, U. Self-organization in nonadditive systems with external noise. *Int. J. Bifurcat. Chaos* **2009**, *19*, 4247–4252. [CrossRef]
28. Tsallis, C.; Plastino, A.R.; Zheng, W.-M. Power-law sensitivity to initial conditions—New entropic representation. *Chaos Solitons Fractals* **1997**, *8*, 885. [CrossRef]
29. Costa, U.M.S.; Lyra, M.L.; Plastino, A.R.; Tsallis, C. Power-law sensitivity to initial conditions within a logisticlike family of maps: Fractality and nonextensivity. *Phys. Rev. E* **1997**, *56*, 245. [CrossRef]
30. Kullback, S.; Leibler, R.A. On information and sufficiency. *Ann. Math. Stat.* **1951**, *22*, 79–86. [CrossRef]
31. Afsar, O.; Bagci, G.B.; Tirnakli, U. Renormalized entropy for one dimensional discrete maps: periodic and quasi-periodic route to chaos and their robustness. *Eur. Phys. J. B* **2013**, *86*, 307. [CrossRef]
32. Kurths, J.; Voss, A.; Saparin, P.; Witt, A.; Kleiner, H.J.; Wessel, N. Quantitative analysis of heart rate variability. *Chaos* **1995**, *5*, 88–94. [CrossRef]
33. Voss, A.; Kurths, J.; Kleiner, H.; Witt, A.; Wessel, N.; Saparin, P.; Osterziel, K.; Schurath, R.; Dietz, R. The application of methods of non-linear dynamics for the improved and predictive recognition of patients threatened by sudden cardiac death. *Cardiovasc. Res.* **1996**, *31*, 419–433. [CrossRef] [PubMed]
34. Kopitzki, K.; Warnke, P.C.; Timmer, J. Quantitative analysis by renormalized entropy of invasive electroencephalograph recordings in focal epilepsy. *Phys. Rev. E* **1998**, *58*, 4859–4864. [CrossRef]
35. Afsar, O.; Tirnakli, U.; Kurths, J. Entropy-based complexity measures for gait data of patients with parkinson's disease. *Chaos* **2016**, *26*, 023115. [CrossRef] [PubMed]
36. Venkatesan, R.C.; Plastino, A. Scaled Bregman divergences in a Tsallis scenario. *Physica A* **2011**, *390*, 2749–2758. [CrossRef]
37. May, R.M. Simple mathematical models with very complicated dynamics. *Nature* **1976**, *261*, 459–467.
38. Schuster, H.G. *Deterministic Chaos: An Introduction*; Wiley-VCH: Weinheim, Germany, 2006.

39. Aaronson, S.; Carroll, S.; Ouellette, L. Quantifying the Rise and Fall of Complexity in Closed Systems: The Coffee Automaton. *arXiv* **2014**, arXiv:1405.6903 .
40. Luciano, G.G.; Blasone, M. *q*-generalized Tsallis thermostatistics in Unruh effect for mixed fields. *Phys. Rev. D* **2021**, *104*, 045004. [CrossRef]
41. Nojiri, S.; Odintsov, S.D.; Saridakis, E.N. Modified cosmology from extended entropy with varying exponent. *Eur. Phys. J. C* **2019**, *79*, 242. [CrossRef]

Some Non-Obvious Consequences of Non-Extensiveness of Entropy

Grzegorz Wilk [1,*] and Zbigniew Włodarczyk [2]

[1] National Centre for Nuclear Research, Department of Fundamental Research, 02-093 Warsaw, Poland
[2] Institute of Physics, Jan Kochanowski University, 25-406 Kielce, Poland
* Correspondence: grzegorz.wilk@ncbj.gov.pl

Abstract: Non-additive (or non-extensive) entropies have long been intensively studied and used in various fields of scientific research. This was due to the desire to describe the commonly observed quasi-power rather than the exponential nature of various distributions of the variables of interest when considered in the full available space of their variability. In this work we will concentrate on the example of high energy multiparticle production processes and will limit ourselves to only one form of non-extensive entropy, namely the Tsallis entropy. We will discuss some points not yet fully clarified and present some non-obvious consequences of non-extensiveness of entropy when applied to production processes.

Keywords: non-additive entropy; Tsallis distribution; multiparticle production processes

1. Introduction

Entropy plays an important role in the study of the production mechanism of elementary particles observed in hadronic and nuclear collisions. This is the case both in the modelling of these processes based on thermodynamics (that is, on the description of distributions of all kinds of observables characterizing multiparticle production processes) and in their description in the language of statistical models (i.e., mainly on the description of their multiplicity distributions).

Over time, more and more new experimental results appeared, which began clearly to indicate that the originally used Boltzmann entropy (in the first case) or Shannon entropy (treated as a measure of information in the second), did not describe the results in the entire range of measured values. Experimentally observed distributions depart from the expected exponential form (in the first case) and from the Poissonian distribution (in the second) [1,2]. This was generally taken as an indication that different mechanisms operate, resulting in the occurrence of various types of correlations and fluctuations, and these do not fit into the scheme of equilibrium thermodynamics or the Shannon information measure [3]. This meant that it was necessary either to add appropriate conditions to the definition of the Boltzmann-Shannon entropy used, or to extend the very concept of entropy so that in its new form it could be applied to more complex systems without any additional conditions (their operation would be replaced by a new form of the entropy formula and by some new parameters appearing in it).

A multitude of new definitions of entropy and related measures of information have appeared in various fields of science (see, for example, [3–7] and references cited therein). In most cases, their distinguishing feature is their non-extensiveness. Here we will consider only the case of Tsallis entropy [5] S_q, which for $q = 1$ becomes Boltzmann-Shannon entropy, $S = S_{q=1}$:

$$S_q = -\int dx f(x) \ln_q f(x) = -\frac{1}{1-q} \int dx f(x) \left[1 - f^{q-1}(x)\right]$$

$$\overset{q \to 1}{\Longrightarrow} \quad S = -\int dx f(x) \ln f(x), \tag{1}$$

which is currently the most widely-used to describe the particle production processes mentioned above (in fact, Tsallis entropy was introduced independently before and then rediscovered by Tsallis in thermodynamics [8,9]. It should be mentioned that from the point of view of information theory, the entropies $S = S_{q=1}$ and S_q are related to a different, specific way of collecting information about the object of interest [10]. This observation has recently been used in cognitive science [11]). The reason for this is the quasi-power nature of the Tsallis distribution $f_q(x)$ that is obtained from it,

$$f_q(x) = \exp_q(-x) = (2-q)[1 - (1-q)x]^{\frac{1}{1-q}} \overset{q \to 1}{\Longrightarrow} \quad f(x) = \exp(-x), \tag{2}$$

and, as it was shown a long time ago in [12–14], it is this type of distribution that is most suitable for describing the distributions of various variables in the full observable range of their variability. In fact, there are a variety of systems that do not comply with the standard equilibrium theory and that fit under the description of non-extensive entropy, thus suggesting that the entropic index q could be a convenient manner for quantifying some relevant aspects of complexity [5].

The Tsallis distribution is obtained by maximizing the Tsallis entropy using some constraints imposed on the distribution function sought. It turns out that in the commonly used version this procedure leads to a rather surprising result, namely that the non-extensiveness parameter q appearing in the definition of entropy is, in a sense, dual to the non-extensiveness parameter q' obtained from the description of the observed distributions. As we show in (Section 2), this result is confirmed by the simultaneous analysis of multiparticle production processes in nucleon and nuclear collisions. In (Section 3) we show how by properly redefining the functions $\exp_q(x)$ and $\ln_q(y)$ this problem of duality can be avoided.

Tsallis entropy S_q is nonadditive, namely

$$S_q(AB) = S_q(A) + S_q(B) + (1-q)S_q(A)S_q(B), \tag{3}$$

where A and B are two systems independent in the sense that $f(AB) = f(A)f(B)$ and the parameter q is simply a measure of the degree of this non-additivity (note that we tacitly assume here and in all subsequent considerations that q is the same in both systems). If, hypothetically, we extended this reasoning to the system of ν independent components (again, with the same q), $A_1, A_2, \ldots, A_\nu$ such that $f(\prod_{i=1}^{\nu} A_i) = \prod_{i=1}^{\nu} f(A_i)$, then we would have some kind of non-linear non-additivity (in parameter q), because now

$$S_q\left(\prod_{i=1}^{\nu} A_i\right) = \sum_{i=1}^{\nu} \binom{\nu}{i}(1-q)^{(i-1)}\prod_{j=1}^{i} S_q(A_j). \tag{4}$$

To better understand the role of the parameter q, let us additionally consider the non-additive versions of conditional probability and conditional entropy. Let us say that the considered system can be divided into two subsystems, A and B, and that $p_{ij}(A, B)$ is the joint normalized probability of finding A in state i and B in state j. Then the conditional probability B with A being in the $i-th$ state, $p_{ij}(B|A)$, is given by Bayes' multiplication law,

$$p_{ij}(A, B) = p_i(A)p_{ij}(B|A), \tag{5}$$

and the corresponding conditional Shannon entropy is

$$S(A, B) = S(A) + S(B|A). \tag{6}$$

By analogy to Equation (3) we can now write the corresponding conditional non-additive Tsallis entropy as

$$S_q(A, B) = S_q(A) + S_q(B|A) \tag{7}$$

where

$$S_q(B|A) = S_q(B)[1 + (1 - q)S_q(A)] \tag{8}$$

(note that because $S_q(B|A) \leq S_q(B)$ one must have $q \geq 1$). This allows us to interpret the nonextensivity parameter q in terms of the conditional entropy as

$$q = 1 + \frac{S_q(B) - S_q(B|A)}{S_q(B)S_q(A)}, \tag{9}$$

and turns out to be crucial for nonadditive (quantum) information theory [15].

In practical applications, the non-extensiveness of the entropy manifests itself in the quasi-power character of the distributions obtained from it, i.e., in the case considered here in the appearance of the non-extensiveness parameter q in the Tsallis distribution. However, there is a problem here that we discuss in Sections 2 and 3, namely that for a certain type of constraints, the parameters q in the definition of entropy and q' in the Tsallis distribution are not identical but dual to each other, i.e., $q + q' = 2$. Usually, the meaning of the non-extensiveness parameter is related to Tsallis distributions rather than to entropy as above. These, in turn, can be obtained in many ways, depending on the details of the described physical process and even from the Shannon entropy, if only the appropriate constraints are applied. We discuss this issue in more detail in Section 4. Section 5 contains our summary and conclusions.

2. From Tsalis Entropy to Tsalis Distribution

The Tsallis distribution (2) (valid for $0 \leq x < \infty$; $1 \leq q \leq 3/2$) is obtained by maximizing the Tsallis entropy (1) using the following constraints [16]:

$$\int dx f(x) = 1; \qquad \int dx x f^q(x) = \langle x \rangle_q. \tag{10}$$

In most cases, it is this form of distribution that is used phenomenologically to describe the various distributions measured in high-energy multiple particle production experiments (with $x = X/T$ and the scaling factor T is usually identified with the temperature and X denotes the energy or momentum of the measured particles; it also appears in the normalization as $1/T$). As shown in Figure 1, using this form of Tsallis distribution one obtains from measurements of different observables (rapidity, multiplicity and transverse momentum) and for high enough energies $q' > 1$ (for low energies, conservation laws are important and they can sometimes push the parameter q' to the $q' < 1$ region). In addition, note that the values of q obtained from different observables are different (but always $q' > 1$). These differences are due to the influence of two factors. The first is whether q' is estimated from the temperature fluctuations obtained from data already averaged over other fluctuations or from data taking other fluctuations into account as well, and the second is that in different analyzes q' is obtained in other regions of the phase space.
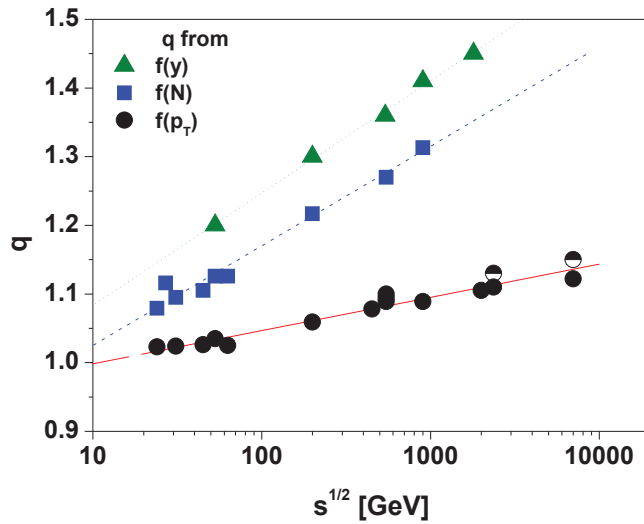
Figure 1. (Color online) Energy $\sqrt{s}$ dependencies of the parameters q obtained from different observables. Squares: q obtained from multiplicity distributions $f(N)$ [17,18] (fitted by $q = 0.88 + 0.063 \ln[\sqrt{(s)}]$). Circles: q obtained from different analyses of the transverse momenta distribution $f(p_T)$. Data points are, respectively, from a compilation of $p + p$ data (full symbols) [19], from CMS data (half filled circles at high energies) [20,21] (fitted by $q = 0.95 + 0.021 \ln[\sqrt{(s)}]$. Triangles: q obtained from analyses of rapidity distributions $f(y)$ [22,23] (and fitted by $q = 0.92 + 0.071 \ln[\sqrt{(s)}]$.

However, this is not the only possible choice of constraints. Instead, using constraints in the form which seems to be more natural from the point of view of physical interpretation, namely that

$$\int dx f(x) = 1; \qquad \int dx x f(x) = \langle x \rangle \tag{11}$$

obtain [16]

$$f(x) = q' \left[1 - (1 - q')x \right]^{\frac{1}{q'-1}}; \qquad 0 \leq x < 1/(1 - q'); \quad 1/2 < q' \leq 1. \tag{12}$$

These two different definitions pertain to two different schemes of the nonextensive statistical mechanics [24]. It should be noted that [25] proposes a parametric technique that shows the equivalence of different schemes (including those discussed here), and [26] once again shows the relationship of both averaging schemes (i.e., Equations (10) and (11)) with duality $q \leftrightarrow 1/q$. Now note that for

$$q' = 2 - q, \tag{13}$$

distribution $f(x)$ from Equation (12) becomes $f(x)$ from Equation (2) (note that in addition to the additive duality represented by Equation (13), multiplicative duality, $q \leftrightarrow 1/q$, was also considered [27,28] shows the potential physical application of a combination of both types of duality to study cosmic ray physics). This means that the imposition of these constraints leads to a situation in which the non-extensiveness parameter q appearing in the definition of entropy is dual to the non-extensiveness parameter q' obtained from describing the observed distributions. The problem of this duality has been raised many times (for example in [29–31]), but it does not seem to have been put to the experimental test yet, at least not in the field of multiparticle production. It turns out, however, that experiments measuring the multiplicities and distributions of particles produced in nuclear (AA) and nucleon (nn) collisions are very useful for this purpose, because they simultaneously

measure the multiplicities (enabling the estimation of the entropy produced) and particle distributions, and thus allow for the simultaneous determination and comparison of the non-extensiveness of the above mentioned relevant parameters and to verify the hypothesis of their duality.

Nuclear collisions are usually described by increasingly complex statistical models that try to account for all possible collective effects [32–34]. Because, however, for our purposes, the mutual relation between the entropies of AA and nn collisions will be important, to estimate the entropy in the nuclear collision, it will therefore be more convenient to use the phenomenological description based on the assumption that it can be described by a certain superposition of collisions of single nucleons (taking into account only nucleons that collided at least once and assuming that their collisions are independent—these are the so-called "wounded nucleons") [35]. (The reason for this choice may be the fact that, despite its apparent simplicity, this model is still able to describe a surprisingly large number of experimental results [36,37]).

In this approach, the total observed multiplicity N is the sum of the multiplicities $n_{i=1,...,\nu}$ of particles emitted from ν individual sources, and the average total multiplicity $\langle N \rangle$ is the product of the average number of sources, $\langle \nu \rangle$, and the average multiplicity from the source, $\langle n_i \rangle$, (which here is assumed to be the same for each source):

$$N = \sum_{i=1}^{\nu} n_i, \quad \text{and} \quad \langle N \rangle = \langle \nu \rangle \langle n_i \rangle. \tag{14}$$

The identity of the sources assumed here means that their entropies are equal, so using the relationship (4) the entropy ν of such sources is

$$S_q^{(\nu)} = \sum_{k=1}^{\nu} \binom{\nu}{k} (1-q)^{(k-1)} \left[S_q^{(1)} \right]^k = \frac{\left[1 + (1-q) S_q^{(1)} \right]^{\nu} - 1}{1-q}. \tag{15}$$

In further considerations, ν will denote the number N_P of nucleons of the incident nucleus participating in the collision (i.e., participants), and $\nu = N_W/2$, where N_W is the number of wounded nucleons. Continuing in the same vein and assuming that the total entropy is proportional to the average multiplicity of particles produced in the collision,

$$S = \alpha \langle N \rangle, \tag{16}$$

we can relate the average multiplicities in nuclear (AA) and nucleon (NN) collisions, namely

$$\alpha \langle N \rangle_{AA} = \frac{\left[1 + (1-q) \alpha \langle N \rangle_{pp} \right]^{N_P} - 1}{1-q}. \tag{17}$$

This simple dependence already allows for some preliminary assessment of the q parameter. It turns out that the observed N_{AA} grows non-linearly with N_P, $\langle N \rangle_{AA} > N_P \langle N \rangle_{pp}$ [38]. Considering this observation from the point of view of entropy, it is clear that we must have $q < 1$ here.

However, this is only a very rough estimate, because, strictly speaking, formula (17) is not fully correct with respect to the S_q entropy. We will therefore return to Equation (15) denoting now the entropy for the whole particle production process by s and the corresponding non-extensiveness parameter by $\tilde{q}$, and their equivalents for nucleon collisions by S and q, respectively. The relation (15) for N particles now looks like this:

$$s_{\tilde{q}}^{(N)} = \frac{\left[1 + (1-\tilde{q}) s_{\tilde{q}}^{(1)} \right]^N - 1}{1-\tilde{q}} \xrightarrow{\tilde{q} \to 1} N \cdot s_{\tilde{q}}^{(1)} = \alpha N \tag{18}$$

where $s_{\tilde{q}}^{(1)} = \alpha$ is the entropy for a single particle. In the $A + A$ collision with ν nucleons participating Equation (15) results in

$$S_q^{(\nu)} = \frac{\left[1 + (1 - q)S_q^{(1)}\right]^\nu - 1}{1 - q} \qquad (19)$$

where $S_q^{(1)}$ is the entropy for a single nucleon. Denoting multiplicity in single $N + N$ collisions by n, one can write that the respective entropy is

$$S_q^{(1)} = S_{\tilde{q}}^{(1)} = \frac{\left[1 + (1 - \tilde{q})s_{\tilde{q}}^{(1)}\right]^n - 1}{1 - \tilde{q}}, \qquad (20)$$

whereas the entropy in $A + A$ collisions for N produced particles is

$$S_{\tilde{q}}^{(N)} = \frac{\left[1 + (1 - \tilde{q})s_{\tilde{q}}^{(1)}\right]^N - 1}{1 - \tilde{q}}. \qquad (21)$$

This means therefore that

$$S_{\tilde{q}}^{(N)} = S_q^{(\nu)}. \qquad (22)$$

Parameters q and $\tilde{q}$ are usually not the same. However, from analyzes in [38,39] one obtains that for NN collisions (where $N_P = 1$) $\tilde{q} = 1$. On the other hand, for $\tilde{q} = q$ Equation (22) corresponds to the situation encountered in superpositions as now one obtains

$$\left[1 + (1 - q)s_q^{(1)}\right]^N = \left[1 + (1 - q)s_q^{(1)}\right]^{n\nu} \qquad \text{or} \qquad N = n\nu. \qquad (23)$$

In the general case, we obtain the formula for the ratio $N/(\nu \cdot n))$

$$\frac{N}{\nu \cdot n} = \frac{1}{\nu n \cdot \ln c_1} \ln \left[\frac{(c_2 c_1^n + 1 - c_2)^\nu - (1 - c_2)}{c_2} \right], \qquad (24)$$

where

$$c_1 = 1 + (1 - \tilde{q})s_{\tilde{q}}^{(1)}; \qquad c_2 = \frac{1 - q}{1 - \tilde{q}}, \qquad (25)$$

which for $N = \langle N_{AA} \rangle >$, $n = \langle N_{pp} \rangle$ and $\nu = N_P$ is presented in Figure 2 for different reactions (see [40] for more details). Note that for energies $\sqrt{s} > 7\,\text{GeV}$ one has $c_1 > 1$. This means that $\tilde{q} < 1$ and (because $c_2 > 0$) also $q < 1$, confirming therefore previous estimates based on Equation (17).

This, however, is as much as can be said for sure, because while the distributions can give exact values of the parameter q', the same cannot be said about q except that $q < 1$ (at least in a certain energy range). We still have too many free parameters here, e.g., unknown a priori entropy $s_q^{(1)}$. Therefore, while the statement that mostly we have $q' > 1$ and $q < 1$ seems certain, it is not known how exactly (if at all) the duality $q' + q = 2$ (13) is satisfied.
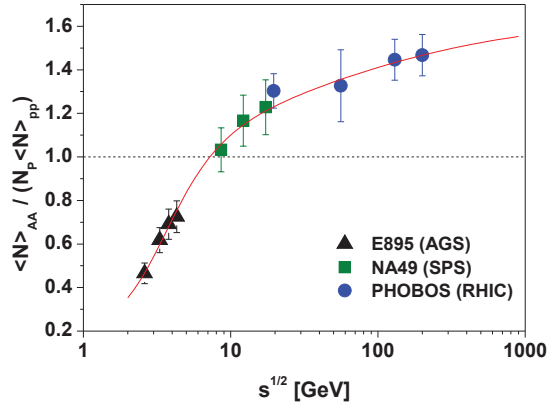
Figure 2. (Color online) Energy dependence of the charged multiplicity for nucleus-nucleus collisions divided by the superposition of multiplicities from proton-proton collisions using Equation (24) with $c_2 = 1.7$ and with c_1 depending on energy $\sqrt{s}$ according to $c_1(s) = 1.0006 - 0.036s^{-1.035}$. Experimental data on multiplicity are taken from the compilation of Ref. [41].

3. More Thorough Screening of Duality

We will now deal with the problem of duality in more detail. Figure 3 shows the entropies S_q obtained from the distributions (12) for $0.5 < q' \leq 1$,

$$S_q = \frac{q^q - (2q-1)}{(1-q)(2q-1)},$$ (26)

(here, q' was changed to $2q - 1$), and for $1 \leq q < 1.5$,

$$S_q = \frac{1 - (2q-1)^q}{1-q}.$$ (27)
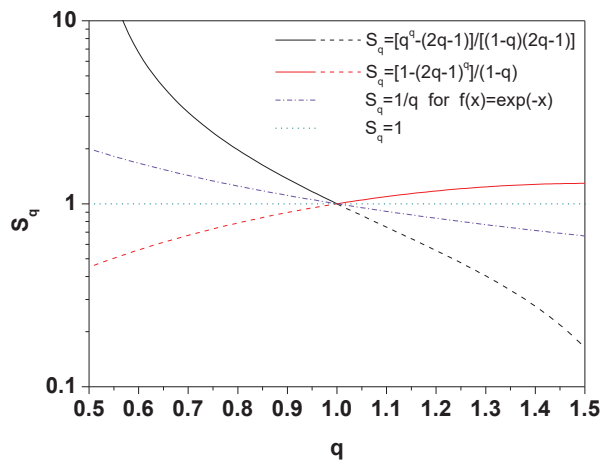
Figure 3. (Color online) Tsallis entropy for different nonextensivity parameter (see text for details).

Let us note that for values of q outside the range of variability declared for a given entropy, $S_q < 1$, i.e., it is always lower than unity, which is less than the Shannon entropy. From Figure 3 it can be seen that the entropy formula S_q, which could be used in the entire

allowable range of the parameter q, describing both q cases and $2 - q$ dual to them, must contain both elements of (26) and (27), i.e., have the following form:

$$S_q = \frac{1}{1-q} \frac{(1 - |1 - q|)^q - 1}{q - |1 - q|}. \tag{28}$$

The corresponding Tsallis distribution is now

$$f(x) = \frac{1 - |1 - q'|}{[1 + |1 - q'||x|]^{\frac{1}{1-q'}}}. \quad \text{where} \quad 0.5 < q' < 1.5. \tag{29}$$

A natural question arises as to what should be modified and how in such a case? What we would like to suggest here is the use of appropriately modified definitions of the $\exp_q(x)$ and $\ln_q(x)$ functions, namely to replace $\exp_q(x)$ defined in Equation (2) by

$$\exp_q(x) = [1 + \kappa x]^{\frac{1}{\kappa}} \quad \text{where} \quad \kappa = (q - 1)sign(x) \tag{30}$$

and, accordingly,

$$\ln_q(y) = \frac{y^\kappa - 1}{\kappa} \quad \text{where} \quad \kappa = (q - 1)sign(y - 1). \tag{31}$$

This form works for all x and q values, and there are no additional restrictions on the admissible values of the q parameter depending on whether $x > 0$ or $x < 0$. Formally, this corresponds to replacing $q \to q' = 2 - q$ when changing the sign of x. Figure 4 shows behaviour of the functions $\exp_q(x)$ and $\ln_q(x)$. Note that using this form we now have

$$\exp_q(-x) \cdot \exp_q(x) = 1 \tag{32}$$

and the ocupation numbers of particles $n_q(x)$ and antiparticles $n_q(-x)$ satisfy relation

$$n_q(-x) + n_q(x) = -\zeta \tag{33}$$

for all values of q ($\zeta = +1$ for bosons and -1 for fermions). The naive replecement of the Euler-exponential with another, deformed exponential function (namely given by Equation (2)) can lose the particle-hole symmetry, inherent in the traditional Fermi distribution above and below the Fermi level. Previously, these relationships had a dual form,

$$\exp_q(-x) \cdot \exp_{2-q}(x) = 1 \quad \text{and} \quad n_q(x) + n_{2-q}(-x) = -\zeta. \tag{34}$$
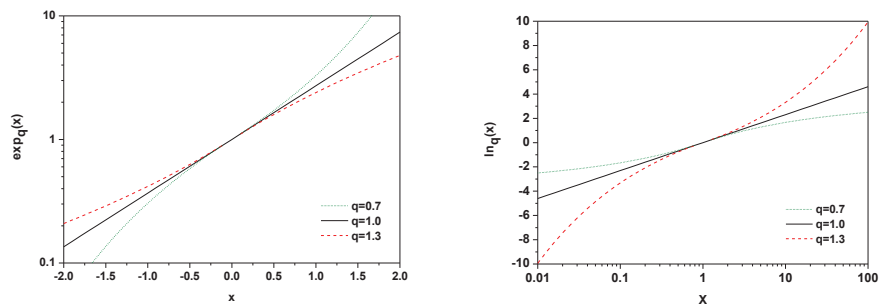
Figure 4. (Color online) Illustration of the behavior of the function $\exp_q(x)$ defined by Equation (30) and the function $\ln_q(x)$ defined by Equation (31) for different values of the parameters q.

This means that such an approach avoids not only the problem of duality discussed earlier in Section 2, but also preserves the particle-hole symmetry concerning distribution above and below the Fermi level which is fundamental in field theory and was discussed in [42,43].

In the above considerations, we must remember that the modified functions $\exp_q(x)$ and $\ln_q(y)$ are not differentiable everywhere because the functions $sign(x)$ (in the first case) and $sign(1-y)$ (in the second) have a discontinuity at $x = 0$ or $y = 1$. Therefore, by their derivatives for $x = 0$ (or $y = 1$), we understand their limits for $x \to 0$ (or $y \to 1$). In this approach, the first derivatives $\exp_q(x)$ and $\ln_q(y)$ are the same for $x = 0$ and $y = 1$ as the first derivatives $\exp(x)$ and $\ln(y)$, while their n-th derivatives already depend on q in the following way:

$$\lim_{x \to 0} \frac{d^n \exp_q(x)}{dx^n} = \prod_{i=1}^{n} [i - (i-1)]q] \tag{35}$$

and

$$\lim_{y \to 1} \frac{d^n \ln_q(y)}{dy^n} = \prod_{i=2}^{n} (-i + q). \tag{36}$$

4. Other Sources of Tsallis Distribution

Note that since Equation (2) describes the data in the entire measured area of phase space, i.e., both those associated with the thermal approach and those associated with hard collisions, the justification of this formula cannot be reduced to the Tsallis entropy only. It is worth noting that for each probability distribution the appropriate form of entropy can be given and for each probability distribution one can also give the constraints which, when used together with the Shannon entropy, lead to this probability distribution [44]. For our considerations, it is important to note that when selecting the constraints in such a way that they best take into account the most important dynamic features of the examined system, one could basically stop at the Shannon entropy [45]. For example, condition $\langle x \rangle = const$ provides to the usual exponential distribution, $\langle x^2 \rangle$ gives Gaussian distribution, $\langle \ln(x) \rangle = const$ gamma distribution, whereas $\langle \ln(1 + x^2) \rangle$ gives a Cauchy distribution. In general, for some function $h(x)$, the maximum entropy density for $f(x)$ satisfying the constraint $\int dx f(x)h(x) = const$ has the form $f(x) = \exp[\lambda_0 + \lambda h(x)]$ where parameters λ_0 and λ are fixed by the requirement of normalization for $f(x)$ and by the above constraint. To obtain the Tsallis distribution in this way,

$$f(x) = \frac{2-q}{x_0} \left[1 - (1-q) \frac{x}{x_0} \right]^{\frac{1}{1-q}} \tag{37}$$

we need to use a constraint like this:

$$\left\langle \ln \left[1 - (1-q) \frac{x}{x_0} \right] \right\rangle = \frac{q-1}{2-q}. \tag{38}$$

The Tsallis distribution understood as a quasi-power distribution can also be obtained in many ways without referring to any form of entropy [46]. We will now discuss a few of them in more detail.

Superstatistics. This approach extends the exponential description, $f(E) = \frac{1}{T} \exp(-\frac{E}{T})$, characterized by some parameter of the scale, T, by allowing fluctuations of this parameter [47]. In particular, if they are described by a gamma distribution,

$$g\left(\frac{1}{T}\right) = \frac{1}{\Gamma\left(\frac{1}{q-1}\right)} \frac{T_0}{q-1} \left(\frac{1}{q-1} \frac{T_0}{T} \right)^{\frac{2-q}{q-1}} \exp\left(-\frac{1}{q-1} \frac{T_0}{T} \right), \tag{39}$$

the total result is a Tsallis distribution [29,48], the $f_q(E) = \frac{2-q}{T}\left[1 - (1-q)\frac{E}{T}\right]^{\frac{1}{1-q}}$, where the parameter q characterizing the strength of fluctuations in T is given by its variance, $\omega_T^2 = \frac{Var(T)}{\langle T \rangle^2} = q - 1$. Since in thermal models ω_T^2 is related to the heat capacity C_V, one possible meaning of the parameter q is its relationship to the heat capacity, $q = 1 + 1/C_V$ (note that here $q > 1$ always). Other classes of generalized statistics can also be obtained, and with small variance of fluctuations they all behave universally [47].

Preferential attachment. This approach describes a situation where the scale parameter depends linearly on the variable under consideration, as is the case when preferential attachment correlations are encountered in the system under consideration, e.g., when $x_0 \to x_0 + (q-1)x$. This changes the equation defining the distribution, resulting in the Tsallis distribution with $q > 1$ [49,50],

$$\frac{df(x)}{dx} = \frac{f(x)}{x_0} \to \frac{df(x)}{dx} = \frac{f(x)}{x_0 + (q-1)x} \to f(x) = \frac{2-q}{x_0}\left[1 - (1-q)\frac{x}{x_0}\right]^{\frac{1}{1-q}}. \quad (40)$$

Tsallis distribution from multiplicative noise. The Tsallis distribution may also mean that the described process has a stochastic character defined by the additive, $\gamma(t)$, and multiplicative, $\xi(t)$, noise and described by the Langevin equation,

$$\frac{dp}{dt} + \gamma(t)p = \xi(t). \quad (41)$$

The corresponding Fokker-Planck equation has the form

$$\frac{\partial f}{\partial t} = -\frac{\partial(K_1 f)}{\partial p} + \frac{\partial^2(K_2 f)}{\partial p^2}, \quad (42)$$

$$K_1 = E(\xi) - E(\gamma)p \quad \text{and} \quad K_2 = Var(\xi) - 2Cov(\xi, \gamma)p + Var(\gamma)p^2, \quad (43)$$

and for stationary solutions

$$\frac{d(K_2 f)}{dp} = K_1 f. \quad (44)$$

When both noises are uncorrelated (i.e., when $Cov(\xi, \gamma) = 0$) and when there is no drift caused by additive noise (i.e., $E(\xi) = 0$) the solution to Equation (44) is the Tsallis distribution in p^2 [51]:

$$f(p) = \left[1 + (q-1)\frac{p^2}{T}\right]^{\frac{q}{1-q}} \quad \text{where} \quad T = \frac{2Var(\xi)}{E(\gamma)}, \quad q = 1 + \frac{2Var(\gamma)}{E(\gamma)}. \quad (45)$$

The Tsallis distribution with p (as in Equation (2)) and not p^2 is obtained for the more complicated case of $T = T(q)$ when [46]

$$T(q) = (2-q)[T_0 + (q-1)T_1] \quad \text{where} \quad T_0 = -\frac{Cov(\xi, \gamma)}{E(\gamma)} \text{ and } T_1 = \frac{E(\xi)}{2E(\gamma)}. \quad (46)$$

Note that T now depends non-linearly on q, which significantly makes the Tsallis distribution more flexible, allowing for the analysis and comparison of various types of processes (cf. [46]).

At this point, it is worth noting that there is a relationship between the type of noise and the condition imposed in MaxEnt. In the case of Shannon entropy, a condition imposed on the arithmetic mean corresponds to additive noise, while the use of a condition imposed on the geometric mean corresponds to multiplicative noise and leads to a power distribution [52].

Conditional probability. The methods for obtaining the Tsallis distribution presented so far are basically limited to cases with $q > 1$. Cases with $q < 1$ can only be observed

in constrained systems. Consider for example N independent energies, $E_{i=1,\ldots,N}$, where each of them follows the Boltzman distribution, $g_i(E_i) = \frac{1}{\lambda}\exp\left(-\frac{E_i}{\lambda}\right)$, and their sum, $E = \sum_{i=1}^{N} E_i$, has a gamma distribution, $g_N(E) = \frac{1}{\lambda^{(N-1)}}\left(\frac{E}{\lambda}\right)^{N-1}\exp\left(-\frac{E}{\lambda}\right)$. However, if the available energy is bounded, $E = N\alpha = const$, these energies will no longer be independent and will be described by conditional probabilities in the form of Tsallis distributions with $q < 1$:

$$f(E_i | E = N\alpha) = \frac{g_1(E_i)g_{N-1}(N\alpha - E_i)}{g_N(N\alpha)} = \frac{2-q}{\lambda}\left[1 - (1-q)\frac{E_i}{\lambda}\right]^{\frac{1}{1-q}}, \qquad (47)$$

$$\lambda = \frac{\alpha N}{N-1}, \quad q = \frac{N-3}{N-2} < 1. \qquad (48)$$

One could obtain a Tsallis-like distribution with $q > 1$ only if the scale parameter λ fluctuates in the same way as in the case of superstatistics.

Statistical physics. A Tsallis distribution with $q < 1$ also follows from statistical physics. Consider an isolated system with energy $U = const$ and ν degrees of freedom (particles). We choose one of them with energy $E \ll U$, then the rest of the system has energy $E_r = U - E$. If this particle is in one well-defined state then the number of states of the entire system is $\Omega(E_r)$, and the probability that the energy of the selected particle is E is $P(E) \propto \Omega(U - E)$. Expanding $\ln\Omega(U - E)$ around U and keeping only the first two terms one obtains

$$\ln P(E) \propto \ln\Omega(E) \propto -\beta E \implies P(E) \propto e^{-\beta E}, \qquad (49)$$

that is a Boltzman distribution with

$$\beta = \frac{1}{k_B T} \stackrel{def}{=} \frac{\partial \ln\Omega(E_r)}{\partial E_r}. \qquad (50)$$

However, it is usually expected that $\Omega(E_r) \propto \left(\frac{E_r}{\nu}\right)^{\alpha_1 \nu - \alpha_2}$ with $\alpha_1, \alpha_2 \sim O(1)$. Choosing $\alpha_1 = 1$ and $\alpha_2 = 2$ (because the number of states in the reservoir has decreased by one), therefore

$$\frac{\partial^k \beta}{\partial E_r^k} \propto (-1)^k k! \frac{\nu - 2}{E_r^{k+1}} = (-1)^k k! \frac{\beta^{k-1}}{(\nu - 2)^k}. \qquad (51)$$

This allows us to write the probability of selection of energy E as:

$$P(E) \propto \frac{\Omega(U - E)}{\Omega(E)} = C\left(1 - \frac{1}{\nu - 2}\beta E\right)^{(\nu - 2)} = \beta(2 - q)[1 - (1-q)\beta E]^{\frac{1}{1-q}}, \qquad (52)$$

that is, in the form of the Tsallis distribution with $q = 1 - \frac{1}{\nu - 2} \le 1$, such as in the case of conditional probability above.

5. Summary and Conclusions

Entropy has always played an important role in the study of the production mechanisms of particles produced in high-energy hadronic and nuclear collisions, either in their description based on thermodynamics [2] or in descriptions using elements of information theory [4].

In the application of the non-extensive approach, we encounter the problem of a certain duality manifested in the parallel occurrence of the parameter q and $2 - q$, which is best illustrated by the parallel description of particle production processes in nucleon and nuclear collisions discussed in Section 2. The second manifestation of duality appears in an attempt at a non-extensive description of quantum statistical distributions. As suggested by the results of [42,43] they are inconsistent with the conventional description using Tsallis distributions (and prefer the nonextensive Kaniadakis distribution). The point here is the necessity to preserve the particle-hole symmetry requiring that $\exp(-x) \cdot \exp(x) = 1$, while

using the original q-exponential Tsallis distribution it leads to $\exp_q(-x) \cdot \exp_{2-q}(x) = 1$. In Section 3 we propose a new formula defining the non-extensive function $\exp_q(x)$ which restores this symmetry and we have a nonextensive version of particle-hole symmetry again which restores this symmetry in the form $\exp_q(-x) \cdot \exp_q(x) = 1$.

From a more technical perspective, it is worth noting that both Shannon's and Tsallis' entropies have the same generating function, $f(x) = \sum_i p_i^x$, and that the difference in their forms is just due to the form of adopted differentiation operator. For standard first-order differentiation, $df(x)/dx$, we obtain the Shannon entropy, whereas adopting the Jackson q-derivative, $D_q f(x) = \frac{f(qx) - f(x)}{qx - x}$, yields the Tsallis entropy. In fact, other expressions for entropy can be obtained by using yet other forms of differentiation operators [7].

Author Contributions: G.W. and Z.W. contributed equally to all stages of this work: conceived the problem, calculations and preparation of the manuscript. All authors have read and agreed to the published version of the manuscript.

Institutional Review Board Statement: Not applicable.

Data Availability Statement: Not applicable

Conflicts of Interest: The authors declare no conflict of interest.

References

1. Kittel, W.; De Wolf, E.A. *Multihadron Dynamics*; World Scientific: Singapore, 2005.
2. Schlögl, F. *Probability and Heat—Fundamentals of Thermostatistics*; Springer Fachmedien Wiesbaden GmbH: Wiesbaden, Germany, 1989.
3. Biró, T.S. *Is there a Temperature? Conceptual Challenges at High Energy, Acceleration and Complexity*; Springer: New York, NY, USA; Dordrecht, The Netherlands; Heidelberg, Germany; London, UK, 2011.
4. Arndt, C. *Information Measures—Information and its Description in Science and Engineering*; Springer: Berlin/Heidelberg, Germany; New York, NY, USA, 2001.
5. Tsallis, C. *Introduction to Nonextensive Statistical Mechanics*; Springer: New York, NY, USA, 2009.
6. Naudts, J. *Generalised Thermostatistics*; Springer: London, UK; Dordrecht, The Netherlands; Heidelberg, Germany; New York, NY, USA, 2011.
7. Lopes, A.M.; Machado, J.A. A Review of Fractional Order Entropies. *Entropy* **2020**, *22*, 1374. [CrossRef] [PubMed]
8. Havrda, J.; Charvat, F. Quantification Method of Classification Processes—Concept of Structural α-Entropy. *Kybernetica* **1967**, *3*, 30–34.
9. Daroczy, Z. Generalized information functions. *Inf. Control* **1970**, *16*, 36–51. [CrossRef]
10. Wilk, G.; Włodarczyk, Z. Example of a possible interpretation of Tsallis entropy. *Phys. A* **2008**, *387*, 4809–4813. [CrossRef]
11. Neuman, Y.; Cohen, Y.; Neuman, Y. How to (better) find a perpetrator in a haystack. *J. Big Data* **2019**, *6*, 1–17. [CrossRef]
12. Michael, C.; Vanryckeghem, L. Consequences of momentum conservation for particle production at large transverse momentum. *J. Phys. G* **1977**, *3*, L151–L156. [CrossRef]
13. Michael, C. Large transverse momentum and large mass production in hadronic interactions. *Prog. Part. Nucl. Phys.* **1979**, *2*, 1–39. [CrossRef]
14. Hagedorn, R. Multiplicities, p_T Distributions and the Expected Hadron → Quark-Gluon Phase Transition. *Riv. Nuovo Cim.* **1983**, *6*, 1–50. [CrossRef]
15. Abe, S. Nonadditive conditional entropy and its significance for local realism. *Phys. A* **2001**, *289*, 157–164. [CrossRef]
16. Rathie, P.N.; Da Silva, S. Shannon, Lévy, and Tsallis: A Note. *Appl. Math. Sci.* **2008**, *2*, 1359–1363.
17. Dash, A.K.; Mohanty, B.M. Extrapolation of multiplicity distribution in $p + p(\bar{p})$ collisions to LHC energies. *J. Phys. G* **2010**, *37*, 025102. [CrossRef]
18. Geich-Gimbel, C. Particle production at collider energies. *Int. J. Mod. Phys. A* **1989**, *4*, 1527–1680. [CrossRef]
19. Wibig, T. The non-extensivity parameter of a thermodynamical model of hadronic interactions at LHC energies. *J. Phys. G* **2010**, *37*, 115009. [CrossRef]
20. Khachatryan, V.; Sirunyan, A.M.; Tumasyan, A.; Adam, W.; Bergauer, T.; Dragicevic, M.; Erö, J.; Friedl, M.; Fruehwirth, R.; Ghete, V.M.; et al. Transverse-momentum and pseudorapidity distributions of charged hadrons in pp collisions at $\sqrt{s} = 0.9$ and 2.36 TeV. *J. High Energ. Phys.* **2010**, *2*, 041-1–041-19. [CrossRef]

21. Khachatryan, V.; Sirunyan, A.M.; Tumasyan, A.; Adam, W.; Bergauer, T.; Dragicevic, M.; Erö, J.; Fabjan, C.; Friedl, M.; Fruehwirth, R.; et al. Transverse-Momentum and Pseudorapidity Distributions of Charged Hadrons in pp Collisions at $\sqrt{s} = 7$ TeV. *Phys. Rev. Lett.* **2010**, *105*, 022002. [CrossRef]

22. Navarra, F.S.; Utyuzh, O.V.; Wilk, G.; Włodarczyk, Z. Information theory approach (extensive and nonextensive) to high-energy multiparticle production processes. *Phys. A* **2004**, *340*, 467–476. [CrossRef]

23. Rybczyński, M.; Włodarczyk, Z.; Wilk, G. Rapidity spectra analysis in terms of non-extensive statistic approach. *Nucl. Phys. B (Proc. Suppl.)* **2003**, *122*, 325–328. [CrossRef]

24. Tsallis, C.; Mendes, R.S.; Plastino, A.R. The role of constraints within generalized nonextensive statistics. *Physica A* **1998**, *261*, 534–554. [CrossRef]

25. Ferri, G.L.; S Martínez, S.; Plastino, A. Equivalence of the four versions of Tsallis's statistics. *J. Stat. Mech.* **2005**, *P04009*, 1–14. [CrossRef]

26. Parvan, A.S. Equivalence of the phenomenological Tsallis distribution to the transverse momentum distribution of q-dual statistics. *Eur. Phys. J. A* **2020**, *56*, 106. [CrossRef]

27. Tsallis, C. On the foundations of statistical mechanics. *Eur. Phys. J. Spec. Topics* **2017** *226* 1433–1443. [CrossRef]

28. Yalcin, G.C.; Beck, C. Generalized statistical mechanics of cosmic rays: Application to positron-electron spectral indices. *Sci. Rep.* **2018**, *8*, 1764. [CrossRef] [PubMed]

29. Biró, T.S.; Jakovác, A. Power-Law Tails from Multiplicative Noise. *Phys. Rev. Lett.* **2005**, *94*, 132302. [CrossRef]

30. Biró, T.S.; Purcel, G; Ürmösy, K. Non-extensive approach to quark matter *Eur. Phys. J. A* **2009**, *40*, 325–340.

31. Karlin, I.V.; Grmela, M.; Gorban, N. Duality in nonextensive statistical mechanics. *Phys. Rev. E* **2002**, *65*, 036128. [CrossRef]

32. Gaździcki, M.; Gorenstein, M.; Seybothe, P. Onset of Deconfinement in Nucleus–Nucleus Collisions: Review for Pedestrians and Experts. *Acta Phys. Polon. B* **2011**, *42*, 307–351. [CrossRef]

33. Gaździcki, M.; Rybicki, A. Overview of results from NA61/SHINE: Uncovering critical structures. *Acta Phys. Polon. B* **2019**, *50*, 1057–1070. [CrossRef]

34. Noronha, J. Collective effects in nuclear collisions: Theory overview. *Nucl. Phys. A* **2019**, *982*, 78–84. [CrossRef]

35. Białas, A.; Błeszynski, M.; Czyż, W. Multiplicity distributions in nucleus-nucleus collisions at high energies. *Nucl. Phys. B* **1976**, *111*, 461–476. [CrossRef]

36. Fiałkowski, K.; Wit, R. RHIC Multiplicity Distributions and Superposition Models. *Acta Phys. Pol. B* **2010**, *41*, 1317–1325.

37. Fiałkowski, K.; Wit, R. Superposition models and the multiplicity fluctuations in heavy-ion collisions. *Eur. Phys. J. A* **2010**, *45*, 51–55. [CrossRef]

38. Wilk, G.; Włodarczyk, Z. Multiplicity fluctuations due to the temperature fluctuations in high-energy nuclear collisions. *Phys. Rev. C* **2009**, *79*, 054903. [CrossRef]

39. Shao, M.; Yi, L.; Tang, Z.; Chen, H.; Li, C.; Xu, Z. Examination of the species and beam energy dependence of particle spectra using Tsallis statistics. *J. Phys. G* **2010**, *37*, 085104. [CrossRef]

40. Wilk, G.; Włodarczyk, Z. The imprints of superstatistics in multiparticle production processes. *Cent. Eur. J. Phys.* **2012**, *10*, 568–575. [CrossRef]

41. Backet, B.B.; Baker, M.D.; Barton, D.S.; Betts, R.R.; Ballintijn, M.; Bickley, A.A.; Bindel, R.; Budzanowski, A.; Busza, W.; Carroll, A.; et al. Centrality and energy dependence of charged-particle multiplicities in heavy ion collisions in the context of elementary reactions. *Phys. Rev. C* **2006**, *74*, 021902. [CrossRef]

42. Biró, T.S.; Shen, K.M.; Zhang, B.W. Non-extensive quantum statistics with particle–hole symmetry. *Phys. A* **2015**, *428*, 410–415. [CrossRef]

43. Biró, T.S. Kaniadakis Entropy Leads to Particle–Hole Symmetric Distribution. *Entropy* **2022**, *24*, 1217. [CrossRef]

44. Papalexiou, S.M.; Koutsoyiannis, D. Entropy Maximization, *P*-Moments and Power-Type Distributions in Nature. Available online: http://itia.ntua.gr/1127 (accessed on 8 April 2011).

45. Rufeil Fiori, E.; Plastino, A. A Shannon–Tsallis transformation. *Phys. A* **2013**, *392*, 1742–1749.

46. Wilk, G.; Włodarczyk, Z. Quasi-power law ensembles. *Acta Phys. Pol. B* **2015**, *46*, 1103–1122. [CrossRef]

47. Beck, C.; Cohen, E.G.D. Superstatistics. *Phys. A* **2003**, *322*, 267–275. [CrossRef]

48. Wilk, G.; Włodarczyk, Z. Interpretation of the Nonextensivity Parameter q in Some Applications of Tsallis Statistics and Lévy Distributions. *Phys. Rev. Lett.* **2000**, *84*, 2770–2773. [CrossRef] [PubMed]

49. Wilk, G.; Włodarczyk, Z. Nonextensive information entropy for stochastic networks. *Acta Phys. Pol. B* **2004**, *35*, 871–879.

50. Soares, D.J.B.; Tsallis, C.; Mariz, A.M.; da Silva,L.R. Preferential attachment growth model and nonextensive statistical mechanics. *Europhys. Lett.* **2005**, *70*, 70–76. [CrossRef]

51. Anteneodo, C.; Tsallis, C. Multiplicative noise: A mechanism leading to nonextensive statistical mechanics. *J. Math. Phys.* **2003**, *44*, 5194–5203. [CrossRef]

52. Rostovtsev A. On a geometric mean and power-law statistical distributions. *arXiv* **2005**, arXiv:cond-mat/0507414.

Testing Nonlinearity with Rényi and Tsallis Mutual Information with an Application in the EKC Hypothesis

Elif Tuna [1], Atıf Evren [1], Erhan Ustaoğlu [2], Büşra Şahin [3] and Zehra Zeynep Şahinbaşoğlu [1,*]

[1] Department of Statistics, Faculty of Sciences and Literature, Yildiz Technical University, Davutpasa, Esenler, 34210 Istanbul, Turkey

[2] Department of Informatics, Faculty of Management, Marmara University, Göztepe, 34180 Istanbul, Turkey

[3] Department of Computer, Faculty of Engineering, Halic University, Eyupsultan, 34060 Istanbul, Turkey

[*] Correspondence: zeynepsahinbasoglu@gmail.com; Tel.: +90-532-2123-311

Abstract: The nature of dependence between random variables has always been the subject of many statistical problems for over a century. Yet today, there is a great deal of research on this topic, especially focusing on the analysis of nonlinearity. Shannon mutual information has been considered to be the most comprehensive measure of dependence for evaluating total dependence, and several methods have been suggested for discerning the linear and nonlinear components of dependence between two variables. We, in this study, propose employing the Rényi and Tsallis mutual information measures for measuring total dependence because of their parametric nature. We first use a residual analysis in order to remove linear dependence between the variables, and then we compare the Rényi and Tsallis mutual information measures of the original data with that the lacking linear component to determine the degree of nonlinearity. A comparison against the values of the Shannon mutual information measure is also provided. Finally, we apply our method to the environmental Kuznets curve (EKC) and demonstrate the validity of the EKC hypothesis for Eastern Asian and Asia-Pacific countries.

Keywords: nonlinearity; Rényi mutual information; Tsallis mutual information; EKC hypothesis

1. Introduction

An analysis of the dependence between two or more random variables can be traced back to the late 19th century, beginning with the works of mathematicians such as Gauss and Laplace. Later, Galton created the concept of correlation, which enabled Pearson to derive the correlation coefficient that has been extensively used in all kinds of statistical analyses since then [1]. When the dependence is linear or approximately linear, the correlation coefficient is the most effective indicator of the relationship between the random variables. It also provides a simple interpretation for the direction of the relation, whether positive or negative. When the dependence departs from the linearity, the linear correlation coefficient is of no use, and various methods have been proposed for evaluating nonlinearity. One of these measures is Spearman's correlation coefficient, which is nonparametric and uses ranked values to assess monotonic nonlinearity between two random variables [2]. Another measure for nonlinear dependence is the correlation ratio, which expresses the relationship between random variables as a single valued function. In the case of nonlinear relationships, the value of the correlation ratio is greater than the correlation coefficient, and therefore, the difference between the correlation ratio and the correlation coefficient refers to the degree of the nonlinearity of dependence [3]. Polynomial regression has also been used for modeling nonlinear dependence in various phenomena. Although nonparametric regression models have been used more often, polynomial regression is still being deployed for modeling dependence in some areas of application, such as biomechanics [4], cosmology [5], climatization [6], and chemistry [7]. As more and more-complex data have been produced through technological development, the need for analyzing these data have

given rise to a new field, called functional data analysis, which also includes functional regression. Functional regression models assume functional relationships between responses and predictors, and for polynomial models, these relationships are in polynomial form rather than linear [8].

Shannon entropy plays a central role in information theory as a measure of information choice and uncertainty. Conditional entropy can also be used as a measure of missing information [9]. Conditional entropy or mutual information do not assume any underlying distribution and reflect the stochastic relationship between random variables as a whole—linear or nonlinear [10]. These properties have made mutual information a good choice for analyzing dependencies. Hence, mutual information is extensively used for dependency analysis, especially in finance [11–13] and in genetics [14–16]. Although mutual information is an effective method for determining the dependency between random variables, it does not provide any information on the nature of the dependence as being linear or nonlinear. Very few attempts have been made to investigate the nature of the dependence by extracting the linear component of Shannon mutual information, though some have, such as [1,17].

The environmental Kuznets curve (EKC) hypothesis states that there is an inverse U-shape relationship between per capita gross domestic product (GDP) and measures of environmental degradation [18]. Because carbon dioxide (CO_2) is the major factor for greenhouse gas emissions, it is accepted as the main reason for the environmental degradation. Hence, the same relationship is assumed between GDP and CO_2. So the EKC is an indication of the "stages of economic growth" that economies pass through as they make a transition from agriculturally based to industrial and then to postindustrial service-based economies. In a way, EKC provides a visual representation of the stages of economic growth, as seen in Figure 1 (Panayatou 1993).
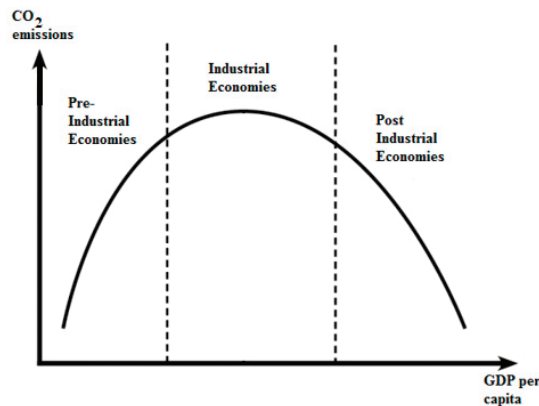
Figure 1. Environmental Kuznets curve.

There are various methods in the literature to test the EKC. Some studies have used panel data, while others have used time series data [19]. Panayotou [20], who first suggested the term EKC, used cross-sectional data and empirically tested the relation between environmental degradation and economic development for the late 1980s. He discovered quadratic patterns in a sample of developing and developed countries. Antle and Heidebrink [21] found turning points for the EKC curve by using cross-sectional data. Vasilev [22] also studied EKC with cross-sectional data.

Although the determination of the exact shape of the Kuznets curve is important, demonstrating its nonlinearity will help support the EKC hypothesis. We aim to determine nonlinearity by deploying mutual information with an application on EKC. The Rényi and Tsallis mutual information types are used in determining the nonlinearity of EKC, and the results are compared with that of Shannon. By demonstrating the confirmation of the EKC hypothesis, it can be concluded that the "grow and pollute now, clean later" strategy

revealed by the hypothesis has enormous environmental costs, so alternative strategies should be developed for growth.

The structure of our study is as follows: Section 2 describes the tests for nonlinearity on the basis of mutual information. Section 3 starts with the application by conducting a cross-sectional analysis using ordinary least squares (OLS) and then adds the application of nonlinearity tests. Finally, Section 4 concludes.

2. Relative Entropy, Mutual Information, and Dependence

2.1. Mutual Information

Relative entropy is a special case of statistical divergence. It is a measure of the inefficiency of assuming that the probability distribution is q when the true distribution is p [23]. Shannon, Rényi, and Tsallis relative entropies for the discrete case are defined as follows:

$$D_S = (p\|q) = \sum P(x) \log \frac{P(x)}{q(x)} \tag{1}$$

$$D_R = (p\|q) = \frac{1}{\alpha - 1} \log \sum P(x) \left(\frac{P(x)}{q(x)} \right)^{\alpha - 1} \tag{2}$$

$$D_T = (p\|q) = \frac{1}{\alpha - 1} \sum P(x) \left[\left(\frac{P(x)}{q(x)} \right)^{\alpha - 1} - 1 \right] \tag{3}$$

Bivariate extensions are as follows:

$$D_S(p(x,y)\|q(x,y)) = \sum \sum p(x,y) \log \frac{p(x,y)}{q(x,y)} \tag{4}$$

$$D_R(p(x,y)\|q(x,y)) = \frac{1}{\alpha - 1} \log \sum \sum p(x,y) \left(\frac{p(x,y)}{q(x,y)} \right)^{\alpha - 1} \tag{5}$$

$$D_T((p(x,y)\|q(x,y)) = \frac{1}{\alpha - 1} \sum \sum p(x,y) \left[\left(\frac{p(x,y)}{q(x,y)} \right)^{\alpha - 1} - 1 \right] \tag{6}$$

To check the independence of variables, the null and alternative hypotheses can be stated as follows:

$$H_0 : p_{X,Y}(x,y) = q_{X,Y}(x,y) \tag{7}$$

$$H_A : p_{X,Y}(x,y) \neq q_{X,Y}(x,y) \tag{8}$$

where $q_{X,Y}(x,y) = p_X(x) \cdot p_Y(y)$ for all $(x,y) \in R^2$.

Mutual information can be seen as the divergence of the joint probability function from the product of the two marginal probability distributions. In other words, mutual information is derived as a special case of divergence or relative entropy. Three alternative formulations of mutual information are due to Shannon, Rényi, and Tsallis. Shannon mutual information (or Kullback—Leibler divergence) is defined as follows:

$$M(X,Y) = D_S(p_{X,Y}(x,y)\|p_X(x)p_Y(y)) = \sum \sum p(x,y) \log \frac{p(x,y)}{p_X(x)p_Y(y)} \tag{9}$$

Mutual information formulated this way is also called as cross entropy.

Rényi order-α divergence (or Rényi mutual information) of $p_{X,Y}(x,y)$ from $p_X(x)p_Y(y)$ is given as follows:

$$D_R(p_{X,Y}(x,y)\|p_X(x)p_Y(y)) = \frac{1}{\alpha - 1} \log \sum \sum \frac{p_{X,Y}(x,y)^\alpha}{(p_X(x)p_Y(y))^{\alpha - 1}} \tag{10}$$

Tsallis order-α divergence of $p_{X,Y}(x,y)$ from $p_X(x)p_Y(y)$ (or Tsallis mutual information) is given as follows:

$$D_T(p_{X,Y}(x,y)\|p_X(x)p_Y(y)) = \frac{1 - \sum\sum \frac{p_{X,Y}(x,y)^\alpha}{(p_X(x)p_Y(y))^{\alpha-1}}}{1-\alpha} \tag{11}$$

In the case of independence, the Rényi and Tsallis mutual information types are 0, just like Shannon mutual information. As $\alpha \to 1$, the Rényi and Tsallis mutual information types approach Shannon mutual information [24]. The mutual information of two variables reflects the reduction in the variability of one variable, by knowing the other. Mutual information becomes 0 if and only if the random variables are independent. It should also be emphasized that mutual information measures general dependence, whereas the correlation coefficient measures linear dependence [15].

2.2. Testing Linearity by Using Mutual Information

The application of the Shannon mutual information measure on the problem of detecting nonlinearity was suggested by Tanaka, Okamoto, and Naito [17] and by Smith [1].

This method utilizes the residuals obtained by the ordinary linear regression model. Note that a linear regression model that fits data well is a good indicator of linear relation between variables so that the residuals obtained from a linear model are considered to include no linear dependence on independent variables:

$$\xi_i = Y_i - b_0 - \sum_{j=1}^{p} b_j X_j \tag{12}$$

Next, the mutual information between residuals and observed values of the independent variable is calculated. The mutual information between independent and dependent variables $M(X,Y)$ can be computed, as can the mutual information between independent variable and the residuals obtained from linear regression $M(X,\xi)$. Note that the later statistic reflects the nonlinear dependence between the original variables. If the mutual information between the independent variable and residuals does not differ much from the mutual information between the dependent and independent variables, then the relation is nonlinear. By comparing $M(X,\xi)$ with $M(X,Y)$, we can evaluate the degree of nonlinearity in the dependence [1,17].

We suggest that nonlinearity can be detected better by the Rényi and Tsallis mutual information measures because of their parametric nature.

Especially becuause the Tsallis mutual information measure is calculated on the basis of the power of α, the larger the α value, the larger the Tsallis mutual information was becoming, so the difference between these two common mutual information measures cannot be interpreted. Therefore, we suggest a new measure that still leads to the same result, as seen in Equation (13):

$$\lambda_{S,R,T} = \left| 1 - \frac{M(X,\xi)}{M(X,Y)} \right| \tag{13}$$

The letters *S*, *R*, and *T* in the index indicate the Shannon, Rényi, and Tsallis mutual information measures, respectively. As $M(X,\xi)$ and $M(X,Y)$ become closer to each other, λ converges to zero, implying nonlinearity. This hypothesis is tested by using two simulated data sets, one of which represents a linear relationship and the other one reflects curvilinearity. The number of simulated pairs of X and Y values is 1000. The simulated data representing the linear and the curvilinear relationships are modeled by Equations (14) and (15):

$$Y = a + bX + e \tag{14}$$

$$Y = a + bX + cX^2 + e \tag{15}$$

Various α values between 0 and 5 are selected randomly from a uniform distribution for assessing the effect of α on nonlinearity measures. Table 1 provides 50 randomly generated observations from a uniform distribution for different values of α and the corresponding λ values for the Rényi and Tsallis measures.

Table 1. λ values for linear and curvilinear relationships, based on simulations.

α	Linear Relationship		Curvilinear Relationship	
	λ_R	λ_T	λ_R	λ_T
0.07	0.9956	0.9906	0.0489	0.0308
0.13	0.9917	0.983	0.0457	0.0263
0.17	0.9894	0.9788	0.0447	0.0247
0.18	0.9888	0.9778	0.0445	0.0244
0.35	0.9808	0.9664	0.0433	0.0228
0.41	0.9785	0.964	0.0431	0.0232
0.48	0.976	0.9619	0.0429	0.024
0.56	0.9734	0.9604	0.0429	0.0254
0.67	0.9702	0.9595	0.0435	0.0281
0.69	0.9696	0.9595	0.0437	0.0287
0.74	0.9684	0.9596	0.0444	0.0304
0.82	0.9668	0.9605	0.0464	0.0339
0.87	0.9663	0.9618	0.0483	0.0369
1.36	0.9473	0.964	0.0087	0.0099
1.46	0.9446	0.9662	0.003	0.0037
1.86	0.9323	0.9749	0.0129	0.0214
2.11	0.9236	0.9797	0.0138	0.0271
2.18	0.9209	0.981	0.0139	0.0285
2.44	0.9102	0.9851	0.0139	0.0334
2.54	0.9056	0.9865	0.0138	0.0352
2.73	0.8962	0.9888	0.0136	0.0386
2.78	0.8935	0.9893	0.0136	0.0395
2.8	0.8924	0.9895	0.0136	0.0398
2.83	0.8908	0.9898	0.0135	0.0403
2.84	0.8902	0.9899	0.0135	0.0405
2.92	0.8856	0.9907	0.0134	0.0419
3.01	0.8801	0.9914	0.0133	0.0436
3.02	0.8795	0.9915	0.0133	0.0437
3.04	0.8782	0.9917	0.0133	0.0441
3.09	0.8749	0.9921	0.0132	0.045
3.23	0.8652	0.9931	0.0131	0.0476
3.29	0.8608	0.9934	0.0131	0.0487

Table 1. *Cont.*

α	Linear Relationship		Curvilinear Relationship	
	λ_R	λ_T	λ_R	λ_T
3.34	0.857	0.9937	0.013	0.0497
3.38	0.8538	0.994	0.013	0.0504
3.4	0.8522	0.9941	0.013	0.0508
3.5	0.844	0.9946	0.0129	0.0528
3.57	0.8379	0.9949	0.0128	0.0542
3.71	0.8249	0.9954	0.0128	0.057
3.74	0.822	0.9956	0.0128	0.0576
3.77	0.8191	0.9957	0.0127	0.0583
3.88	0.808	0.996	0.0127	0.0607
3.97	0.7985	0.9963	0.0127	0.0627
4.04	0.7908	0.9964	0.0127	0.0643
4.17	0.7762	0.9967	0.0127	0.0673
4.54	0.7318	0.9974	0.0128	0.0769
4.62	0.7219	0.9975	0.0128	0.0792
4.71	0.7108	0.9976	0.0129	0.0818
4.76	0.7046	0.9976	0.0129	0.0833
4.85	0.6934	0.9977	0.013	0.0861
4.94	0.6822	0.9978	0.0131	0.089
λ_S	0.9589		0.0121	
Mean	0.8783	0.9848	0.0211	0.0443
Std. Dev.	0.0869	0.0134	0.0143	0.0199

Because λ values close to 1 indicate a linear relationship, λ_T, λ_S, and λ_R support the linearity hypothesis. It can be observed that λ_T detects linearity more strongly than does λ_R for $\alpha > 1$; conversely, λ_R captures linearity better for $\alpha < 1$. The mean and the standard deviation for each mutual information measure are also presented in Table 1 for checking the variability of each measure against various α values. The standard deviation values for λ_T are lower than those for λ_R, pointing out the consistency of Tsallis in the case of linearity.

On the other hand, nonlinearity is captured by λ_T better than by λ_R for $\alpha < 1$ and vice versa for $\alpha > 1$. When the standard deviations are considered, λ_R is more stable in determining nonlinearity.

Changing the scale parameter α of mutual information measures naturally changes the sensitivity of this measure, and by plotting λ values against the scale parameter α, the change in sensitivity can be graphically displayed. In order to visually interpret the results, the λ_R and λ_T values, according to the different α values, are as seen in the graphs:

As can be seen from Figure 2, for $\alpha > 1$, λ_T is more succesful and stable than λ_R for a linear relationship. In addition, the λ_T measure consistently takes values close to 1, whereas λ_R gets smaller as α values increase.
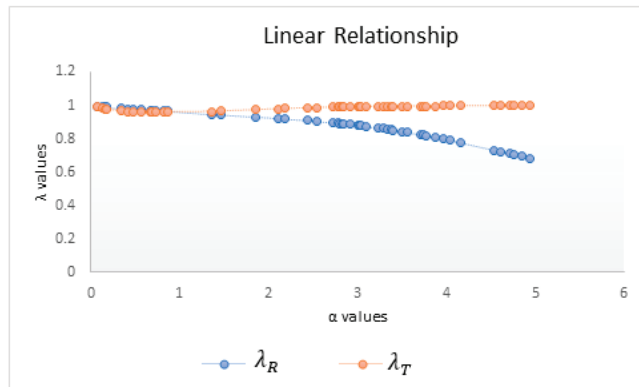
Figure 2. λ values versus α in the case of linearity.

As seen in Figure 3, in the curvilinear relationship, λ_T started to grow after alpha 1.4; λ_R takes values close to zero in all values of alpha. However, λ_T also takes a maximum value of 0.09101. Both common information measures can be used as criteria in nonlinearity. However, λ_R more consistently indicates nonlinearity. Because there is no logarithmic function in the Tsallis mutual information formula, when α takes a value greater than 1, Tsallis mutual information makes deviations from linearity less important than Rényi mutual information does. Therefore, λ_T will make it less sensitive to nonlinearity than λ_R and therefore more unresponsive to nonlinearity than λ_S and λ_T. For the same reason, λ_T will represent linearity better than Rényi will in linear relationship.
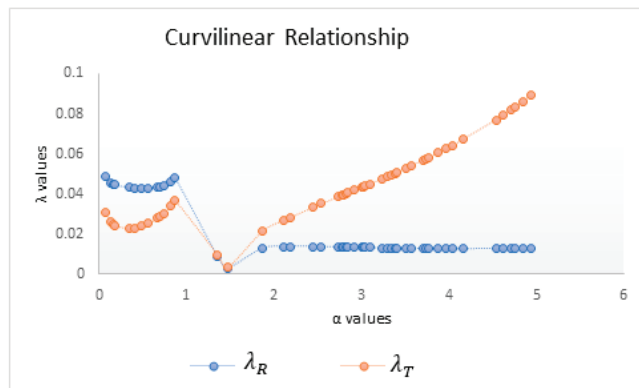
Figure 3. λ values versus α in the case of curvilinearity.

An important general property of Rényi entropy is that for a given probability distribution, Rényi entropy is a monotonically decreasing function of α, where α is an arbitrary real number other than 1. Therefore, as can be seen in Figure 2, increasing α values will not provide additional information, so α values are limited to 5.

2.3. Method for Bin-Size Selection

Mutual information depends mainly on both the bin size and the sample size; thus, a natural question arises about the optimal choice of one parameter given the value of another. Here, we use the Freedman–Diaconis rule for finding the optimal number of bins. According to this rule, the optimal number of bins can be calculated on the basis of the interquartile range ($IQR = Q_3 - Q_1$) and the number of data points n. Freedman and

Diaconis use the IQR of the data instead of the standard deviation; therefore, this method is described as more robust than some of the other methods.

$$\Delta_{bin} = 2 \times \frac{IQR(X)}{\sqrt[3]{n}} \tag{16}$$

The Freedman–Diaconis rule takes into account the asymmetry of the data and sets the bin size to be proportional to the IQR [25].

3. Checking the EKC Hypothesis for East Asian and Asia-Pacific Countries (1971–2016)

3.1. Model

To test the EKC hypothesis, a simple linear regression model is applied. Using the ordinary least squares procedure, we find a quadratic relationship ("inverted U-hypothesis") between CO_2 emissions (metric tons per capita) and GDP per capita (current USD) in a time series of East Asia and Asia-Pacific countries (excluding high-income countries) over a 46-year period.

East Asia and Asia-Pacific countries were classified initially as low income (LIC) in the 1990s, then as lower middle income (LMC) in 2010. In fact, the highest growth rate of CO_2 emissions (5.6% (1990–2008)) was observed in the East Asia and the Asia-Pacific region, where the highest GDP growth rates (7.2% (1990–2000) and 9.4% (2000–2010)) were achieved.

We first examine the residual diagrams from a linear regression model to determine whether there are serious deviations from assumptions. In Figure 4a, nonlinearity is apparent, whereas in Figure 4b, the deviation from normality assumption can be seen:
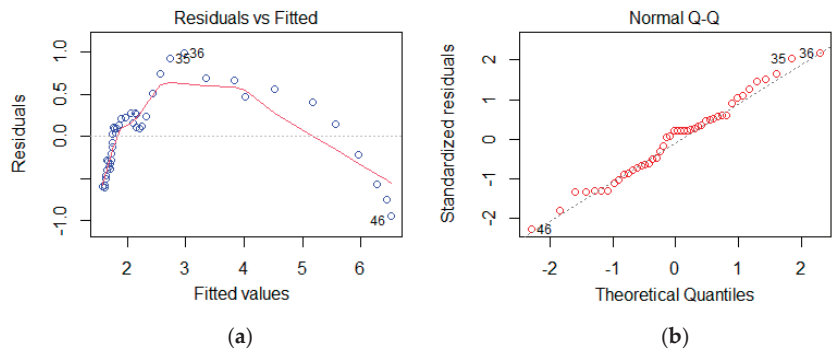
Figure 4. Residual plots listed as (**a**) fitted values to residuals and (**b**) normal Q-Q plot of standardized residuals.

According to a quick visual check of the residuals in Figure 4a, a quadratic model seems to be more appropriate. In Table 2, the results of quadratic models are given. The scatter diagram of CO_2 and GDP variables is shown in Figure 5.

Table 2. Summary of the model.

	a	b	c	F	R^2
Parameter Estimates	1.0121	0.0016	1.4×10^{-7}		
Standard Error	0.04599	5.9×10^{-5}	9.35×10^{-9}	1581.224	0.986
p-Value	4.99×10^{-25}	4.39×10^{-29}	5.08×10^{-19}		
Model		$CO_2 = 1.021 + 0.0016 GDP - \left(1.4 \times 10^{-7}\right) GDP^2$			

a: constant; b and c: coefficients of model; F: F test; R^2: coefficient of determination.
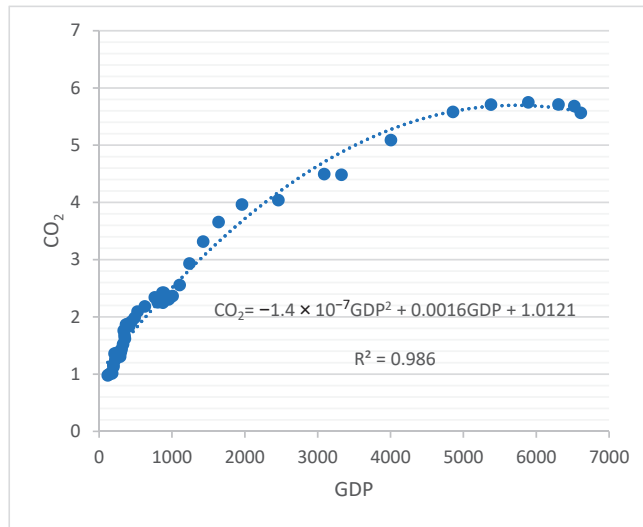
Figure 5. Quadratic regression model estimation.

To test the appropriateness of a simple linear regression function, the null and alternative hypotheses are given as follows:

$$H_0 : E(Y) = \beta_0 + \beta_1 X \tag{17}$$

$$H_a : E(Y) \neq \beta_0 + \beta_1 X \tag{18}$$

The general linear test statistic for simple regression model is as follows:

$$F^* = \frac{SSLF}{c-2} \div \frac{SSPE}{n-c} = \frac{1.641}{0.107} = 15.209$$

When we look at the results, shown in Table 3, $F* > F(0.05; 3.41) = 2.833$, so we reject null hypothesis H_0. This means that the linear regression function does not provide a good fit for the data. The dependence measures are $r^2 = 0.91$ and $\eta^2_{XY} = 0.96$. A nonzero value of $\eta^2_{YX} - r^2$ is associated with a departure from linearity. The calculated value of this difference is $\eta^2_{YX} - r^2 = 0.05$. To test the significance of this difference, the alternatives are given as follows:

H_0: The relationship between X and Y is linear.
H_a: The relationship between X and Y is not linear.

Table 3. Related ANOVA table.

Source of Variation	Df	Sum of Squares	Mean Squares
Explained variation by linear regression	1	SSR = 98.658	98.658
Explained variation by nonlinear regression	3	SSLF = 4.925	1.641
Unexplained variation	41	SSPE = 4.425	0.107
Total	45	SST = 108.01	

The test statistic is as follows:

$$F^* = \frac{n-c}{c-2} \cdot \frac{\eta_{XY}^2 - r^2}{1 - \eta_{XY}^2} = \frac{41}{3} * \frac{0.05}{0.04} = 17.083$$

This value of F also indicates a significant departure from linearity.

3.2. Testing Linearity on the Basis of Shannon, Rényi, and Tsallis Mutual Information Measures

The Tanaka, Okamoto, and Naito [17] and Smith [1] method is based on comparing the Shannon mutual information between the original data series with that between the new ones obtained by removing linear dependence from the original ones.

Entropy and mutual information calculations are based on a contingency table. A possible reason for the EKC hypothesis may lie in the fact that in poor countries, most of the output is produced in the agricultural sector. So CO_2 emissions are lower in these countries than in other countries. In middle-income countries, pollution begins to increase. As the country grows, it tends to switch to cleaner technologies.

Here, on the basis of the Freedman–Diaconis rule, the optimal number of bins is calculated and presented in Table 4:

Table 4. Optimal number of bins.

Variables	n_{bins}
CO_2	7
GDP	14
Residuals	9

To detect nonlinearity by using the Shannon, Rényi and Tsallis mutual information measures, the following table for different values of alpha may help. To evaluate the degree of nonlinearity included in the dependence, the two mutual information measures were compared. When $M(X, \xi) = M(X, Y)$, the dependence is interpreted to be based on nonlinearity, so the proposed λ_S, λ_R, and λ_T measures are considered as criteria of nonlinearity.

As seen in the Table 5, λ_S, λ_R, and λ_T are close to zero, so the relationship is nonlinear. As can be checked from the simulation data in Table 1, $\alpha < 1$ λ_T and $\alpha > 1$ λ_R more successfully reveal the curvature. Therefore, the results obtained from the EKC data also support this situation. As a result, the λ_S, λ_R, and λ_T values nearly zero indicate a curvilinear relationship, which supports the EKC hypothesis.

Table 5. λ values for EKC data.

α	λ_R	λ_T	α	λ_R	λ_T
0.07	0.3892	0.3655	3.01	0.0649	0.1460
0.13	0.3809	0.3444	3.02	0.0646	0.1459
0.17	0.3741	0.3323	3.04	0.0640	0.1458
0.18	0.3722	0.3295	3.09	0.0625	0.1455
0.35	0.3355	0.2902	3.23	0.0587	0.1453
0.41	0.3221	0.2797	3.29	0.0573	0.1455
0.48	0.3071	0.2690	3.34	0.0562	0.1457
0.56	0.2910	0.2586	3.38	0.0553	0.1460
0.67	0.2708	0.2466	3.4	0.0549	0.1461
0.69	0.2673	0.2447	3.5	0.0530	0.1471

Table 5. *Cont.*

α	λ_R	λ_T	α	λ_R	λ_T
0.74	0.2590	0.2402	3.57	0.0518	0.1481
0.82	0.2468	0.2339	3.71	0.0497	0.1505
0.87	0.2400	0.2307	3.74	0.0493	0.1511
1.36	0.1735	0.1961	3.77	0.0489	0.1518
1.46	0.1631	0.1913	3.88	0.0476	0.1545
1.86	0.1271	0.1743	3.97	0.0467	0.1570
2.11	0.1087	0.1653	4.04	0.0461	0.1591
2.18	0.1040	0.1630	4.17	0.0451	0.1635
2.44	0.0888	0.1556	4.54	0.0430	0.1782
2.54	0.0837	0.1532	4.62	0.0427	0.1817
2.73	0.0751	0.1494	4.71	0.0423	0.1858
2.78	0.0731	0.1486	4.76	0.0421	0.1881
2.8	0.0723	0.1483	4.85	0.0418	0.1923
2.83	0.0711	0.1479	4.94	0.0415	0.1965
2.84	0.0708	0.1477	λ_S	0.2181	0.2181
2.92	0.0679	0.1468	Mean	0.1313	0.1914
			St. Dev.	0.1147	0.0607

The relationship between λ and α can be seen in Figure 6:
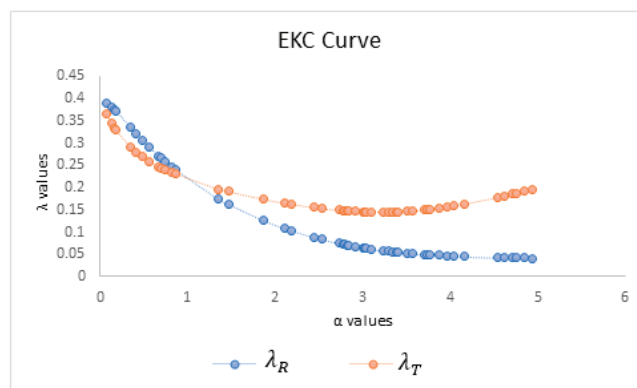
Figure 6. λ values against different α values for EKC data.

4. Conclusions

The environmental Kuznets curve (EKC) hypothesizes that the relationship between environmental quality and real output has an inverted U-shaped quality. Using the ordinary least squares estimation procedure, we have found a quadratic relationship between CO_2 emission and GDP in a time series of East Asia and Asia-Pasific countries (excluding high-income countries) over a period of 46 years. One technique to check the EKC hypothesis utilizes an F test, by which we have concluded that the linear model does not provide a good fit for the data. As a second technique, comparing the linear determination coefficient with the correlation ratio may be useful. Again, for the EKC data, the difference between these two association measures was found to be significant, addressing curvilinearity. Alternatively, the difference between two dependence measures on the basis of mutual

information can be used. Although Shannon mutual information has been used more often in the literature, we suggested that the Rényi and Tsallis mutual information measures catch the nature of the relation between the variables better because of their parametric flexibility.

In this study, the mutual information between dependent and independent variables ($M(X,Y)$) was found first. Secondly, by using a simple linear regression model, the residuals (ξ) were calculated. Then, the mutual information between the independent variable and the residuals ($M(X,\xi)$) was obtained. Finally, by comparing these two mutual information measures, the degree of nonlinearity included in the dependence was determined. We also proposed a measure of nonlinearity, λ, and demonstrated that the Rényi and Tsallis mutual information measures determined nonlinearity better for certain ranges of α values compared with the Shannon mutual information measure.

Applications of all these measures on CO_2 emissions and GDP data underlined curvilinearity, and hence, the presumed pattern by the EKC hypothesis was realistic. The result concludes that the "growth and pollute now, clean later" strategy is wasting a lot of resources and has enormous environmental costs. Therefore, countries should seek alternative growth strategies.

References

1. Smith, R. A Mutual Information Approach to Calculating Nonlinearity. *Stat* **2015**, *4*, 291–303. [CrossRef]
2. Yi, W.; Li, Y.; Cao, H.; Xiong, M.; Shugart, Y.Y.; Jin, L. Efficient Test for Nonlinear Dependence of Two Continuous Variables. *BMC Bioinform.* **2015**, *16*, 260.
3. Weatherburn, C.E. *A First Course Mathematical Statistics*; Cambridge University Press: Cambridge, UK, 1961.
4. Pestaña-Melero, F.L.; Haff, G.; Rojas, F.J.; Pérez-Castilla, A.; García-Ramos, A. Reliability of the Load-Velocity Relationship Obtained Through Linear and Polynomial Regression Models to Predict the 1-Repetition Maximum Load. *J. Appl. Biomech.* **2018**, *34*, 184–190. [CrossRef] [PubMed]
5. Gómez-Valent, A.; Amendola, L. H0 from Cosmic Chronometers and Type Ia Supernovae, with Gaussian Processes and the Novel Weighted Polynomial Regression Method. *J. Cosmol. Astropart. Phys.* **2018**, *2018*, 51. [CrossRef]
6. Akhlaghi, Y.G.; Ma, X.; Zhao, X.; Shittu, S.; Li, J. A Statistical Model for Dew Point Air Cooler Based on the Multiple Polynomial Regression Approach. *Energy* **2019**, *181*, 868–881. [CrossRef]
7. Gajewicz-Skretna, A.; Kar, S.; Piotrowska, M.; Leszczynski, J. The Kernel-Weighted Local Polynomial Regression (Kwlpr) Approach: An Efficient, Novel Tool for Development of Qsar/Qsaar Toxicity Extrapolation Models. *J. Cheminform.* **2021**, *13*, 9. [CrossRef]
8. Morris, J.S. Functional Regression. *Annu. Rev. Stat. Its Appl.* **2015**, *2*, 321–359. [CrossRef]
9. Shannon, C.E. A Mathematical Theory of Communication. *ACM SIGMOBILE Mob. Comput. Commun. Rev.* **2001**, *5*, 3–55. [CrossRef]
10. Darbellay, G.A.; Wuertz, D. The Entropy as a Tool for Analysing Statistical Dependences in Financial Time Series. *Phys. A Stat. Mech. Its Appl.* **2000**, *287*, 429–439. [CrossRef]
11. Dionisio, A.; Menezes, R.; Mendes, D.A. Mutual Information: A Measure of Dependency for Nonlinear Time Series. *Phys. A Stat. Mech. Its Appl.* **2004**, *344*, 326–329. [CrossRef]
12. BBarbi, A.; Prataviera, G. Nonlinear Dependencies on Brazilian Equity Network from Mutual Information Minimum Spanning Trees. *Phys. A Stat. Mech. Its Appl.* **2019**, *523*, 876–885. [CrossRef]
13. Mohti, W.; Dionísio, A.; Ferreira, P.; Vieira, I. Frontier Markets' Efficiency: Mutual Information and Detrended Fluctuation Analyses. *J. Econ. Interact. Coord.* **2019**, *14*, 551–572. [CrossRef]
14. Wu, X.; Jin, L.; Xiong, M. Mutual Information for Testing Gene-Environment Interaction. *PLoS ONE* **2009**, *4*, e4578. [CrossRef] [PubMed]

15. Li, J.; Dong, W.; Meng, D. Grouped Gene Selection of Cancer Via Adaptive Sparse Group Lasso Based on Conditional Mutual Information. *IEEE/ACM Trans. Comput. Biol. Bioinform.* **2017**, *15*, 2028–2038. [CrossRef]
16. Rosas, F.E.; Mediano, P.A.; Gastpar, M.; Jensen, H.J. Quantifying High-Order Interdependencies Via Multivariate Extensions of the Mutual Information. *Phys. Rev. E* **2019**, *100*, 032305. [CrossRef]
17. Tanaka, N.; Okamoto, H.; Naito, M. Detecting and Evaluating Intrinsic Nonlinearity Present in the Mutual Dependence between Two Variables. *Phys. D Nonlinear Phenom.* **2000**, *147*, 1–11. [CrossRef]
18. Grossman, G.M.; Krueger, A.B. Economic Growth and the Environment, Quarterly Journal of Economics, Cx, May, 353–377. *Int. Libr. Crit. Writ. Econ.* **2002**, *141*, 105–129.
19. Selden, T.M.; Song, D. Neoclassical Growth, the J Curve for Abatement, and the Inverted U Curve for Pollution. *J. Environ. Econ. Manag.* **1995**, *29*, 162–168. [CrossRef]
20. Panayotou, T. *Empirical Tests and Policy Analysis of Environmental Degradation at Different Stages of Economic Development*; Tech. & Emp. Prog.: Geneva, Switzerland, 1993.
21. Antle, J.M.; Heidebrink, G. Environment and Development: Theory and International Evidence. *Econ. Dev. Cult. Chang.* **1995**, *43*, 603–625. [CrossRef]
22. Vasilev, A. *Is There an Environmental Kuznets Curve: Empirical Evidence in a Cross-Section Country Data*; ZBW: Kiel, Germany, 2014.
23. Thomas, M.T.C.A.J.; Joy, A.T. *Elements of Information Theory*; Wiley-Interscience: Hoboken, NJ, USA, 2006.
24. Ullah, A. Entropy, Divergence and Distance Measures with Econometric Applications. *J. Stat. Plan. Inference* **1996**, *49*, 137–162. [CrossRef]
25. Freedman, D.; Diaconis, P. On the Histogram as a Density Estimator: L 2 Theory. *Z. Für Wahrscheinlichkeitstheorie Und Verwandte Geb.* **1981**, *57*, 453–476. [CrossRef]

Non-Additive Entropy Composition Rules Connected with Finite Heat-Bath Effects

Tamás Sándor Biró [1,2,†]

1   Wigner Research Centre for Physics, 1121 Budapest, Hungary; biro.tamas@wigner.hu
2   Institute for Physics, University Babeş-Bolyai, 400294 Cluj, Romania
†   External Faculty Member at Complexity Science Hub, 1080 Vienna, Austria.

Abstract: Mathematical generalizations of the additive Boltzmann–Gibbs–Shannon entropy formula have been numerous since the 1960s. In this paper we seek an interpretation of the Rényi and Tsallis q-entropy formulas single parameter in terms of physical properties of a finite capacity heat-bath and fluctuations of temperature. Ideal gases of non-interacting particles are used as a demonstrating example.

Keywords: entropy; finite heat-bath; superstatistics

1. Introduction

Entropy is a great tool in thermodynamics and statistical physics. Conceptualized originally by Clausius [1] as a state descriptor, that distinguishes it from heat, it became a basic principle for statistical and informatics calculations. Its classical form, the Boltzmann entropy has a wide use [2–5]. Nevertheless, mostly in mathematical approaches to informatics, its generalizations occurred: altered, non-logarithmic formulas between the probability of a given sate and the total entropy of the system [6–10].

Still, the classical logarithmic formula is of widest use, having a number of properties that make it destined to be a convex measure of information and probability. The most known generalization is due to Alfred Renyi [6], who constructed a formula being also additive for factorizing joint probability, but abandoned the logarithm as the sole function with this property. There is a parameter, occurring as a power of probability, denoted by q or α. The classical formula emerges in the $q \to 1$ limit, formally.

As interesting as the Renyi entropy is, its form is not an expectation value. The q-entropy as an expectation value was suggested by C. Tsallis [11–13], as that form is not additive for factorizing joint probabilities (or being additive for correlated, non-factorizing probabilities). Other and further generalizations, naming more parameters, were also suggested formulated in terms of leading order corrections to the Boltzmann formula in the thermodynamical limit or just utilizing more parameters for possible deformations of the original formula [9,14–19]. Properties of generalized entropy formulas were intensely studied, for two selected examples with respect to the Tsallis entropy see [20,21].

In the present paper another viewpoint is presented: (i) first we identify deviations from the classical logarithmic formula derived from deviations from additivity; (ii) then we demonstrate how phase space finiteness effects cause corrections to the additivity of entropy in coincidence with the factorization of probability in a microcanonical approach; (iii) and finally we ask the question of which modified entropy can be the most additive one in this respect. More closely, a general group entropy [22] is considered following non-addition rules and a limit of its infinite repetitions on small amounts is considered as an asymptotic rule of composition [23]. Associative rules form group operations, therefore a logarithm of the formal group can be derived from a general composition law, which is then additive. This will be the content of the next section.

There were decade-long discussions about the physical (or statistical) meaning of the parameter q, the first non-universal parameter occurring in generalized entropy formulas. It may be bound to the sort of the system under discussion, to its material properties, but at the same time it occurs generally in a given class of statistical systems, including informatics, statistical mechanics, dynamics at the edge of chaos, and complex random networks. A few approaches in the quest of uncovering physical mechanisms determining the value of q in particular cases in which the present author was involved, are in Refs. [23–27]. Similar studies by others are copiously cited in review books, cf. [12,24].

Following this, a physical interpretation of the parameter q will be established connected to the finite heat capacity of an environment [28] and to possible fluctuations in phase space dimensionality. The latter is akin to the superstatistical approach [29–33]. A balance between physical factors reducing and increasing the value of q may ensure the classical $q = 1$ case, however, in a general setting it is not provided. One is then tempted to restore additivity at best—since classical thermodynamics is based on this property. The attempt is made by using a logarithm of the formal group of entropy composition instead of the original entropy, $S \rightarrow K(S)$, and deriving again the associated q_K parameter. Then $q_k = 1$ generates a differential equation for the $K(S)$ function, and due to that, a new composition rule.

Finally some examples will be discussed and families of $K(S)$ forms will be established. The Boltzmann, Renyi, Tsallis entropies are all special cases, and they represent physical extremes in terms of the heat container capacity and the relative size of superstatistical fluctuations.

2. Logarithm of the Formal Group

It is worth starting our mathematical considerations with the composition law of entropy, or any other real valued physical quantity, when contacting and combining two systems to a bigger, unified one. Abandoning additivity, which ensures the co-extensivity properties of entropy and other extensive quantities, constructed also as expectation values, further composition rules are considered for non-extensive statistical mechanics [12]. The Abe-Tsallis composition law,

$$S_{12} = S_1 + S_2 + (q-1)S_1S_2, \tag{1}$$

is a particular case for a more general one, described by a two-variable function, $x \oplus y = h(x,y)$. In such composition rules the entropies, S_i (i = 1, 2, or 12) can be any state functions, $S(E, N, X_1, \ldots)$ and assumed to be valid in general, both for equilibrium and non-equilibrium entropies. Here we do not address such questions, just look for the consequences of adopting non-additive rules for the entropy. The value of the parameter q is usually in the open interval $(0, 2)$, in measured cases very often close but not equal to $q = 1$. Formally, however, it can be any real number, even negative. Certainly for $q < 1$, the entropies cannot be too large in order to avoid a negative composite result. In thermodynamics we deal mostly with large systems; thus, the requirement of associativity is natural:

$$h(h(x,y),z) = h(x,h(y,z)). \tag{2}$$

Having the third law in mind, on the other hand, zero entropy is a valid value, and its addition must be trivial:

$$h(x,0) = x, \tag{3}$$

and similarly $h(0,y) = y$. These two requirements already circumvent composition as a group operation. The question of inverse building remains only nontrivial.

Here, the logarithm of the formal group is helpful. It can be shown that, from the associativity Equation (2), it follows the existence of a monotonous and hence invertible mapping, which maps the general rule to the addition:

$$K(h(x,y)) = K(x) + K(y). \tag{4}$$

The function $K(z)$ is the formal logarithm; it can be constructed asymptotically from the rule $h(x, y)$ as follows. Imagine we compose from x to $x \oplus y = h(x, y)$ by adding small amounts, Δy, a number of time, N, so that $N\Delta y = y$. Then, in a general step, one proceeds as

$$x_{n+1} \;=\; x_n \oplus \Delta y \;=\; h(x_n, \Delta y) \;=\; h(x_n, 0) + \Delta y \frac{\partial h}{\partial y}(x_n, 0) + ldots \tag{5}$$

The index n in this change is additive, while x and y are not. Seeking for a continuous limit in the variable $t = n/N$ between zero and one, we arrive at

$$\int_{x(0)}^{x(1)} \frac{dx}{\frac{\partial h}{\partial y}(x, 0)} \;=\; \int_0^1 y \, dt \;=\; y. \tag{6}$$

Here $x(0) = x$ and $x(1) = x \oplus y$. Denoting the primitive function of the above integral by $K(z)$, our result reads as

$$K(x \oplus y) - K(x) \;=\; y. \tag{7}$$

This form breaks the symmetry between x and y. We remedy this problem by re-defining $\Delta y = K(y)/N$, i.e., taking steps by the additive quantity $K(y)$. By this we obtain the K-additivity

$$K(x \oplus y) = K(x) + K(y). \tag{8}$$

This is the sought mapping to additivity; therefore, $K(x)$ is called the formal logarithm. We note by passing this point that due to the continuous limit in the above derivation, the new rule is only asymptotic:

$$h_\infty(x, y) \;=\; K^{-1}(K(x) + K(y)) \tag{9}$$

does not always coincide with the starting rule, $h(x, y)$. Such asymptotic rules, however, build attractors among all composition rules. The result Equation (6) can also be obtained by taking the partial derivative of Equation (4) at $y = 0$, using $h(x, 0) = x$ and integrating. The asymptotic rule is a reconstruction of the composition rule from its first derivative at a very small (zero) second argument.

Here, we mention examples. The Tsallis-Abe rule, $h(x, y) = x + y + axy$ with $a = q - 1$, leads to the formal logarithm $K(x) = \frac{1}{a} \ln(1 + ax)$ and does not change in the asymptotics: $h_\infty(x, y) = x + y + axy$. A more general rule, using a general function of the product of the composables, $h(x, y) = x + y + f(xy)$ on the other hand leads back to the Tsallis-Abe rule with $a = f'(0)$. Triviality requires $f(0) = 0$, of course. The properties $K(0) = 0$ and $K'(0) = 1$ also do hold.

Lesser-known, more complex rules can also be investigated. For example, $h(x, y) = (x + y)A(xy) + B(xy)$ results in a logarithm of a rational function for $K(x)$. Instead of listing more and more examples, however, let us close this section with a more general comment. Once we change the simple additivity to K-additivity, equivalent to the use of an associative composition rule, the entropy formula in terms of the probability also changes.

Considering an ensemble in the Gibbs sense, the state i is realized W_i times, while altogether, $W = \sum_i W_i$ instances are investigated. The probability of being in state i approaches the $p_i = W_i/W$ ratio. Since the individual contribution to entropy would be $-\ln p_i$ in the classical approach, a composition of W such instances from which the i-th is repeated W_i times shall be constructed by K-additivity. The logarithm of the probability being additive for factorizing joint probabilities, a non-additive entropy can be constructed by the inverse function of the formal logarithm:

$$S_{\text{tot,non-add}} \;=\; \sum_i W_i K^{-1}(-\ln p_i). \tag{10}$$

In this way the generalized entropy formula belongs to an ensemble average value (or expectation value):

$$K^{-1}(S) = \sum_i p_i K^{-1}(-\ln p_i). \qquad (11)$$

This formula may need a little more explanation. Since we replaced the original additivity assumption with K-additivity, the additive quantities, reflected in the $\ln(1/p_i)$ formula which is additive for factorizing probabilities, must be a K-function of the non-additive ones. The above Equations (10) and (11) are for the non-additive quantities; therefore, the inverse function, K^{-1} is used on the additive log.

With the example of the Tsallis–Abe composition law, we have $K(S) = \frac{1}{a}\ln(1 + aS)$ and $K^{-1}(z) = (e^{az} - 1)/a$. This delivers the Tsallis entropy,

$$S_T = K^{-1}(S) = \frac{1}{a}\sum_i \left(p_i^{1-a} - p_i\right), \qquad (12)$$

with $q = 1 - a$ as the non-additive, but expectation value-like construction, with the corresponding Rényi entropy,

$$S_R = K(S_T) == \frac{1}{a}\ln\left(\sum_i p_i^{1-a}\right), \qquad (13)$$

as the version additive for factorizing probabilities, but not being an expectation value (ensemble average).

Consequently, equilibrium distributions when maximizing the entropy or its monotonous function, $K(S)$, deliver corresponding solutions of

$$\frac{\partial S}{\partial p_i} = \alpha + \beta\epsilon_i, \qquad (14)$$

while keeping an average energy fixed. Both for the Rényi and Tsallis q-entropy the resulting canonical distribution becomes a cut power law in the individual energy, ϵ_i:

$$p_i = \frac{1}{Z}\left(1 + a\frac{\epsilon_i}{T}\right)^{-1/a}. \qquad (15)$$

In the $a \to 0$ ($q \to 1$) limit the Boltzmann-Gibbs exponential emerges. The factor Z ensures the normalization, $\sum_i p_i = 1$.

3. *q* Parameter in the Boltzmannian Approach

At a first glance, it seems arbitrary which composition rule, and consequently which formal logarithm, is to be used in our models. However, the parameters occurring in a modification of the entropy addition law need some connection to physical reality. In this section we first extend the familiar textbook derivation of the exponential canonical distribution by going a step further in the thermodynamical limit expansion and then compare the result with the cut power-law canonical distribution. This gives rise to a possible physical interpretation of the parameter q.

Following the classical argumentation, there is a factor in the probability of a subsystem having energy ϵ out of the total E occurring as a ration of corresponding phase space volumes:

$$\rho(\epsilon) = \langle\frac{\Omega(E - \epsilon)}{\Omega(E)}\rangle. \qquad (16)$$

Here, the averaging is over parallel ensemble copies of the same system, allowing for microscopical fluctuations in parameters beyond the total energy, E, like particle numbers, charges, etc. The occupied phase space volumes are connected to the entropy, $\Omega(E) = e^{S(E)}$.

Expanding the expression Equation (16) up to first order in $\epsilon \ll E$ one arrives at the well known canonical factor

$$\rho_1(\epsilon) = \langle e^{-\epsilon S'(E)} \rangle = e^{-\epsilon \langle S'(E) \rangle} = \frac{1}{Z} e^{-\epsilon/T}. \tag{17}$$

Here Z is a normalization factor ensuring $\int_0^E \rho(\epsilon)d\epsilon = E$. The temperature is interpreted as $1/T = \langle S'(E) \rangle$. The information about the environment (heat bath) is comprised into this single parameter, traditionally.

Now we look at the consequences of going one step further, i.e., performing an $\mathcal{O}(\epsilon^2)$ expansion:

$$\rho_2(\epsilon) = \langle e^{-\epsilon S'(E) + \epsilon^2 S''(E)/2} \rangle = 1 - \epsilon \langle S'(E) \rangle + \frac{1}{2}\epsilon^2 \langle S''(E) + S'(E)^2 \rangle. \tag{18}$$

This result is to be compared with the canonical distribution following from the Rényi and Tsallis entropy, to the Tsallis–Pareto distribution [12,34] to the same order

$$\left(1 + (q-1)\frac{\epsilon}{T}\right)^{-\frac{1}{q-1}} = 1 - \frac{\epsilon}{T} + \frac{q}{2}\frac{\epsilon^2}{T^2}. \tag{19}$$

Term by term comparison between Equations (18) and (19) interprets the parameters T and q in the Tsallis–Pareto distribution as being

$$\frac{1}{T} = \langle S'(E) \rangle, \qquad \frac{q}{T^2} = \langle S''(E) \rangle + \langle S'(E)^2 \rangle. \tag{20}$$

Denoting $S'(E) = \beta$ as a fluctuating quantity, one uses its variance in the above interpretation of q, besides the derivative of the temperature $dT/dE = 1/C$, with C being the total capacity of the heat bath in the formula $\langle S''(E) \rangle = \frac{d}{dE}\frac{1}{T} = -1/CT^2$:

$$q = 1 - \frac{1}{C} + T^2 \Delta\beta^2. \tag{21}$$

This result allows for q values both smaller and larger than one; the $q = 1$ remaining a special choice. Indeed, textbooks [35] suggest that the $q = 1$ is the only possible choice and then conclude that $T\Delta\beta = 1/\sqrt{C}$ argues for the "one over square root law" for energy fluctuations. This argumentation is, however, misleading: the physical situation and size of the heat bath actually present must determine the value of the parameter q.

4. Optimal Restoration of Additivity

In the present section we shall optimize the choice of $K(S)$ instead of S in estimating the phase space volumes above in order to achieve $q_K = 1$. This requirement leads to a differential equation restricting the function $K(S)$. Since according to the Tsallis-Abe composition law $q = 1$ is the additive case, seeking for $q_K = 1$ we call restoration of additivity. This is the best result possible, keeping in mind that the Tsallis-Pareto distribution is also an approximation in case of finite heat bathes, although one term improved beyond the traditional Boltzmann–Gibbs exponential.

The canonical statistical factor in this case transmutes to

$$\rho_K = \langle e^{K(S(E-\epsilon))-K(S(E))} \rangle. \tag{22}$$

Expanding up to (ϵ^2) terms, as in the previous section, with the assumption that the $K(S)$ function is universal, i.e., independent from the energy stored in the heat bath, we obtain

$$\rho_K = 1 - \epsilon \langle S' \rangle K' + \frac{\epsilon^2}{2}\left[\langle S'' \rangle K' + \langle S'^2 \rangle (K'^2 + K'') \right] + \dots \tag{23}$$

Comparing this with a Tsallis–Pareto distribution of the same approximation, we obtain another temperature and different variance parameters, T_K and q:

$$\frac{1}{T_K} = \langle S' \rangle K'$$

$$q_K = \langle S'' \rangle \frac{T^2}{K'} + \langle S'^2 \rangle \left(1 + \frac{K''}{K'^2}\right). \tag{24}$$

The requirement, $q_K = 1$, singles out a $K(S)$ formal logarithm for the entropy composition rule, which optimizes to the subleading order $\mathcal{O}(\epsilon^2)$ in general. This results in a simple, solvable differential equation for $F = 1/K'$:

$$q_K = -\frac{1}{C} F + (1 + T^2 \Delta \beta^2)(1 - F') = 1. \tag{25}$$

Here, we again used the fact that $\langle S' \rangle = 1/T$ and $\langle S'' \rangle = -1/CT^2$. Ordering this equation to F' one obtains

$$F' + \frac{1/C}{1 + T^2 \Delta \beta^2} F = \frac{T^2 \Delta \beta^2}{1 + T^2 \Delta \beta^2}. \tag{26}$$

Such an equation can be solved by quadrature even for complicated functions of the entropy.

The simplest physical system is an ideal gas: in this case, the heat capacity is independent of the total entropy, so $1/C$ is a constant. On the other hand, we may also assume that the relative variance in temperature, comprised in the term $T\Delta \beta = \Delta \beta / \langle \beta \rangle$, is also a constant with respect to the total entropy. In this simplest case, it is straightforward to obtain the optimal formal logarithm, $K(S)$ from Equation (26).

Here we present the solution, which contains two parameters:

$$K(S) = \frac{1}{\mu} \ln\left(1 + \frac{\mu}{\lambda}(e^{\lambda S} - 1)\right). \tag{27}$$

This ansatz is a "to and back" construction in a $K(S) = h_\mu(h_\lambda^{-1}(S))$ form with $h_\mu(x) = \frac{1}{\mu} \ln(1 + \mu x)$ being the formal logarithm associated to the Tsallis–Abe composition rule. The reciprocal inverse of the first derivative of $K(S)$ is obtained as

$$F(S) = \frac{1}{K'(S)} = \frac{\mu}{\lambda} + \left(1 - \frac{\mu}{\lambda}\right) e^{-\lambda S} \tag{28}$$

satisfying the $F(0) = 1$ condition. Substituting this function and its first derivative into Equation (26) we conclude that $F' + \lambda F = \mu$ with

$$\mu = \frac{T^2 \Delta \beta^2}{1 + T^2 \Delta \beta^2},$$

$$\lambda = \frac{1/C}{1 + T^2 \Delta \beta^2}. \tag{29}$$

It is interesting to check some limits of this expression. For $\mu \ll \lambda$ or in the $\mu = 0$ case, corresponding to zero fluctuations in the thermodynamical temperature, one obtains

$$K(S) = \frac{1}{\lambda}\left(e^{\lambda S} - 1\right) = C(e^{S/C} - 1). \tag{30}$$

This generates a non-additive entropy formula

$$K^{-1}(S) = C \sum_i p_i \ln\left(1 - \frac{1}{C} \ln p_i\right). \tag{31}$$

The corresponding canonical distribution is a complicated expression involving Lambert's function.

In the other extreme, $\lambda = 0$, meaning the presence of an infinite heat capacity (ideal) heat bath, we arrive at

$$K(S) \; = \; \frac{1}{\mu} \ln(1 + \mu S). \tag{32}$$

In this case the non-additive entropy formula delivers a Tsallis entropy, cf. Equations (11) and (12), and the canonical distribution is a Tsallis–Pareto distribution.

It is most intriguing that the choice $\mu = \lambda$, i.e., stating that the temperature fluctuations are exactly following the inverse square root law, $T\Delta\beta = 1/sqrtC$; and therefore, $\mu = \lambda = 1/(C+1)$, always the Boltzmann–Gibbs formula emerges:

$$K(S) \; = \; S, \tag{33}$$

and S itself is additive.

One realizes that the balance between ensemble fluctuations and the finiteness of the heat bath determines which is the optimally additive entropy formula. It is convenient to use the formal logarithm $K(S)$ instead of S as an additive quantity. Still, the traditional balance derived from $q = 1$ ($\lambda = \mu$) is not always given in physical situations. Some might find it strange that the parameter q depends on the heat capacity controlling the reservoir. Here the relation is with the same system's heat capacity. Analogously, a much simpler correspondence is true for a fixed volume of photon gas, where $C = 3S$, since the equation of state is given by $S \sim E^{3/4}V^{1/4}$, stemming from $E/V \sim T^4$ and $S/V \sim T^3$.

5. Fluctuations in Phase Space Dimension

One of the most prominent cases when fluctuations are "external", occurring due to the way of collecting data and not stemming from the finiteness of the heat bath, is the study of single particle energy spectra in high energy collisions. Hadronization makes n particles, event by event a different number, while the total energy shared by them is approximately constant. This situation is opposite to the energy fluctuations with a fixed number of particles (atoms).

In this case the phase space to be filled by individual energies has a fluctuating dimension, while the total energy determining the microcanonical hypersurface is fixed. Then, depending on the actual probability of making n hadrons in a single collision event, P_n, the summed distribution of single particle energy, frequently measured by the transverse momentum for very energetic particles, will differ from the traditionally expected exponential or Gaussian. In order to dwell on this problem, let us first review how the microcanonical phase space is calculated at a given total energy, E, and how dimensions for n particles move in some spatial dimensions.

Phase space is over momenta. Individual energies are functions of momenta according to the corresponding dispersion relation. A number of such relations look like a power of the absolute value, so they can be comprised into an L_p-norm:

$$\left(\sum_{i=1}^{n} |p_i|^p \right)^{1/p} \leq R(E) \tag{34}$$

with p_i individual momentum components, altogether n-dimension in phase space and E total energy. The $R(E)$ function also reflects the dispersion relation between energy and momenta. For a one dimensional jet $E = |\vec{p}|$, here simply $R(E) = E$ and the L_1 norm is to be used. For nonrelativistic ideal gases $E = |\vec{p}|^2/2m$, therefore, $R(E) = \sqrt{2mE}$ and the L_2 norm is used.

For extreme relativistic particles $p = 1$, and $R(E) = E$ measures the volume satisfying

$$\sum_{i=1}^{n} |p_i| \leq E. \tag{35}$$

The general formula reads as

$$\Omega_n^{(p)}(R) = \frac{\Gamma(1/p+1)^n}{\Gamma(n/p+1)} (2R)^n. \tag{36}$$

Originally Dirichlet obtained this formula in a french publication [36]. More contemporary popularizations are due to Smith and Vamanamurthy [37] from 1989 and Xianfu Wang [38] from 2005. Wikipedia also has an entry on this formula [39] and a recursive proof in few lines can be obtained from [40]. A microcanonical constrained hypersurface is the derivative of the above volume formula against the total energy

$$G_n^{(p)}(E) = \frac{\mathrm{d}}{\mathrm{d}E} \Omega_n^{(p)}(R(E)). \tag{37}$$

Meanwhile the surface is the derivative against R.

We define a ratio of volumes, and consider the $p = 1$ case, related to relativistic particles in a 1-dimensional jet:

$$r_n^{(1)} = \frac{\Omega_1^{(1)}(\epsilon)\Omega_{n-1}^{(1)}(E-\epsilon)}{\Omega_n^{(1)}(E)} = n \frac{\epsilon}{E} \left(1 - \frac{\epsilon}{E}\right)^{n-1}. \tag{38}$$

For normalization we use the pure environmental factor, the above ratio without the single particle factor:

$$\rho_n^{(1)} = \frac{\Omega_{n-1}^{(1)}(E-\epsilon)}{\Omega_n^{(1)}(E)} = \frac{n}{2E} \left(1 - \frac{\epsilon}{E}\right)^{n-1}. \tag{39}$$

This $\rho_n^{(1)}(\epsilon, E)$ is normalized over an integral in the single-particle phase space. This means an integral over p between $-E$ and $+E$, while $\epsilon = |p|$ with the absolute value:

$$\int_{-E}^{+E} \rho_n^{(1)} dp = \frac{n}{2E} \int_{-E}^{+E} \left(1 - \frac{|p|}{E}\right)^{n-1} dp = 1. \tag{40}$$

Due to the $|p|$ absolute value expression, this integral is twice of that between 0 and E, whence the factor 2 in the denominator becomes cancelled.

Once its integral is normalized to 1, also the mixture

$$\rho^{(1)}(\epsilon; E) = \sum_{n=0}^{\infty} P_n \rho_n^{(1)}(\epsilon) \tag{41}$$

is normalized to 1, provided that the $\sum_n P_n = 1$ sum is also normalized.

Finally, note that the ratio of volumes and energy shells in the 1-dimensional, relativistic case are simply related:

$$G_n^{(p)}(E) = \frac{\mathrm{d}}{\mathrm{d}E} \Omega_n^{(p)}(R(E)) = \Omega_n^{(p)}(R(E)) \frac{\mathrm{d}}{\mathrm{d}E} \ln(R^n), \tag{42}$$

in the $p = 1$ (relativistic) L_1-norm delivers due to $R(E) = E$

$$G_n^{(1)}(E) = \frac{n}{E} \Omega_n^{(1)}(E). \tag{43}$$

So we have $G_1^{(1)}(\epsilon) = \frac{1}{\epsilon}\Omega_1^{(1)} = 2$ and

$$g_n^{(1)}(\epsilon; E) \;=\; \frac{G_1^{(1)}(\epsilon)G_{n-1}^{(1)}(E-\epsilon)}{G_n^{(1)}(E)} \;=\; \frac{n-1}{E}\left(1-\frac{\epsilon}{E}\right)^{n-2}. \tag{44}$$

Finally, we have

$$r_n^{(1)}(\epsilon; E) \;=\; \epsilon\, g_{n+1}^{(1)}(\epsilon; E). \tag{45}$$

In this case the microcanonical ratio, $g_{n+1}^{(1)}$ is normalized to 1 for an integral over ϵ between 0 and E.

For ideal gases, one considers $S = \ln c_n + n \ln E$, delivering

$$\frac{1}{T} \;=\; \frac{\langle n \rangle}{E}; \qquad \text{and} \qquad \frac{q}{T^2} \;=\; \frac{\langle n(n-1) \rangle}{E^2}. \tag{46}$$

Here, q is actually the measure of non-Poissonity,

$$q \;=\; 1 - \frac{1}{\langle n \rangle} + \frac{\Delta n^2}{\langle n \rangle^2}. \tag{47}$$

For the negative binomial distribution (NBD) $q = 1 + 1/(k+1)$, for the Poissonian exactly $q = 1$. In hadronization statistics the Tsallis–Pareto distribution extracted from transverse momentum distributions and the multiplicity fluctuations event by event go hand in hand [41–43]. Such distributions may be a consequence of dynamical random processes, too, as it is investigated in the framework of the Local Growth Global Reset (LGGR) model recently on the master equation level [44], or earlier in the framework of the generalization of Boltzmann's kinetic approach and the related H theorem [45–47].

6. Conclusions

In conclusion, we investigated the physical background for applying non-additive entropy in three steps: (i) we reviewed associative composition rules and the derivation of their asymptotic version valid in the thermodynamic limit, (ii) we have optimized which formal logarithm of the entropy, $K(S)$, is to be used in phase space occupation probability arguments, including but not restricted to the case for Tsallis entropy, and finally, (iii) we reviewed phase space ratios in high energy jets as an application for superstatistical fluctuation in the dimensionality of phase space volumes. The coupling of these three aspects in a particular chain concludes that even ideal gases in a finite heat bath environment and away from thermal equilibrium can show a certain ambiguity, best removed by using non-additive entropy formulas.

To show an example, a certain ambiguity for estimating the heat capacity from maximizing the mutual entropy between observed subsystem and heat bath is discussed in detail for ideal gases in the Appendix A. We demonstrate in Appendix B that using $K(S)$ instead of S indeed clears the mismatch between statistical informatics—postulating mutual entropy maximum in equilibrium—and thermodynamics, obtaining the heat capacity of a subsystem independently of the heat bath, i.e., using the Universal Thermostat Independence (UTI) principle.

Appendix A. Ideal Gas with Finite Heat-Bath

First, we describe how a finite heat capacity heat bath influences the heat capacity of an observed subsystem. The effect stems from maximizing the mutual entropy instead of the subsystem's entropy alone.

We consider ideal gases, occupying phase space volumes according to the N-Ball in L_p norm picture. N is the number of degrees of freedom, or particles, while dimensionality factorizes. For one-dimensional extreme relativistic particles, the radius is $R(E) = E$ and one uses the diamond shape, L_1-norm. For traditional, nonrelativistic particles the radius is $R(E) = \sqrt{2mE}$ and one uses the spherical, L_2-norm.

In both cases the entropy is given as

$$S = \ln(a(N)) + kN \ln E. \tag{A1}$$

We have $k = 1$ for one-dimensional jets, and $k = 3/2$ for traditional ideal gases in 3 dimensions. The first derivative wrsp the energy defines the $\beta = 1/T$ variable:

$$\beta \equiv S'(E) = k\frac{N}{E} = 1/T. \tag{A2}$$

The second derivative defines implicitly the heat capacity:

$$C \equiv \left.\frac{dQ}{dT}\right|_V = \frac{dE}{dT} = \frac{dE}{d(1/\beta)} = kN \tag{A3}$$

with

$$S''(E) = -\frac{1}{CT^2} = -\frac{\beta^2}{kN}. \tag{A4}$$

For a subsystem connected with another system (may be called reservoir if large enough) not the individual, but the mutual entropy maximum describes the most probable energy for a subsystem. We have $I_{12} = S(E_1, N_1) + S(E_2, N_2) - S(E_1 + E_2, N_1 + N_2)$ and when fixing E_2 and all N-s from that the first derivative,

$$\frac{\partial I_{12}}{\partial E_1} = k\frac{N_1}{E_1} - k\frac{N_1 + N_2}{E_1 + E_2}, \tag{A5}$$

and the second derivative against E_1 is given by

$$\frac{\partial^2 I_{12}}{\partial E_1^2} = -k\frac{N_1}{E_1^2} + k\frac{N_1 + N_2}{(E_1 + E_2)^2}. \tag{A6}$$

Due to $\rho(E_1) \sim e^{I_{12}}$, the most probable energy value for the subsystem is obtained from the vanishing of the first derivative of I_{12}. This occurs at $\beta_1 = \beta_{12}$, according to the definition of β and Equation (A5). At this point from the second derivative, an effective, intercorrelated heat capacity for the subsystem appears. We have

$$\left.\frac{\partial^2 I_{12}}{\partial E_1^2}\right|_{max} = -k\beta^2 \frac{N_2}{N_1(N_1 + N_2)}, \tag{A7}$$

and from that the effective heat capacity

$$C_{1,I_{12}=max} = \frac{C_1}{C_2}(C_1 + C_2) = C_1 + \frac{C_1^2}{C_2}. \tag{A8}$$

Exactly the correction C_1^2/C_2 is the effect of a finite heat bath reservoir which vanishes in the thermodynamical limit, $C_2 \to \infty$.

A similar result can be derived when fixing the total energy, $E = E_1 + E_2$, and then looking for the most probable subsystem energy, E_1. We get

$$C_{1,I_{12}=max} = C_1 - \frac{C_1^2}{C}. \tag{A9}$$

In this case the total system has fixed parameters (energy, heat capacity). Again, in the thermodynamical limit the correction vanishes.

Appendix B. Universal Thermostat Independence

The above corrections, in one case positive, in another negative, make the concept of heat capacity ambiguous. In order to avoid this discrepancy, we can follow two strategies: (i) ignore the problem and restrict to the infinite capacity reservoir limit, or (ii) compensate for this leading effect near to the maximal probability. Choosing the second strategy is equivalent with admitting that the original additive concept of mutual entropy has to be generalized.

Following the second option, we consider the maximum of the mutual K-entropy instead of the original entropy, and the additive quantity associated to a possibly non-additive entropy, $K(S)$, is constructed in a way that the corresponding heat capacity appears infinite.

It is easy to achieve by choosing $K(S)$ accordingly. All usual quantities, temperature, heat capacity acquire a K index by doing so and we obtain

$$
\begin{aligned}
\frac{1}{T_k} &= \frac{\partial}{\partial E} K(S) = K'(S) \frac{\partial S}{\partial E} = \frac{K'}{T} \\
-\frac{1}{C_K T_K^2} &= \frac{\partial}{\partial E} \frac{1}{T_K} = \frac{1}{T^2} \left(-K'' + (K')^2 \frac{1}{C} \right).
\end{aligned} \tag{A10}
$$

Solving it for the *K*-capacity of heat, we have

$$\frac{1}{C_K} = -\frac{K''}{(K')^2} + \frac{1}{C}. \tag{A11}$$

The universal thermostat independence requires that $1/C_K = 0$, which is a second order differential equation for $K(S)$, quoted as the UTI principle in [28,48],

$$\frac{K''(S)}{(K'(S))^2} = \frac{1}{C}. \tag{A12}$$

With the boundary conditions $K(0) = 0$ (for the sake of keeping the third law of thermodynamics) and $K'(0) = 1$ (just keeping the Boltzmann constant at its original value $k_B = 1$), we arrive at a solution for a constant C, independent of S, as being

$$K(S) = -C \ln(1 - S/C). \tag{A13}$$

Applying now *K*-additivity with this formula, we require zero mutual K-entropy reflecting total independence of the energy states of reservoir and subsystem,

$$K(S_1) + K(S_2) - K(S_{12}) = 0, \tag{A14}$$

we derive the Tsallis–Abe composition law. From Equations (A13) and (A14), one writes

$$-C \ln(1 - S_1/C) - C \ln(1 - S_2/C) = -C \ln(1 - S_{12}/C). \tag{A15}$$

From here, a product rule follows,

$$\left(1 - \frac{S_1}{C} \right) \cdot \left(1 - \frac{S_2}{C} \right) = \left(1 - \frac{S_{12}}{C} \right), \tag{A16}$$

which in turn simplifies to

$$S_{12} = S_1 + S_2 - \frac{1}{C}S_1 S_2. \tag{A17}$$

Comparing this with the Tsallis–Abe rule Equation (1) one obtains $q = 1 - 1/C$. This is already a part of the result presented in Equation (21). For the total result, previously known temperature fluctuation can already be counted for, which may or may not under- or overcompensate this effect.

References

1. Clausius, R. *Théorie Mécanique de la Chaleur*; Librarie Scientifique, Industrielle et Agricole, Série B, No. 2; Eugéne Lacroix: Paris, France, 1868.
2. Boltzmann, L. Weitere Studien über das Wärmegleichgewicht unter Gasmolekülen. *Wien. Ber.* **1872**, *66*, 275.
3. Boltzmann, L. Über die Beziehung einer allgemeine mechanischen Satzes zum zweiten Hauptsatze der Wärmetheorie. *Sitzungsberichte K. Akad. Wiss. Wien* **1877**, *75*, 67.
4. Gibbs, J.W. *Elementary Principles in Statistical Mechanics*; C. Scriber's Sons: New York, NY, USA, 1902.
5. Shannon, C. A mathematical theory of communication. *Bell. Syst. Tech. J.* **1948**, *27*, 379–423; ibid 623–656. [CrossRef]
6. Renyi, A. On measures of information and entropy. In Proceedings of the Fourth Berkeley Symposium on Mathematics, Statistics and Probability, Berkeley, CA, USA, 20 June–30 July 1960; Volume 1, pp. 547–561.
7. Havrda, J.; Charvat, F. Quantification Method of Classification Processes. Concept of Structural Entropy. *Kybernetika* **1967**, *3*, 30–35.
8. Daróczy, Z. Generalized Information Functions. *Inf. Control* **1970**, *16*, 36. [CrossRef]
9. Sharma, B.D.; Mittal, D.P. New nonadditive measures of inaccuracy. *J. Math. Sci.* **1975**, *10*, 122.
10. Nielsen, F.; Nock, R. A closed-form expression for the Sharma-Mittal entropy of exponential families. *J. Phys. A* **2011**, *45*, 032003. [CrossRef]
11. Tsallis, C. Possible generalization of Boltzmann–Gibbs statistics. *J. Stat. Phys.* **1988**, *52*, 479. [CrossRef]
12. Tsallis, C. *Introduction to Non-Extensive Statistical Mechanics: Approaching a Complex World*; Springer Science+Business Media LLC: New York, NY, USA, 2009.
13. Tsallis, C. Nonadditive entropy: The concept and its use. *EPJ A* **2009**, *40*, 257–266. [CrossRef]
14. Hanel, R.; Thurner, S. A comprehensive classification of complex statistical systems and an axiomatic derivation of their entropy and distribution functions. *EPL* **2011**, *93*, 20006. [CrossRef]
15. Hanel, R.; Thurner, S. When do generalized entropies apply? How phase space volume determines entropy. *EPL* **2011**, *96*, 50003. [CrossRef]
16. Landsberg, P.T. Is equilibrium always an entropy maximum? *J. Stat. Phys.* **1984**, *35*, 159. [CrossRef]
17. Tisza, L. *Generalized Thermodynamics*; MIT Press: Cambridge, MA, USA, 1961.
18. Maddox, J. When entropy does not seem extensive. *Nature* **1993**, *365*, 103. [CrossRef]
19. Zapirov, R.G. *Novije Meri i Metodi b Teorii Informacii*; New Measures and Methods in Information Theory; Kazan State Tech University: Kazan, Russia, 2005, ISBN 5-7579-0815-7.
20. Abe, S. Axioms and uniqueness theorem for Tsallis entropies. *Phys. Lett. A* **2000**, *271*, 74. [CrossRef]
21. Santos, R.J.V. Generalization of Shannon's theorem for Tsallis entropy. *J. Math. Phys.* **1997**, *38*, 4104. [CrossRef]
22. Jensen, H.J.; Tempesta, P. Group Entropies: From Phase Space Geometry to Entropy Functionals via Group Theory. *Entropy* **2018**, *20*, 804. [CrossRef]
23. Biro, T.S. Abstract composition rule for relativistic kinetic energy in the thermodynamical limit. *EPL* **2008**, *84*, 56003. [CrossRef]
24. Biro, T.S. *Is There a Temperature? Conceptual Challenges at High Energy, Acceleration and Complexity*; Springer Series on Fundamental Theories of Physics 1014; Springer Science+Business Media LLC: New York, NY, USA, 2011.
25. Biro, T.S.; Jakovac, A. Power-law tails from multiplicative noise. *Phys. Rev. Lett.* **2005**, *94*, 132302. [CrossRef]
26. Biro, T.S.; Purcsel, G. Non-extensive Boltzmann-equation and hadronization. *Phys. Rev. Lett.* **2005**, *95*, 062302. [CrossRef]
27. Biro, T.S.; Purcsel, G.; Urmossy, K. Non-extensive approach to quark matter. *EPJ A* **2009**, *40*, 325–340. [CrossRef]
28. Biro, T.S.; Van, P.; Barnafoldi, G.G.; Urmossy, K. Statistical Power Law due to Reservoir Fluctuations and the Universal Thermostat Independence Principle. *Entropy* **2014**, *16*, 6497–6514. [CrossRef]
29. Beck, C.; Cohen, E.G.D. Superstatistics. *Physica A* **2003**, *322*, 267–275. [CrossRef]
30. Cohen, E.D.G. Superstatistics. *Physica D* **2004**, *193*, 35. [CrossRef]
31. Beck, C. Recent developments in superstatistics. *Braz. J. Phys.* **2009**, *38*, 357. [CrossRef]
32. Beck, C. Superstatistics in high-energy physics, Application to cosmic ray energy spectra and $e^+ e^-$ annihilation. *EPJ A* **2009**, *40*, 267–273. [CrossRef]
33. Beck, C. Dynamical foundations of nonextensive statistical mechanics. *Phys. Rev. Lett.* **2001**, *87*, 180601. [CrossRef]
34. Available online: https://en.wikipedia.org/wiki/Pareto_distribution#Generalized_Pareto_distributions (accessed on 26 October 2022).

35. Landau, L.D.; Lifshitz, E.M. *Course of Theoretical Physics*; Statistical Physics; Elsevier Science: Amsterdam, The Netherlands, 2013; Volume 5; ISBN 9781483103372.
36. Dirichlet, L.P.G. Sur une nouvelle méthode pour la détermination des intégrales multiples. *J. Math. Pures Appl.* **1839**, *4*, 164–168.
37. Smith, D.J.; Vamanamurthy, M.K. How Small Is a Unit Ball? *Math. Mag.* **1989**, *62*, 101–167. [CrossRef]
38. Wang, X. Volumes of Generalized Unit Balls. *Math. Mag.* **2005**, *78*, 390–395. [CrossRef]
39. Available online: htps://en.wikipedia.org/wiki/Volume_of_an_n-ball (accessed on 26 October 2022).
40. Available online: https://math.stockexhange.com/questions/301506/hypervolume-of-a-n-dimensional-ball-in-p-norm (accessed on 26 October 2022).
41. Wilk, G.; Wlodarczyk, Z. On the interpretation of nonextensive parameter q in Tsallis statistics and Levy distributions. *Phys. Rev. Lett.* **2000**, *84*, 2770. [CrossRef]
42. Wilk, G. Fluctuations, correlations and non-extensivity. *Braz. J. Phys.* **2007**, *37*, 714. [CrossRef]
43. Wilk, G.; Wlodarczyk, Z. Power laws in elementary and heavy-ion collisions. A story of fluctuations and nonextensivity? *EPJ A* **2009**, *40*, 299–312. [CrossRef]
44. Biro, T.S.; Neda, Z. Unidirectional random growth with resetting. *Physica A* **2018**, *499*, 335–361. [CrossRef]
45. Kaniadakis, G. Non-linear kinetics underlying generalized statistics. *Physica A* **2001**, *296*, 405. [CrossRef]
46. Kaniadakis, G. H-theorem and generalized entropies within the framework of nonlinear kinetics. *Phys. Lett. A* **2001**, *288*, 283. [CrossRef]
47. Kaniadakis, G. Relativistic entropy and related Boltzmann kinetics. *EPJ A* **2009**, *40*, 275–287. [CrossRef]
48. Biró, T.S.; Barnaföldi, G.G.; Ván, P. New entropy formula with fluctuating reservoir. *Phys. A* **2015**, *417*, 215–220. [CrossRef]

Article

Entropy Optimization, Generalized Logarithms, and Duality Relations

Angel R. Plastino [1], Constantino Tsallis [2,3,4,*], Roseli S. Wedemann [5] and Hans J. Haubold [6]

[1] CeBio y Departamento de Ciencias Básicas, Universidad Nacional del Noroeste de la Província de Buenos Aires, UNNOBA, CONICET, Roque Saenz Peña 456, Junin B6000, Argentina
[2] Centro Brasileiro de Pesquisas Físicas and National Institute of Science and Technology for Complex Systems, Rua Xavier Sigaud 150, Rio de Janeiro 22290-180, RJ, Brazil
[3] Santa Fe Institute, 1399 Hyde Park Road, Santa Fe, NM 87501, USA
[4] Complexity Science Hub Vienna, Josefstädter Straße 39, 1080 Vienna, Austria
[5] Instituto de Matemática e Estatística, Universidade do Estado do Rio de Janeiro, Rua São Francisco Xavier 524, Rio de Janeiro 20550-900, RJ, Brazil
[6] Office for Outer Space Affairs, United Nations, Vienna International Center, 1400 Vienna, Austria
[*] Correspondence: tsallis@cbpf.br

Abstract: Several generalizations or extensions of the Boltzmann–Gibbs thermostatistics, based on non-standard entropies, have been the focus of considerable research activity in recent years. Among these, the power-law, non-additive entropies $S_q \equiv k\frac{1-\sum_i p_i^q}{q-1}$ ($q \in \mathbb{R}$; $S_1 = S_{BG} \equiv -k\sum_i p_i \ln p_i$) have harvested the largest number of successful applications. The specific structural features of the S_q thermostatistics, therefore, are worthy of close scrutiny. In the present work, we analyze one of these features, according to which the q-logarithm function $\ln_q x \equiv \frac{x^{1-q}-1}{1-q}$ ($\ln_1 x = \ln x$) associated with the S_q entropy is linked, via a duality relation, to the q-exponential function characterizing the maximum-entropy probability distributions. We enquire into which entropic functionals lead to this or similar structures, and investigate the corresponding duality relations.

Keywords: generalized entropies; generalized logarithms; duality relations; entropy optimization; S_q entropies

PACS: 05.90.+m

1. Introduction

Extensions of the maximum entropy principle based on non-standard entropic functionals [1–4] have proven to be useful for the study of diverse problems in physics and elsewhere, particularly in connection with complex systems [5,6]. These lines of enquiry were greatly stimulated by research into a generalized thermostatistics advanced in the late 80s, in which the canonical probability distributions optimize the S_q power-law, non-additive entropies [7]. The S_q thermostatistics was successfully applied to the analysis of a wide range of systems and processes in physics, astronomy, biology, economics, and other fields [8–11]. Motivated by the work on the S_q entropies, researchers also explored the properties and possible applications of several other entropic measures, such as those introduced by Borges and Roditi [12], by Anteneodo and Plastino [13], by Kaniadakis [14], and by Obregón [15]. Recent reviews on these and other entropic forms can be found in [16,17]. These developments, in turn, led to the investigation of general properties of entropic variational principles, in order to elucidate which features are shared by large families of entropic forms, or are even universal, and, on the contrary, which features characterize specific entropies, such as the S_q ones. Several aspects of general entropic variational principles have been studied along those lines, including, for instance, the Legendre transform structure [18–20], the maximum entropy–minimum norm approach to inverse problems [21],

the implementation of dynamical thermostatting schemes [22,23], the interpretation of superstatistics in terms of entropic variational prescriptions [24], and the derivation of generalized maximum-entropy phase-space densities from Liouville dynamics [25].

Of all the thermostatistics associated with generalized entropic forms, the thermostatistics derived form the S_q entropies has been the most intensively studied and fruitfully applied one. The S_q-thermostatistics exhibits some intriguing structural similarities with the standard Boltzmann–Gibbs one. The aim of the present contribution is to explore one of these similarities, within the context of thermostatistical formalisms based on general entropic functionals. As is well known, the Boltzmann–Gibbs entropy S_{BG} of a normalized probability distribution can be expressed as minus the mean value of the logarithms of the probabilities. Or, alternatively, as the mean value of the logarithms of the inverse probabilities. On the other hand, the probability distribution that optimizes S_{BG} under the constraints imposed by normalization and by the energy mean value, has an exponential form, where the exponential is the inverse function of the above mentioned logarithm function. In a nutshell: the entropy is the mean value of a logarithm (evaluated on the inverse probabilities), while the maximum-entropy probabilities are given by an exponential function, which is the inverse function of the logarithm. This structure turns out to be nontrivial, and, up to a duality condition, is shared by the S_q-thermostatistics. Indeed, it is possible to define a q-logarithm function, and its inverse function, a q-exponential, both parameterized by the parameter q, such that the S_q entropy is the mean value of a q-logarithm (evaluated on the inverse probabilities), while the probability distribution optimizing S_q has a q-exponential form. The alluded duality condition, however, imposes that the value of the q-parameter associated with the aforementioned q-logarithm should not be the same as the value of the parameter associated with the q-exponential. Both q-values are connected via the duality relation $q \leftrightarrow 2 - q$, which is ubiquitous in the S_q-thermostatistics. In the present work, we shall explore which entropic measures generate similar structures, linking the entropic functional, regarded as the mean value of a generalized logarithm, with the form of the maximum-entropy distributions.

This paper is organized in the following way. In Section 2, we provide a brief review of the S_q-thermostatistical formalism, focusing on the q-logarithm duality relation. In Section 3, we explore which entropic functionals give rise to structures, and duality relations, similar to those characterizing the S_q-thermostatistics. More general scenarios are considered in Section 3. Finally, some conclusions are drawn in Section 4.

2. S_q Entropies, q-Logarithms, and q-Exponential Maximum-Entropy Probability Distributions

The S_q-thermostatistics is constructed on the basis of the non-additive, power-law entropy S_q [5] defined as

$$S_q = \frac{k}{1-q} \sum_{i=1}^{W} \left(p_i^q - p_i \right), \tag{1}$$

where $q \in \mathbb{R}$ is a parameter characterizing the degree of non-additivity exhibited by the entropy, k is a constant chosen once and for ever, determining the dimensions and the units in which the entropy is measured, and $\{p_i, \ i = 1, \ldots, W\}$ is an appropriately normalized probability distribution for a system admitting W microstates. In what follows, we shall assume that $k = 1$. The limit $q \to 1$ corresponds to the standard Boltzmann–Gibbs (BG) entropy, that is, $S_1 = S_{BG} = -k \sum_{i=1}^{W} p_i \ln p_i$. The power-law entropy S_q constitutes a distinguished and founding member of the club of generalized entropies, which is nowadays the focus of intensive research activity [3,4,16].

The q-logarithm function, given by

$$\ln_q(x) = \frac{x^{1-q} - 1}{1-q} \quad (x > 0; \ \ln_1 x = \ln x), \tag{2}$$

and its inverse function, the q-exponential

$$\exp_q(x) = \begin{cases} [1 + (1-q)x]^{\frac{1}{1-q}}, & \text{if } 1 + (1-q)x > 0, \\ 0, & \text{if } 1 + (1-q)x \le 0 \end{cases} \tag{3}$$

constitute essential ingredients of the S_q thermostatistical formalism. For the sake of completeness, it is worth mentioning that sometimes people use an alternative notation for the q-exponential, given by $\exp_q(x) = [1 + (1-q)x]_+^{\frac{1}{1-q}}$. The q-logarithm and the q-exponential functions arise naturally when one considers the constrained optimization of the entropy S_q [5,9]. Moreover, it is central to the q-thermostatistical theory that the S_q entropy itself can be expressed in terms of q-logarithms,

$$S_q = k \sum_{i=1}^{W} p_i \ln_q \left(\frac{1}{p_i} \right) = k \left\langle \ln_q \left(\frac{1}{p_i} \right) \right\rangle. \tag{4}$$

Note that, for $q \to 1$, the above equation reduces to the well-known one, $S_{BG} = k \sum_{i=1}^{W} p_i \ln \left(\frac{1}{p_i} \right)$.

The gist of the S_q thermostatistics is centered on the optimization of S_q under suitable constraints. The S_q entropic variational problem can be formulated using standard linear constraints or nonlinear constraints based on escort probability distributions [26,27]. When working with more general entropic functionals, it is not well understood what are the appropriate escort mean values to be used, and few or no concrete applications of escort mean values to particular problems have been developed. Consequently, in order to investigate and clarify the distinguishing features of the S_q formalism within the context of more general entropic formalisms, it is convenient to restrict our considerations to the optimization of the S_q entropy under linear constraints. The main instance of the S_q variational problem is the one yielding the generalized canonical probability distribution, which corresponds to the optimization of S_q under the constraints corresponding to normalization,

$$\sum_{i=1}^{W} p_i = 1, \tag{5}$$

and to mean energy. We assume that the ith microstate of the system under consideration, which has probability p_i, has energy ϵ_i. The mean energy is then

$$E = \sum_{i=1}^{W} p_i \epsilon_i. \tag{6}$$

Introducing the Lagrange multipliers α and β, corresponding to the constraints of normalization (5) and the mean energy (6), the optimization of S_q leads to the variational problem

$$\delta \left[S_q - \alpha \left(\sum_{i=1}^{W} p_i \right) - \beta E \right] = 0, \tag{7}$$

yielding

$$p_i^{q-1} = \frac{1}{q} \left[1 - (q-1)(\alpha + \beta \epsilon_i) \right]. \tag{8}$$

For later comparison with thermostatistical formalisms based on general entropic forms, it will prove convenient to recast the above equation as

$$p_i^{q-1} = 1 + (q-1) \left[\mathcal{A} - \mathcal{B}(\alpha + \beta \epsilon_i) \right], \tag{9}$$

with $\mathcal{A} = -1/q$ and $\mathcal{B} = 1/q$. At first glance, it might seem cumbersome to introduce the parameters $\mathcal{A}$ and $\mathcal{B}$, since, within the context of the S_q-thermostatistics, they are

simple functions of the entropic parameter q. The new parameters, however, will prove essential when exploring the duality properties exhibited by thermostatitsical formalisms based on other generalized entropies, and when comparing those properties with the ones corresponding to the S_q entropy. In those scenarios, the parameters $\mathcal{A}$ and $\mathcal{B}$ have other values, depending on the parameterized form of the relevant entropic functionals. Using the $\mathcal{A}$ and $\mathcal{B}$ parameters, the maximum S_q entropy probability distribution can be expressed in terms of a q-exponential, as follows:

$$p_i = \exp_{\tilde{q}}[\mathcal{A} - \mathcal{B}(\alpha + \beta \epsilon_i)] = \ln_{\tilde{q}}^{(-1)}[\mathcal{A} - \mathcal{B}(\alpha + \beta \epsilon_i)], \qquad (10)$$

where

$$\tilde{q} = 2 - q. \qquad (11)$$

Comparing now the Equation (4) for the entropy, with the Equation (10) for the probabilities optimizing the entropy, we see that the S_q entropy can be expressed in terms of a q-logarithm function, while the optimal probabilities are given by an inverse q-logarithm function (that is, by a q-exponential function). However, the value of the q-parameter that appears in the first q-logarithm, associated with the entropy, does not coincide with the one, denoted by $\tilde{q}$, that appears in the inverse q-logarithm defining the optimal probabilities. This pair of q-values satisfy the duality relation (11). It is important to emphasize that the duality relation (11) has the property

$$\tilde{\tilde{q}} = q. \qquad (12)$$

In other words, the dual of the dual of q is equal to q itself. Note also that, in the Boltzmann–Gibbs limit, $q \to 1$, the duality relation reduces to $\tilde{q} = q = 1$. The Boltzmann–Gibbs thermostatistics, regarded as a particular member of the S_q-thermostatistical family, is self-dual. The duality relation (12) between the values of the q-parameters characterizing two q-logarithm functions, can be reformulated as a duality relation between the q-logarithms themselves. Indeed, one has that

$$\ln_{\tilde{q}}(x) = -\ln_q\left(\frac{1}{x}\right). \qquad (13)$$

For $q \to 1$, the self-dual condition $q = \tilde{q} = 1$ is obtained, and the relation (13) reduces to the well-known property of the standard logarithm, $\ln(x) = -\ln(1/x)$.

3. Generalized Entropies and Logarithms

Now, we shall consider a generic trace-form entropy S_G. It can always be written in the form

$$S_G = \sum_{i=1}^{W} p_i \ln_G\left(\frac{1}{p_i}\right), \qquad (14)$$

expressed in terms of an appropriate generalized logarithm function $\ln_G(x)$. The specific form of the generalized logarithmic function $\ln_G(x)$ depends on which particular thermostatistical formalism one is considering. For example, in the case of the S_q-based thermostatistics, $\ln_G(x)$ is given by the generalized logarithm $\ln_q(x)$. Note that the subindex "G" stands for "generalized", and it does not represent a numerical parameter. In order to lead to a sensible entropy, the function $\ln_G(x)$ has to be continuous and two-times differentiable, has to comply with $(x \ln_G(1/x)) > 0$ for $0 < x < 1$ and $\lim_{x \to 0}(x \ln_G(1/x)) = \lim_{x \to 1}(x \ln_G(1/x)) = 0$, and has to satisfy the concavity requirement given by $\frac{d^2}{dx^2}\left[x \ln_G\left(\frac{1}{x}\right)\right] < 0$.

One can optimize the entropic measure (14) under the constraints imposed by normalization (5) and by the energy mean value (6). The corresponding variational problem reads

$$\delta\left[S_G - \alpha\left(\sum_{i=1}^{W} p_i\right) - \beta E\right] = 0,$$

(15)

where α and β are the Lagrange multipliers corresponding to the normalization and the mean energy constraints. The solution to the variational problem is given by a probability distribution complying with the equations

$$\frac{1}{p_i}\ln'_G\left(\frac{1}{p_i}\right) - \ln_G\left(\frac{1}{p_i}\right) = -\alpha - \beta\epsilon_i, \quad (i = 1, \ldots, W),$$

(16)

where $\ln'_G(x) = \frac{d}{dx}\ln_G(x)$.

Equation (16) arises from a generic entropy optimization problem. Basically, the optimization of any trace form entropy leads to an equation of the form (16). Here, we want to consider a particular family of entropies, leading to maximum entropy distributions satisfying a special symmetry requirement. We want the maximum entropy distribution p_i to be of the form

$$p_i = \ln_{\tilde{G}}^{(-1)}(\xi_i),$$

(17)

where $\xi_i = \mathcal{A} + \mathcal{B}(-\alpha - \beta\epsilon_i)$, with $\mathcal{A}$ and $\mathcal{B}$ appropriate constants ($\mathcal{B} > 0$), and $\ln_{\tilde{G}}^{(-1)}$ is the inverse of a generalized logarithmic function $\ln_{\tilde{G}}(x)$, related to $\ln_G(x)$ through a *duality relationship*. A few clarifying remarks are now in order. First, ξ_i is, up to the additive and multiplicative constants $\mathcal{A}$ and $\mathcal{B}$, equal to the right-hand side of (16). Second, the constants A and B depend only on the form of the entropy (14), and not on any details of the system under consideration, such as the number of microstates W, the values of the microstates' energies ϵ_i, or the values of the Lagrange multipliers α and β. Last, the duality relation connecting the functions $\ln_G(x)$ and $\ln_{\tilde{G}}(x)$ is such that the dual of the dual is equal to the original function, that is

$$\ln_{\tilde{\tilde{G}}}(x) = \ln_G(x).$$

(18)

Combining Equations (16) and (17), one obtains

$$\frac{1}{p_i}\ln'_G\left(\frac{1}{p_i}\right) - \ln_G\left(\frac{1}{p_i}\right) = \frac{1}{\mathcal{B}}\left(\ln_{\tilde{G}}(p_i) - \mathcal{A}\right).$$

(19)

Introducing the constants $A = -\mathcal{A}/\mathcal{B}$ and $B = 1/\mathcal{B}$, the above equation can be cast in the more convenient form

$$\frac{1}{p_i}\ln'_G\left(\frac{1}{p_i}\right) - \ln_G\left(\frac{1}{p_i}\right) = A + B\ln_{\tilde{G}}(p_i).$$

(20)

For a given duality relation $\ln_G(x) \rightarrow \ln_{\tilde{G}}(x)$, and given values of the parameters A and B, Equation (20) can be regarded as a differential equation that has to be obeyed by the generalized logarithmic function $\ln_G(x)$. For solving the differential equation, one needs an initial condition, given by the value $\ln_G(x_0)$ adopted by the generalized logarithm at some particular point x_0. We shall assume, as an initial condition, that $\ln_G(1) = 0$.

Different forms of the duality relation $\ln_G(x) \rightarrow \ln_{\tilde{G}}(x)$ are compatible with different forms of the generalized logarithm, and with different forms of the generalized entropy. In what follows, we shall explore some instances of duality relations, in order to determine which entropic forms are compatible with them.

3.1. The Duality Condition Satisfied by the S_q Thermostatistics

Motivated by the S_q-based thermostatistics, we shall first adopt the duality condition

$$\ln_{\tilde{G}}(x) = -\ln_G(1/x), \tag{21}$$

which is precisely the relation (13) satisfied by the S_q-thermostatistics. Equation (20) then becomes

$$\frac{1}{p_i} \ln'_G \left(\frac{1}{p_i} \right) - \ln_G \left(\frac{1}{p_i} \right) = A - B \ln_G \left(\frac{1}{p_i} \right). \tag{22}$$

Therefore, in order to find the form of $\ln_G(x)$, we have to solve the differential equation

$$\ln'_G(x) = \frac{1}{x} \left[A + (1 - B) \ln_G(x) \right], \tag{23}$$

with the initial condition $\ln_G(1) = 0$. The (unique) solution of Equation (23) is then

$$\ln_G(x) = A \left(\frac{x^{1-B} - 1}{1 - B} \right). \tag{24}$$

We see that, up to the multiplicative constant A, the only generalized logarithmic function leading to an entropy optimization scheme compatible with the duality condition (21) is the q-logarithm

$$\ln_q(x) = \frac{x^{1-q} - 1}{1 - q}. \tag{25}$$

The parameter B appearing in (22) coincides with the parameter q of the S_q-thermostatistics.

3.2. The Simplest Duality Relation

We shall now consider the simplest possible duality relation, which is

$$\ln_{\tilde{G}}(x) = \ln_G(x). \tag{26}$$

In spite of its simplicity, this duality relation is worthy of consideration, because *it includes the standard logarithm (and the corresponding Boltzmann–Gibbs scenario) as a particular case*. It is interesting, therefore, to explore which entropic forms are compatible with the simplest conceivable condition (26), even if this exploration is not a priori motivated by a generalized entropy of known physical relevance.

Combining the general Equation (20) with the duality relation (26), one obtains

$$\frac{1}{p_i} \ln'_G \left(\frac{1}{p_i} \right) - \ln_G \left(\frac{1}{p_i} \right) = A + B \ln_G(p_i). \tag{27}$$

Then, we have to solve the ordinary differential equation

$$\frac{1}{x} \ln'_G \left(\frac{1}{x} \right) - \ln_G \left(\frac{1}{x} \right) = A + B \ln_G(x), \tag{28}$$

or, equivalently,

$$\frac{d \ln_G}{dx} = \frac{1}{x} \left[\ln_G(x) + A + B \ln_G \left(\frac{1}{x} \right) \right], \tag{29}$$

with the condition $\ln_G(1) = 0$. At first sight, Equation (29) may look like a standard ordinary differential equation. It has, however, the peculiarity that in the right-hand side of (29), the unknown function $\ln_G$ is evaluated at two different values of its argument: x and $1/x$. This situation is similar to the one that occurs, for instance, with differential equations describing dynamical systems with delay. In the case of (29), this difficulty can

be removed by recasting the equation as a pair of coupled ordinary differential equations. Let us introduce the functions

$$
\begin{aligned}
F(x) &= \ln_G(x), \\
G(x) &= \ln_G(1/x).
\end{aligned}
\tag{30}
$$

The differential Equation (28) can be reformulated as the two coupled differential equations

$$
\begin{aligned}
\frac{dF}{dx} &= \frac{1}{x}\Big[F(x) + B\,G(x) + A\Big], \\
\frac{dG}{dx} &= -\frac{1}{x}\Big[G(x) + B\,F(x) + A\Big],
\end{aligned}
\tag{31}
$$

with the conditions $F(1) = G(1) = 0$. To find a solution for (31), we propose the ansatz

$$
\begin{aligned}
F(x) &= c_1 x^{\gamma_1} + c_2 x^{\gamma_2} + c_3, \\
G(x) &= c_1 x^{-\gamma_1} + c_2 x^{-\gamma_2} + c_3.
\end{aligned}
\tag{32}
$$

If one inserts the ansatz (32) into the differential Equations (31), one can verify that (32) constitutes a solution, provided that

$$
\begin{aligned}
\gamma_1 &= -\gamma_2 \geq 0, \\
c_1/c_2 &= -\frac{1}{B}\Big(1 + \sqrt{1 - B^2}\Big), \quad 0 \leq B^2 \leq 1, \\
c_3 &= -A/(1 + B),
\end{aligned}
\tag{33}
$$

and

$$
\gamma = \sqrt{1 - B^2},
\tag{34}
$$

where $\gamma = \gamma_1 = -\gamma_2$. It follows from (33) and (34) that $0 \leq \gamma \leq 1$, and that

$$
c_2 = -\sqrt{\frac{1-\gamma}{1+\gamma}}\,c_1.
\tag{35}
$$

The relations (33)–(35), together with the initial conditions $F(1) = G(1) = 0$, lead to

$$
F(x) = \frac{A}{1+B}\left(\frac{\sqrt{1+\gamma}\,x^{\gamma} - \sqrt{1-\gamma}\,x^{-\gamma}}{\sqrt{1+\gamma} - \sqrt{1-\gamma}} - 1\right),
\tag{36}
$$

and

$$
G(x) = \frac{A}{1+B}\left(\frac{\sqrt{1+\gamma}\,x^{-\gamma} - \sqrt{1-\gamma}\,x^{\gamma}}{\sqrt{1+\gamma} - \sqrt{1-\gamma}} - 1\right).
\tag{37}
$$

The solution to the system of differential Equations (31) is completely determined by the conditions $F(1) = G(1) = 0$. Therefore, given these conditions, and for $0 \leq B \leq 1$, the solution (36) and (37) is unique. Now, the entropy S_γ compatible with the duality relation (26) is $S_\gamma = \sum_i p_i \ln_G(\frac{1}{p_i})$, with $\ln_G(x) = F(x)$. Therefore, for $0 \leq B \leq 1$, one has

$$
S_\gamma = \frac{A}{1+B}\sum_i\left(\frac{\sqrt{1+\gamma}\,p_i^{1-\gamma} - \sqrt{1-\gamma}\,p_i^{1+\gamma}}{\sqrt{1+\gamma} - \sqrt{1-\gamma}} - p_i\right),
\tag{38}
$$

which, after some algebra, can be recast in the more convenient form

$$
S_\gamma = \frac{A}{2}\left(\frac{\sqrt{1+\gamma} + \sqrt{1-\gamma}}{1 + \sqrt{1-\gamma^2}}\right)\sum_i\left[\sqrt{1+\gamma}\left(\frac{p_i^{1-\gamma} - p_i}{\gamma}\right) + \sqrt{1-\gamma}\left(\frac{p_i^{1+\gamma} - p_i}{-\gamma}\right)\right].
\tag{39}
$$

Introducing now the parameters $q = 1 - \gamma$, $(0 \le q \le 1)$ and $q^* = 1 + \gamma = 2 - q$, $(1 \le q^* \le 2)$, the entropy (39) can be expressed as a linear combination of two S_q entropies,

$$S_\gamma = \mathcal{K} \left(\sqrt{q^*}\, S_q + \sqrt{q}\, S_{q^*} \right), \tag{40}$$

where

$$\mathcal{K} = \frac{A}{2} \left(\frac{\sqrt{q} + \sqrt{q^*}}{1 + \sqrt{q\, q^*}} \right). \tag{41}$$

In the limit $B \to 1$, which corresponds to $\gamma \to 0$, $q \to 1$, and $q^* \to 1$, the generalized entropy (40) is, up to a multiplicative constant, equal to the Boltzmann–Gibbs entropy S_{BG}.

3.3. More General Duality Relations

It is possible to consider duality relations more general than the ones discussed previously. One can consider scenarios where the relation between a generalized logarithm and its dual is defined in terms of a pair of functions $h_{1,2}(x)$, as

$$\ln_{\tilde{G}}(x) = h_1(\ln_G(h_2(x))), \tag{42}$$

where the functions $h_{1,2}(x)$ satisfy

$$h_1(h_1(x)) = x, \quad \text{and} \quad h_2(h_2(x)) = x. \tag{43}$$

For example, the duality relation associated with the S_q entropy corresponds to $h_1(x) = -x$ and $h_2(x) = 1/x$, while the duality relation associated with the entropy S_γ corresponds to $h_1(x) = h_2(x) = x$.

Other duality relations can be constructed, for instance, in terms of the Moebius transformations

$$M(x) = \frac{m_1 x + m_2}{m_3 x + m_4}, \tag{44}$$

with $m_1 m_4 - m_2 m_3 \ne 0$. The inverse of (44) is

$$M^{(-1)}(x) = \frac{m_4 x - m_2}{-m_3 x + m_1}. \tag{45}$$

Moebius transformations that are self-inverse (that is, transformations coinciding with their own inverse: $M(x) = M^{(-1)}(x)$) are candidates for the functions $h_{1,2}(x)$ from which possible duality relations for generalized logarithmic functions can be constructed. Examples of self-inverse Moebius transformations are those of the form

$$M(x) = \frac{m_1 x + m_2}{m_3 x - m_1}, \tag{46}$$

which have $m_4 = -m_1$. Notice that, for $m_1 \ne 0$, the above form of $M(x)$ depends on only two parameters, as follows: $M(x) = \frac{x + (m_2/m_1)}{(m_3/m_1)x - 1}$. Another self-inverse Moebius transformation, not included in the family (46), is the identity function, $M(x) = x$, corresponding to $m_1 = m_4 \ne 0$ and $m_2 = m_3 = 0$ (see also [28]). The duality relations corresponding to the entropic measures S_q and S_γ are both constructed in terms of particular instances of Moebius transformations. The duality relation associated with the entropy S_q is constructed with $h_1(x) = -x$ and $h_2(x) = 1/x$, which are the self-inverse Moebious transformation corresponding, respectively, to $m_1 = 1$, $m_4 = -1$, and $m_2 = m_3 = 0$, and to $m_1 = m_4 = 0$ and $m_2 = m_3 = 1$. The duality relation for the entropy S_γ is constructed with $h_1(x) = h_2(x) = x$, which correspond to $m_1 = m_4 = 1$ and $m_2 = m_3 = 0$.

A generalized logarithmic function $\ln_G(x)$ defining a trace-form entropy (14), for which the associated entropic optimization principle leads to the duality relation (42), must satisfy the differential equation

$$
\begin{aligned}
\frac{1}{x} \ln'_G\left(\frac{1}{x}\right) - \ln_G\left(\frac{1}{x}\right) &= A + B \ln_{\tilde{G}}(x) \\
&= A + B h_1(\ln_G(h_2(x))),
\end{aligned}
\tag{47}
$$

with the condition $\ln_G(1) = 0$. For expression (14) to represent a sensible (i.e., concave) entropy, the generalized logarithm satisfying (47) has to comply with the requirement

$$
\frac{d^2}{dx^2}\left[x \ln_G\left(\frac{1}{x}\right)\right] = -B \frac{d}{dx}\left[h_1(\ln_G(h_2(x)))\right] < 0.
\tag{48}
$$

For duality relations more general than the two ones already analyzed by us in detail (corresponding to the entropies S_q and S_γ), the associated differential Equation (47) has, presumably, to be treated numerically.

3.4. Duality Relations: The Inverse Problem

One can also consider the following inverse problem. Given a parameterized family of non-negative, monotonically increasing functions $J(x; \lambda)$, depending on one or more parameters (that we collectively denote by λ), find out if the inverse function $J^{(-1)}(x; \lambda)$ is related to a generalized logarithmic function defining a sensible entropy (14), and satisfying a duality relation (42) defined in terms of appropriate functions $h_{1,2}(x)$. The problem is the following: for the inverse function $J^{(-1)}(x; \lambda)$, determine if suitable functions $h_{1,2}(x)$ exist, and identify them. We assume that the integral

$$
\mathcal{I} = \int_0^1 J^{(-1)}(x'; \lambda) \, dx',
\tag{49}
$$

converges.

In order to formulate this inverse problem, we consider a thermostatistical formalism, based on a generalized entropy, which yields optimizing-entropy canonical probability distributions of the form

$$
p_i = J(\xi_i; \lambda),
\tag{50}
$$

where $\xi_i = \mathcal{A} + \mathcal{B}(-\alpha - \beta \epsilon_i)$. In the latter expression, α and β are, as usual, the Lagrange multipliers associated with normalization of mean energy, and $\mathcal{A}$ and $\mathcal{B}$ are constants, possibly depending on the parameters λ characterizing the function $J(x; \lambda)$.

The associated entropy S_J can be expressed as

$$
S_J = \sum_i \mathcal{C}(p_i),
\tag{51}
$$

where the function $\mathcal{C}(x)$ is defined as the integral

$$
\mathcal{C}(x) = \int_x^1 \left[J^{(-1)}(x'; \lambda) - \mathcal{I}\right] dx'.
\tag{52}
$$

The function $\mathcal{C}(x)$ satisfies the following properties,

$$
\begin{aligned}
\mathcal{C}(x) &> 0, \quad \text{for } 0 < x < 1, \\
\mathcal{C}(0) &= \mathcal{C}(1) = 0, \\
d\mathcal{C}/dx &= \mathcal{I} - J^{(-1)}(x; \lambda), \\
d^2\mathcal{C}/dx^2 &= -dJ^{(-1)}(x; \lambda)/dx < 0,
\end{aligned}
\tag{53}
$$

which guarantee that S_J, defined by (51), is a sensible entropy. For $J(x) = \exp(x)$, one has $J^{(-1)}(x) = \ln(x)$, $\mathcal{I} = -1$, $\mathcal{C}(x) = -x \ln(x)$, and S_J coincides with the Boltzmann–

Gibbs entropy. If we compare the expression (51) for S_J with the expression (14) for a generalized entropy in terms of a generalized logarithm, we find that the generalized logarithm associated with S_J is

$$\ln_G^{(J)}\left(\frac{1}{x}\right) = \frac{1}{x}\int_x^1 \left[J^{(-1)}(x';\lambda) - \mathcal{I}\right]dx',$$ (54)

or, equivalently,

$$\ln_G^{(J)}(x) = x\int_{x^{-1}}^1 \left[J^{(-1)}(x';\lambda) - \mathcal{I}\right]dx'.$$ (55)

On the other hand, if we compare the form (17) for a generalized canonical distribution, with the form (50) corresponding to the function S_J, we obtain

$$\ln_{\tilde{G}}^{(J)}(x) = J^{(-1)}(x;\lambda).$$ (56)

The present inverse problem consists of determining what type of duality relation, if any, exists between the functions (55) and (56). It seems that this is a difficult problem, which has to be tackled in a case-by-case way. As an intriguing example of this inverse problem, we can consider the one posed by probability distributions related to the Mittag-Leffler function $E_{a,b}(x)$ (see [29] and references therein). The Mittag-Leffler function is given, for a general complex argument z, by the power series expansion

$$E_{a,b}(z) = \sum_{k=0}^{\infty}\frac{z^k}{\Gamma(b+ak)}, \quad a,b \in C, \ \Re(a) > 0, \ \Re(b) > 0, \ z \in C,$$ (57)

with $E_a(z) \equiv E_{a,1}(z)$. Notice that, in the literature [29], the two parameters a and b characterizing the Mittag-Leffler function are sometimes referred to as α and β.

The Mittag-Leffler function has several applications in physics and other fields. In particular, it plays a distinguished role in the study of non-standard diffusion processes involving fractional calculus operators [29]. In the present context, we consider only real values of the parameters (a,b) and real arguments. A few examples of the Mittag-Leffler function, and of its inverses, are respectively depicted in Figures 1 and 2, for $b = 1$ and different values of the parameter a.
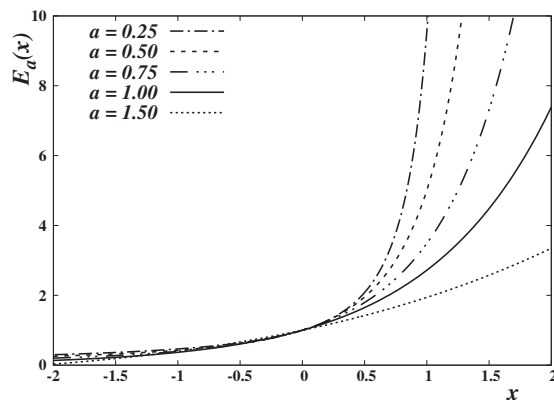
Figure 1. Plot of the Mittag-Leffler function $E_{a,b}(x)$, for $b = 1$ and illustrative values of the parameter a; $E_{1,1}(x) = e^x$.
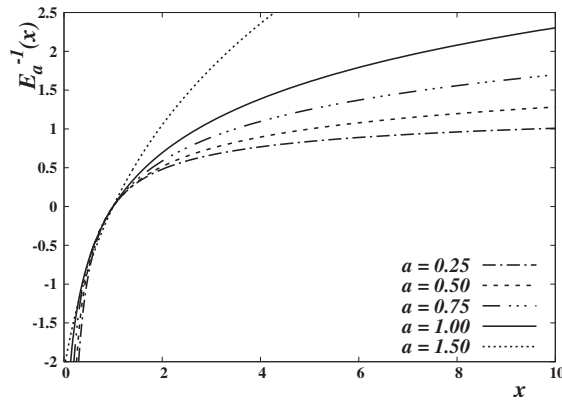
Figure 2. Plot of the inverse Mittag-Leffler function, $E_{a,b}^{(-1)}(x)$, for $b = 1$ and specific values of the parameter a; $E_{1,1}^{(-1)}(x) = \ln x$.

In the context of a Mittag-Leffler-based thermostatistical formalism, some possible choices for the function $J(x;\lambda)$ would be

$$
\begin{aligned}
J(x;\lambda) &= E_{a,b}(x), \quad \text{or,} \\
J(x;\lambda) &= E_{a,b}(x^2),
\end{aligned}
\tag{58}
$$

where $\lambda = (a,b)$ is the set of parameters characterizing the Mittag-Leffler function. For each of these choices, provided that the values of the parameters λ are such that the appropriate conditions are fulfilled, it is possible to explore the existence of functions $h_{1,2}$ for which the Mittag-Leffler-related generalized logarithms, (55) and (56), satisfy a differential equation of the form (47). For $J(x;\lambda) = E_{a,1}(x) = E_a(x)$, the corresponding generalized entropy (51) is defined in terms of the function $\mathcal{C}(x)$, given by (52). A few examples of $\mathcal{C}(x)$, which we obtained by numerically solving the integrals (49) and (52) for particular values of the parameter a, are plotted in Figure 3.
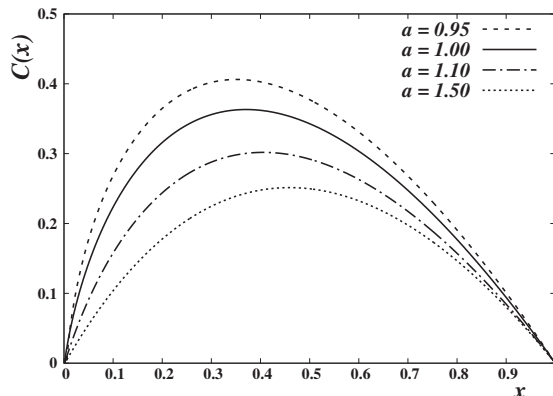
Figure 3. Plot of the function $\mathcal{C}(x)$ corresponding to $J(x) = E_a(x)$, for different values of the parameter a. The function $\mathcal{C}(x)$ appears in the definition of a trace-form entropic measure (51), and is given by Equation (52). For $a = 1$, one has $E_1(x) = \exp(x)$ and $C(x) = -x \ln x$.

4. Conclusions

Several generalizations or extensions of the notion of entropy have been advanced and enthusiastically investigated in recent years. The associated entropic optimization problems seem to provide valuable tools for the study of diverse problems in physics and

other fields, particularly when applied to the analysis of complex systems. Among the growing number of entropic forms that have been advanced, the non-additive, power-law S_q entropies exhibit the largest number of successful applications. It is clear by now, however, that the S_q entropies are not universal: some systems or processes seem to be described by entropic forms not belonging to the S_q family. Given this state of affairs, it is imperative to investigate in detail the properties of the various entropies, and of the associated thermostatistics, in order to elucidate and clarify the deep reasons that make them suitable for treating specific problems. In particular, the structural features of the S_q thermostatistics are certainly worthy of close scrutiny. In the present work, we investigated one of these features, according to which the q-exponential function describing the maximum-entropy probability distributions are linked, via a duality relation, with the q-logarithm function in terms of which the S_q entropy itself can be defined. We investigated which entropic functionals lead to this kind of structure and explored the corresponding duality relations.

The main take-home message of the present work is that there is a close connection between the aforementioned duality relations, and the forms of the entropic measures. The S_q thermostatistics exhibits a particular duality connection, which, in the limit of the Boltzmann–Gibbs thermostatistics, reduces to a self-duality. We proved that there is no other entropic functional satisfying the duality relation associated with S_q, namely, Equation (21). This constitutes what may be regarded as a brand new uniqueness theorem leading to S_q, in addition to those already existing, such as the Enciso–Tempesta theorem [30] and those indicated therein. Assuming other types of duality relation, it is possible to formulate differential equations that lead to new entropic measures complying with the assumed duality. We studied in detail a duality relation leading to a differential equation that admits closed analytical solutions, and corresponds to a new generalized entropy, which we denoted by S_γ. The duality relations characterizing the entropies S_q and S_γ seem to be exceptional, in that the concomitant differential equations can be solved analytically. In many other cases, the differential equations resulting from duality relations have to be treated numerically. The investigation of these equations, associated with thermostatistical scenarios different from, or more general than, those based on the entropies S_q and S_γ, would certainly be worthwhile. It would also be valuable to identify new duality relations admitting an analytical treatment. The exploration of the ensuing thermostatistical scenarios may suggest interesting new applications of generalized entropies. Another promising direction for future research is to extend the present study to scenarios involving non-trace-form entropies [31], or involving escort mean values [27,32]. We would be delighted to see further advances along these or related lines.

Author Contributions: A.R.P., C.T., R.S.W., H.J.H. contributed equally to this paper. All authors have read and agreed to the published version of the manuscript.

Conflicts of Interest: The authors declare no conflict of interest.

References

1. Tsallis, C. Entropy. *Encyclopedia* **2022**, *2*, 264–300. [CrossRef]
2. Jizba, P.; Korbel, J. Maximum entropy principle in statistical inference: Case for non-Shannonian entropies. *Phys. Rev. Lett.* **2019**, *122*, 120601. [CrossRef]
3. Naudts, J. *Generalised Thermostatistics*; Springer: London, UK, 2011.
4. Beck, C. Generalised information and entropy measures in physics. *Contemp. Phys.* **2009**, *50*, 495–510. [CrossRef]
5. Tsallis, C. *Introduction to Nonextensive Statistical Mechanics—Approaching a Complex World*; Springer: New York, NY, USA, 2009.

6. Hanel, R.; Thurner, S. A comprehensive classification of complex statistical systems and an axiomatic derivation of their entropy and distribution functions. *EPL* **2011**, *93*, 20006 . [CrossRef]

7. Tsallis, C. Possible generalization of Boltzmann-Gibbs statistics. *J. Stat. Phys.* **1988**, *52*, 479–487. [CrossRef]

8. Gell-Mann, M.; Tsallis, C. *Nonextensive Entropy: Interdisciplinary Applications*; Oxford University Press: Oxford, UK, 2004.

9. Tsallis, C. The nonadditive entropy S_q and its applications in physics and elsewhere: Some remarks. *Entropy* **2011**, *13*, 1765–1804. [CrossRef]

10. Tsallis, C. Beyond Boltzmann-Gibbs-Shannon in physics and elsewhere. *Entropy* **2019**, *21*, 696 [CrossRef] [PubMed]

11. Sánchez Almeida, J. The principle of maximum entropy and the distribution of mass in galaxies. *Universe* **2022** *8*, 214. [CrossRef]

12. Borges, E.P.; Roditi, I. A family of nonextensive entropies. *Phys. Lett. A* **1998**, *246*, 399–402. [CrossRef]

13. Anteneodo, C.; Plastino, A.R. Maximum entropy approach to stretched exponential probability distributions. *J. Phys. A Math. Gen.* **1999**, *32*, 1089–1097. [CrossRef]

14. Kaniadakis, G. Statistical mechanics in the context of special relativity. *Phys. Rev. E* **2002**, *66*, 056125. [CrossRef] [PubMed]

15. Obregón, O. Superstatistics and gravitation. *Entropy* **2010**, *12*, 2067–2076. [CrossRef]

16. Amigó, J.M.; Balogh, S.G.; Hernández S. A brief review of generalized entropies. *Entropy* **2018**, *20*, 813. [CrossRef] [PubMed]

17. Ilic, V.M.; Korbel, J.; Gupta, S.; Scarfone, A.M. An overview of generalized entropic forms. *EPL* **2021**, *133*, 50005. [CrossRef]

18. Plastino, A.; Plastino, A.R. On the universality of thermodynamics' Legendre transform structure. *Phys. Lett. A* **1997**, *226*, 257–263. [CrossRef]

19. Mendes, R.S. Some general relations in arbitrary thermostatistics. *Physical A* **1997**, *242*, 299–308. [CrossRef]

20. Curado, E.M.F. General aspects of the thermodynamical formalism. *Braz. Journ. Phys.* **1999**, *29*, 36–45. [CrossRef]

21. Plastino, A.R.; Miller, H.G.; Plastino, A.; Yen G.D. The role of information measures in the determination of the maximum entropy-minimum norm solution of the generalized inverse problem. *J. Math. Phys* **1997** *38*, 6675–6682. [CrossRef]

22. Roston, G.B.; Plastino, A.R.; Casas, M.; Plastino, A.; Da Silva, L.R. Dynamical thermostatting and statistical ensembles. *Eur. Phys. J. B* **2005**, *48*, 87–93. [CrossRef]

23. Plastino, A.R.; Anteneodo C. A dynamical thermostatting approach to nonextensive canonical ensembles. *Ann. Phys.* **1997** *255*, 250–269. [CrossRef]

24. Tsallis, C.; Souza, A.M.C. Constructing a statistical mechanics for Beck-Cohen superstatistics. *Phys. Rev. E* **2003**, *67*, 026106. [CrossRef] [PubMed]

25. Saadatmand, S.N.; Gould, T.; Cavalcanti, E.G.; Vaccaro, J.A. Thermodynamics from first principles: Correlations and nonextensivity. *Phys. Rev. E* **2020**, *101*, 060101. [CrossRef] [PubMed]

26. Curado, E.M.F.; Tsallis, C. Generalized statistical mechanics: Connection with thermodynamics. *J. Phys. A* **1991**, *24*, L69. [CrossRef]

27. Tsallis, C.; Mendes, R.S.; Plastino, A.R. The role of constraints within generalized nonextensive statistics. *Phys. A* **1998**, *261*, 534–554. [CrossRef]

28. Gazeau, J.P.; Tsallis, C. Moebius transforms, cycles and q-triplets in statistical mechanics. *Entropy* **2019**, *21*, 1155. [CrossRef]

29. Haubold, H.J.; Mathai, A.M.; Saxena, R.K. Mittag-Leffler Functions and Their Applications. *J. Appl. Math.* **2011**, *2011*, 298628. [CrossRef]

30. Enciso, A.; Tempesta, P. Uniqueness and characterization theorems for generalized entropies. *J. Stat. Mech.* **2017**, *2017*, 123101. [CrossRef]

31. Tempesta, P.; Jensen, H.J. Universality classes and information-theoretic measures of complexity via group entropies. *Sci. Rep.* **2020**, *10*, 1–11. [CrossRef] [PubMed]

32. Furuichi, S. On the maximum entropy principle and the minimization of the Fisher information in Tsallis statistics. *J. Math. Phys.* **2009**, *50*, 013303. [CrossRef]

Article

Information Shift Dynamics Described by Tsallis $q = 3$ Entropy on a Compact Phase Space

Jin Yan [1] and Christian Beck [2,3,*]

[1] Max Planck Institute for the Physics of Complex Systems, 01187 Dresden, Germany
[2] School of Mathematical Sciences, Queen Mary University of London, London E1 4NS, UK
[3] The Alan Turing Institute, London NW1 2DB, UK
[*] Correspondence: c.beck@qmul.ac.uk

Abstract: Recent mathematical investigations have shown that under very general conditions, exponential mixing implies the Bernoulli property. As a concrete example of statistical mechanics that are exponentially mixing we consider the Bernoulli shift dynamics by Chebyshev maps of arbitrary order $N \geq 2$, which maximizes Tsallis $q = 3$ entropy rather than the ordinary $q = 1$ Boltzmann-Gibbs entropy. Such an information shift dynamics may be relevant in a pre-universe before ordinary space-time is created. We discuss symmetry properties of the coupled Chebyshev systems, which are different for even and odd N. We show that the value of the fine structure constant $\alpha_{el} = 1/137$ is distinguished as a coupling constant in this context, leading to uncorrelated behaviour in the spatial direction of the corresponding coupled map lattice for $N = 3$.

Keywords: information shift; Tsallis entropy; Chebyshev maps; fine structure constant

1. Introduction

The foundations of statistical mechanics are a subject of continuing theoretical interest. It is far from obvious that a given deterministic dynamics can ultimately be described by a statistical mechanics formalism. The introduction of generalized entropies (such as, for example, the non-additive Tsallis entropies [1–3]) leads to a further extension of the formalism relevant for systems with long-range interactions, or with a fractal or compactified phase space structure, or with non-equilibrium steady states exhibiting fluctuations of temperature or of effective diffusion constants [4,5]. Generalized entropies have been shown to have applications for a variety of complex systems, for example, in high energy physics [6–10] or for turbulent systems [11–13]. In this paper we go back to the basics and explore the properties of a particular statistical mechanics, namely that of an information shift dynamics described by Tsallis entropies with the entropic index $q = 3$ on a compact phase space.

Our work is inspired by recent mathematical work [14] that shows that the exponential mixing property automatically implies the Bernoulli property, under very general circumstances. This theorem is of utmost interest for the foundations of statistical mechanics. Namely, by definition the systems we are interested in when dealing with statistical mechanics relax to an equilibrium fairly quickly (under normal circumstances). That is to say, we have the exponential mixing property. However, this then implies that somewhere (on a suitable subset of the phase space) there must exist a Bernoulli shift dynamics in suitable coordinates.

We will work out one of the simplest example systems that is consistent with a generalized statistical mechanics formalism, and at the same time is exponentially mixing and ultimately conjugated to a Bernoulli shift. These are discrete-time dynamical systems on the interval $[-1, 1]$ as generated by N-th order Chebyshev maps T_N [15–18]. Chebyshev maps are exponentially mixing and are conjugated to a Bernoulli shift of N symbols. We will review and investigate their properties in detail in the following sections. It is needless to

say that Chebyshev maps do not live in ordinary physical space but just on a compactified space, the interval $[-1, 1]$. The simplest examples are given by the $N = 2$ and $N = 3$ cases, i.e., $T_2(x) = 2x^2 - 1$ and $T_3(x) = 4x^3 - 3x$. Despite their simplicity, a statistical mechanics formalism can be constructed as an effective description (see also Refs. [19,20]). In contrast to ordinary statistical mechanics (described by states where the $q = 1$ Boltzmann–Gibbs–Shannon entropy has a maximum subject to constraints), in our case the relevant entropy is the $q = 3$ Tsallis entropy S_q. This leads to interesting properties. Our physical interpretation is that the above information shift dynamics may be relevant in a pre-universe, i.e., in an extremely early stage of the universe where ordinary space-time has not yet formed. The dynamics evolves in a fictitious time coordinate (different from physical time) which is relevant for stochastic quantization [21,22] (this idea has been worked out in more detail in Refs. [19,23,24]).

While we will work out the properties of Chebyshev maps in further detail in the following sections, what we mention right now as a prerequisite is that the invariant density $p(x)$ of Chebyshev maps T_N of arbitrary order $N \geq 2$ is given by

$$p(x) = \frac{1}{\pi\sqrt{1 - x^2}}, \quad x \in [-1, 1]. \tag{1}$$

This density describes the probability density of iterates under long-term iteration. The maps T_N are ergodic and mixing. In suitable coordinates, iteration of the map T_N corresponds to a Bernoulli shift dynamics of N symbols. In the following we give a generalized statistical mechanics interpretation for the above invariant density, identifying Chebyshev maps as one of the simplest systems possible for which a generalized statistical mechanics can be defined. The interesting aspect of this low-dimensional simplicity is that $q = 3$ is relevant, rather than $q = 1$ as for ordinary statistical mechanics.

This paper is organized as follows. In Section 2 we derive the generalized canonical distributions obtained from the q-entropies S_q, and discuss the special distinguished features obtained for $q = 3$ (or $q = -1$ if so-called escort distributions [20,25] are used). In Section 3 we discuss the exponential mixing property, which is fixed by the second largest eigenvalue of the Perron–Frobenius operator. In fact, we will present formulas for *all* eigenvalues and eigenfunctions, thus completely describing the exponential mixing behaviour. In Section 4 we couple two maps, thus gradually expanding the phase space, and investigate how the coupling structure induces certain symmetries in the attractor, which are different for odd N and even N. The degeneracy of the canonical distribution (of the invariant density) is removed by the coupling, and all attractors become N-dependent. Finally, in Section 5 we consider a large number of coupled maps on a one-dimensional lattice space. This is the realm of the so-called 'chaotic strings', which have previously been shown to have relevant applications in quantum field theory [17,19,23]. We confirm, by numerical simulations, that the $N = 3$ string distinguishes a value of the coupling constant given numerically by $1/137$, which numerically coincides with the low-energy limit of the fine structure constant fixing the strength of electric interaction. A physical interpretation for that will be given, in the sense that we assume that the chaotic shift dynamics, described by $q = 3$ Tsallis entropies in a statistical mechanics setting, is a fundamental information shift dynamics that helps to fix standard model parameters in a pre-universe, before ordinary space-time is created.

2. Generalized Canonical Distributions from Maximizing q-Entropy Subject to Constraints

The relevant probability density (1) mentioned above can be regarded as a generalized canonical distribution in non-extensive statistical mechanics [1]. As it is well known, one defines for a dimensionless continuous random variable X with probability density $p(x)$ the Tsallis entropies as

$$S_q = \frac{1}{q-1}\left(1 - \int p(x)^q dx\right). \tag{2}$$

Here $q \in (-\infty, \infty)$ is the entropic index. The Tsallis entropies contain the Boltzmann–Gibbs–Shannon entropy $S_1 = -\int p(x) \log p(x) dx$ as a special case for $q \to 1$, as can be easily checked by writing $q = 1 + \epsilon$ and taking the limit $\epsilon \to 0$ in the above equation.

We now do statistical mechanics for general q. Typically one has some knowledge on the system. This could be, for example, a knowledge of the mean energy U of the system. Extremizing S_q subject to the constraint

$$\int p(x)E(x)dx = U \tag{3}$$

one ends up with q-generalized canonical distributions (see, e.g., Refs. [2,12] for a review). These are given by

$$p(x) \sim (1 + (q-1)\beta E(x))^{-\frac{1}{q-1}}, \tag{4}$$

where E is the energy associated with microstate x, and $\beta = 1/kT$ is the inverse temperature. Of course, for $q \to 1$ one obtains the usual Boltzmann factor $e^{-\beta E}$.

Alternatively, one can work with the so-called escort distributions, defined for a given parameter q and a given distribution $p(x)$ as [20]

$$P(x) = \frac{p(x)^q}{\int p(x)^q dx}.$$

The escort distribution sometimes helps to avoid diverging integrals, thus 'renormalizing' the theory under consideration, see Ref. [26] for more details. If the energy constraint (3) is implemented using the escort distribution $P(x)$ rather than the original distribution $p(x)$, one obtains generalized canonical distributions of the form

$$P(x) \sim (1 + (q-1)\beta E(x))^{-\frac{q}{q-1}}. \tag{5}$$

Again the limit $q \to 1$ yields ordinary Boltzmann factors $e^{-\beta E}$.

Let us now apply a q-generalized statistical mechanics formalism to the chaotic dynamics $x_{n+1} = T_N(x_n)$ as generated by Chebyshev maps. We may regard these Chebyshev maps as the simplest possibility to microscopically generate a dynamics that exactly follows a generalized canonical distribution, and at the same time lives on a compact phase space $[-1, 1]$. We might identify $E = \frac{1}{2}mX^2$ as a formal kinetic energy associated with the chaotic fields X, interpreting X as a kind of velocity and m as a mass. Or, we might regard it as a harmonic oscillator potential, regarding X as a kind of position. We then get, by comparing Equations (1) and (4),

$$\begin{aligned} q &= 3 \\ \beta^{-1} &= -m. \end{aligned}$$

Note that the mass that formally comes out of this approach is negative. A formal problem of this approach is that the $q = 3$ Tsallis entropy of the distribution (1) as defined by the integral Equation (2) does not exist, since the integral $\int_{-1}^{1}(1-x^2)^{-3/2}dx$ diverges. This problem, however, can be avoided by proceeding to the escort distribution, which has a different effective q index. For escort distributions, all relevant integrals are well-defined, as we will show in the following.

If the escort formalism [20,25,26] is used, then by comparing the functional form of the invariant density $\pi^{-1}(1-x^2)^{-\frac{1}{2}}$ with Equation (5) we get

$$\begin{aligned} q &= -1 \\ \beta^{-1} &= m. \end{aligned}$$

We obtain the result that our shift-of-information model behaves similar to an ideal gas in the non-extensive formalism but with an entropic index of either $q = 3$ or $q = -1$,

rather than $q = 1$, as in ordinary statistical mechanics. The 'velocity' v is given by the dimensionless variable $v = X$, the 'kinetic energy' by the non-relativistic formula $E = \frac{1}{2}mv^2$, and the inverse temperature is $\beta = m^{-1}$. This non-extensive gas has the special property that the temperature coincides with the mass of the 'particles' considered. Alternatively, it corresponds to a harmonic oscillator potential if X is interpreted as a fluctuating position variable that lives on a compact interval. The idea can also be worked out for coupled systems, i.e., for spatially coupled Chebyshev maps on a lattice, and applied to vacuum fluctuations in quantum field theory, see Ref. [19] for more details.

We can now evaluate all interesting thermodynamic properties of the system using the escort formalism. Regarding the invariant density of our system as an escort distribution $P(x) = \frac{1}{\pi}(1 - x^2)^{-\frac{1}{2}}$, we have, by comparing the exponent with that in Equation (5), $q = -1$. The original distribution $\hat{p}(x)$ is then given by $\hat{p}(x) \sim P(x)^{\frac{1}{q}} = P(x)^{-1}$ which gives

$$\hat{p}(x) = \frac{2}{\pi}\sqrt{1 - x^2}, \tag{6}$$

where the prefactor is fixed by the normalisation condition $\int_{-1}^{1} \hat{p}(x)dx = 1$. For the Tsallis entropy of the chaotic fields, we obtain from Equations (2) and (6)

$$S_q[\hat{p}] = \frac{1}{4}(\pi^2 - 2) = S_q[P].$$

It is invariant under the transformation $\hat{p} \to P$, which is a distinguished property of the entropic index $q = \pm 1$. For the generalized internal energy we obtain

$$U_q[P] = \int_{-1}^{1} P(x)\frac{1}{2}mx^2 dx = \frac{1}{4}m$$

and for the generalized free energy

$$F_q = U_q - TS_q = \frac{m}{4}(3 - \pi^2).$$

All expectations formed with the invariant measure can be regarded as corresponding to escort expectations within the more general type of thermodynamics that is relevant for our chaotically evolving information-shift fields. Whereas ordinary statistical physics is described by a statistical mechanics with $q = 1$, the chaotic fields underlying our information shift are described by $q = -1$ or $q = 3$, depending on whether the escort formalism is used or not. In general, one can easily verify that the entropic indices $q = +1$ and $q = -1$ are very distinguished cases: Only for these two cases is the Tsallis entropy of the escort distribution equal to the Tsallis entropy of the original distribution, for arbitrary distributions $p(x)$.

An important distinction comes from the non-additivity property of Tsallis entropies. Consider a factorization of probabilities, i.e., write

$$p(x) = p^I(x)p^{II}(x)$$

where I and II are independent subsystems. A general property of Tsallis entropy is

$$S_q^{I,II} = S_q^I + S_q^{II} - (q-1)S_q^I \cdot S_q^{II}$$

which is true for arbitrary factorizing probability densities and arbitrary q.

The cases $q = -1$ and $q = 3$ are distinguished as they satisfy the relation

$$S_q^{I,II} - S_q^I - S_q^{II} = (S_q^I \pm S_q^{II})^2 - (S_q^I)^2 - (S_q^{II})^2.$$

That is to say, linear entropy differences on the left-hand side are connected with squared entropy differences on the right-hand side.

We should mention here that the case $q = 3$, respectively $q = -1$, is a kind of extreme case where $|q - 1|$ is not small. Usually, the difference $|q - 1|$ is assumed to be small in typical applications of Tsallis statistics to cosmology and quantum field theory, see e.g., Refs. [27–29] for some recent work in this direction. Note that for our information shift dynamics, the Kolmogorov–Sinai entropy h_{KS} is still given by the standard Lyapunov exponent $h_{KS} = \log N > 0$ as we have a strongly chaotic dynamics for which everything can be calculated analytically since the invariant density is known. This means there is on average a linear growth of information in each iteration step [20]. All n-point higher-order correlation functions of the dynamics can be calculated by implementing a graph-theoretical method developed in Ref. [16]. The deformation from ordinary statistical mechanics is visible in the shape of the invariant density, which strongly differs from a Gaussian, as it is described by a q-Gaussian with $q = 1 \pm 2$. This anomaly is due to the fact that the statistical mechanics we consider has as a phase space a compactified space—it simply lives on the interval $[-1, 1]$. Our physical interpretation is that this information shift dynamics is not living in the ordinary space-time of the current universe but describes a pre-universe dynamics on a compactified space. Only later, when ordinary space-time unfolds, does q start getting closer to 1, because the available phase space then becomes much bigger and the many more degrees of freedom will start to contribute. We may assume that there is a complex transition scenario from $q = 3$ to $q = 1$ on that way towards ordinary statistical mechanics.

3. Relaxation Properties of Chebyshev Dynamical Systems

Formally, the Chebyshev maps are a family of discrete dynamical systems defined by

$$x_{n+1} = T_N(x_n), \quad n = 0, 1, 2, \ldots, \tag{7}$$

where

$$T_N(x) = \cos(N \arccos x), \quad x \in [-1, 1], \quad N = 2, 3, 4, \ldots, \tag{8}$$

which can be written as polynomials, for example,

$$\begin{aligned}
T_2(x) &= 2x^2 - 1, \\
T_3(x) &= 4x^3 - 3x, \\
T_4(x) &= 8x^4 - 8x^2 + 1, \\
&\vdots
\end{aligned} \tag{9}$$

They are proven to be topologically conjugated to tent-like maps via the conjugacy function $h(x) = \frac{1}{\pi} \arccos(-x)$, and as a consequence, they are conjugated to Bernoulli shifts of N symbols. Furthermore, one can show that the (higher-order) correlation functions of Chebyshev maps are vanishing identically, except for special sets of tuples described by appropriate N-ary graphs [15,16], which is a distinguished feature compared to other maps conjugated to a Bernoulli shift.

The transfer (or Perron–Frobenius) operator $\mathcal{L}$ for a given map describes the time evolution of a distribution of points characterised by a density function. Consider the eigenvalue equation $\mathcal{L}\rho = \lambda\rho$: if we write an initial distribution as a linear combination of eigenfunctions of $\mathcal{L}$, then the time evolution of the distribution is just applications of the (linear) transfer operator, which is simply multiplying the eigenfunctions in the expansion of the initial density with the corresponding eigenvalues.

For a one-dimensional discrete dynamical system T the Perron–Frobenius operator is given by $\mathcal{L}\rho(y) = \sum_{x \in T^{-1}(y)} \frac{\rho(x)}{|T'(x)|}$, where T' denotes the derivative of the map T and

$\sum_{x \in T^{-1}(y)}$ is summing over all the preimages of a point y. It was shown [15] that for Chebyshev maps $T = T_N$, we have $\mathcal{L}\rho^{(n)}(x) = \lambda^{(n)}\rho^{(n)}(x)$, $n = 0, 1, 2, \dots$ with

$$\lambda^{(n)} = N^{-2n},$$

$$\rho^{(n)}(x) = \begin{cases} \frac{1}{\pi\sqrt{1-x^2}} B_{2n}\left(\frac{1}{2\pi}\arccos(-x) + \frac{1}{2}\right) \text{ if } N = 2, 4, \dots \text{ is even;} \\ \begin{cases} \rho^{(n,1)}(x) = \frac{1}{\pi\sqrt{1-x^2}} B_{2n}\left(\frac{1}{\pi}\arccos(-x)\right) \\ \rho^{(n,2)}(x) = \frac{1}{\pi\sqrt{1-x^2}} E_{2n-1}\left(\frac{1}{\pi}\arccos(-x)\right) \end{cases} \text{ if } N = 3, 5, \dots \text{ is odd;} \end{cases}$$

where $B_n(x)$ and $E_n(x)$ are the Bernoulli and Euler polynomials, respectively. The graphs of the first few eigenfunctions are shown below. They form a basis of the functional space under consideration.

The invariant density of the Chebyshev map T_N is the eigenfunction of the transfer operator $\mathcal{L}$ associated with the unit eigenvalue, with $\lambda^{(0)} = 1$ we recover Equation (1): $\rho^{(0)}(x) = \frac{1}{\pi\sqrt{1-x^2}} = p(x)$. The graph can be found in blue in Figure 1a or Figure 1b.

(a)   **(b)**   **(c)**
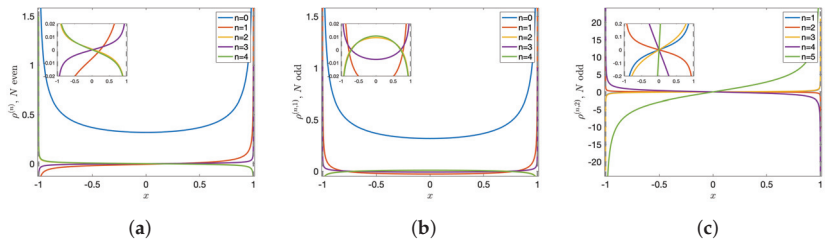
Figure 1. First five eigenfunctions of the transfer operator $\mathcal{L}$ for Chebyshev maps T_N ($N \in \mathbb{N}_{\geq 2}$) with **(a)** even N, and **(b,c)** odd N. Each inset captures the graph close to the origin.

The remaining eigenvalues are related to relaxation times of the dynamical system and in particular, the second one $\lambda^{(1)} = N^{-2} < 1$ characterises the mixing rate in the following sense:

Consider an arbitrary initial distribution $\rho_0(x)$ in a suitable functional space, it can then be expressed as a linear combination of the eigenfunctions of $\mathcal{L}$

$$\rho_0(x) = \sum_{i=0}^{\infty} c_i \rho^{(i)}(x),$$

where the c_i are some real coefficients. Applying the transfer operator $\mathcal{L}$ m times gives

$$\rho_m(x) = \mathcal{L}^m \rho_0(x) = \sum_{i=0}^{\infty} c_i (\lambda^{(i)})^m \rho^{(i)}(x) = c_0 p(x) + R_m,$$

where $p(x)$ is the invariant density and $R_m := \sum_{i=1}^{\infty} c_i (\lambda^{(i)})^m \rho^{(i)}(x)$ denotes the sum of the remaining terms. Since $|\lambda^{(i)}| = N^{-2i} < 1$ for all $i = 1, 2, \dots$ and $N \in \mathbb{N}_{\geq 2}$, we have $R_m \to 0$ as $m \to \infty$. The decay of R_m will be dominated by the second largest eigenvalue. In other words, $\lambda^{(1)}$ determines the rate of approaching the equilibrium state (or invariant density) $p(x)$.

The *exponential mixing* property of a map means that an arbitrary density approaches the invariant density exponentially fast: $|\rho_m(x) - p(x)| \sim e^{-rm}$, where r^{-1} is referred to as *relaxation time* and it is related to the second largest eigenvalue $\lambda^{(1)}$ by $e^{-r} = |\lambda^{(1)}|$ [20]. In our case we have $\lambda^{(1)} = N^{-2}$ and hence the relaxation time for the Chebyshev map T_N is given by $r^{-1} = (2\ln N)^{-1}$.

4. Symmetries in the Attractors of Coupled Chebyshev Map Systems of Small Size

We have shown in the previous section that the invariant density of a Chebyshev map T_N is independent of the order $N \in \mathbb{N}_{\geq 2}$. We will now couple the maps [17–19,23,30,31]. The independence of N will be removed by the coupling and all the attractors will become N-dependent.

Consider a one-dimensional lattice of size $J \geq 2$ with periodic boundary conditions, and on each lattice site we impose an identical Chebyshev dynamics. The simplest coupling scheme is the nearest-neighbour coupling and it is described as follows:

$$x_{n+1}^{(j)} = (1-c)T_N(x_n^{(j)}) + \frac{c}{2}\left[T_N(x_n^{(j-1)}) + T_N(x_n^{(j+1)})\right], \tag{10}$$

where the superscripts $j = 1, 2, \ldots, J$ and subscripts $n = 0, 1, 2, \ldots$ of the dynamical variable x denote the spatial position of the lattice site and the number of time steps of iterations, respectively, and $c \in [0, 1)$ is the coupling strength.

It is usually assumed that for a very weak coupling, ergodicity still holds if the uncoupled system is ergodic. It is still an open mathematical question whether the coupled Chebyshev systems are ergodic or not for a range of the coupling strength for a given order N. However, we can numerically investigate their behaviour for a large time.

For a system of two ($J = 2$) coupled T_N maps, Figure 2 shows the attractors and the associated probability measures (in colour) for $N = 2, 3, 4$ and 5 with various values of the coupling strength c. In general, the attractor shrinks to the diagonal ($x^{(1)} = x^{(2)}$) as the coupling strength c increases, where the system achieves a completely synchronized state, before which spikes (small regions in red) occur at various c values, indicating high concentrations of probability; a pair of symmetric islands implies that the two lattice sites have opposite-sign dynamics ($x^{(1)}x^{(2)} < 0$).

Apart from their intricate and complicated structures, one notices that for odd N, the attractor is symmetric also with respect to the anti-diagonal $x^{(1)} = -x^{(2)}$ while for even N this symmetry is not present. This is simply due to the fact that $T_N(x)$ is an odd function when N is odd: As $T_N(-x) = -T_N(x)$, the coupled map Equation (10) is invariant if we multiply the variables by -1, while this is not true for even N. The videos for Figure 2, showing the dynamics of the attractor when the coupling strength c is slowly changed, are available online [32].

Figure 3 shows similar symmetry behaviour for a system of three ($J = 3$) coupled T_N maps of order $N = 2, 3, 4$ and 5 with some arbitrarily chosen coupling strength c, as indicated in each caption. Each three-dimensional attractor is projected onto the $(x^{(1)}, x^{(2)})$-plane, in other words, the marginal density $\int_{-1}^{1} \rho(x^{(1)}, x^{(2)}, x^{(3)})dx^{(3)}$ is shown.

In Refs. [19,23] four types of coupled map systems were introduced for applications in stochastically quantized field theories. They differ from the current model (Equation (10), so-called *forward diffusive coupling*) by changing the sign of the second term (*antidiffusive*) or replacing $T_N(x_n^{(j\pm1)})$ by $x_n^{(j\pm1)}$ (*backward coupling*, taking into account the propagation time along the lattice). All of them have interesting physical applications, but in this paper we solely focus on the model Equation (10). In the next section, we show that in this simple model of coupled information shifts there might be a deep connection to a fundamental constant of particle physics—the fine structure constant. For more details on this type of approach fixing standard model parameters, see Refs. [19,23].
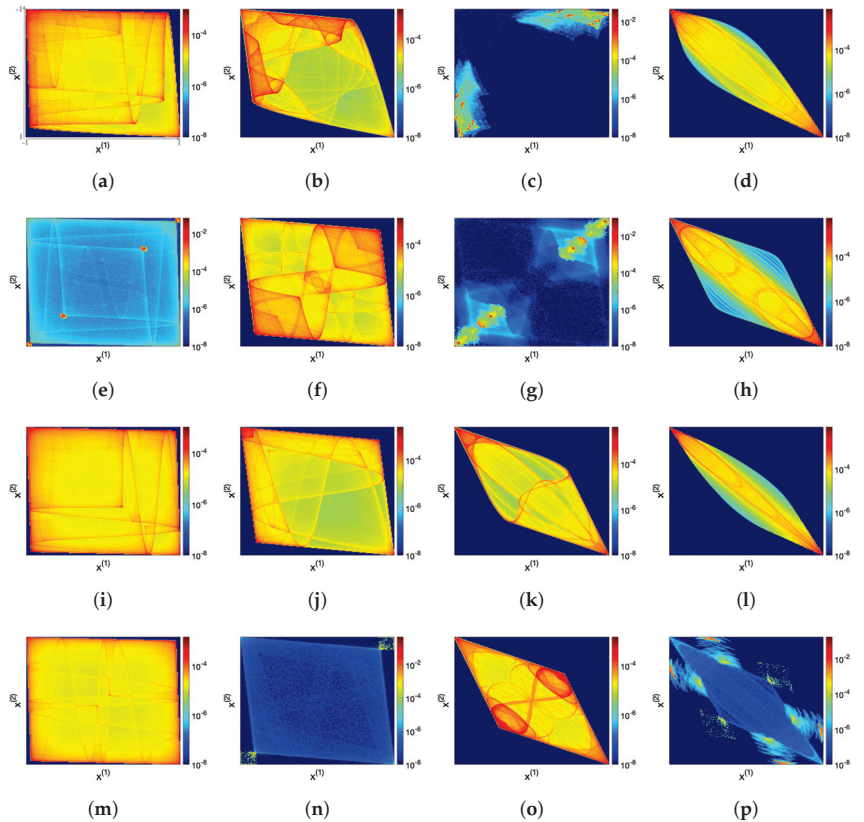
Figure 2. Probability densities on attractors of two coupled T_2 (row 1), T_3 (row 2), T_4 (row 3) and T_5 (row 4) systems, with different coupling strengths c (indicated in each caption). The x- and y-axes intervals are $x^{(1)} \in [-1, 1]$ (the value increases horizontally from left to right) and $x^{(2)} \in [-1, 1]$ (the value increases vertically from top to bottom). The colour codes show the averaged probability of 10,000 trajectories, randomly chosen initially, each iterated for 10,100 (-100 transient) time steps. The colour coding is in log scaling for a better representation; dark blue indicates lower probability and dark red indicates higher probability; each heatmap uses 200×200 bins. Videos of the shown dynamics are available online https://sites.google.com/view/jinyan-cmls/home (accessed on 25 October 2022). (**a**) T_2: $c = 0.027$, (**b**) T_2: $c = 0.1$, (**c**) T_2: $c = 0.12$, (**d**) T_2: $c = 0.22$, (**e**) T_3: $c = 0.027$, (**f**) T_3: $c = 0.093$, (**g**) T_3: $c = 0.12$, (**h**) T_3: $c = 0.29$, (**i**) T_4: $c = 0.027$, (**j**) T_4: $c = 0.1$, (**k**) T_4: $c = 0.29$, (**l**) T_4: $c = 0.35$, (**m**) T_5: $c = 0.027$, (**n**) T_5: $c = 0.093$, (**o**) T_5: $c = 0.29$, (**p**) T_5: $c = 0.35$.
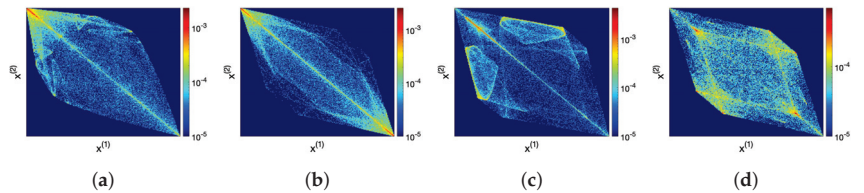
Figure 3. Probability densities on attractors of three coupled T_N systems projected onto the $(x^{(1)}, x^{(2)})$-plane of the full $(x^{(1)}, x^{(2)}, x^{(3)})$-space (i.e., marginal densities are shown). The value of the coupling strength c is indicated in each caption. The axes and colour coding are the same as in Figure 2. The averaged probability is obtained from 500 trajectories, randomly chosen initially, each iterated for 300 (-100 transient) time steps. (**a**) T_2: $c = 0.22$, (**b**) T_3: $c = 0.35$, (**c**) T_4: $c = 0.3$, (**d**) T_5: $c = 0.35$.

5. Vanishing Spatial Correlations Related to the Fine Structure Constant

For applications in quantum field theory and high energy physics it is meaningful to extend the coupled map system to a larger size, and ultimately to take the thermodynamic limit $J \rightarrow \infty$.

In this section we numerically study the *spatial* nearest-neighbour correlations (SNNC) of the system described by Equation (10), and show that the value of the fine structure constant is distinguished as a coupling constant for which the SNNC (with local T_3 maps) vanishes, implying that the underlying dynamics is uncorrelated in the spatial direction, thus achieving maximal randomness.

The spatial nearest-neighbour correlation (SNNC) for the coupled map system (10) of size J (large) is defined as

$$\text{SNNC} := \lim_{K \rightarrow \infty} \frac{1}{KJ} \sum_{n=1}^{K} \sum_{j=1}^{J} x_n^{(j)} x_n^{(j+1)},$$

where the superscripts j and subscripts n of x denote the lattice location and iteration times, respectively, as previously.

Here we choose the local Chebyshev map T_N of order $N = 3$. The reader can refer to Refs. [15,19] for results on other orders. Figure 4 shows our results for SNNC as a function of the coupling c, as obtained from new numerical simulations. One notices in Figure 4a that for the coupling strength c being very small, there is a zero of SNNC around $c \in [0.0072, 0.0074]$, and by magnifying this region in Figure 4b with higher precision, we can observe that the zero is located at a particular value c^*. Our simulations were repeated 11 times for different random initial conditions and the averaged result is $c^* = 0.0073084(48)$, where the statistical error is estimated from the small deviations that are observed for each of the 11 runs. This value is in good agreement with the numerical value of the fine structure constant $\alpha_{el} \approx 1/137 \approx 0.00730$ as observed in nature. In fact, the fine structure constant $\alpha_{el}(E)$ is a running coupling constant and depends on the energy scale E considered [19]. Our numerical results are consistent with the range $m_e \lesssim E \lesssim 3m_e$, where m_e is the electron mass. Our simulations were performed on lattices of size J = 50,000 with periodic boundary conditions. The iteration time for each run was K = 50,100, with 100 initial iterations discarded to avoid transients. At smaller lattice sizes J, we observe a small tendency of the zero c^* to decrease with the increasing lattice size, so there may also be tiny systematic errors due to the finite lattice size used in our simulations.

(a) (b)
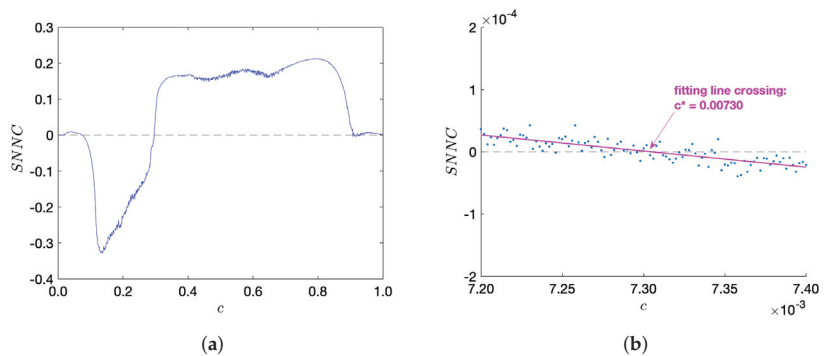
Figure 4. The graph of spatial nearest-neighbour correlation (SNNC) for coupled 3rd-order Chebyshev maps (T_3) as a function of the coupling strength $c \in [0, 1)$. The space×time size for the first plot is $1000 \times 1100(-100$ for transient), and for the second plot is $50,000 \times 50,100$ (-100); all initial points are randomly chosen from a uniform distribution in the interval $[-1, 1]$. (a) SNNC for $c \in [0, 1)$, (b) zoomed-in for $c \in [0.0072, 0.0074]$.

The general idea of this approach is that in a pre-universe, before the creation of a 4-dimensional space-time, the coupled information shift dynamics is already evolving and fixing standard model parameters, such as the fine structure constant, as states of maximum randomness (realized as a state of zero SNNC), given the constraint that we have a deterministic (chaotic) dynamics on microscopic scales.

More extensive numerical simulations can in principle be performed on supercomputers to locate the exact numerical value of c^*, making the result more precise. Within the precision obtained in our simulations, the coupled Chebyshev system (with local T_3 maps) gives a possible distinction of a fundamental constant of particle physics, by making the coupled chaotic system uncorrelated: for $c = c^*$, the deterministic system appears completely random (in the spatial direction) in the sense of vanishing nearest-neighbour correlations.

Of course, one might argue that perhaps the value of the zero-crossing in Figure 4b is just a random coincidence, i.e., it just by chance happens to coincide with the observed value of the fine structure constant. However, coincidences with other values of standard model coupling constants (weak and strong interactions) were also observed for other types of chaotic strings, see Refs. [19,23,24] for more details. Thus, a pure random coincidence of all these observed values appears quite unlikely, see Ref. [19] for quantitative estimates of the likelihood.

One can also study in a similar way the *temporal* nearest-neighbour correlations (TNNC), see Ref. [15], and also other higher-order statistics. Our results seem to indicate that the distinction comes only from the spatial two-point correlation function, not from other types of higher-order correlation functions.

6. Conclusions

In this paper we have considered an information shift dynamics that is deterministic and chaotic, and which maximizes Tsallis $q = 3$ entropy in a generalized statistical mechanics formalism. It is, in a sense, the simplest example of a low-dimensional statistical mechanical system that lives on a compact phase space and is ergodic and mixing. We consider it as a candidate dynamics for a pre-universe information shift dynamics that has the ability to fix standard model parameters (such as the fine structure constant) if a coupled version is considered.

Conflicts of Interest: The authors declare no conflict of interest.

References

1. Tsallis, C. Possible generalization of Boltzmann-Gibbs statistics. *J. Stat. Phys.* **1988**, *52*, 479. [CrossRef]
2. Tsallis, C. *Introduction to Nonextensive Statistical Mechanics*; Springer: Berlin/Heidelberg, Germany, 2009.
3. Jizba, P.; Korbel, J. Maximum entropy principle in statistical inference: Case for non-Shannonian entropies. *Phys. Rev. Lett.* **2019**, *122*, 120601. [CrossRef] [PubMed]
4. Beck, C.; Cohen, E.G.D. Superstatistics. *Physica A* **2003**, *322*, 267. [CrossRef]
5. Metzler, R.; Superstatistics and non-Gaussian diffusion. *Eur. Phys. J. Special Topics* **2020**, *229*, 711. [CrossRef]
6. Bediaga, I.; Curado, E.M.F.; De Miranda, J.M. A nonextensive thermodynamical equilibrium approach in $e^+e^- \to$ hadrons. *Physica A* **2000**, *286*, 156. [CrossRef]
7. Beck, C. Non-extensive statistical mechanics and particle spectra in elementary interactions. *Physica A* **2000**, *286*, 164. [CrossRef]
8. Biro, T.S.; Purcsel, G.; Urmossy, K. Non-extensive approach to quark matter. *Eur. Phys. J. A* **2009**, *40*, 325. [CrossRef]
9. Marques, L.; Cleymans, J.; Deppman, A. Description of high-energy pp collisions using Tsallis thermodynamics: Transverse momentum and rapidity distributions. *Phys. Rev. D* **2015**, *91*, 054025. [CrossRef]
10. Wong, C.Y.; Wilk, G.; Cirto, L.J.; Tsallis, C. From QCD-based hard-scattering to nonextensive statistical mechanical descriptions of transverse momentum spectra in high-energy pp and $p\bar{p}$ collisions. *Phys. Rev. D* **2015**, *91*, 114027. [CrossRef]
11. Beck, C.; Lewis, G.S.; Swinney, H.L. Measuring nonextensivity parameters in a turbulent Couette-Taylor flow. *Phys. Rev. E* **2001**, *63*, 035303R. [CrossRef]

12. Beck, C. Generalised information and entropy measures in physics. *Contemp. Phys.* **2009**, *50*, 495. [CrossRef]
13. Yoon, P.H. Thermodynamic, non-extensive, or turbulent quasi-equilibrium for the space plasma environment. *Entropy* **2009**, *21*, 820. [CrossRef]
14. Dolgopyat, D.; Kanigowski, A.; Rodriguez-Hertz, F. Exponential Mixing Implies Bernoulli. *arXiv* **2021**, arXiv:2106.03147.
15. Yan, J.; Beck, C. Distinguished Correlation Properties of Chebyshev Dynamical Systems and Their Generalisations. *Chaos Solitons Fractals X* **2020**, *5*, 100035. [CrossRef]
16. Hilgers, A.; Beck, C. Higher-order correlations of Tchebyscheff maps. *Physica D* **2001**, *56*, 1. [CrossRef]
17. Groote, S.; Veermae, H. Short chaotic strings and their behaviour in the scaling region. *Chaos Solitons Fractals* **2009**, *41*, 2354. [CrossRef]
18. Dettmann, C.P.; Lippolis, D. Periodic orbit theory of two coupled Tchebyscheff maps. *Chaos Solitons Fractals* **2005**, *23*, 43. [CrossRef]
19. Beck, C. *Spatio-Temporal Chaos and Vacuum Fluctuations of Quantized Fields*; World Scientific: Singapore, 2002.
20. Beck, C.; Schlögl, F. *Thermodynamics of Chaotic Systems*; Cambridge University Press: Cambridge, UK, 1993.
21. Parisi, G.; Wu, Y. Perturbation theory without gauge fixing. *Sci. Sin.* **1981**, *24*, 483.
22. PDamgaard, H.; Hüffel, H. (Eds.) *Stochastic Quantization*; World Scientific: Singapore, 1988.
23. Beck, C. Chaotic strings and standard model parameters. *Phys. D* **2002**, *171*, 72. [CrossRef]
24. Beck, C. Chaotic scalar fields as models for dark energy. *Phys. Rev. D* **2004**, *69*, 123515. [CrossRef]
25. Tsallis, C.; Mendes, R.S.; Plastino, A.R. The role of constraints within generalized nonextensive statistics. *Physica A* **1998**, *261*, 534. [CrossRef]
26. Beck, C. Nonextensive scalar field theories and dark energy models. *Physica A* **2004**, *340*, 459. [CrossRef]
27. Luciano, G.G. Tsallis statistics and generalized uncertainty principle. *Eur. Phys. J. C* **2021**, *81*, 672. [CrossRef]
28. Luciano, G.G.; Blasone, M. q-generalized Tsallis thermostatistics in Unruh effect for mixed fields. *Phys. Rev. D* **2021**, *104*, 045004. [CrossRef]
29. Nojiri, S.; Odintsov, S.D.; Saridakis, E.N. Modified cosmology from extended entropy with varying exponent. *Eur. Phys. J. C* **2019**, *79*, 242. [CrossRef]
30. Kaneko, K. Period-doubling of kink anti-kink patterns, quasiperiodicity in antiferro-like structures and spatial intermittency in coupled logistic lattice. *Progr. Theor. Phys.* **1984**, *72*, 480. [CrossRef]
31. Mackey, M.; Milton, J. Asymptotic stability of densities in coupled map lattices. *Physica D* **1995**, *80*, 1. [CrossRef]
32. Available online: https://sites.google.com/view/jinyan-cmls/home (accessed on 25 October 2022).

Brief Review on the Connection between the Micro-Canonical Ensemble and the S_q-Canonical Probability Distribution

Angel R. Plastino [1] **and Angelo Plastino** [2,*]

[1] CeBio y Departamento de Ciencias Básicas, Universidad Nacional del Noroeste de la Província de Buenos Aires, UNNOBA, CONICET, Roque Saenz Peña 456, Junin 6000, Argentina

[2] Facultad de Ciencias Exactas, Departamento de Física, UNLP and CONICET-CCT-IFLP, La Plata 1900, Argentina

[*] Correspondence: angeloplastino@gmail.com

Abstract: Non-standard thermostatistical formalisms derived from generalizations of the Boltzmann–Gibbs entropy have attracted considerable attention recently. Among the various proposals, the one that has been most intensively studied, and most successfully applied to concrete problems in physics and other areas, is the one associated with the S_q non-additive entropies. The S_q-based thermostatistics exhibits a number of peculiar features that distinguish it from other generalizations of the Boltzmann–Gibbs theory. In particular, there is a close connection between the S_q-canonical distributions and the micro-canonical ensemble. The connection, first pointed out in 1994, has been subsequently explored by several researchers, who elaborated this facet of the S_q-thermo-statistics in a number of interesting directions. In the present work, we provide a brief review of some highlights within this line of inquiry, focusing on micro-canonical scenarios leading to S_q-canonical distributions. We consider works on the micro-canonical ensemble, including historical ones, where the S_q-canonical distributions, although present, were not identified as such, and also more resent works by researchers who explicitly investigated the S_q-micro-canonical connection.

Keywords: generalized entropies; micro-canonical ensemble; S_q non-additive entropies

1. Introduction

To speak about things, it is often useful to have names for them. Otherwise, one faces a plight similar to that of Garcia Marquez's celebrated Macondo characters, who lived when "*the world was so recent that many things lacked names, and in order to indicate them it was necessary to point*" [1]. One of the tasks of scientists is to identify and baptize things, including abstract mathematical objects, that deserve to have a name. The probability distributions, nowadays called q-exponentials and q-Gaussians (q-distributions, for short), constitute nice illustrations of physically relevant mathematical objects that, for a long time, lacked a deserved name. Since the very inception of statistical mechanics, the q-distributions are discernible in the scientific literature. These distributions are closely related to the micro-canonical ensemble, and are central to some standard derivations of the Gibbs canonical probability distribution from the micro-canonical one. The relevance of the q-distributions, however, remained unrecognized for more than a century. The unnoticed distributions remained unnamed.

In 1988 Tsallis advanced a thermo-statistical formalism based on the non-additive entropy S_q, characterized by the parameter q [2]. The new formalism soon attracted the attention of a few adventurous theoreticians because of its mathematical elegance and its physically appealing features. Then, after some concrete applications were identified in the early and mid 1990s, research activity on the S_q-thermo-statistics increased dramatically, and the field expanded in myriad new directions [3]. In particular, the connection with the micro-canonical ensemble describing finite systems, discovered in 1994 [4], established

a direct link between Tsallis theory and some basic ideas of statistical mechanics dating from the very beginnings of this branch of physics. It became clear that the probability distributions (or densities) optimizing the S_q entropy were already present in some early works by the founding fathers of statistical mechanics, as well as in some modern textbooks. Nowadays, those distributions, first identified as important in their own right by Tsallis in 1988, are endowed with well-deserved short, catchy names: q-exponentials and q-Gaussians (the latter are special instances of the former).

The link between the micro-canonical ensemble and either the q-exponential or q-Gaussians has been, since 1994, investigated by several researchers, from diverse points of view. The aim of the present effort is to provide a brief review of this subject, summarizing its historical background, and discussing recent developments.

This paper is organized in the following way. In Section 2, we describe briefly the S_q-thermo-statistical formalism and the probability distributions that optimize the S_q entropy. The basic connection between the S_q-thermostatistics and the micro-canonical ensemble is reviewed and explained in Section 3. In Section 4, we provide some historical background, on works prior to 1994, where the q-exponential related to the micro-canonical ensemble can be identified. Recent developments on these matters are reviewed in Section 5. Finally, some concluding remarks are given in Section 6.

2. Probability Distributions Optimizing the S_q Non-Additive Entropies

Generalizations of the maximum entropy principle based on non-standard entropies [5–11] have been applied to the study of a variety of systems and processes in physics and other fields, especially in relation to complex systems [3,12,13]. This line of endeavor started in earnest around the mid and late 1990s, stimulated, to a large extent, by the early applications of a generalized thermostatistics advanced by Tsallis in 1988. Within the Tsallis proposal, the canonical probability distributions arise from the optimization of the S_q non-additive entropies [2]. The S_q-based thermostatistics has been applied successfully to diverse fields, including physics, astronomy, and biology, among various others [14–19]. Of all the thermo-statistics derived from generalized entropic forms, the thermo-statistics associated with the S_q entropies has been the one that attracted more attention and the one that generated the largest and most diverse set of fruitful applications. In this section, we shall briefly review the main features of the S_q-thermo-statistics.

The S_q-thermo-statistics is derived from the non-additive, entropy S_q [3] which is given by the expression

$$S_q \; = \; \frac{k}{q-1} \sum_{i=1}^{\mathcal{W}} \left(p_i - p_i^q \right), \tag{1}$$

where the parameter q determines the degree of non-additivity exhibited by the entropy, the constant k determines both the dimensions and the units in which the entropy is measured, and $\{p_i, \; i = 1, \ldots, \mathcal{W}\}$ constitutes a set of normalized probabilities associated with a system that has $\mathcal{W}$ microstates. Here, we assume that $k = 1$. In the limit $q \to 1$, the standard Boltzmann–Gibbs entropy is recovered: $S_1 = -k \sum_{i=1}^{\mathcal{W}} p_i \ln p_i = S_{\mathrm{BG}}$. Central to the S_q thermo-statistical formalism are the q-logarithm and the q-exponential functions. The q-logarithm is defined as

$$\ln_q(x) \; = \; \frac{1 - x^{1-q}}{q-1}, \tag{2}$$

and its inverse function, the q-exponential, is given by

$$\exp_q(x) = [1 + (1-q)x]_+^{\frac{1}{1-q}}, \tag{3}$$

where

$$[1 + (1-q)x]_+^{\frac{1}{1-q}} = \begin{cases} [1 + (1-q)x]^{\frac{1}{1-q}}, & \text{if } 1 + (1-q)x > 0, \\ 0, & \text{if } 1 + (1-q)x \leq 0. \end{cases} \tag{4}$$

The q-logarithm and the q-exponential functions are inextricably linked to the constrained optimization of the S_q entropies [3]. It is worth mentioning that the S_q entropy itself can be expressed in terms of q-logarithms,

$$S_q = k \sum_{i=1}^{W} p_i \ln_q(1/p_i) = k \left\langle \ln_q(1/p_i) \right\rangle. \tag{5}$$

In the limit $q \to 1$, the above expression coincides with the well-known one, $S_{\text{BG}} = k \sum_{i=1}^{W} p_i \ln(1/p_i)$.

The S_q thermo-statistics revolves around the optimization of the entropic form S_q under appropriate constraints. The concomitant variational problem can be formulated in terms of standard linear constraints, or in terms of power-law nonlinear constraints related to escort distributions [3]. For our present purposes, which are to consider some connections between the S_q formalism and the micro-canonical ensemble, it is convenient to consider standard linear constraints. The use of linear constraints also makes it easier to consider more general entropic functionals, for which it is still not well understood what type of escort mean values should be used. S_q-based canonical probability distribution is obtained when the S_q entropy is optimized under the constraints imposed by normalization,

$$\sum_{i=1}^{W} p_i = 1, \tag{6}$$

and by the system's mean energy. If the ith microstate of the system has energy ϵ_i and probability p_i, the mean energy is given by

$$E = \sum_{i=1}^{W} p_i \epsilon_i. \tag{7}$$

We assume that the energies of the system are bounded from below, and that for all states, $\epsilon_i \geq 0$. The optimization of the entropy S_q under the constraints (6) and (7) leads to

$$\delta \left[S_q - \alpha \left(\sum_{i=1}^{W} p_i \right) - \beta E \right] = 0, \tag{8}$$

where α and β are the Lagrange multipliers associated with the constraints of normalization (6) and the mean energy (7). It follows from (8) that

$$p_i^{q-1} = \frac{1}{q} \left[1 - (q-1)(\alpha + \beta \epsilon_i) \right], \tag{9}$$

and

$$p_i = \left(\frac{1}{q} \right)^{\frac{1}{q-1}} \left[1 - (q-1)(\alpha + \beta \epsilon_i) \right]_{+}^{\frac{1}{q-1}}, \tag{10}$$

which constitutes the S_q-canonical probability distribution. The probabilities (10) can be recast as

$$p_i = \mathcal{C} \left[1 - (q-1)\tilde{\beta}\epsilon_i \right]_{+}^{\frac{1}{q-1}}, \tag{11}$$

where $\mathcal{C} = \left[\left(\frac{1}{q} \right) \frac{\beta}{1-(q-1)\alpha} \right]^{\frac{1}{q-1}}$ and $\tilde{\beta} = \frac{\beta}{1-(q-1)\alpha}$. Expression (11) for the S_q-canonical probabilities coincides with the one obtained by Tsallis in his seminal paper of 1988 [2] (compare (11) with Equation (12) from [2], making the identifications $\tilde{\beta} \to \beta$ and $\mathcal{C} \to 1/Z_q$). In what follows, we shall use expression (11), focusing on scenarios satisfying $q > 1$ and $\tilde{\beta} > 0$, which, as we shall see, are related to the micro-canonical ensemble. It is also worth

emphasizing that the probabilities (11) can be expressed in the standard q-exponential form, as

$$p_i = \mathcal{C} \, \exp_{\tilde{q}}\left[-\tilde{\beta}\epsilon_i\right], \tag{12}$$

where

$$\tilde{q} = 2 - q. \tag{13}$$

That is, the expression (11) constitutes just a particular way of parameterizing a q-exponential probability distribution. Since, as we already explained, we are going to use the parameterization (11), all the q-values mentioned in this review correspond to this parameterization. In order to compare our q-values with those of the authors, who use the parameterization (12), one has to apply the relation (13). In what follows, when we use (11) or (12), we shall drop the tilde from $\tilde{\beta}$. When deriving (11), we considered a set of discrete energy levels. In the case of classical Hamiltonian systems with a Hamiltonian H and continuous phase space, the optimization of the S_q entropy under the normalization and mean energy constraints leads to a phase space S_q-canonical probability density of the form

$$\mathcal{F}(\omega) = \mathcal{C}\left[1 - (q-1)\beta H(\omega)\right]_+^{\frac{1}{q-1}}, \tag{14}$$

where $\omega = (q_i, q_2, \ldots; p_1, p_2, \ldots)$ denotes the set of generalized coordinates and conjugate momenta.

3. The Micro-Canonical Path towards the S_q-Canonical Distribution

Now, we shall review how the S_q canonical distribution can arise from the micro-canonical ensemble. We shall consider a composite system $A + B$ consisting of two weakly coupled subsystems A and B. The subsystem A has energy levels ϵ_i, $i = 1, 2, \ldots$. The "total" system $A + B$ is described by the Gibbs micro-canonical ensemble, and has a total energy lying in the interval $(E_T - \Delta, E_T + \Delta)$ with $\Delta \ll E_T$. The level distribution of subsystem B is assumed to be quasi-continuous. Under these assumptions, it is possible to show that, if the number of states of system B having energies less or equal to E grows as a power of E, then the marginal probability distribution associated with subsystem A has the same form as the S_q-canonical distribution (11) (or, equivalently, as (12)).

The proof of the above statement is based on the fact that the probability p_i of finding the system A in a particular state i with energy i is proportional to the total number ν of configurations of the complete system $A + B$ that are compatible with the state of affairs. In order to determine ν, we introduce the assumption, already mentioned, that the number $\mathcal{N}(E)$ of states of system B having energies less or equal to E complies with the power law,

$$\mathcal{N}(E) \propto E^\eta, \tag{15}$$

The above power law implies that the number of states of system B having energies within the range $(E - \Delta, E + \Delta)$ is proportional to

$$2\Delta E^{\eta-1}, \tag{16}$$

from which it follows that the number ν of configurations of the total system $A + B$ compatible with finding A in a state with energy ϵ_i satisfies,

$$\nu \propto (E_T - \epsilon_i)^{\eta-1}. \tag{17}$$

It is plain from the above relation that the probabilities p_i to find the system A is in its different states $i = 1, 2, \ldots$, comply with

$$\frac{p_i}{p_j} = \frac{(E_T - \epsilon_i)^{\eta-1}}{(E_T - \epsilon_j)^{\eta-1}} = \frac{[1 - (\epsilon_i/E_T)]^{\eta-1}}{[1 - (\epsilon_i/E_T)]^{\eta-1}}. \tag{18}$$

After introducing a normalization factor $\mathcal{C}$, defined by the relation

$$\mathcal{C}^{-1} = \sum_i \left[1 - (\epsilon_i/E_T)\right]^{\eta-1}, \tag{19}$$

the probabilities p_i, associated with the states of system A, can be finally cast as

$$p_i = \mathcal{C} \left[1 - (\epsilon_i/E_T)\right]^{\eta-1}. \tag{20}$$

Setting now

$$q = \frac{\eta}{\eta - 1}, \tag{21}$$

and

$$\beta = \frac{\eta - 1}{E_T}, \tag{22}$$

it follows that the marginal probability distribution describing the system A has the same form as the S_q-canonical distribution, given by (11) (or, alternatively, by (12)).

The main assumptions made in the above arguments can be summarized as follows:

- We have two weakly interacting systems, A and B, jointly described by the micro-canonical ensemble.
- The energy level distribution of subsystem B is quasi-continuous, and the number of states of system B with energy less than or equal to E grows as a power E^η.

Some comments are in order with regards to the second assumption. First, systems complying with that assumption are not rare. Systems such that the number of states grows with a power η of the system's energy can be realized in a number of ways. Particular examples are the following: a system B consisting of N quantum harmonic oscillators, for which one has $\eta = N$; a set of N free non-relativistic quantum particles moving in a D-dimensional box, for which $\eta = DN/2$; and a system of N rigid, quantum plane rotators, for which $\eta = N/2$. As can be appreciated in these examples, in order to exhibit the desired behavior, B has to be finite. If one interprets B as a heat bath, it follows that one of the physical scenarios leading to the S_q-canonical distribution is the one corresponding to systems in equilibrium with a finite heath bath. This is, indeed, a sensible interpretation. The finite-bath interpretation is not, however, essential for our present purposes, and we shall not emphasize it. In order to establish the connection between the S_q-canonical distribution and the micro-canonical ensemble, it is enough to consider a system consisting of two weakly coupled subsystems, in which one of the subsystems (our system B) is such that the number of states grows as a power of energy.

Notice that in all the above-mentioned instances of a system B for which the number of states depends on E according to the appropriate power-law behavior, the exponent η is proportional to the number N of constituents of B. If one lets $N \to \infty$ and $E_T \to \infty$, keeping the quotient E_T/N constant, one also has $\eta \to \infty$, with η/E_T constant. It can be verified that, if one takes that limit, then q goes to unity, and the probability distribution associated with system A becomes the standard canonical exponential one,

$$p_i = \frac{1}{Z} \exp(-\beta\epsilon_i), \tag{23}$$

where

$$Z = \sum_i \exp(-\beta\epsilon_i). \tag{24}$$

If B is interpreted as an infinite heat bath (resulting from taking the thermodynamic limit $N \to \infty$ and $E_T \to \infty$), the above argument is, essentially, the one provided in many textbooks in order to derive the Gibbs canonical distribution (23). In particular, this is the case in Feynman's celebrated lectures on statistical mechanics [20] (for instance, q-distributions are clearly identifiable in page 4 of [20], although they are not explicitly

parameterized, nor referred to, as "*q*-distributions", nor are they, for that matter, given any specific name). The *q*-distributions appear and play a central role in these derivations, although this fact usually remains unnoticed because the connection with the S_q-based thermostatistics is not recognized. Since 1994, the connection between the s_q-thermo-statistics and the micro-canonical ensemble has been investigated by several researchers. Baranger, an outstanding contributor to S_q-thermo-statistics, and an influential commentator on the field [3], hailed the S_q-canonical-micro-canonical connection as a key ingredient in answering the question "*Why Tsallis Statistics?*". In a paper published in 2002, Baranger re-visited the argument advanced in [4] and made the bold conjecture that the argument may be extended beyond equilibrium scenarios, helping to explain the phenomenological success of Tsallis statistics in describing diverse non-equilibrium situations [21]. Baranger suggested that, during an out-of-equilibrium process, a subsystem may interact with a finite number of effective degrees of freedom of the rest of the system, establishing a quasi-equilibrium situation described by the S_q-statistics.

Our previous arguments were formulated in terms of systems having discrete energy levels. The main arguments, however, are still valid if one considers classical Hamiltonian systems with a continuous phase space. Let us consider a classical composite system $A + B$, consisting of two weakly interacting subsystems, governed by a Hamiltonian $H = H_A(\omega_A) + H_B(\omega_B)$, where ω_A denotes the set of canonical phase-space variables describing the state of system A, and ω_B stands for the set of variables describing the state of system B. Let us assume that the volume $\Phi_B(E)$ in the phase space of system B, corresponding to $H_B(\omega_B) \leq E$, is proportional to a power η of E. That is,

$$\Phi_B(E) = \int\limits_{H(\omega_B) \leq E} d\omega_B \propto E^{\eta}, \tag{25}$$

where $d\omega_B$ denotes the volume element in the phase space of system B. If the condition (25) is satisfied, one can follow essentially the same argument as before, and reach a similar conclusion: if the composite system $A + B$ is described by the micro-canonical ensemble with total energy E_T, then the marginal probability density corresponding to system A has the S_q-canonical form

$$\mathcal{F}_A(\omega_A) = \mathcal{C} \left[1 - (q-1)\beta H_A(\omega_A) \right]_+^{\frac{1}{q-1}}, \tag{26}$$

where $\mathcal{C}$ is an appropriate normalization constant, and q and β are related to η and E_T through Equations (21) and (22). Note that the above setting is applicable even in situations in which A and B do not, strictly speaking, represent subsystems of a Hamiltonian system. The above results are also applicable when A denotes a subset of the canonical variables characterizing the system, B denotes the remaining canonical variables, and the total Hamiltonian can be separated as $H = H_A + H_B$, with the term H_A depending only on the variables associated with A, the term H_B only on the variables associated with B. Then, if one assumes that the total system is in the micro-canonical ensemble, and that the volume $\Phi_B(E)$ of the region determined by $H_B \leq E$ (the volume $\Phi_B(E)$ is computed with respect to the set of canonical variables associated with B) grows as a power η of E, the marginal probability distribution for the canonical variables in A has the S_q-canonical shape (26). As an example, we can consider a classical Hamiltonian system in which the kinetic energy is a homogeneous quadratic function of the momenta, and does depend on the configuration coordinates. If A denotes the n configuration coordinates of the system, and B denotes the set of n momenta, then one has that $\Phi_B(E) \propto E^{n/2}$. Consequently, if the system is described by the micro-canonical ensemble, the marginal probability density for the configuration coordinates is proportional to $[1 - (V/E_T)]^{\frac{n}{2}-1}$, where V is the system's potential energy, and E_T is the total energy (here, V plays the role of H_A). We see that the configuration probability density is a *q*-exponential with $q = n/(n-2)$. As we shall see in the next

section, this scenario was already discussed by Maxwell in 1879, although the connection with the S_q-statistics was not recognized at the time.

A paradigmatic scenario (closely related to the previous example) leading to the S_q-canonical distribution (26) is given by a composite classical Hamiltonian system $A + B$, where the subsystem B consists of N free particles of mass m moving in a D-dimensional box (that is, B is a D-dimensional finite classical ideal gas). In such a case, one can see that the volume $\Phi_B(E)$ given by (26), is proportional to the volume of a ND-dimensional hyper-sphere of radius $E^{1/2}$. That is,

$$\Phi_B(E) \propto E^{ND/2}. \tag{27}$$

Therefore, the power η is equal to $ND/2$. It then follows that, if the composite $A + B$ is jointly described by the micro-canonical ensemble with total energy E_T, the probability density $\mathcal{F}_A(\omega_A)$ associated with subsystem A is proportional to

$$\left[1 - \frac{H_A}{E_T}\right]^{\eta - 1} = \left[1 - \frac{H_A}{E_T}\right]^{\frac{ND-2}{2}}. \tag{28}$$

The density $\mathcal{F}_A(\omega_A)$ is thus of the S_q-canonical form (26), with the q-index given by (21), yielding,

$$q = \frac{\eta}{\eta - 1} = \frac{ND}{ND - 2} \tag{29}$$

As already mentioned, the early successes of the S_q theory motivated the exploration of alternative thermostatistical frames based on other entropic forms, and also the comparative investigation of the structural features exhibited by general entropic variational principles. The aim of these latter endeavors was to clarify which are the properties that are shared by large families of entropies, or even that are universal, and, on the other hand, which are the distinguishing properties that characterize particular entropies, such as the S_q ones. Diverse aspects of entropy optimization principles were investigated in this regard. See, for instance [22,23] and references therein. Within this context, it is natural to ask whether the connection with the micro-canonical ensemble is a specific feature of the S_q-thermostatistics or, on the contrary, is a feature shared by larger families of thermo-statistical formalisms. It is clear, on the one hand, that the connection with the S_q-thermostatistics arises from the power law behavior of the function $\mathcal{N}(E)$ (Equation (15)) describing the number of states of system B with energies less or equal E. If the function $\mathcal{N}(E)$ associated with B does not exhibit a power-law behavior, the probability distribution describing the system A will not be S_q-canonical. It will have a different form, which may be interpreted as optimizing an entropic measure different from S_q. In that sense, the link with the micro-canonical ensemble may be shared by other entropies. On the other hand, systems whose energy levels (or phase-space volumes) do exhibit the appropriate power-law behavior, and consequently lead to S_q-canonical distributions, are not rare in nature. As we shall see in the following sections, scenarios in which the S_q-canonical distribution arises from the micro-canonical ensemble have been discovered and investigated by many researchers, including some of the pioneers of statistical mechanics. This situation, not shared by other generalized entropies, suggests that there may be, perhaps, something unique to the link between the S_q-thermostatistics and the micro-canonical ensemble.

4. When q-Exponentials Lacked a Name: From Maxwell to the Mid 1990s

Interesting examples of q-exponential distributions can already be identified in one of Maxwell's pioneering works on statistical mechanics, his celebrated paper "On Boltzmann's Theorem on the Average Distribution of Energy in a System of Material Points", published in 1879 [24] (the paper can also be found in Maxwell's collected scientific works [25]). In this paper, Maxwell developed a statistical treatment for the dynamics of a closed system of interacting particles having a constant total energy. Maxwell considered a large

number of copies of the system, distributed uniformly on a phase-space hyper-surface of constant energy. In essence, Maxwell's idea was to describe the system by recourse to what, in modern parlance, we now call the micro-canonical ensemble. In Equation (41) of [24], Maxwell determined that "the number of systems whose configuration is specified by the variables $b_1, \ldots, b_n$ while the momenta may have any values consistent with the equation of energy" (in Maxwell's notation $b_1, \ldots, b_n$ denotes the complete set of configuration coordinates) [24]. In other words, Equation (41) of Maxwell's paper corresponds to the marginal distribution in configuration space, obtained from the micro-canonical ensemble after tracing over the particles' momenta. Maxwell proved that the distribution in configuration space is proportional to

$$(E - V)^{\frac{n-2}{2}},\tag{30}$$

where E is the system's total energy, and $V(b_1, \ldots, b_n)$ is the the system's total potential energy. If the potential energy is bounded from below, we can choose the zero of energy in such a way that $E, V > 0$. The configuration density $\mathcal{F}(b_1, \ldots, b_n)$ can then be written as

$$\mathcal{F}(b_1, \ldots, b_n) = \mathcal{C} \left(1 - \frac{V(b_1, \ldots, b_n)}{E} \right)^{\frac{n-2}{2}},\tag{31}$$

which is clearly a q-exponential of the potential energy V, with a q index given by

$$q = \frac{n}{n-2}.\tag{32}$$

It goes without saying that Maxwell himself, working a century before Tsallis, did not identify the configuration density as a q-exponential.

As already emphasized, q-distributions play an important role in many textbooks' derivation of the Gibbs canonical distribution [20]. They can also be found in some remarkable works from the 1990s on the micro-canonical approach to finite classical Hamiltonian systems [26,27], although in none of these works were the q-distributions identified as such, nor was their connection with the S_q-thermo-statistics discussed.

In [26], the authors investigate the micro-canonical approach to classical systems consisting of a small number of particles. The authors point out that the momentum distribution of small systems described by the micro-canonical ensemble is non-Maxwellian. The authors prove that the single-particle momentum distribution (see Equation (12) of [26]) is of the form,

$$\mathcal{F}(\mathbf{p}) = \mathcal{C} \left[1 - \frac{\mathbf{p}^2}{2mE} \right]^{[D(N-1)-2]/2},\tag{33}$$

where m is the mass of one particle, $\mathbf{p}$ is the momentum of one particle, E is the total energy of the system, N is the number pf particles in the system, and D is the dimensionality of space (in references [26,27] the authors refer to the spatial dimension as f, but we denote it by D, consistently with the rest of this review). The momentum distribution (33) is clearly a q-Gaussian with

$$q = 1 + \frac{D(N-1) - 2}{2}.\tag{34}$$

In their derivation of the single-particle momentum distribution (33), the authors use, as an intermediate step, the configuration distribution (30) discussed by Maxwell in [24]. As a matter of fact, the developments reported in [26] can, to some extent, be regarded as an interesting re-formulation and elaboration, from a modern point of view, of ideas that were already implicit in Maxwell's seminal paper.

In [27], the authors provide a nice detailed discussion of the micro-canonical approach to a classical ideal gas in a uniform gravitational field confined to a D-dimensional vessel. As in reference [26], the system considered by the authors of [27] is assumed to have a finite

number N particles and a total energy E. Its single-particle distribution, which is provided in Equation (10) of [27], is proportional to

$$\left(1 - \frac{\mathbf{p}^2}{2mE} - \frac{mgz}{E} \right)^{[(D/2)+1]N-[(D/2)+2]}, \tag{35}$$

where m is the mass of a particle, $\mathbf{p}$ is the momentum of a particle, and $z > 0$ denotes the height of particle measured from the bottom of the vessel. As a consequence of the above result, the single-particle distribution can then be expressed as

$$\mathcal{F}(z, \mathbf{p}) = \mathcal{C} \left[1 - \frac{\epsilon}{E} \right]^{[(D/2)+1]N-[(D/2)+2]}, \tag{36}$$

where $\mathcal{C}$ is an appropriate normalization constant and

$$\epsilon = \frac{\mathbf{p}^2}{2m} + mgz \tag{37}$$

is the single-particle energy. The distribution (36) has the S_q-canonical form. It is a q-exponential in the single-particle energy ϵ, with the q parameter given by

$$q = 1 + \{[(D/2) + 1]N - [(D/2) + 2]\}^{-1} \tag{38}$$

The single-particle distributions studied in [26,27] fit into the general picture described in the previous section if one identifies system A with one of the system's particles, and system B with the remaining $N - 1$ particles.

5. The Many Facets of the S_q-Statistics-Micro-Canonical Connection

The connection between the micro-canonical ensemble and the q-exponentials and q-Gaussians for finite systems has been analyzed and discussed by several researchers, expanding this venue of inquiry into various interesting directions [28–42]. In this section, we shall review the main developments along these lines. We shall restrict our discussion to works centered on the S_q-canonical-micro-canonical relation per se, focusing on how the q-distributions arise from such a relation. Some of these works are presented in terms of finite or small heat baths, but they contribute to our main concern here: how the q-distributions originate from micro-canonical scenarios. We shall not discuss works revolving around interpretative issues related to the finite-bath approach. Those constitute, no doubt, interesting and relevant efforts, but they are outside the scope of our present review.

The most powerful formulation of the micro-canonical approach to the S_q-thermostatistics for finite classical Hamiltonian systems with a continuous phase space is, arguably, the one advanced by Adib, Moreira, Andrade Jr, and Almeida (AMAA) in [29]. In terms of our discussion in Section 3, the main ideas in [29] can be interpreted as follows. Let us consider a finite classical system with a Hamiltonian that can be expressed as

$$H = H_A(\omega_A) + \sum_{k=1}^{J} H_k(\omega_k), \tag{39}$$

where each of the terms $H_A, H_1, \ldots, H_J$, depends on a different subset of canonical variables. The term H_A of the Hamiltonian depends on the subset ω_A of canonical variables, and each term H_k $(1 \leq k \leq J)$ depends on the subset ω_k. Each of the system's canonical variables belongs to one and only one of the subsets $\{\omega_A, \omega_1, \ldots, \omega_J\}$. Let us assume that each of the terms H_k $(1 \leq k \leq J)$ depends on n_k canonical variables (the set ω_k has n_k components) and is a homogeneous function of degree l_k. That is, if

$$\omega_k = (z_1^{(k)}, \ldots, z_{n_k}^{(k)}), \quad k = 1, \ldots, J \tag{40}$$

is the set of n_k canonical variables $z_{n_k}^{(k)}$ on which H_k depends, one has,

$$
\begin{aligned}
H_k(\lambda \omega_k) &= H_k(\lambda z_1^{(k)}, \dots, \lambda z_{n_k}^{(k)}), \\
&= \lambda^{l_k} H_k(\omega_k), \qquad k = 1, \dots, J.
\end{aligned}
\tag{41}
$$

Let $\omega_A = (z_1^{(A)}, \dots, z_{n_A}^{(A)})$ stand for the set of canonical variables on which the term H_A depends. Then, the total number of canonical variables describing the complete system, is $n_t = n_A + \sum_{k=1}^{J} n_k$. The above requirements define a class of classical Hamiltonian systems that admits, as particular instances, concrete systems of practical relevance in Physics. For instance, the Hamiltonian corresponding to a system of N interacting classical point particles in D dimensions can be cast in the form (39), if one identifies the subset ω_A with the complete set of ND configuration coordinates, and the subset ω_1 with the complete set of ND components of momenta. In this example, one has $J = 1$, $n_1 = ND$, and $l_1 = 2$. Other concrete examples will be mentioned later.

Under the above assumptions, the authors of [29] proved that, if the complete system is described by the micro-canonical distribution, then the marginal distribution corresponding to the variables ω_A has the S_q-canonical form. Let us take a closer look at this result from the view point of the general argument outlined in Section 3. Let us define H_B as

$$
H_B(\omega_1, \dots, \omega_J) = \sum_{k=1}^{J} H_k(\omega_k),
\tag{42}
$$

and consider the volume $\Phi_B(E)$ in the space characterized by the set of variables $(\omega_1, \dots, \omega_k)$, for which $H_B \leq E$. We have

$$
\Phi_B(E) = \int_{H_B(\omega_1, \dots, \omega_J) \leq E} d\omega_1 \dots d\omega_J,
\tag{43}
$$

where

$$
d\omega_k = dz_1^{(k)} \dots dz_{n_k}^{(k)}, \quad k = 1, \dots, J.
\tag{44}
$$

Given a value E of the total energy and a reference value E_0, let us choose a set of dimensionless parameters λ_k in such a way that

$$
\lambda_k = \left(\frac{E}{E_0} \right)^{1/l_k}, \quad k = 1, \dots, J.
\tag{45}
$$

We then have, taking into account the homogeneity of the H_ks, that

$$
\frac{H_k(\lambda_k \omega_k)}{H_k(\omega_k)} = \lambda_k^{l_k} = \frac{E}{E_0}, \quad k = 1, \dots, J,
\tag{46}
$$

which implies that

$$
\begin{aligned}
\Phi_B(E) &= \int_{H_B(\omega_1, \dots, \omega_J) \leq E} d\omega_1 \dots d\omega_J \\
&= \left(\prod_{k=1}^{J} \lambda_k^{n_k} \right) \int_{H_B(\omega_1', \dots, \omega_J') \leq E_0} d\omega_1' \dots d\omega_J' \\
&= \left(\prod_{k=1}^{J} \lambda_k^{n_k} \right) \Phi_B(E_0) \\
&= \left(\frac{E}{E_0} \right)^{\sum_{k=1}^{J} (n_k/l_k)} \Phi_B(E_0).
\end{aligned}
\tag{47}
$$

We then see that the volume $\Phi_B(E)$ grows as a power of E,

$$\Phi_B(E) = \Phi_B(E_0) \left(\frac{E}{E_0} \right)^\eta, \tag{48}$$

with

$$\eta = \sum_{k=1}^{J} \frac{n_k}{l_k}. \tag{49}$$

One is then precisely within the scenario discussed in Section 3, from which it follows that the marginal probability density corresponding to the variables ω_A is of the S_q canonical form

$$\mathcal{F}(\omega_A) = \mathcal{C} \left[1 - \frac{H_A(\omega_A)}{E_T} \right]^{\frac{1}{q-1}}, \tag{50}$$

where E_T is the total energy of the system, and

$$q = \frac{\eta}{\eta - 1} = 1 + \left[\left(\sum_{k=1}^{J} \frac{n_k}{l_k} \right) - 1 \right]^{-1}. \tag{51}$$

All the examples discussed in the previous section can be analyzed in terms of the AMAA formulation. In the systems discussed in [26,27], one has to identify the subsystem A with one particle of the system, and the subsystem B with the remaining $N - 1$ particles. In the case discussed in [26], one has $J = 1$, $n_1 = D(N - 1)$, and $l_1 = 2$. Then, (49) and (51) determine the values of η and q, and the latter coincides with (34). In the case discussed in [27], one has $J = 2$, $n_1 = D(N - 1)$, $n_2 = N - 1$, $l_1 = 2$, and $l_2 = 1$. Then, from (49) and (51), one obtains the same value of q as (38).

Remarkably, AMAA performed numerical experiments on a system consisting of a chain of anharmonic oscillators, described by the Hamiltonian,

$$H = \sum_{i=1}^{N} \frac{p_i^2}{2} + \sum_{i=1}^{N} \frac{q_i^4}{2} + \sum_{i=1}^{N} \frac{(q_{i+1} - q_i)^4}{4}, \tag{52}$$

where q_i and p_i $(i = 1, \ldots, N$ are the coordinates and momenta of the N particles in the system. The chain of anharmonic oscillators governed by the Hamiltonian (52) was inspired by the celebrated Fermi–Pasta–Ulam system. The Hamiltonian (52) has the form (39). For instance, if one identifies the set ω_A with the set of N momenta, and the set ω_1 with the set of N coordinates (we then have $J = 1$, $n_1 = N$ and $l_1 = 4$), it follows that the marginal probability distribution corresponding to the momenta will be a q-exponential, provided that the system is described by the micro-canonical ensemble. The numerical experiments conducted by AMAA, based on the numerical integration of the canonical equations of motion, confirmed that the micro-canonical description is in this case appropriate, and that the probability distribution of the momenta is indeed q-exponential [29]. The numerical experiments reported by AMAA are of considerable relevance because they provide a concrete example of a highly nonlinear system, exhibiting complex dynamics, for which the micro-canonical path toward the S_q-canonical distributions is explicitly verified.

In [32], Hanel and Thurner provide a clever analysis of the general conditions under which micro-canonical scenarios in classical statistical mechanics naturally lead to power-law distributions of the q-exponential type. In [33], Naudts and Baeten point out that the configuration probability density of a classical gas always has the S_q-canonical form. Therefore, the authors establish the connection between this scenario and the S_q-thermo-statistics. The authors explore various aspects of this problem, and discuss the possible role of Renyi entropy (which, once optimized, shields the same probability distributions as Tsallis entropy, although parameterized in a different way).

In [34], Bagci and Oikonomou explore interesting aspects of the micro-canonical setting associated with a classical Hamiltonian system interacting with a finite heat bath. These authors focus on how different assumptions on the heat capacity of the bath lead to different versions of the S_q-canonical distribution. The authors reach the conclusions that a finite bath with positive heat capacity leads to q-exponentials with compact support (that is, with a cut-off), while a heat bath with negative heat capacity leads to q-exponentials with fat tails. Within the present review, we restrict our discussion to micro-canonical scenarios generating q-exponentials with a cut-off. We find, however, that Bagci and Oikonomuu's analysis of situations with finite baths of negative heat capacity is intriguing and worthy of further consideration. In [35], Ramshaw re-visits the micro-canonical treatment of a system in contact with a finite heat bath. The author analyzes the concomitant deviations of the system's probability distribution from the exponential Boltzmann–Gibbs one. The author's analysis confirms that, under appropriate conditions, probability distributions of the S_q-canonical form are obtained. The author suggests that, although the S_q entropy may play a direct role here, the presence of q-exponentials is not in itself enough to establish that that is the case. There may be something to the author's point of view. This is an issue that certainly deserves further investigation. In [36], Biró, Barnaĺdi, and Ván apply the S_q-micro-canonical connection to the analysis of some aspects of the physics of the quark–gluon plasma and to the interpretation of experimental data on heavy ion collisions. An intriguing extension of these matters to complex values of the Tsallis parameter q is discussed by Wilk and Wlodarczyk in [37].

In [38], Lima and Deppman re-visit the micro-canonical approach to an ideal gas constituted by a finite number N of particles and provide a detailed analysis of its relation with the S_q-based thermostatistics. The authors investigate in detail how, as $N \to \infty$, the standard Boltzmann–Gibbs scenario is approached. In particular, they compute the two-particle correlation function and study how the amount of correlation decreases as one considers an increasing number of particles in the system. The micro-canonical ensemble for an ideal gas with a finite number of molecules is also considered by Shim in [39], where the S_q-canonical shape of the single-particle distribution is also investigated.

6. Conclusions

A growing number of generalizations of the concept of entropy are nowadays attracting the attention of scientists. Researchers are actively exploring diverse applications of these ideas, particularly in connection with entropic optimization methods. To a large extent, this broad field of inquiry got its initial inspiration in the S_q-thermostatistics advanced by Tsallis in 1988. The non-additive S_q entropies still play a distinguished role within the zoo of generalized entropies. Among the different distributions optimizing non-standard entropies, those optimizing the S_q measures are the ones that provide useful descriptions for the largest number of scenarios in physics and elsewhere. It is, therefore, imperative, in order to explain this state of affairs, to study in detail the particular features of the S_q-thermo-statistics that make it so special. The present review dealt with one of these distinguishing features: the remarkable connection between the S_q-thermostatistics and the micro-canonical ensemble. This connection is nowadays generally acknowledged as constituting the basis of an important mechanism generating S_q-optimizing distributions in physical systems. For instance, the significance of the fact that "research showed that finite ideal gas followed q-exponential distributions" [40], was recently highlighted by Deppman, a leading researcher in nuclear and particle physics, and in the application of Tsallis' non-extensive statistics to these fields. Deppman and collaborators advanced an interesting theoretical framework, based on the concept of thermofractals, for the study of systems that exhibit a finite effective number of degrees of freedom, independently of the system's size [41]. This scenario, which leads to a description similar to the micro-canonical one, generating q-distributions even for large systems, has been applied to problems in high-energy physics [41].

In spite of the considerable amount of research that has been devoted to investigate the micro-canonical approach to the S_q-canonical ensemble, we believe that the study of this aspect of S_q-thermostatistics is still in its infancy. There is still much work to be done, particularly in order to establish links between the micro-canonical setting and other facets of S_q-thermostatistics. In this regard, it would be interesting to explore Baranger's conjecture that the micro-canonical approach may be relevant to explain the emergence of S_q-thermo-statistics within non-equilibrium scenarios [21]. A promising first step in this direction was taken by Megias, Lima, and Deppman in [42], where the authors consider transport phenomena on the light of the connection between the S_q-thermostatstical and the micro-canonical setting. Another issue that deserves further scrutiny is the connection of the entropy functional S_q itself with the micro-canonical setting. Up to now, the main theoretical indication of a connection between the S_q-based thermostatistics and the micro-canonical scenario is based on the presence of the q-distributions, rather than on a more direct connection with the S_q functional itself. The presence of q-distributions is generally construed, by a large part of the research community, as evidence for the S_q-based thermostatistics. This is the case not only with regards to the micro-canonical scenarios but also within more general contexts. In particular, most of the empirical evidence for the S_q-thermostatistics rests on the experimental observation of q-distributions [17,19]. This situation is not surprising since the distributions that describe a system are more amenable of experimental or observational investigation than an entropic functional. The fact that probability distributions optimizing a particular functional, the S_q entropy, appear so frequently, both in theoretical models and in experimental settings, strongly suggests that the S_q entropy is playing an important role. This is consistent with the general notion that variational principles provide the most fundamental description of physical systems or processes. It is significant, in this regard, that even researchers who doubt that the S_q-based optimization principle is the correct explanation for the presence of q-distributions, nevertheless entertain the idea that an alternative variational principle may be at work. For instance, Ramshaw recently observed that the non-exponential distributions describing subsystems in micro-canonical contexts, can be derived from an entropy-optimization prescription if one, instead of changing the entropic form, replaces the standard energy constraint by an adroitly chosen non-linear generalization [43]. Ramshaw's proposal is intriguing, and certainly deserves further consideration. It nicely illustrates the belief of many theoreticians that the identification of an appropriate entropic variational principle leading to the non-exponential distributions observed on micro-canonical scenarios will contribute to achieving a deep understanding of these distributions. Among the proposals that have been advanced in this respect, the one based on the S_q-entropy has been, so far, the most actively investigated, as attested by the works reviewed here.

The S_q canonical distributions, which exhibit the q-exponential (or, in particular cases, are q-Gaussian) form, arise naturally as marginal probability distributions describing parts of systems represented by the micro-canonical ensemble. In this regard, the q-distributions can be identified in some works dating from the very beginnings of statistical mechanics. They have also been appearing, along the years, in papers' and textbooks' discussions on the micro-canonical ensemble. The relevance of these ubiquitous distributions, however, was for a long time unrecognized. Until the development of the S_q thermo-statistics, they lacked a name. The significance of their relationship with the micro-canonical ensemble, which links them to the origins and history of statistical mechanics, has been highlighted in recent times by the research efforts conducted by several scientists, who explored its interesting and manifold implications. Intriguing results along these lines continue to appear. What new developments the future will bring, we cannot tell. However, we can be sure of one thing: like Holly's cat in *Breakfast at Tiffany's* [44], these long-neglected distributions finally got a name, and the name is here to stay.

References

1.   Garcia Marquez, G. *One Hundred Years of Solitude*; Avon Books: New York, NY, USA, 1971.
2.   Tsallis, C. Possible generalization of Boltzmann-Gibbs statistics. *J. Stat. Phys.* **1988**, *52*, 479–487. [CrossRef]
3.   Tsallis, C. *Introduction to Nonextensive Statistical Mechanics—Approaching a Complex World*; Springer: New York, NY, USA, 2009.
4.   Plastino, A.; Plastino, A.R. From Gibbs microcanonical ensemble to Tsallis generalized canonical distribution. *Phys. Lett. A* **1994**, *193*, 140–143. [CrossRef]
5.   Tsallis, C. Entropy. *Encyclopedia* **2022**, *2*, 264–300. [CrossRef]
6.   Jizba, P.; Korbel, J. Maximum Entropy Principle in statistical inference: Case for non-Shannonian entropies. *Phys. Rev. Lett.* **2019**, *122*, 120601. [CrossRef]
7.   Naudts, J. *Generalised Thermostatistics*; Springer: London, UK, 2011.
8.   Beck, C. Generalised information and entropy measures in physics. *Contemp. Phys.* **2009**, *50*, 495–510. [CrossRef]
9.   Amigó, J.M.; Balogh, S.G.; Hernández, S. A Brief Review of Generalized Entropies. *Entropy* **2018**, *20*, 813. [CrossRef]
10. Ilic, V.M.; Korbel, J.; Gupta, S.; Scarfone, A.M. An overview of generalized entropic forms. *EPL* **2021**, *133*, 50005. [CrossRef]
11. dos Santos, M.A.F.; Nobre, F.D.; Curado, E.M.F. Entropic form emergent from superstatistics. *Phys. Rev. E* **2023**, *107*, 014132. [CrossRef]
12. Hanel, R.; Thurner, S. A comprehensive classification of complex statistical systems and an axiomatic derivation of their entropy and distribution functions. *EPL* **2011**, *93*, 20006. [CrossRef]
13. Amigó, J.M.; Dale, R.; Tempesta, P. Complexity-based permutation entropies: From deterministic time series to white noise. *Commun. Nonlinear Sci. Numer. Simul.* **2022**, *105*, 106077. [CrossRef]
14. Gell-Mann, M.; Tsallis, C. *Nonextensive Entropy: Interdisciplinary Applications*; Oxford University Press: Oxford, UK, 2004.
15. Lenzi, E.K; Dos Santos, M.A.F.; Michels, F.S.; Mendes, R.S.; Evangelista, L.R. Solutions of Some Nonlinear Diffusion Equations and Generalized Entropy Framework. *Entropy* **2013**, *15*, 3931–3940. [CrossRef]
16. Livadiotis, G.; McComas, D.J. Understanding Kappa Distributions: A Toolbox for Space Science and Astrophysics. *Space Sci. Rev.* **2013**, *175*, 183. [CrossRef]
17. Tsallis, C. Beyond Boltzmann-Gibbs-Shannon in physics and elsewhere. *Entropy* **2019**, *21*, 696. [CrossRef] [PubMed]
18. Sánchez Almeida, J. The Principle of Maximum Entropy and the Distribution of Mass in Galaxies. *Universe* **2022**, *8*, 214. [CrossRef]
19. Wild, R.; Nötzold, M.; Simpson, M.; Tran, T.D.; Wester, R. Tunnelling measured in a very slow ion–molecule reaction. *Nature* **2023**, *615*, 425–429. [CrossRef] [PubMed]
20. Feynman, R. *Statistical Mechanics: A Set of Lectures*; Addison-Wesley: Reading, MA, USA, 1972.
21. Baranger, M. Why Tsallis statistics? *Physica A* **2002**, *305*, 27–31. [CrossRef]
22. Saadatmand, S.N.; Gould, T.; Cavalcanti, E.G.; Vaccaro, J.A. Thermodynamics from first principles: Correlations and nonextensivity. *Phys. Rev. E* **2020**, *101*, 060101. [CrossRef]
23. Plastino, A.R.; Tsallis, C.; Wedemann, R.S.; Haubold, H.J. Entropy Optimization, Generalized Logarithms, and Duality Relations. *Entropy* **2022**, *24*, 1723. [CrossRef]
24. Maxwell, J.C. On Boltzmann's Theorem on the Average Distribution of Energy in a System of Material Points. *Trans. Camb. Philos. Soc.* **1879**, *XII*, 547–570.
25. Niven, W.D. (Ed.) *The Scientific Papers Of James Clerk Maxwell*; Cambridge University Press: Cambridge, UK, 1890; Volume II.
26. Ray, J.R.; Graben, H.W. Small systems have non-Maxwellian momentum distributions in the microcanonical ensemble. *Phys. Rev. A* **1991**, *44*, 6905. [CrossRef]
27. Román, F.L.; White, J.A.; Velasco, S. Microcanonical single-particle distributions for an ideal gas in a gravitational field. *Eur. J. Phys.* **1995**, *16*, 83. [CrossRef]
28. Velazquez, L.; Guzmán, F. Remarks about the Tsallis formalism. *Phys. Rev. E* **2002**, *65*, 046134. [CrossRef] [PubMed]
29. Adib, A.B.; Moreira, A.A.; Andrade, J.S., Jr.; Almeida, M.P. Tsallis thermostatistics for finite systems: A Hamiltonian approach. *Physica A* **2003**, *322*, 276–284. [CrossRef]
30. Almeida, M.P. Thermodynamical entropy (and its additivity) within generalized thermodynamics. *Physica A* **2003**, *325*, 426–438. [CrossRef]
31. Potiguar, F.Q.; Costa, U.M.S. Thermodynamical relations for systems in contact with finite heat baths. *Physica A* **2004**, *344*, 614. [CrossRef]
32. Hanel, R.; Thurner, S. Derivation of power-law distributions within standard statistical mechanics. *Physica A* **2005**, *351*, 260–268. [CrossRef]

33. Naudts, J.; Baeten, M. Non-extensivity of the configurational density distribution in the classical microcanonical ensemble. *Entropy* **2009**, *11*, 285–294. [CrossRef]
34. Bagci, G.B.; Oikonomou, T. Tsallis power laws and finite baths with negative heat capacity. *Phys. Rev. E* **2013**, *88*, 042126. [CrossRef] [PubMed]
35. Ramshaw, J.D. Supercanonical probability distributions. *Phys. Rev. E* **2018**, *98*, 020103. [CrossRef] [PubMed]
36. Biró, T.S.; Barnaföldi, G.G.; Van, P. Quark-gluon plasma connected to finite heat bath. *Eur. Phys. J. C* **2013**, *49*, 110:1–110:5. [CrossRef]
37. Wilk, G.; Włodarczyk, Z. Tsallis Distribution Decorated with Log-Periodic Oscillation. *Entropy* **2015**, *17*, 384–400. [CrossRef]
38. Lima, J.A.S.; Deppman, A. Tsallis meets Boltzmann: q-index for a finite ideal gas and its thermodynamic limit. *Phys. Rev. E* **2020**, *101*, 040102. [CrossRef] [PubMed]
39. Shim, J.W. Entropy formula of N-body system. *Sci. Rep.* **2020**, *10*, 14029. [CrossRef] [PubMed]
40. Deppman, A. Thermofractals, Non-Additive Entropy, and q-Calculus. *Physics* **2021**, *3*, 290–301. [CrossRef]
41. Deppman, A.; Megías, E.; Menezes, D.P. Fractal Structures of Yang–Mills Fields and Non-Extensive Statistics: Applications to High Energy Physics. *Physics* **2020**, *2*, 455–480. [CrossRef]
42. Megías, E.; Lima, J.A.S.; Deppman, A. Transport Equation for Small Systems and Nonadditive Entropy. *Mathematics* **2022**, *10*, 1625. [CrossRef]
43. Ramshaw, J.D. Maximum entropy and constraints in composite systems. *Phys. Rev. E* **2022**, *105*, 024138. [CrossRef]
44. Capote, T. *Breakfast at Tiffany's*; Penguin Classics: New York, NY, USA, 2000.